The Hydrogeochemistry of Spring and Gorge Waters of the Karijini National Park, Pilbara, Western Australia.

A thesis submitted in partial fulfilment of the requirements for the Degree

of Master of Engineering Geology

in the

University of Canterbury

by P.J Hedley

University of Canterbury

2009

Frontispiece

“What makes the desert beautiful is that somewhere it hides a well”

~ Antoine de Saint-Exupery ~

Abstract

Isotopes and hydrochemistry were used to define groundwater flow systems and better understand the hydrogeological setting of the Karijini National Park within the Central Pilbara region, this study was initiated because of the near proximity of the Marandoo iron ore mine to the National Park. Based on the stable isotope composition of the water samples, two main groups of water can be identified. Groundwater is characterised by depleted δD and $\delta^{18}O$, suggesting no significant evaporation effect. Surface water on the other hand is more enriched in δD and $\delta^{18}O$ due to evaporation. The relatively high concentration of Cl- compared to rainfall and depleted δD and $\delta^{18}O$ values of groundwater indicate that recharge of the aquifers is occurring during intense rainfall events when rapid infiltration occurs. Evapotranspiration then acts to concentrate ionic species prior to recharge. The presence of CFCs in the groundwater indicates the presence of modern recharge water.

Relationships between various ionic species has shown that infiltration through the Tertiary sequence and subsquent dissolution of carbonate minerals is main influence on increasing concentrations of Ca^{2+} , Mg^{2+}, HCO_3^-.

The TDS concentration of the groundwater in the Marra-Mamba Iron Formation that hosts the Marandoo ore body is higher than most of the water bodies surrounding the mining area. This suggests that either significant chemical modification is occuring or it is recharged by different mechanisms to that of the Karijini groundwater.

Relationships between the major ion concentration and catchment area, surficial Tertiary cover and distance between recharge and discharge were identified. The results show that the hydrochemistry of the water discharging at each location within the National Park can be justified by groundwater evolution within it's own catchment.

Table of Contents

List of Figures and Tables

LIST OF FIGURES

CHAPTER 1

CHAPTER 2

CHAPTER 3

CHAPTER 4

CHAPTER 6

CHAPTER 7

LIST OF TABLES

CHAPTER 1

CHAPTER 3

CHAPTER 4

CHAPTER 5

CHAPTER 6

List of Abbreviations

AMS = Accelerator Mass Spectrometry

BIF = Banded Iron Formation

BRF = Brockman Iron Formation

CFC = Chloroflourocarbon

EC = Electric Conductivity

ET = Evapotranspiration

GMWL = Global Meteoric Water Line

GIS = Geographic Information System

GPS = Global Positioning System

IAEA = International Atomic Energy Agency

KNP = Karijini National Park

LMWL = Local Meteoric Water Line

MM = Mara-Mamba

PMC = Percent modern Carbon

RTIO = Rio Tinto Iron Ore

SAL = Salinity

SFP = Southern Fortescue Borefield

SWL = Sea Water Dilution Line

SMOW = Standard Mean Ocean Water

TDS = Total Dissolved Solids

TR = Tertiary Formation

VSMOW = Vienna Standard Mean Ocean water

WES = Water Equilibration System

WF = Wittenoom Formation

XRD = X-Ray Diffraction

Acknowledgments

A huge recognition needs to go to everybody at Rio Tinto Iron Ore who made it possible for me to conduct my masters through their funding and support. In particular:

Shawan Dogramaci, thank-you very much for all the help you have given me throughout the project and continually encouraging me to think outside the square. **Wade Dodson**: Thank you for all your hydrogeological advise and for all the help with setting up the project and organising my travel. **Jay Matta**: For Hydrogeological/Hydrochemical assistance and great company driving around the outback. **George Domahidy**: For initial involvement in getting the project off the ground and sparking my interest in hydrogeology during my vacation work placement.

From the University of Canterbury I would like to thank my Supervisors **David Bell** and **Travis Horton**. Firstly, David for welcoming me into Engineering Geology at an early stage and passing on your wisdom through the course from which I have learnt a huge amount. Also thanks for your critical review of thesis. Secondly, Travis for always being extremely welcoming whenever I had any issues, hydrochemical or otherwise. Also thanks to Stephen Brown and also Travis for analysis of my rock and water samples.

Thanks is also due to Pippa Gardner for taking the amazing aerial photographs of Karijini on request!

Cheers to the gents from 81 Memorial Ave! You all made home a completely relaxing and hassle free environment, which is a luxury often taken for granted.

Lastly, I would also like to thank Blanche for her immense support, friendship and patience. You gave me the motivation to complete my Master's for which I am truly grateful. Also, dragging me away from the computer for coffee breaks has prevented my eyes from going square.

Glossary

Chloroflourocarbon = A man made molecule of carbon, chlorine, and fluorine. It had many household uses prior to the 1950's. It has not be phased out of use due to it's harmful effects of the Earth's Ozone Layer.

Cosmic rays = Energetic particles originating from outer space that impinge on Earth's atmosphere

Dueterium = An stable isotope of hydrogen with mass number of 2 (^2H).

Evapotranspiration = The composite term to describe the loss of water from a system due to Evaporation and Transpiration.

Fractionation = The difference in mass of the water molecules creates differences in thermodynamic reaction rates which leads to the isotope partitioning isotope

Sea Water Dilution Line = A line defines that ionic ratios of seawater which is retained in sea-water aerosols. Rainwater that contains these aerosols should show similar ionic ratios to seawater.

Salinity = A measure of the concentration of dissolved solutes in a solution.

Unsaturated zone (Vadose Zone) = is the portion of Earth between the ground surface and the phreatic zone or zone of saturation or water table.

Chapter 1

Introduction

1.1 Background and scope of the problem

Rio Tinto Iron Ore are investigating the feasibility of extending the resource at their Marandoo Mine by accessing the ore below the current water table. The mine produces Marra Mamba lump and fine ore, which is a vital part of their Pilbara Blend Iron Ore Product. Extending Marandoo's life will be important in continuing to produce a constant product.

Hydrogeologic Modelling suggests that the water table should be significantly lowered in the vicinity of the mine for effective and safe extraction of the iron ore. A drop in water table of this scale has the potential to have adverse effects on surrounding areas.

Marandoo Mine is located within Karijini National Park (Figure 1.1). The Karijini National Park (hereafter referred to as "the KNP") is a popular tourist destination and provides sanctuary for the Pilbara region biodiversity. A particular attraction for the estimated 100,000 visitors per year is the scenic, perennial water filled gorges in the north of the Park. Thus, there is sensitivity to any dewatering operation in the vicinity of the KNP to ensure that unacceptable impacts do not affect the natural amenities of the park. These features range from 10-40km from the mine itself.

1.2 Scope for thesis

1.2.1 Thesis Objectives

To assess the potential impact of dewatering on the water features of the National park the hydrogeology must be understood to determine groundwater interaction and the flow dynamics. As the ground disruption within the National Park is prohibited due to land tenure

and environmental and heritage values, a drilling programme to define the hydrogeology is not an option.

A hydro-geochemical study of groundwater and surface water within the KNP has therefore been conducted. This is a non-invasive method of determining groundwater interaction and flow dynamics. The variation in the hydrochemistry between different samples of water will indicate the variation in the chemical and physical processes the water has been subjected to as it evolves from recharge to discharge water.

Understanding this unique chemical signature will provide information on groundwater recharge-discharge mechanisms and groundwater hydro-chemical evolution in the Park. The hydraulic relationship between the two locations can therefore be understood to determine likelihood of dewatering having an impact of the water features.

The objective of the thesis will be to analyse water samples collected from the study area and interpret their hydrochemistry to understand the physical and chemical processes controlling chemical evolution. It will then be possible to determine whether the water discharging at the key features of the Karijini National could have evolved (and there for sourced) from Marandoo's Marra-Mamba Aquifer.

1.2.2 Thesis Organisation

Chapter 1: Introduces the background and scope of the thesis. It then progresses into describing the physiography of the study area both at a regional scale and the individual local settings relevant to the study. Descriptions include Hydrology, Hydrogeology and Geology.

Chapter 2: Reviews the use of Environmental Tracers in Hydrogeological studies for determining groundwater evolution. The chapter investigates the processes involved in determining to concentrations of dissolved solutes in the groundwater and the appropriate methods of displaying geochemical data. The use of stable isotopes in groundwater studies is reviewed with particular emphasis on the unique characteristics of an arid region. Lastly

the methods and theory involved with the groundwater dating techniques, Chloroflurocarbons and Radiocarbon is described.

Chapter 3: Describes the methods involved with the collection of water samples in the field and their subsequent laboratory analysis to determine Major Ion concentrations, stable isotopic ratios and CFC and Radiocarbon concentrations.

Chapter 4: Details the results from both field and laboratory analysis. In field observations are compiled and developed in conceptual model for groundwater discharge mechanisms in the Karijini National Park

Chapter 5: Discusses the results and progressively develops a story about how groundwater is evolving within the Karijini National Park. This is achieved by investigating the relationships between major ion concentrations and subsequent isotopic signatures. The processes are finally summarised in a conceptual model of groundwater chemical evolution

Chapter 6: The dimension of time is introduced to further investigate the processes occurring in the hydrologic cycle. A second water sampling programme was undertaken to investigate temporal variation in the hydrochemistry of the waters. The groundwater was also dated with the CFC and ^{14}C method to further understand recharge and discharge processes.

Chapter 7: Presents each Karijini National Park sample location separately and uses the knowledge of groundwater evolution developed in chapter 5 and 6 to systematically assess the likely hood of hydraulic connection between Marandoo Mine and relevant water features.

Chapter 8: Concluding statements and recommendations for future work

A publication entitled: "***The use of Major Ions and Stable Isotope (δD and $\delta^{18}O$) to distinguish groundwater flow in Karijini National Park, Pilbara, WA"*** was produced for the AusIMM Water in Mining 2009 Conference. This details a the major results and conclusions from the thesis. It is located in Appendix iii.

1.3 Physiography

1.3.1 Location and description

The Pilbara region of Western Australia is located 1,100km NNE of Perth City. It is a region that covers an area of 507,800 km² and is rich in mineral resources that have been extracted for the last century. Karijini National Park (Figure 1.1) is a located in the Hamersley Ranges in the Centre of the Pilbara covering an area of 6,300km^2. The Park extends from latitude 23°13'S to 22°13'S (approximately 110 km) and from longitude 117°53'E to 118°45'E (approximately 70 km). It is the second largest national park in Australia and at its nearest point, the Park is approximately 200 km from the coast. The highest point within the park is Mt Bruce, which is the second highest peak in Western Australia at 1 235 m.

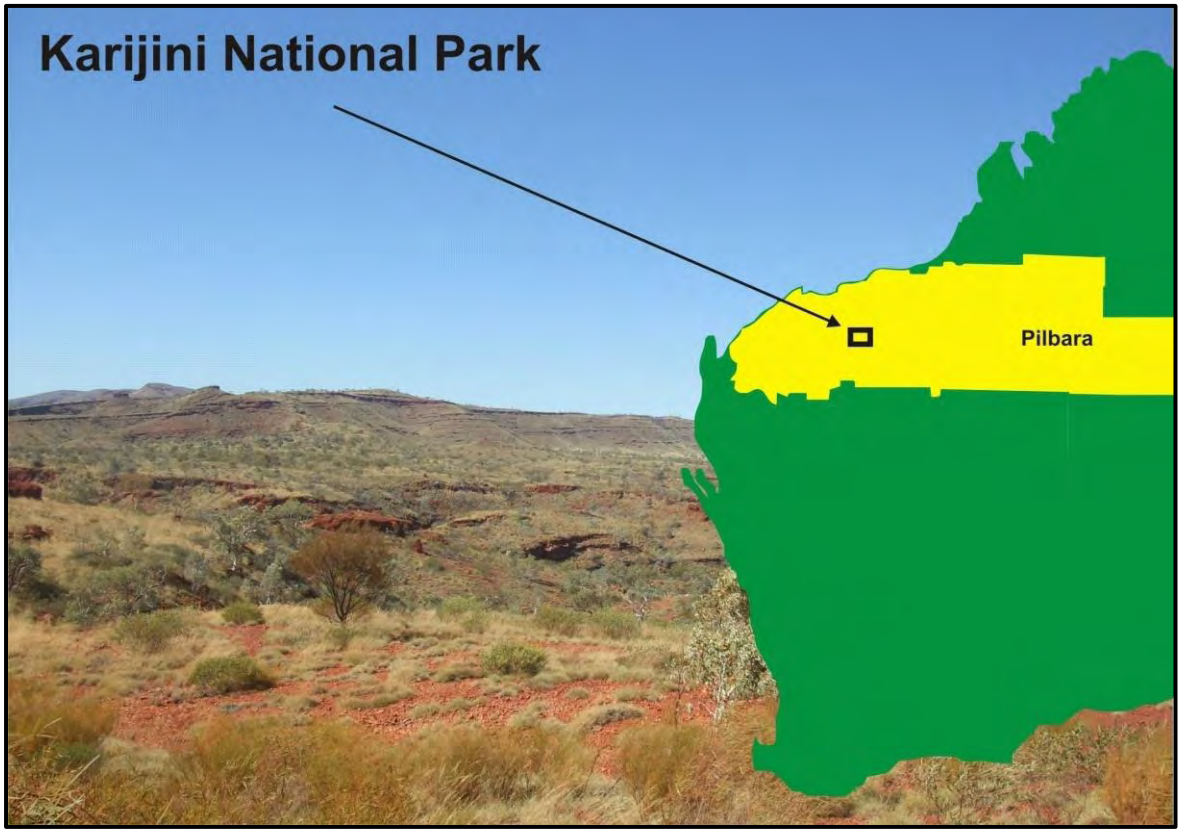

Figure 1.1 Location Map of Karijini National Park, Pilbara, WA

Natural erosive and depositional processes have produced an array of landscape features, best known of which are the picturesque gorges, for which the Park is famous. These have incised through the Banded Iron Formations up to 40m deep. The erosive processes have also deposited a significant thickness of colluvial and alluvial sediments as valley fill during the tertiary period..

1.3.2 Vegetation

The vegetation includes a range of vegetation formations ranging from grasslands to closed forests, with most areas of the Park having hummock grasslands of *Triodia* species with various open shrub and tree layers over them. Generally the shrub layer is dominated by *Acacia* species and the tree layer by *Eucalyptus*.

Other species include, Mulga (*Acacia aneura*) stands on flats and hill slopes, Paperbark (*Melaleuca leucadendra*) forests in gorges, sedge lands around permanent pools and bulrush (*Typha*) stands within them (DEC, 1999).

1.3.3 Aboriginal Significance

The Park and the surrounding areas are of enduring significance to contemporary Panyjima,Yinhawangka and Kurrama Aboriginal people, most of whom now reside in such towns as Onslow, Karratha, Roebourne, Wickham and Port Hedland. Although many disruptions have occurred to traditional life, they seek to retain social, religious and personal bonds that have persisted for countless generations.

The Park and surrounding area is rich in physical evidence of the occupation and use of the land by Aboriginal people from ancient times. A recently discovered habitation site has had its contents dated at 18 000 years old (DEC, 1999). The contemporary and archaeological significance of Karijini National Park to Aboriginal people add important dimensions to the understanding and appreciation of the Park.

1.4 Site Descriptions

The main locations of importance to the study are two borefields, Southern Fortescue Production Borefield and Marandoo Production Borefield, and also a selection of ground and surface water locations that exist within the Karijini National Park. Details of these are now discussed:

1.4.1 Marandoo Borefield

The Main borefield in the study is Marandoo Production Borefield which extracts water from the Mara Mamba Aquifer. This is the major aquifer that will be involved in dewatering. The field comprises five production bores and 13 observation bores. The bores were installed in the early 1990's and were commissioned in 1994, the water is extracted for mine related purposes and pit dewatering. The annual allocation for the borefeild is 2.0GL, which only 30% is currently utilised

The Marandoo borefield draws water from a mixed aquifer system which has developed within a broad paleovalley. The valley has eroded into the Wittenoon Formation and is bounded by outcrops of Marra Mamba and Brockman Iron Formations (Figure 1.2). Within the paleovalley sequence aquifers are associated with calcrete horizons and deeper granular sediments. There is also a deeper aquifer associated with the vuggy / karstic weathered upper section of the Wittenoon Formation (AAR, 2007).

The aquifers are recharged by direct infiltration of rainfall runoff which accumaltes in local drainage lines and subsequently leaks into deeper aquifers (AAR, 2007) . The groundwater flows to the northwest towards the Southern Fortescue River valley and borefield area and discharges via baseflow and borefield abstraction (Aquaterra, 2001). Minthi Spring and Banjima Pool are nearby and therefore significant water features.

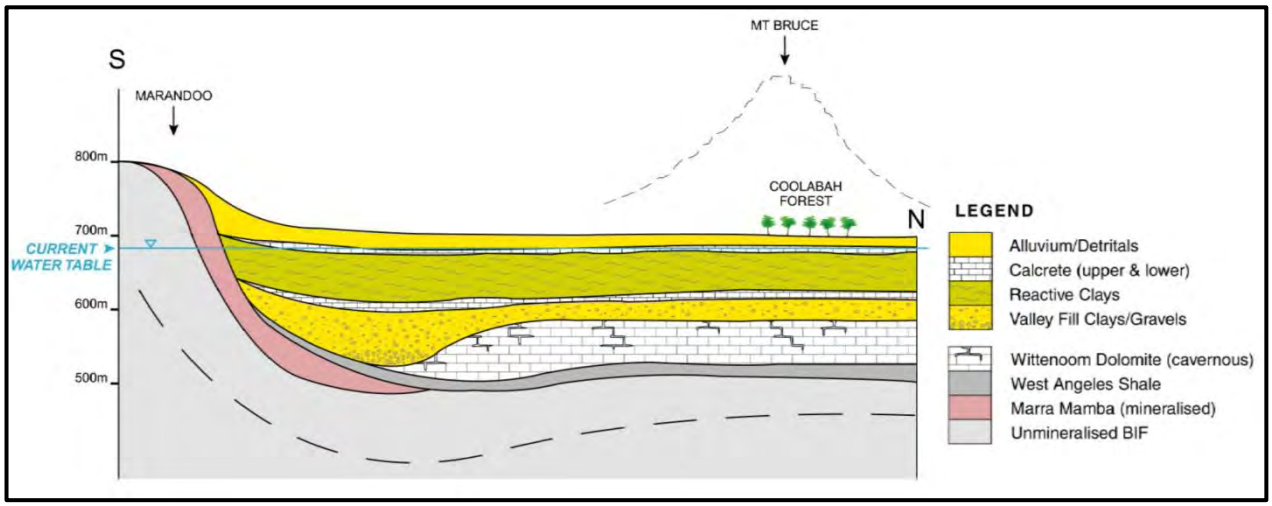

Figure 1.2 Schematic Cross Section of Marandoo Hydrogeology (Adapted from Liquid Earth, 2005)

1.4.2 Southern Fortescue Borefield

The other major borefield associated with this study is the Southern Fortescue Borefield, which is located about 20km North-West of Marandoo and supplies water to both Tom Price mine and Town. The borefield has been operating since the 1970s and currently consist of ten production bores and fifteen observation bores. The annual allocation for the borefeild is 4.68GL (~12ML/day).

The borefield is located within the upper reaches of the Southern Fortescue River Valley, which is bounded to the east and west by outcropping Brockman and Marra Mamba Iron Formations. A thick sequence of alluvial, colluvial and chemical sediments has developed in a palaeovalley, which has eroded down to the underlying Wittenoom Formation (RTIO, 2006).

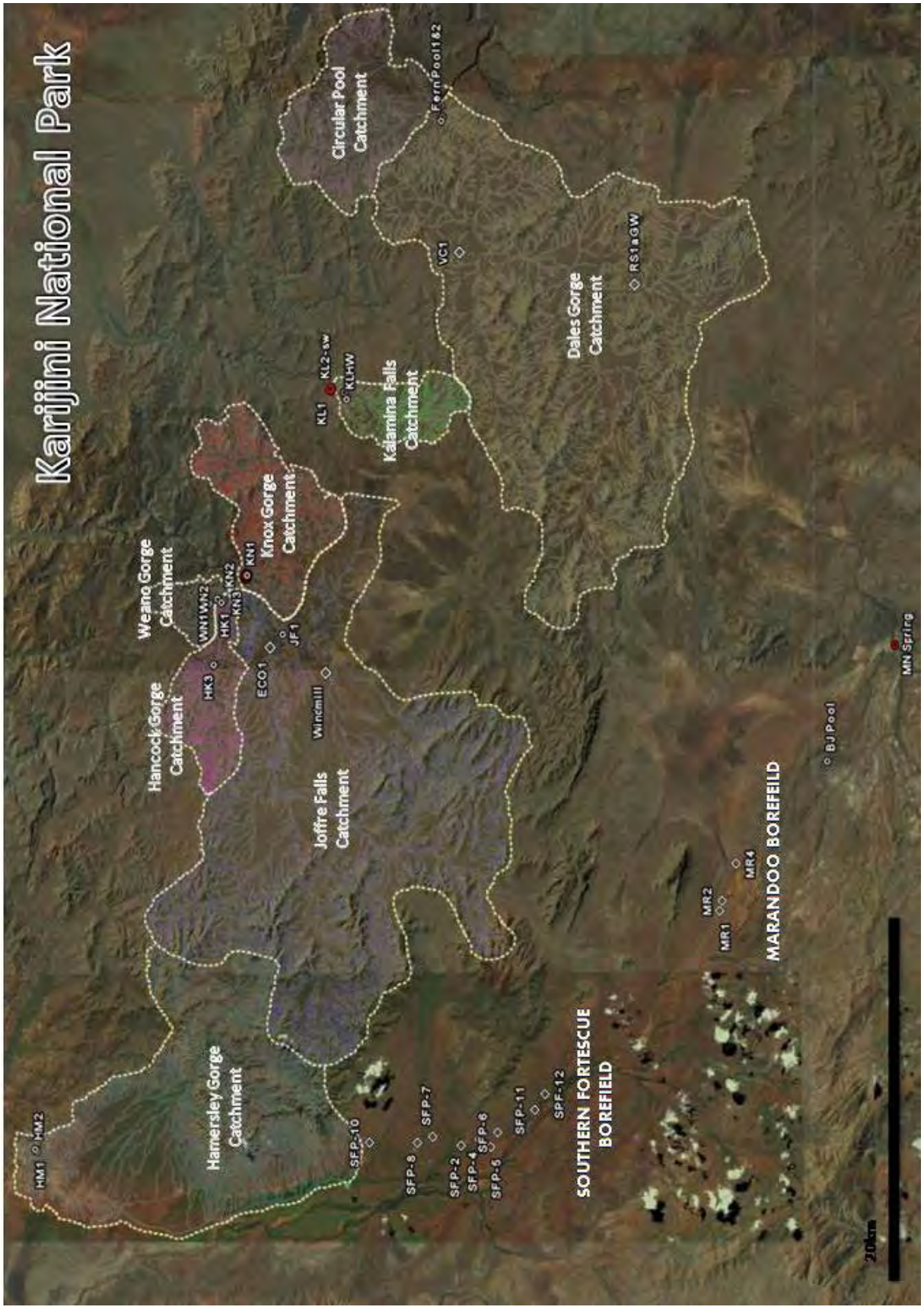

Figure 1.3. Location Map of key locations associated with the study. Dotted lines define the catchment boundaries.

1.3.3 The Gorges of Karijini

The water features of Karijini National Park are contained within a number of gorges scattered throughout the Park. The Gorges have formed in topographic low points, where discharging groundwater has progressively incised through the Brockman Iron Formation. The gorge morphology is generally very steep side gorge walls, which can reach a height of 80m, with a low discharge stream at its base. The gorges generally taper off to a spring (ground water discharge) location at their head. In some locations groundwater can be observed to discharge from joints and fractures in the Brockman Iron Formation gorge walls, but generally the gorge walls are dry.

Surface water is located in perennial pools, low discharge streams and waterfalls. These are generally the first location that surface water can be observed/sampled over the whole catchment system. Each gorge has its own surface water catchment which vary greatly in size across the study area (≈12km^2 - 350km^2). The network of these catchments combine to form the Southern Fortescue River catchment system which drains to the Nor-west.

The beauty of the geology and hydrology of these features attracts 100,000s of Tourists annually. The water features also hold large cultural heritage values to the Local aboriginal people as they traditionally provided a source of fresh water.

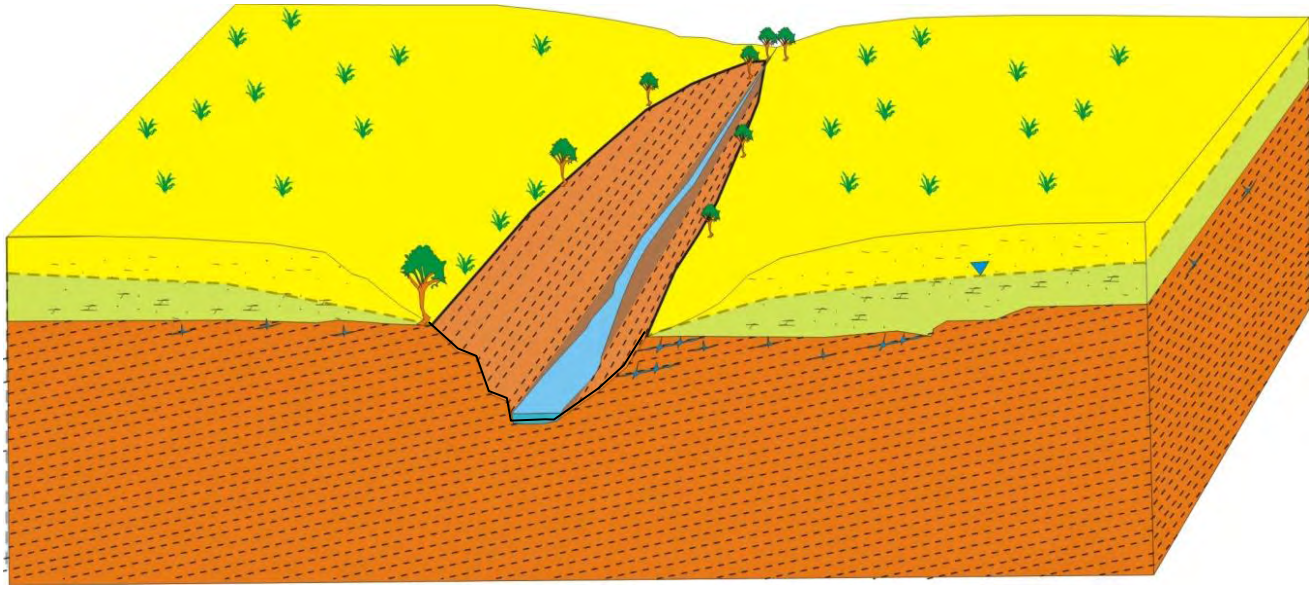

Figure 1.4 Schematic Cross section of a typical Gorge within Karijini National Park

From West to East the samples were collected from the following Gorges and Water features (It is recommended to view appendix I for more detailed description of each feature:

Hamersley Gorge: The most distant gorge in the Nor-western Corner of the Park. Hosts numerous perennial pools and water falls.

Weano Gorge: A small gorge with numerous perennial pools and low discharge streams

Hancock Gorge: A Small gorge exhibiting a network of narrow canyons (Figure 1.5c)

Knox Gorge: A deep gorge hosting a steady flowing low discharge stream(Figure 1.5a) .

Joffre Falls: A significant waterfall feature at the head of Joffre Gorge (Figure 1.5b).

Kalamina Falls: A small waterfall feature at the Head of Kalamina Gorge

Dales Gorge: A large gorge hosting some of the most visited features inclduding; Fortescue Falls, Fern Pool and Circular Pool.

Banjima Pool: A small isolated pool nearby Marandoo Orebody.

Mindthi Spring: A very low discharge spring outcropping on a river bank east of Marandoo Orebody

Figure 1.5 Gorges of Karijini left to right a) Knox Gorge b) Joffre Falls c) Hancock Gorge.

1.5 Local Climate and Hydrology

1.5.1 Climate

The Pilbara Region has a semi-arid climate dominated by two distinct seasons (wet summers and dry winters). These are influenced by two air masses over the region, the Indian Tropical Maritime air moving in from the west or north-west, and the tropical continental air from the inland (ANRA, 2008). In the summer months (November to February) the average maximum temperature is often over 40^0C, while during the winter months it falls to about 25^0C (Figure 1.7).

Average rainfall over the area ranges from about 200mm to 350mm (60 year record), although rainfall may vary widely from the average from year to year. Most of this rain falls between December and March, but can continue through until June. Distinct dry periods are observable predominantly between August and November. The average yearly evapotranspiration (about 2,500mm) exceeds average yearly rainfall (ANRA, 2008). Average rainfall near Marandoo is approximately 400mm (BOM,2009) and is characterised by frequent, low-intensity events related to localised thunderstorms and tropical upper air disturbances, however there are also rare high-intensity events associated with tropical cyclones (Beckett, 2008).

Tropical cyclones occur in the area, usually between January and April, with a frequency of about seven every decade. The rainfall from these events contributes 40% - 60% rainfall to the region during intense precipitation events (ANRA, 2008). These high-intensity events often cause over 100mm of rain within 24hours (Beckett, 2008) which can produce significant surface flow that may recharge the aquifers in the region and cause significant erosion (Figure 1.6).

Figure 1.6 Surface water flooding in the Pilbara after Cyclone Steve, 2000. (Source: Bureau Of Meteorology)

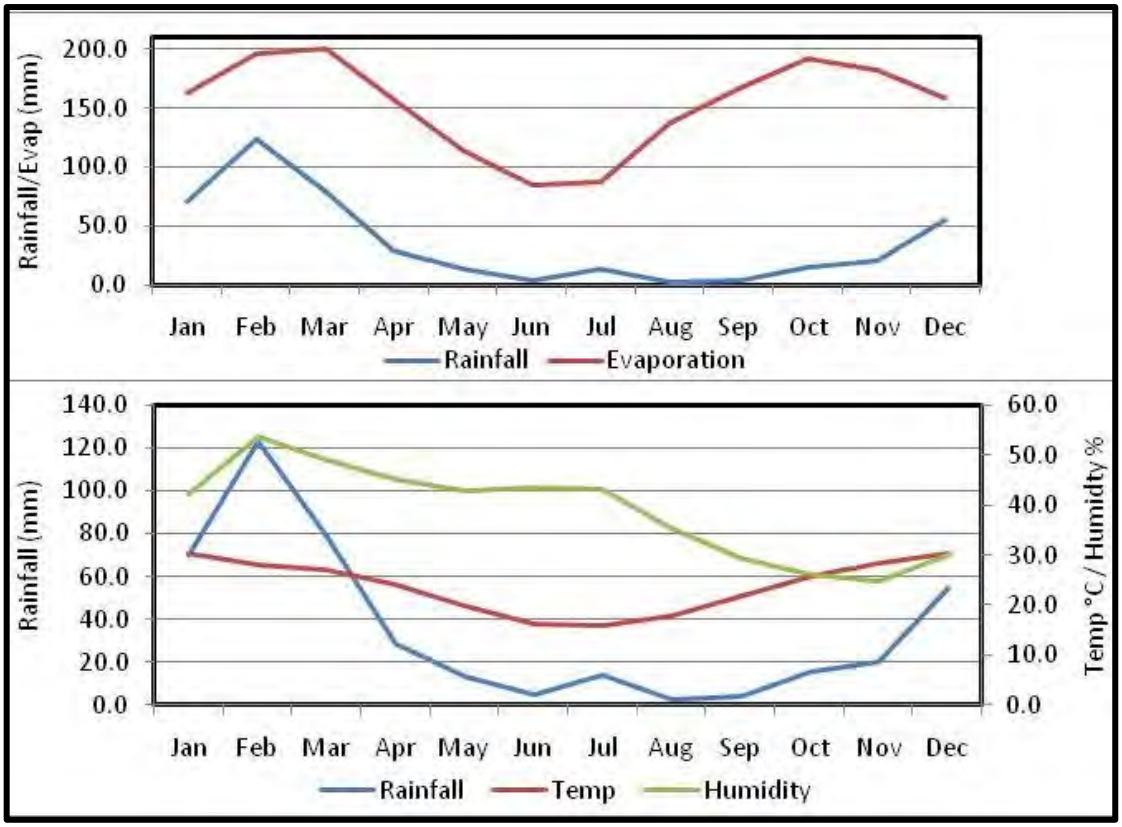

Figure 1.7 Average annual variation in climatic parameters (1999-2006)

1.5.2 Hydrology and Catchment Morphology

The local hydrology is affected by a prominent east-west ridge of the Hamersley Range which divides Marandoo Mine and KNP (Figure 1.8). Rainfall that occurs either side of this will enter a different aquifer system.

Rainfall that falls on the **north** side of the ridge will be collected by a number of catchments ranging in size from 12km^2 – 350km^2 (Figure 1.3). The morphology of each catchment is defined by the resistant BIF ridges that create the significant topography in the area (Figure 1.8) Each catchment is lined with alluvial tertiary sediments, the result of constant erosion. Incision by streams has cut down to the new base level creating deep gorges which provide the location for groundwater discharge to occur.

For the majority of the year, surface water flow in the KNP is relatively low as it is derived completely from base flow. However, a feature of catchments in the Pilbara is their variable rate of surface discharge. Significant stream flow is generated for short periods after intense

rainfall (DEC, 1999). The catchments of the KNP all eventually drain into the Southern Fortescue River.

Rainfall that occurs on the **south** side of the ridge will fall on the Mount Bruce flats (Figure 1.8) which are an internally draining system. Surface water outflows from these flats only occur during extreme rainfall events. When it does occur, surface water will drain in the Ashburton River via Turee Creek.

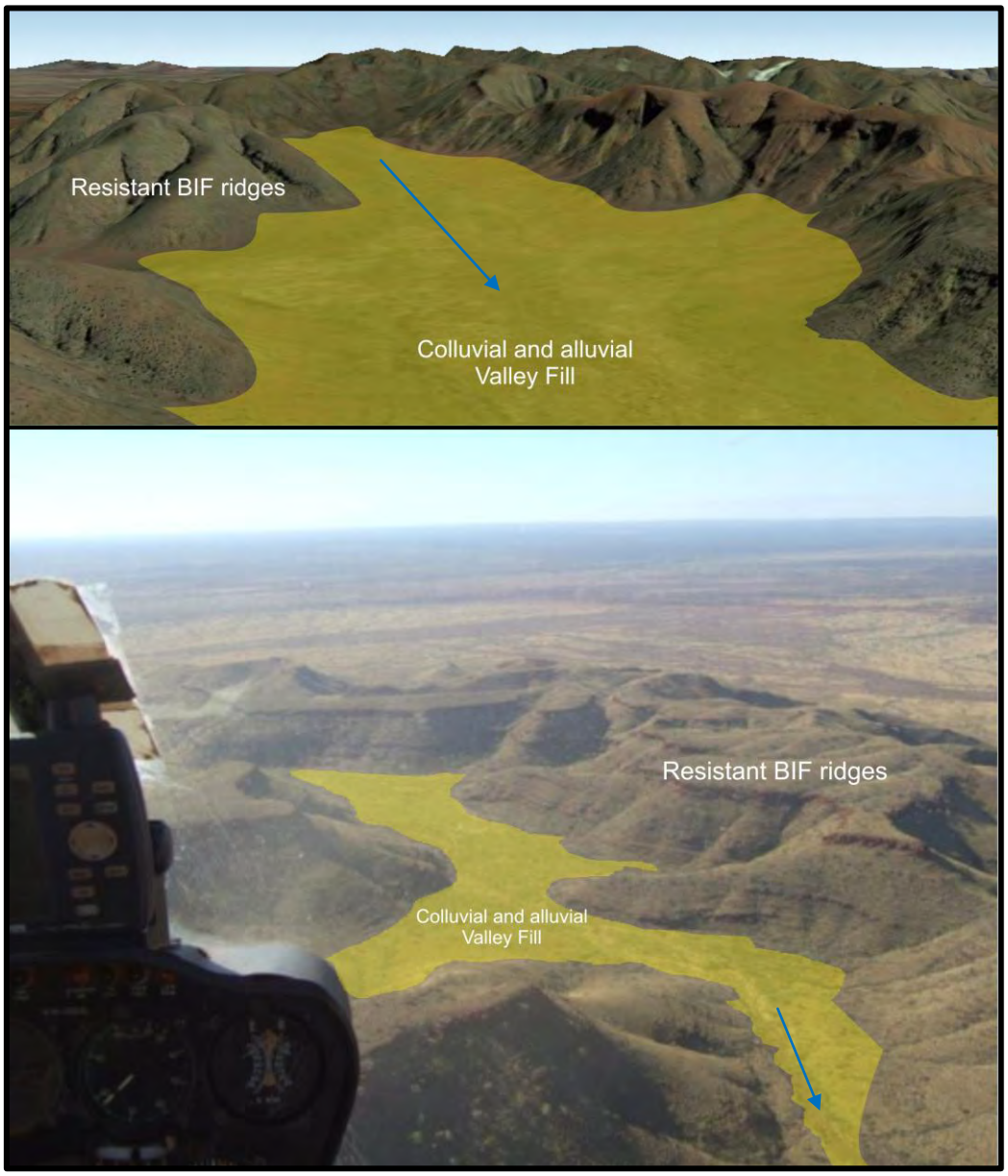

Figure 1.8 Top: Google Earth DEM showing a typical catchment morphology. Bottom: Aerial photo emphasising the stratigraphic relationship between the resistant BIF ridges and the valley fill, also the hydraulic gradient of the catchment is shown by the blue arrow (photo: Pippa Gardner)

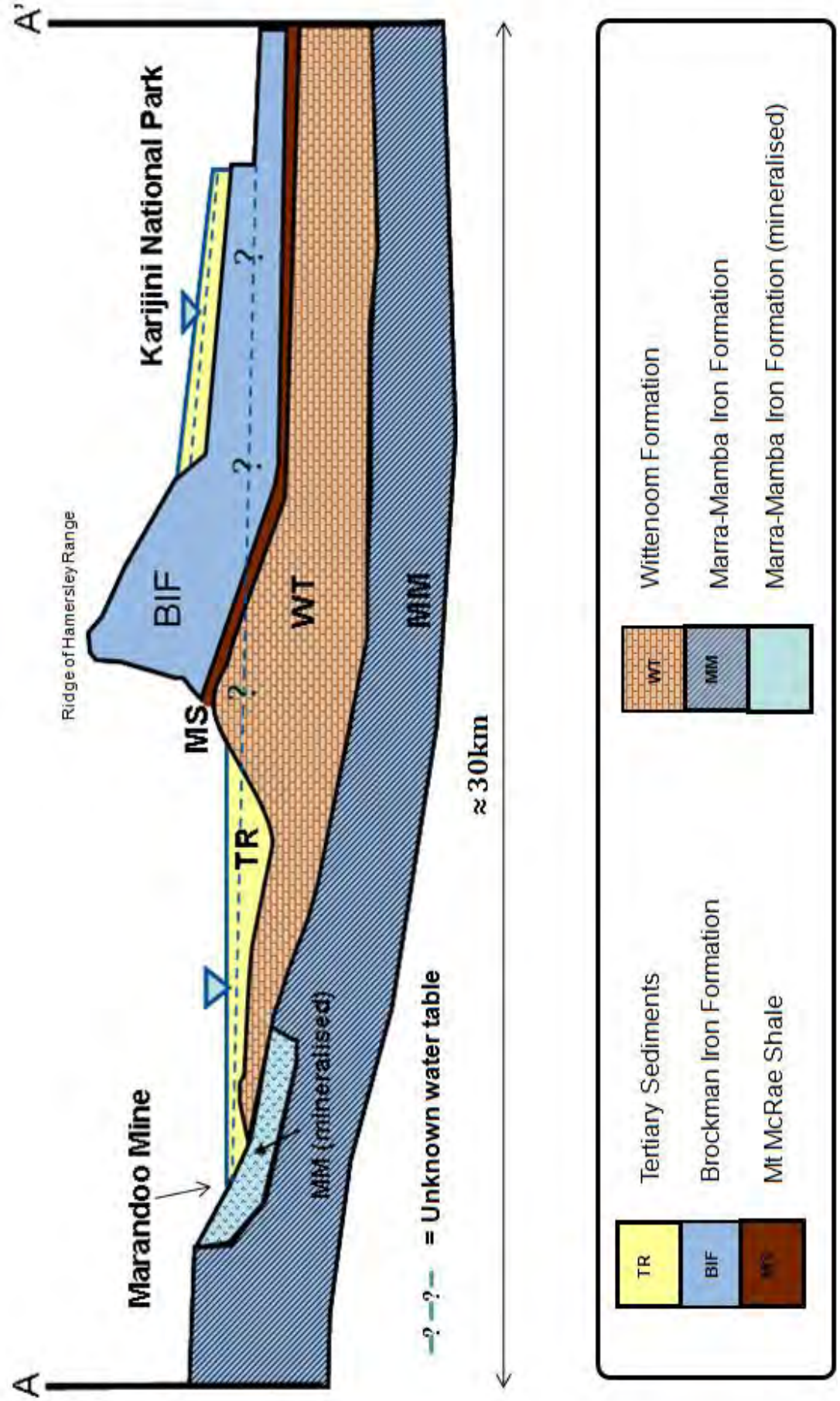

Figure 1.9 Schematic cross section of the local hydrogeology for the study area (A = South Side A' = North Side) See trace on Figure 1.10

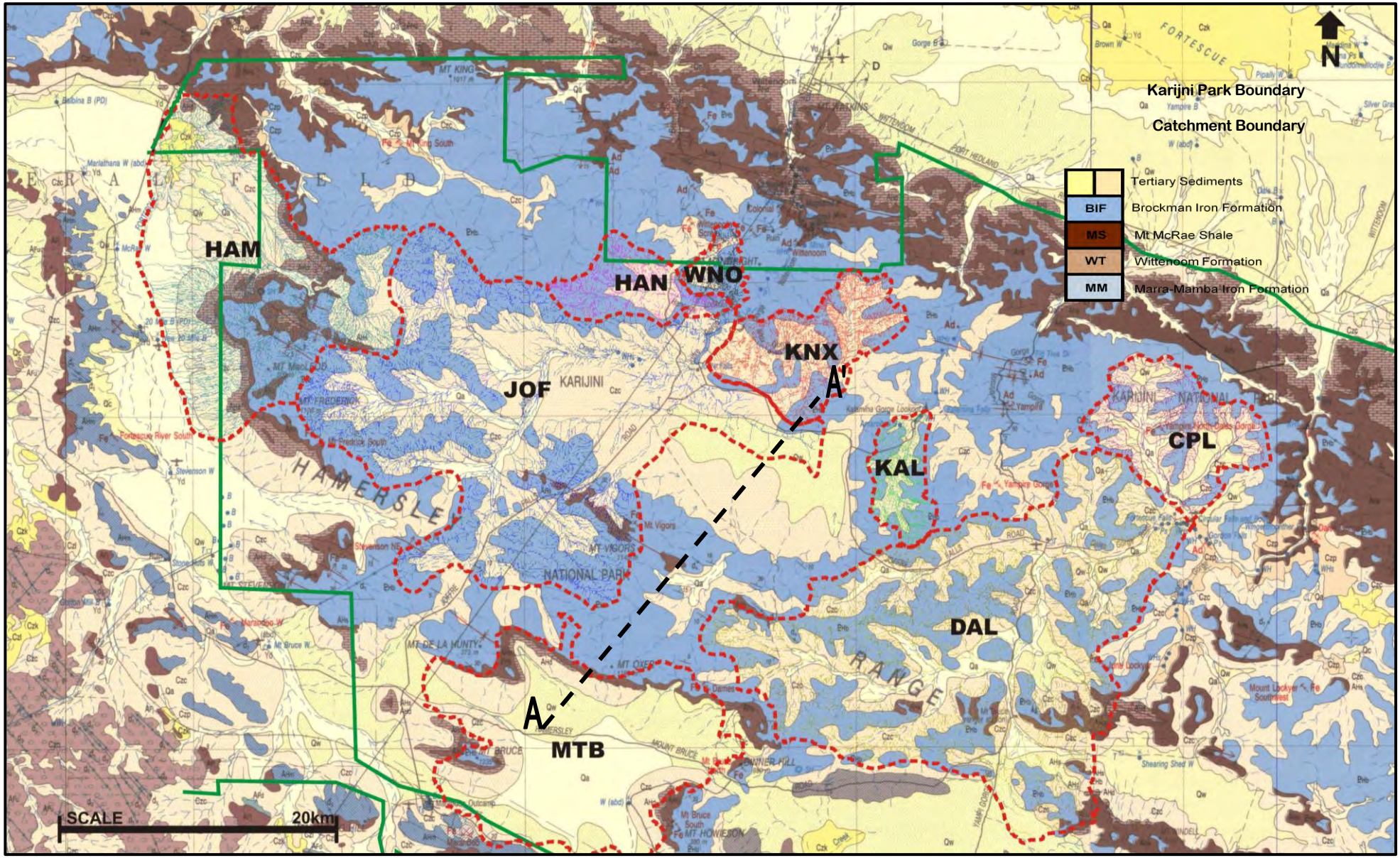

Figure 1.10 The Geology of the catchments within the Study area (HAM = Hamersley Gorge; JOF = Joffre Falls; HAN = Hancock Gorge; WNO = Weano Gorge; KNX = Knox Gorge; KAL = Kalamina Falls; DAL = Dales Gorge; CPL = Circular Pool; MTB = Mount Bruce Flats

1.6 Regional and Local Geology and Hydrogeology

1.6.1 Regional Stratigraphy

The geology of the study area (Figure 1.10) is comprised of a succession of Achaean to Lower Proterozoic rocks from the Hamersley Group. The group consists of various metasedimentary rocks including banded iron formations, inter-bedded with minor felsic volcanic rock and intruded dolerite dykes (Johnson and Wright, 2001). These units have all been deformed, uplifted, weathered and eroded over a prolonged period to form the current landscape. The stratigraphic relationship of the units from the Hamersley Group are shown in (Figure 1.11):

1.6.2 Marra- Mamba Unit

The Mara-Mamba Iron Formation is widely distributed across the province, extending with almost continuous outcrop along the entire northern front of the iron province for more than 480kms. The member outlines main geologic structures and is an invaluable marker horizon. However within the study area the unit has limited outcrop.

The unit exists in both mineralised and unmineralised forms (section 1.7.1.4) which each have unique physical and chemical properties. The total thickness is around 230m. The formation is formally divided into three members. The lowermost Nammuldi Member contains chert-rich BIF and thin discrete shale bands. The middle MacLeod member contains BIF, chert and carbonate with numerous interbedded shales. The uppermost unit Most Newman member comprises BIF with interbedded carbonate and discrete shale bands. The mineralised section of the Marra-Mamba unit contains the iron rich ores and is therefore the location of Marandoo Mine. The Marra-Mamba is the oldest unit relevant to this study (Thorne and Tyler, 1997).

1.6.3 Wittenoom Formation

The Wittenoom Formation is a succession of marine sediments. The formation is 150m thick, and consists of dolomite, chert and dolomitic shale. The lower part of the formation is generally composed of well-bedded grey to bluish grey crystalline dolomite (Simonson, Hassler and Schuble, 1995). Chert and shale intercalations are more abundant towards the upper part. Minor folding is a common feature of the Wittenoom Dolomite. Significant karstic terrain is thought exist within the Dolomite. The Wittenoom Formation outcrop within the study area is limited to a thin band on the .

1.6.4 Mount Sylvia Formation

The Mount Sylvia formation (33m thick) includes three thin, but remarkably persistent, beds of jaspilite with interbedded dolomitic shale. The three jasilite members are prominent along the escarpments of the Hamersley Range and can be followed continuously for many kms. They are excellent marker beds and help define the base of the Brockman Iron formation.

The uppermost jaspilite bed is 5m thick and defines the top of the Mt Sylvia Formation. It exists over most of the Hamersley province with little change in either thickness of lithology. The two lower jaspilite members are thinner and contain a higher proportion of greenish white banded chert than the uppermost unit. The chert as jaspilite beds are separated by blocky calcareous shale/dolomitic intercalations which weather rapidly to give smooth concave slopes from which the jaspilite beds stand out as prominent low cliffs.

1.6.5 Mount McRae Shale

The Mount Mc Rae Shale is about 90m thick and its limits are sharply defined by the overlying Brockman Iron Formation and the uppermost jaspilite of the Mount Sylvia Formation at the base. The formation includes shale, siltstone and dolomitic shale and thin beds of jaspiliite and chert. The shaley sediments offer low resistance to erosion and in cliff sections they weather to concave slopes with white outcrops. Exposures are rare and the

formation is often masked with a veneer of jaspilite scree from the overlying Brockman Iron Formation (BRF).

1.6.6 Brockman Iron Formation

The Brockman Iron Formation is the thickest and most widely exposed formation of the Hamersley Group. It conformably overlies the Mount McRae Shale. This unit has an unmineralised (BIF) thickness of about 620m. Bedding is normally regular and laterally persistent, but pinching and lensing of the beds have been observed. It is divided into four members consisting of shales, BIFs and minor mineralisation. The Dale Gorge Member consists of alternating microbands of Shale and BIF which persist throughout the entire Hamersley Province. The Whaleback Shale comprises shale, BIF and chert. The Joffre Member contains dominantly BIF with minor thin shale bands. The Yandicoogina Shale member consists of interbedded chert and shale with locally intruded dolerite. The jaspilite of this formation has a high resistance to erosion and therefore the Brockman Iron Formation forms many of the prominent hills of the Hamersley Range (Figure 1.8).

1.6.7 Tertiary Sediments

During the Tertiary period paleo-topographic weathering and erosion occurred. This has resulted in the unconformable deposition of various terrestrial clastic and chemical sediments, including coarse-grained clastics, clays, calcrete, geoethite and silicrete. These sediments now infill the major drainage systems within the area. The sediments are well indurated but still exhibit high porosity.

The stratigraphic column below shows the major units within the Hamersley Group. In the study area Tertiary sediments over lie the Brockman Iron Formation (BRF), however in other areas of the Pilbara subsquent Banded Iron formations and Volcanics exist younger than the BRF.

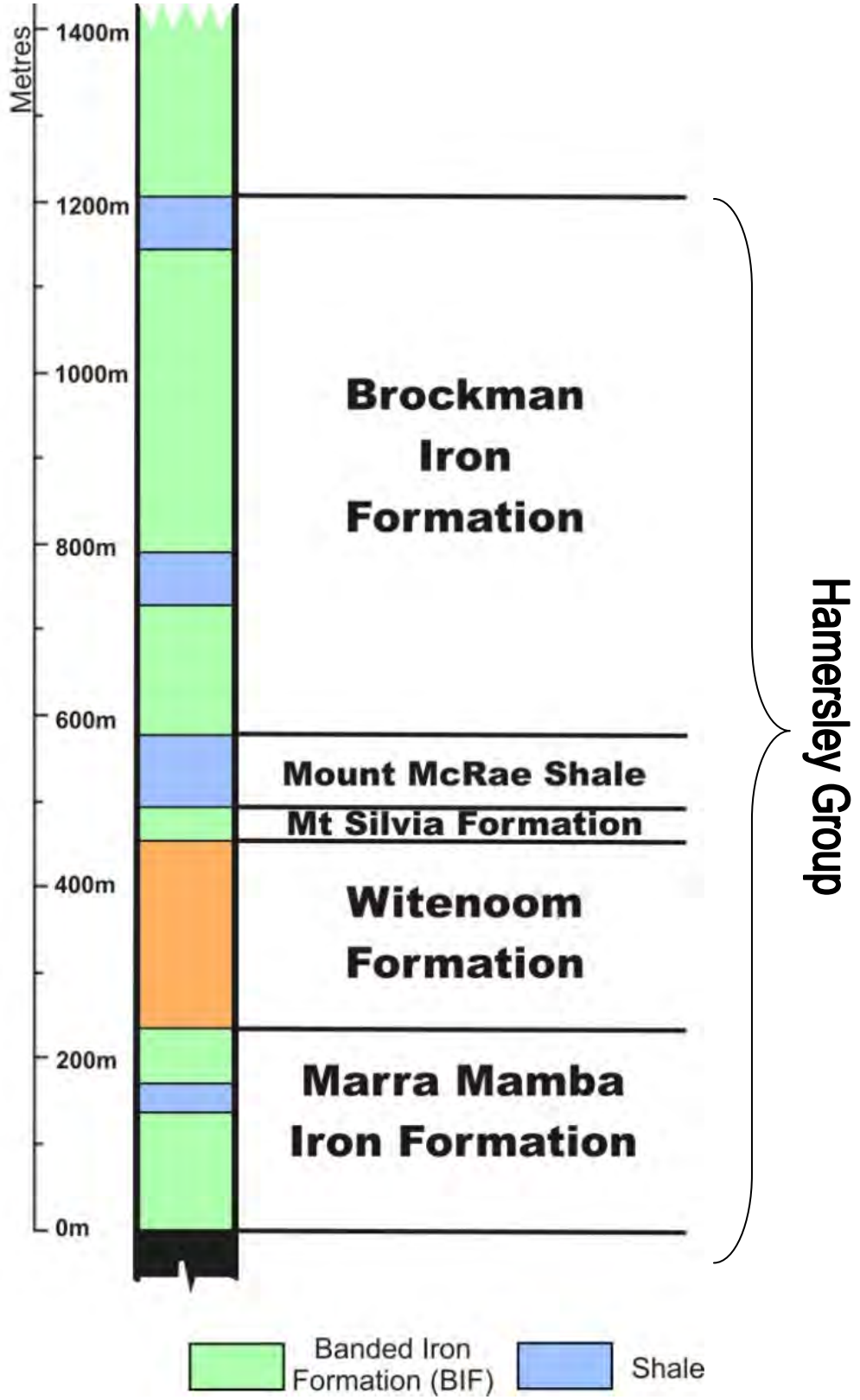

Figure 1.11. Stratigraphic column of the Hamersley Group which outcrops in the study area

1.7 Hydrogeology

The local hydrogeology follows closely the main geologic units. The sedimentary relationship of each unit is shown in (Figure 1.12), Marandoo Mine is located in the highly permeable mineralised section of the Mara Mamba Iron Formation (MM), which is overlain by the Karstic Wittenoom Formation (WF) and the relatively impermeable Mount McRae Shale. These are overlain by the low permeable Brockman Iron Formation (BRF). All units have been subsequently eroded to form the permeable Tertiary sediments (TR) which line the main drainage channels and form local aquifers in the study area. The description of these aquifers follow below and is summarised in Table 1.1.

1.7.1 Aquifer Types in the Study Area

1.7.1.1 Tertiary Aquifer (TR)

The TR aquifers consist of alluvium and colluvium which are shallow and tend to be unconfined. The alluvium is often clayey with inter-bedded sand and gravel lenses, whereas the colluvium comprises cobble-sized detritus within a clay matrix. Chemical deposition has also formed calrete horizons thought to be associated with relict groundwater tables. The thickness of Tertiary material is highly variable (1-50m). Groundwater is contained in the primary porosity of the clastic sediments (K = <1000 kL/day).

Vertical recharge is thought to occur rapidly through calcrete “sink holes” at the surface. The water then travels radially outward (Liquid Earth, 2005). There is thought to be a hydraulic connection with the underlying Brockman Iron Formation aquifer in the KNP and Mara-Mamba aquifer at Marandoo mine site, particularly where the basement is weathered and fractured (Woodward-Clyde, 1995). As the Tertiary alluvial and colluvial sediments are generally associated with major drainage channels, the aquifers are very local and the surface extent of the sediments can be assumed to the aquifer extent (Figure 1.8).

1.7.1.2 Mineralised Mara Mamba (MM) and Wittenoom Formation (WF)

Underlying the Tertiary sediments (in the mine area) is the Wittenoom Formation (WF) and the Mara Mamba (MM) formation. These Proterozioc sediments comprise the deep aquifer. There is no head difference between the two units so they are therefore grouped as one (Liquid Earth, 2005). The high permeability of the MM aquifer is derived from jointing, fractures and mineralisation, which is where the silicates are stripped from the banded ion formation and vugs develop. This creates a variable groundwater yield ranging from 50 to 1800m^2/day (Youngs, 2006).

The Wittenoom Formation is characterised by significant porosity and karstic features that can develop due to the dissolution of dolomite via percolating groundwater (Balleau, 1972), particularly where over lain by Tertiary cover. The hydraulic conductivity (K = <2000kL/day) is dependent on the interconnectivity of the karsts.

1.7.1.3 Unmineralised MM and Brockman Iron Formation (BRF) aquifers

Underlying the Tertiary sediments in the Karijini National Park is the Brockman Banded Iron Formation. This unit exhibits very low primary porosity and therefore generally no groundwater exists. This low hydraulic property of the rock is emphasised by observations that there is an absence of seepage from most of the gorge walls in the KNP, which are comprised of Brockman Iron Formation.

In certain locations the hydraulic conductivity of this unit is increased where secondary porosity occurs due to fractures, joints and weathering. Groundwater occurs here due to downwards percolation from surficial sediments and from direct infiltration at fracture outcrops. In certain locations groundwater can be seen to seep from gorge walls (Section 4.6)

Figure 1.12 illustrates the types of aquifers that are thought to exist within the Hamersley Province

1.7.1.4 Mineralisation Process.

As discussed previously, when BIF is mineralised its physical and chemical properties are altered. It is important to understand these changes to understand the local hydrogeology.

The mineralisation process is known as Supergene Enrichment and only occurs in selective locations. At these locations the iron content of the BIF is increased due to the action of groundwater percolating through the bedding planes and joint fractures. It also requires the presence of artesian pressure and sufficient oxygen.

These conditions result in the oxidation of the Magnetite (Fe_3O_4) to Fe_2O_3 and the silicates, carbonates and other low fe-minerals are leached out and replaced by geoethite (FeO(OH). The physical changes consist of a thinning of the BIF due to the dissolution/replacement and the development of a secondary porosity (Groves et al, 1994). This in turn dramatically increases the hydraulic conductivity of the BIF from around <500 to <2000kL/day.

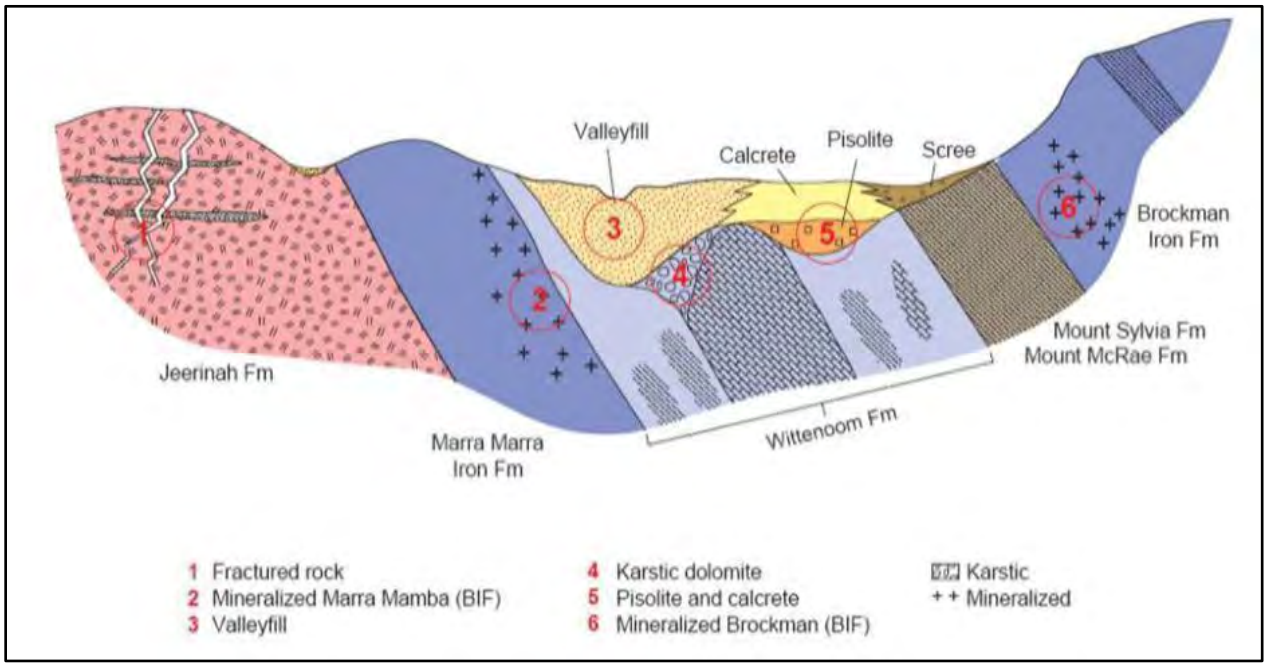

Figure 1.12. Schematic cross section of Pilbara groundwater occurrence (from Johnson and Wright, 2001)

Geological Formation	*Thickness*	*Geological Character*	*Hydrogeological Character*
Quaternary			
Recent Sediments	<10m	Alluvials, colluvials, scree, talus, outwash fans, Clays	**Moderate K (<1000 kL/day)** Localised unconfined aquifers
Tertiary			
Alluvial & Colluvim (TR)	0-100m	Calcrete Canga, pisolites	**Moderate to High K (1500-5000kL/day)** Local aquifers associated with drainage lines
Early Proterozioc			
Brockman Iron Formation	Up to 620m	Shale, Chert and BIF	**Generally Low K (<500kL/day)** (apart from along fracture joints and in weathered zones)
Archean			
Mt McRae Shale	< 120m	Shales, siltstones	**Very Low K** May restrict connection with underlying aquifers
Wittenoom Dolomite	< 150m	Zones of: Shale, Mudstone, Siltstone, Dolomite with minor BIF and chert bands	**Zones of High 2° K (<2000kL/day)** From along fractures and kartsic features. Often a highly productive aquifer
Marra-Mamba Iron Formation *1) Mineralised BIF (Marandoo Orebody)*	40m	Iron ores of haematite, limonite goethite (derived from enrichment of BIF)	**High K (<2000kL/day)** Voids and fissures created during mineralisation create high porosity
2) Unmineralised BIF	< 180m	Chert, jaspillite, banded iron formation	**Generally Low K (<500kL/day)** No 1° K but 2° K is developed from along fracture joints and in weathered zones

Table 1.1 Summary of hydrogeologic units (Source: Johnson and Wright, 2001 and Youngs, 2006)

1.7.2 Local Hydrogeoloic Characteristics of study locations

1.7.2.1 Karijini National Park

The groundwater of the KNP occurs primarily in the Tertiary aquifers and in fractured sections of the BIF. The Tertiary sediments comprise loosely consolidated alluvium, colluvium and indurated chemical (calcrete/goethitic) sediments that act predominantly as sedimentary aquifers (Dodson, 2008). The BIF has zones where it is fractured and jointed and also where bedding planes have parted. These zones may support groundwater flow which is assumed to be sourced from downward percolation via the unconfined Tertiary aquifers.

The gorges of KNP are incised up to 60m into the Brockman Iron Formation (BRF) bedrock with near vertical walls, and have a thickness (0-10m) of Tertiary material on the top. Groundwater is thought to be primarily discharged into the gorges from the contact between the BRF and Tertiary Sediments and where topography intersects the water table. Generally, there is no groundwater discharging from the walls throughout the entire length of the gorge. There are a few cases where groundwater can be seen to seep out of the fractured BIF, in other cases this seepage is indicated by white carbonate precipitate staining on the walls of the gorge (Section 3.2.4 and 4.7).

1.7.2.2 Marandoo and Southern Fortescue Borefields

As discussed before, there are two main borefields associated with this study (Marandoo Mine and Southern Fortescue Borefields). At Marandoo two primary aquifers are recognised. The water table (shallow aquifer) occurs in the tertiary aquifer near the base of an extensive calcrete layer. The calcrete is underlain by a sequence of tight reactive clays commonly 40m in thickness. The clays act as an effective aquitard across most of the Marandoo area. Beneath the clays lie Tertiary clays and gravels of Mara Mamba origin. The Tertiary clays and gravels commonly incorporate a calcrete horizon. Under lying the tertiary sediments are the Wittenoom Dolomite beneath the Mount Bruce Flats and Mara Mamba on the mine lease. These units are commonly group as referred to as the deep aquifer (Liquid Earth, 2005)

The Southern Fortescue borefield is located in the catchment of the Southern Fortescue River. The borefield is located in a thick Tertiary sequence of alluvial, colluvial and other deposits formed from secondary diagenetic process (calcretes, ferricretes etc) that has developed in a palaeovalley. The valley has eroded down to the underlying Wittenoom Formation. These Tertiary aquifers host a large amount of water with hydraulic properties commensurate to that of the MM aquifer (Kendrick, 2006).

1.8 Summary

Rio Tinto are investigating the potential of de-watering their Marandoo Mine to extract ore from below the water table, Marandoo Mine is however located within Karijini National Park. For dewatering to progress it must be shown that there will be no negative impacts on the water features of the National Park.

A Hydrochemical study has been undertaken to investigate groundwater flow dynamics in attempt to determine whether there is any hydraulic connection between Marandoo and Karijini National Park.

The study area is located within a succession of Achean and Lower proterozioc sediments including Banded Iron Formations, Shales and Dolomites. These are unconformably overlain by Tertairy terrestiral sediments which line the valleys and main drainage routes.

The hydrochemistry of various locations was determined including 8 gorges within Karijini National Park and two Major borefields (including the Marandoo Production Borefield). At Marandoo Groundwater is located in the shallow tertiary aquifer and in the Deep aquifer associated the Mineralised Banded Iron Formation and Karstic Dolomite. In Karijini National Park ground water is thought to exist in the saturated tertiary sediments and fractures within the underlying Banded Iron formation Bedrock.

Chapter 2

Use of Environmental Tracers in Hydrogeological Studies

2.1 Introduction

The geo-chemical composition of water is modified as it travels from the atmosphere to the hydrosphere and through the lithosphere. The way the water interacts with its surroundings imparts a unique chemical signature which can be used as a diagnostic tool to understand the history of the water (Fetter, 1994).

This section presents and discusses the theory of methods used for tracing groundwater in this study. Four methods were used:

(i) Major ion geochemistry: The relative concentrations of individual major ions are modified by the water-rock interactions throughout the flow path of water.

(ii) Stable Isotopes: The relative proportions of $\delta^{18}O$ and $\delta^{2}H$ are modified by thermodynamic processes in the atmosphere and they give an indication of the recharge location.

(iii) Chlorofluorocarbons (CFCs): CFC dating is based on comparing the CFC concentration in a sample to a known global atmospheric concentrations over the last half century.

(iv) Carbon- 14: ^{14}C is a radioactive isotope and its concentration decreases with time. It can therefore be used to date groundwater.

2.2 Major Ions

2.2.1 Background

Natural waters always contain small but variable amounts of dissolved solutes. These are derived from interaction between the water and various solids, liquids and gases as the groundwater makes its way from its recharge area to discharge area (Kehew, 2001). More than 90% of the dissolved solids in groundwater can be attributed to eight ions: Na^{+}, Ca^{2+},K^{+},Mg^{2+}, SO_4^{2-},Cl^{-},HCO_3^{-} and CO_3^{2-} (Fetter, 1994). Concentrations of the solutes in different groundwater samples can vary significantly as a function of the mineralogical composition of the aquifers through which the groundwater flows. Therefore the geochemical composition of groundwater can be analysed to determine the path the water has travelled.

The three zones that effect the chemical composition of the water are the (i) atmosphere, (ii) the unsaturated zone, and (iii) Saturated water in the aquifer:

In the Atmosphere, water is in a gaseous state as vapour until the saturation humidity of the air mass becomes too great and it precipitates as rainfall. Rainfall can be expected to be saturated with respect to any gases present in the atmosphere, it also obtains solutes from naturally occurring particulate matter such as terrestrial dust and oceanic salts transported by Aeolian processes (Hem, 1985). Seawater is injected into the air as waves break; the droplets evaporate leaving an aerosol particle which is transported via winds until it is dissolved again by rain. The concentration of the individual ions in the rainfall, will therefore match the ratio found in seawater.

Precipitation that does not runoff or evaporate will infiltrate into the unsaturated zone (Vadose Zone). This zone may consist of soil (which has formed by *in situ* weathering or collection transported material) or unweathered bedrock. As water passes through this zone it acquires solutes from dissolution or partial dissolution of minerals (Drever, 1988). Soil organisms and organic material release soluble organic compounds to the water which

create weak organic acids (Equation 2.1) that accelerate the breakdown of minerals. As rainfall infiltrates the unsaturated zone, evapotranspiration processes will increase the concentration of the dissolved solutes in the water (Allison 1982; Abdalla 2007).

As water leaves the soil zone and passes into the groundwater system, organic complexes decrease (as a result of less organic material) and the concentrations of common major ions increase as a result of water-rock reactions (Equation 2.2). The relative concentration of each ion will depend on the host aquifer mineralogy and the residence time of the water in the aquifer before discharge down gradient.

2.2.2 Factors influencing the concentration of the individual major ions in natural groundwater

The water samples in this study were analysed for the following major Cations: Sodium, Potassium, Calcium, Magnesium and Anions: Chloride, Bicarbonate, Sulphate and Bromide. The following is a summary of the factors that determine ion concentrations in groundwater:

- ***Sodium (Na^+)*** exists in igneous rocks more abundantly than in sediments, however the main source of Na^+ to the hydrologic cycle is from the ocean as air-entrained particles. The Na^+ concentrations in rainfall therefore decrease inland. Na^+ can also be sourced from evaporate sediments, which form in arid conditions where total evaporation of a solution occurs. When Na^+ is brought into solution, it tends to remain in solution, and there are no important precipitation reactions that can maintain low sodium concentrations in water (Hem,1985). Na^+ is however readily retained by adsorption on mineral surfaces, especially such as clays which have high cation-exchange capabilities (Feth, 1964). This is a common process that reduces the Na^+ concentration in groundwater systems.

- ***Calcium (Ca^{2+})*** is introduced into the hydrologic cycle during precipitation/dissolution processes of carbonate minerals in the aquifer and also dissolution of atmospheric dust particles. The Ca^{2+} concentration of water will

increase significantly due to water-rock interactions in the groundwater system. Ca^{2+} can be expected to exist in water that has been in contact with calcium rich rocks. Ca^{2+} is an essential component of igneous rocks being dominant in chain silicates pyroxene, amphibole, and feldspars. However the concentration is generally low due to the slow rate of decomposition of most igneous-rock minerals. In sedimentary rocks Ca^{2+} exists in carbonates (aragonite, calcite, dolomite) and minerals including gypsum ($CaS0_4.2H_20$), anhydrite($CaSO_4$) and fluoride(CaF_2). In detrital rocks eg. sandstone, calcium carbonate is commonly present as a cement between particles (Hem,1985).

- ***Magnesium (Mg^{2+})*** is an alkaline-earth metal and has only one oxidation state of significance in water chemistry, Mg^{2+} (Hem, 1985). Mg^{2+} exists in igneous rocks as a major constituent of the dark-coloured ferromagnesian minerals (Olivine, pyroxenes, amphilboles and biotite). Sedimentary forms of Mg^{2+} include carbonates such as magnesite and hydromagnesite, the hydroxide brucite, and mixtures of magnesium with calcium carbonate. Dolomite has a definite crystal structure in which calcium and Mg^{2+} ions are present in equal amounts. Mg^{2+} occurs in significant amounts in most limestones, the dissolution of this material brings Mg^{2+} into solution, but is not readily reversible. Therefore, the precipitate that forms when a solution has come in contact/reacted with a magnesian limestone may be nearly pure calcite. Mg^{2+} concentration would tend to increase along the flow path of a ground water undergoing such processes, until a rather high [Mg]:[Ca] ratio is reached (Wigley, 1973). Water passing through dolomite should dissolve equal molar amounts of calcium and magnesium (Hem, 1985)

- **Chloride (Cl^-)** exhibits a unique chemical behaviour in natural water, it is relatively inert compared with other major ions that exist in groundwater. Cl^- ions do not significantly enter into oxidation or reduction reactions, form no important solute complexes with other ions unless the Cl^- concentration is extremely high, do not form salts of low solubility, are not significantly adsorbed on mineral surfaces, and

play few vital biochemical roles (Hem, 1985). Cl^- is therefore a conservative ion in groundwater environments and the circulation of Cl^- ions in the hydrologic cycle is largely through physical processes. For this reason Cl^- is commonly used as a reference ion in major ion analysis. Cl^- has lower concentrations in many rock types than the other major constituents of natural water - Ca,Mg,K,Na,Br etc. (Kresic, 2007), However in arid conditions it can dominate. In arid conditions Cl^- can become concentrated in groundwater due to a process known as cyclic wetting and drying:

During a dry period continuous evaporation occurs until all the solutes have been deposited, this is followed by a wet period where partial re-solution occurs. During the dry period the water is evaporated from near surface water in alluvium pores. The resulting deposit may be an efflorescent crust on the surface, or disseminated salts just below the surface. The deposit depends on the salinity of the initial water. The solutes are deposited as a solid phase during evaporation (in the order predicted by the Hardie-Eugster model, 1978 (Drever, 1988) and then re-dissolved in order of solubility. The end result of this evaporation-solution cycle is water that contains more ions that precipitate as highly soluble salts , but fewer of the less soluble ions (Drever, 1988).

The above process requires the complete evporation of the solution as Cl^- will not precipitate untill saturation with respect to Halite (NaCl) is reached (NRC, 1987). Therefore in most case Cl^- is sourced from meteoric water which has had air-entrain Cl^- dissolved in it.

- ***Sulphate*** is a complex ion that displays a strong tendency to form further complex species (Hem, 1985). SO_4^{2-} is abundant in water with low salinity, and its concentration can be highly dependent on its relative saturation with $CaSO_4^-$ (Polevoy, 2003). Sulphates can be introduced to the groundwater system via water-rock reactions. The oxidation of Pyrite and other metal sulphides are the main source of natural SO_4^- in groundwater. The oxidation of these metals in a mining environment (acid mine drainage) is an important environmental concern to be

considered. Dissolution/Precipitation of $MgSO_4$ and $CaSO_4$ is also a common process of increasing or decreasing SO_4^{2-} concentration. Sulphate precipitates tend to occur here extreme evaporation is occurring.SO_4^{2-} concentration in natural water is also reduced by sulphate reduction, often occuring in stagnant pools due to microbial reduction.

- ***Potassium and Bromide*** are generally minor constituents of groundwater. Potassium is most abundant in sedimentary rocks (potassium rich minerals are found in silicate rocks, and in clays). Although potassium is abundant in these sources, it is unusual to observe high K^+ concentrations in groundwater. This is because potassium-rich minerals have a high degree of stability and are therefore not easily dissolved in weathering reactions (Hem, 1985). Also pottasium is readily up-taken during transpiration by plants (Polevoy, 2003).

  Bromine is always present as the bromide ion in natural water and has a similar chemical behaviour to chlorine. It is readily concentrated by Evapotranspiration processes.

2.2.3 A closer look at Carbonate Dissolution and Precipitation

Carbonate minerals are among the most reactive minerals found at the earth's surface. Dissolution of calcite and dolomite, the two most common carbonates exposed to weathering, represents 50% of the chemical denudation of the continents (Stumm, 1992). $CaCO_3$ and other carbonates are also important minerals in aquifers resulting in the addition of Ca^{2+} Mg^{2+} and HCO_3^- , the more abundant ions present in natural waters (Wollast and Mackenzie, 1983). The ions are generally introduced to the groundwater through dissolution of carbonate aquifer minerals.

Neutral water exposed to CO_2 in the atmosphere will dissolved CO_2 equal to the partial pressure. The CO_2 will react with H_2O to form H_2CO_3, a weak acid (Equation 2.1), and the resulting solution will have a pH of about 7.7 (Fetter, 1994). CO_2 is also introduced to

groundwater during plant respiration. Calcite and dolomite are soluble is acid solution, and therefore will be dissolved by the infiltration water, according to the following equations:

$$H_2O + CO_2 \leftrightarrow H_2CO_3 \quad \textbf{(Formation of Weak-Acid)} \quad \textbf{Equation 2.1}$$

$$CaCO_3 + H_2CO_3 \leftrightarrow Ca_{2+} + 2HCO_{3-} \quad \textbf{(Dissolution/Precipitation of Carbonate)} \quad \textbf{Equation 2.2}$$

The reaction (Equation 2.2) is reversible, therefore if the reaction goes to the right (as a result of High CO_2) dissolution of carbonate occurs. If the reaction goes to the left (depletion of CO_2), precipitation will occur (Mazor, 1991).

Dissolution of carbonates can only occur if the solution is thermodynamically under saturated, and pH is an important variable affecting the saturation ratio. At very Low pH, the rate of dissolution is very fast, whereas within the pH range of natural waters, the rate of dissolution (and precipitation) or carbonate minerals is less (Stumm, 1992).

When groundwater is saturated in calcite the water will have a corresponding partial pressure of carbon dioxide. It is at this stage, a 'closed system' with respect to carbon dioxide. When this water reaches a groundwater discharge zone it is brought in contact with the atmosphere and subsequently introduced to a 'open system' with respect to the CO_2 (Krauskopf and Bird, 1995). Consequently, the water will equilibrate with the new conditions. The groundwater may then become undersaturated or supersaturated with calcite, depending on the new partial pressure of carbon dioxide in the discharge area. Most commonly in groundwater will discharge into a zone of lower partial pressure then the above equation will go to the left and precipitation will occur. This brings about the formation of generally white precipitates observed around groundwater seepage, and can also form depositional features such as stalagmites and stalagtites.

Temperature plays a large role in the solubility of $CaCO_{3.}$ In pure water, an increase in temperature will decrease the solubility of calcite, opposite to the behaviour of other rock forming minerals (Krauskopf and Bird, 1995). This is because the solubility of CO_2 decreases with temperature increase. Generally the solubility of carbonates is influenced much more

by this change in solubility of CO_2 than by the temperature dependence of mineral solubility itself.

2.2.4 Evapotranspiration

In Field conditions it is not possible to separate evaporation from transpiration totally. Hydrochemical studies are generally only concerned with water loss, therefore the two terms can be grouped as "Evapotranspiration" (Fetter, 1988).

Dissolved salts which are transported by infiltrating water into the root zone will be concentrated by evapotranspiration (Eriksson, 1985). If recharge areas are covered in vegetation, then the abstraction of water from the soil is almost entirely by root uptake and transpiration of plants. During this process some cations and anions may be taken up by plant roots and absorbed into the plant. The chloride ion however is not up taken by plant roots (Drever, 1994) and therefore the concentration of Chloride in the soil is roughly inversely proportional to the water content of the soil (Eriksson, 1985). In an semi-arid environment where evapotranspiration greatly outweighs precipitation, ionic concentrations in soil water can be very high.

2.2.5 Sulphate Reduction

Sulphate reduction is also a common process that reduces the concentration of SO_4^{2-} ions in natural water. Under anaerobic conditions sulphate-reducing bacteria (prokaryotes) reduce sulphate to hydrogen sulphide (Mackenzie, 2005) by using organic compounds or hydrogen as electron donor, as shown below:

SO42- + 2 CH2O → H2S + 2 HCO3- **Equation 2.3**

The oxidation of electron donors produces alkalinity (e.g. HCO_3^-) which neutralizes acidic water:

HCO3- + H+ → CO2(g) + H2O **Equation 2.4**

Therefore, the location where sulphate reduction is occurring can commonly be identified by low SO_4^{2-} concentrations and a high pH. Anaerobic conditions can commonly occur where discharge rates are low and water can become stagnant.

2.2.6 Other Removal Processes for major species

Ion exchange is another process in which the concentration of ions can be reduced. This process is common where clay minerals exist. Clay minerals in fresh water have their exchange sites occupied generally by calcium, however when these clays encounter more saline water the Ca^{2+} can be replace by Na^{+}, K^{+} and Mg^{2+} (Drever, 1988). This process is particularly important in the removal of Na^{+} and therefore the subsequent increase in Ca^{2+} in solution.

Another process is the precipitation of sulphates such and anhydrite. This can occur due to a combination of high calcium concentrations and elevated temperatures. Along with sulphate reduction these two processes are the main removal processes of sulphate from solution.

2.2.7 Units of concentration

Knowing the amount of dissolved solute within a water sample is an important factor in numerical analysis of groundwater systems. There are several different systems of concentration in use:

2.2.7.1 Mass Concentrations (mg/L and ppm)

The most common method of expressing the concentration of solutes in a water sample is to use mass concentrations. This expresses the weight of the solutes that is contained within a volume of solution, common units are mg/L or µg/L. Parts per Milllion (ppm) is another mass unit system which is commonly used by laboratories, ppm relates the mass of the solutes to the mass of the solution. The two systems are related by density (ρ) of the solution, if the density of the solution approximates that of pure water (ρ=1.0kg/L) then ppm and mg/L will be equal.

2.2.7.2 Molar concentrations

This unit system expresses the amount of moles present in a litre of water, units are generally mol/L or mmol/L. Conversion from mass units to molar units is achieved by using the molecular weight of the solute. Molar concentration is often used when investigating the dissolution of a compound into its individual solutes eg. Dissolution of carbonate into Mg^{2+}, Ca^{2+} and HCO_3^-.

2.2.7.3 Equivalents

The equivalent unit system takes into account the valence of ionic solutes. An equivalent is determined by multiplying the molar concentration by the charge of the ion. Positive and negative charges must balance, therefore the sum of the equivalent weight of each solute in a solution will equal zero. Equivalents are commonly expressed in the form of milli-equivalents per litre (meq/L) and are used when investigating inter-elemental relationships and to check the accuracy of the laboratory analysis. Before any chemical analysis is undertaken, a cation-anion balance is usually undertaken. This is achieved by converting all the concentrations to meq/L and comparing the sum of the anions versus the cations. If the sum of the cations is not within a few percent of the anions, then either there is a problem with the chemical analysis or a major ionic species has not be identified. Freeze and Cherry (1979) recommended that 5% is a reasonable limit for accepting the analysis as valid.

2.3 Presentation and Analyses of Geochemical data

Groundwater chemistry can be displayed in many ways, each method has its own advantages and disadvantages. It can therefore be common practice to use two or more methods to best investigate and display data. The following are common was of graphically displaying hydrochemical day

2.3.1 Schoeller Diagram

A Schoeller Diagram is a two axis plot, with concentrations in meq/L versus each individual ion. The concentration of the ionic species in a sample is displayed as a single line. This allows a visual comparison to be made between waters of different composition

, many water types can be plotted on the same graph.

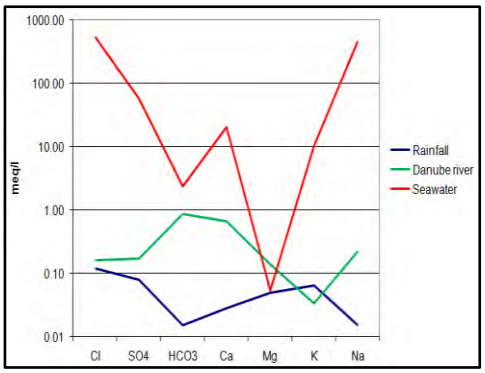

Figure 2.1. A typical Schoeller Diagram

2.3.2 Stiff Graph

The stiff graph is another way of quickly comparing different water samples. A polygonal shape is created from four parallel axes which extend either side from a vertical zero axis. Ion concentrations are plotted along the horizontal axes, each of which represents an individual ion (Cations on the left and Anions on the right of the vertical axis).

When the data is plotted the points can be connected to form a polygon. Each different water type will have a unique polygon and therefore different water types can be quickly compared visually. The polygons produced from Stiff graph can be added to a map at appropriate locations to effectively illustrate spatial variation in water types. This method is very usefull as a simple way of displaying hydrochemical data to an audience with limited experience in hydrochemistry. It is also often used as a starting point to identify patterns in the data that warrant further indepth investigation

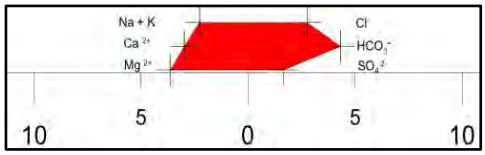

Figure 2.2. Example of Stiff graph

2.3.3 Piper Plot

The piper plot is another tool for classifying water types based on the locations of plotted points in the ion triangles (Figure 2.3). The classes of water types are known as chemical facies. Examples of chemical facies names are the calcium-bicarbonate and the sodium-chloride facies. In either the cation or anion composition falls within the region of no dominant type, the facies name would be mixed cation or mixed anion (Kehew 2001). Piper plots are used as a quick illustration of the variation in water chemistry over the whole study area. They are ideal for identifying any clustering that may exist in the data which indicates a common trend.

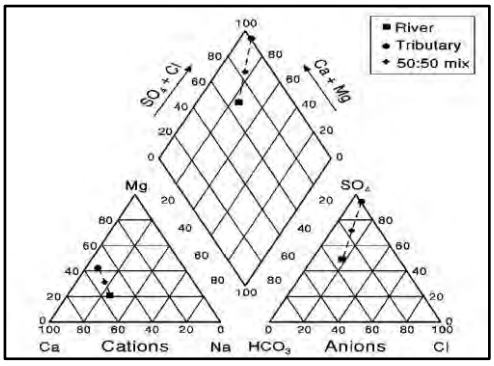

Figure 2.3. Example of a Piper plot

2.3.4 Inter-Element relationships.

To further understand the physical and chemical factors that are effecting the concentration of the solutes in natural groundwater, inter-elemental relationships are often investigated. This is generally achieved by plotting two species against each other on a binary diagram. The variation of the ratio between two ion species across the study area can highlight any chemical or physical processes that are occurring. The following are common relationships that are often used within hydrochemistry and their application:

2.3.4.1 Magnesium:Calcium Ratio

The ratio between Mg^{2+} and Ca^{2+} is commonly explored in groundwater systems that contain any type of carbonate. It is used as a method of indicating the length of a flow path through an aquifer, and therefore its residence time in the aquifer (Cardenal, Benavente et al. 1994; Edmunds, Cook et al. 1987; Kloppmann, Dever et al. 1998; Lo´pez-Chicano, M. et al. 2001; Musgrove and Banner 2004; McIntonsh and Walter 2006).

The variation in the two species concentration is proposed to be due to differences in dissolution kinetics. Observed increases in groundwater Mg/Ca ratios with increasing residence time may be due to progressive water-rock interaction processes such as the incongruent dissolution of dolomite, and the recrystallization of calcite (Wigley, 1973; Plummer 1977; Lohmann, 1988). This is especially relevant in an arid environment like the Pilbara where the recrystallization of calcite is commonly observed as white precipitate staining where groundwater seepage exists.

2.3.4.2 Cation:HCO3-

A high concentration of HCO_3- in solution indicates CO_2-induced interactions with the aquifer matrix, and by balancing the HCO_3^- ions with the cations also in solution, this may indicate the types of minerals present. When minerals are dissolved in a solution they separate into their different ionic species. If a mineral of the 2:1 molar form is being dissolved, then you would expect the ionic species to exist in solution at the same 2:1 ratio (if there are no other solute sources). For example, if pure calcite ($CaCO_3$) was dissolving then it is expected to observe Ca^{2+} and HCO_3^- at a molar ratio of 2:1 (Drever, 1988). This

concept is often illustrated by a plot of Ca^{2+} against HCO_3^- with a 2:1 line regression line plotted. The data that correlates to this line can be assumed to be from a calcite source (Rosen 1998; Dindane 2003).

2.3.4.3 Ion:Cl

Many factors can determine the chemical composition of groundwater, one of these factors is the degree of evaporation that has occurred on the body of water. Of the eight principal solutes that dominate the chemistry of natural waters, chloride is usually conserved over the widest concentration range, because ion exchange is minor and Cl- remains in solution until halite saturation. This makes Chloride a very reliable indicator of the degree of evaporation (Eugster and Jones 1979).

The chloride concentration should reflect the amount of evaporation that has taken place since the water was precipitated as rainfall. If the concentration of any other ion is plotted against chloride concentration, the extent to which the concentration of that ion is controlled by evaporation becomes apparent, and the degree to which other processes are influencing its concentration can be seen (Drever, 1988; Jones, 1977)

If no water-rock interaction or precipitation is occurring, then progressive evapotranspiration should cause data to show an increasing linear relationship. The data is compared to A Sea water dilution line (SWL), this line defines the ionic ratios of seawater which is retained in sea-water aerosols. Rainwater that contains these aerosols should show similar ionic ratios to seawater (Khider, 2004).

2.4 Stable Isotopes

2.4.1 Background

Stable Isotopes are naturally occurring and are routinely used in groundwater investigations for determining recharge sources when complimented with geochemistry and physical hydrogeology. The stable isotopic composition of water is modified by a number of processes as it moves through the hydrological cycle. These processes will be unique to a location, therefore the water that is recharged into the aquifer in a particular environment will have a characteristic isotopic signature. The signature then serves as a natural tracer for the provenance (source) of the groundwater.

The most commonly used isotopes in hydrogeology are Oxygen (^{18}O) and Hydrogen (^{2}H), commonly referred to as Dueterium (δD). This is because they are fundamental components of a water molecule and therefore move at the same rate as the water.

Stable environmental isotopes are measured as the ratio of the two most abundant isotopes of a given element. For example, the most abundant oxygen isotopes are ^{16}O and ^{18}O. ^{18}O has a terrestrial abundance of 0.204% whereas ^{16}O represents 99.796 of terrestrial oxygen (Clark and Fritz, 1991). Because the variation in isotopic abundance is often relatively small, stable isotope ratios are reported relative to a standard as δ values, in units of parts per thousand.

The apparent ratio is usually calculated using gas source mass spectrometry. Isotopic concentrations are expressed as the difference between the measured ratios of the sample and a known reference over the measured ratio of the reference. The ratio is expressed in per mil (‰) deviations from a standard. These deviations are written δD for deuterium, and $\delta^{18}O$ for ^{18}O:

$$\delta D‰ = \left((D/H)_{sample} - (D/H)_{SMOW} \right) / (D/H)_{SMOW} \times 1000 \qquad \text{Equation 2.5}$$

$$\delta^{18}O‰ = \left((^{18}O/^{16}O)_{sample} - (^{18}O/^{16}O)_{SMOW} \right) / (^{18}O/^{16}O)_{SMOW} \times 1000 \qquad \text{Equation 2.6}$$

Water with less deuterium than the standard has a negative δD, and water with more deuterium than the standard has a positive δD, and this is the same for ^{18}O (Mazor,1991).

The commonly used standards is "Vienna Standard Mean Ocean Water (VSMOW), which is a universal standard defined by the IAEA, a recalibration of Craig's 1967 SMOW that was derived from a mixture of ocean water from around the globe. Samples are either analyzed at the same time as this reference standard, or with some internal laboratory standard that has been calibrated relative to the international standard.

2.4.2 Global and Local Meteoric water Lines

Most fresh waters in the world have deuterium and oxygen-18 ratios that plot against each other along a straight line. This line is known as the 'Global meteoric water line' (Figure 2.4), and it defines the relationship between ^{18}O and ^{2}H in worldwide fresh surface waters. The line was produced during a study by Harmon Craig published in 1961. Craig (1961) collected 400 samples from many parts of the world and determined a relationship for the deuterium and oxygen-18 concentrations in natural meteoric waters. The relationship is defined by the equation shown in Figure 2.4.

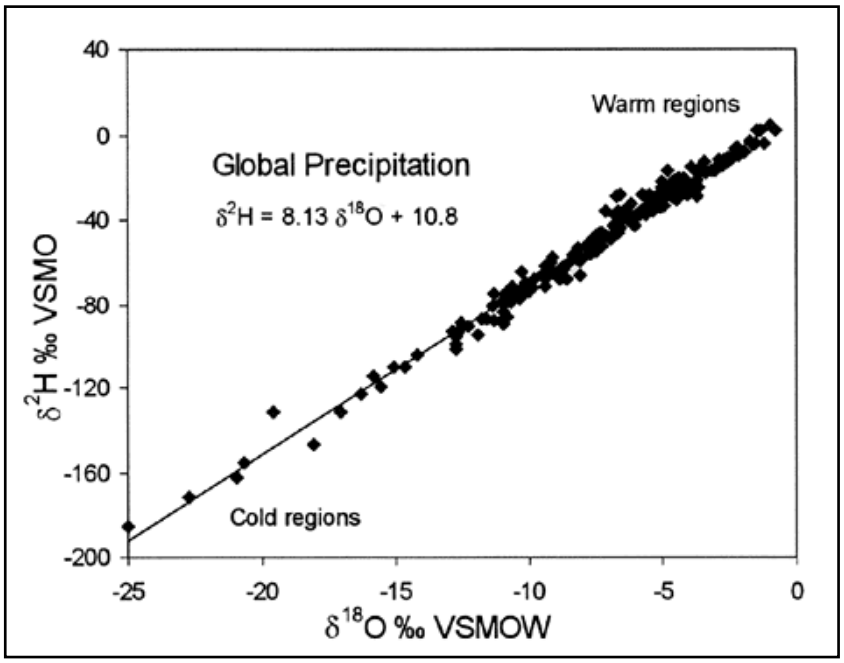

Figure 2.4. The Global Meteoric Water Line (Clark and Fritz 1997, p. 37, as compiled in Rozanski et al. 1993, modified by permission of American Geophysical Union).

The global meteoric water line is used as a method of comparing local precipitation. A "local meteoric water line" can be determined from individual rainfall events at the study location. A local line will differ from the global line in both slope and deuterium intercept. This variation illustrates local processes that are occurring to the rainwater, and these processes are dependent on variations of local climatic and geographic parameters. The processes are known as effects.

2.4.3 Fractionation and Local Effects

The process that makes it possible to use stable isotopes in groundwater provenance studies is fractionation. The variation in molecular weight of a water molecule is dependent on the relative atomic weights of the hydrogen and oxygen Isotopes. Heavy water ($^{2}H_{2}{}^{16}O$), has a mass of 20 compared to normal water ($^{1}H_{2}{}^{16}O$), which has a mass of 18. The difference in mass of the water molecules creates differences in thermodynamic reaction rates which leads to the isotope partitioning or *fractionation* described by Urey (1947). The difference in reaction rates will leave a body of water 'enriched' in the heavy isotopes. So therefore water from different sources, that has been subjected to different kinetic conditions, can be distinguished by variations in isotopic ratios.

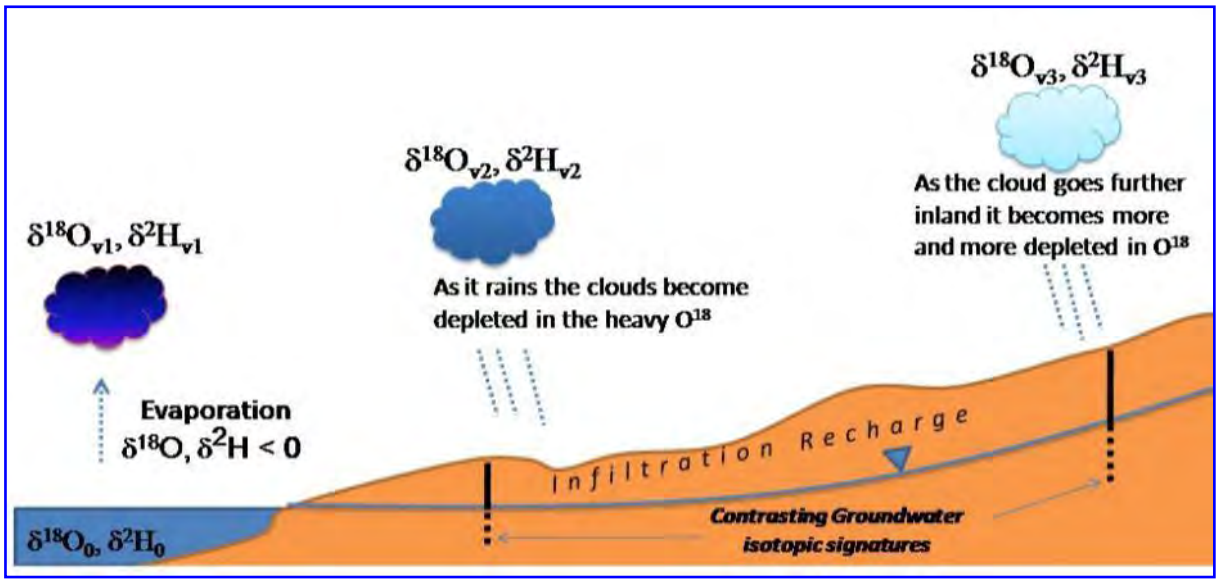

Figure 2.5 Example of Continental effect on the groundwater isotopic signature (v = vapour)

When studying groundwater recharge, local variations in the isotopic composition of the precipitation must be clearly understood. Local topography, climate and hydrologic features can cause characteristic variations to the isotopic composition of the precipitation which can be used to indentify recharge source.

2.4.3.1 Temperature Effect

Temperature is a major parameter that determines the isotopic values of precipitation. The composition of precipitation depends on the temperature at which the oceanic water is evaporated into the air and, even more importantly the temperature of condensation at which clouds and rain or snow are formed (Mazor, 1991). The large variation of isotopic composition of groundwater is largely due to the temperature effect.

2.4.3.2 Amount Effect

The amount of rain that falls during a single event will also have an effect on the isotopic composition of precipitation. The heavier the rain event- the more negative are the δD and ^{18}O values. This is due to: 1) Lower ambient temperatures cause the formations of clouds with lighter composition and lower temperatures also cause heavier rains.2) Falling rain may undergo evaporation which therefore enriches the precipitation in heavy isotopes. This effect is less severe both when ambient temperatures are low, and when the amount of rain is large.

2.4.3.3 Continental Effect

During the condensation of atmospheric vapour the liquid phase (i.e. rain droplets) gets isotopically enriched, the vapour phase gets isotopically depleted. However, the amount of vapour in a cloud is limited. As this process continues, the isotopic signature of the vapour, and consequently of the condensed water, is continuously changing. This leads to a situation in which both the precipitation and groundwater are found depleted with respect to heavy isotopes as the distance away from the coast increases (Figure 2.5). This effect can often be masked by other effects, e.g temperature effect and altitude effect (Mazor, 1991).

2.4.3.4 Altitude Effect

Orographic precipitation will occur when a vapour mass encounters topographic relief. At higher altitudes where temperatures are colder, precipitation will be isotopically depleted. For ^{18}O the depletion varies between about -0.15 to -0.5‰ per 100m rise in altitude with a corresponding decrease of about -1 to -4‰ for ^{2}H (Clark and Fritz 1997) . This effect is very useful in hydrogeological studies, as it distinguishes groundwaters recharged at high altitudes from those recharged on the plains.

2.4.4 Isotopic Studies in Arid Regions

Groundwater that has been recharged in an arid region may have some unique characteristics. The water tends to have a long residence time within the zone of evaporation. This will cause the water to become enriched in heavy isotopes, and it may plot off the meteoric water line relative to water that recharges during flood events (Cook and Herczeg, 2000). Therefore it can be possible to establish the rate that recharge is occurring in an arid region by observing whether the isotopic signature of groundwater shows significant enrichment.

Another isotopic method to quantify recharge rates is detailed by Cook and Herczeg (2000): In arid regions where recharge is intermittent, the isotope method has potential for estimating recharge rates. Precipitation will wash down the evaporativley enriched water down through the soil profile. The isotopically enriched water mixes with regional water and the bulk water is shifted away from the meteoric water line. The recharge rate should be proportional to the magnitude of this shift.

2.5 Chlorofluorocarbon Dating of Modern water

2.5.1 Basic Method

Determining the age and proportion of the modern water recharging an aquifer can give a good indication of factors such as, recharge, flow rates and storage volume. These factors are important when considering the vulnerability of a water resource to change from other influencing factors such as dewatering. The modern input of groundwater to the KNP aquifers was determined with the use of Chloroflourocarbons.

Chlorofluorocarbons (CFCs) are man-made organic compounds that have been produced for a range of industrial and domestic purposes since the 1950s (Busenberg and Plummer, 1992). The concentration of CFCs in the atmosphere has increased between the 1950s-1990s. As CFCs are soluble they enter the groundwater systems during recharge. Their concentrations in the groundwater therefore record the atmospheric concentration when the water was recharged, and this gives an indication of the age of the water.

CFCs exist as three different molecules: CFC-11 (CFCl3), CFC-12 (CF2Cl2) and CFC-13 (C2F3Cl-3), with relatively long residence times in the atmosphere (44, 180 and 85 years respectively) (Cunnold et al. 1994).

Production and release of CFCs to the atmosphere rose rapidly through the 1970s and 1980s. Annual production of CFC-11 and CFC-12 peaked in 1987 at 382,000 and 425,000 metric tonnes, respectively, and that of CFC-13 peaked in 1989 at 251,000 metric tonnes (Cook and Herczeg, 2000). This peak was due to CFCs being identified as a prime contributor to stratospheric ozone depletion. Therefore in 1987, 37 nations agreed to limit the release of CFCs based on guidelines in the Montreal Protocol on substances that deplete the ozone layer. This means that CFCs concentrations are decreasing and are therefore not as effective for dating groundwater recharged after around 1990.

Apparent CFC ages are obtained by converting measured CFC concentrations in groundwater to equivalent air concentrations using known solubility relationships and

recharge temperature. The groundwater concentration is then compared with the atmospheric concentration curve to obtain an apparent CFC age.

The age of the groundwater, when based on the concentration of CFCs in the water, refers to the time elapsed since recharge and isolation of the newly recharged water from the soil atmosphere. The rate at which a parcel of water becomes isolated from the unsaturated zone air is, in part, a function of recharge rate, porosity of the unsaturated zone soil, aqueous and gaseous diffusion coefficients, and magnitude of water table fluctuations (Cook and Herczeg 2000).

Although it is often referred to as 'dating the groundwater, in actual fact the age applies to the date of introduction of the chemical substance, and not the water. Therefore the physical and chemical factors that affect the concentrations of CFCs in the aquifer must be considered. These occur both during recharge and in the groundwater environment. The accuracy of the determined age depends in part on how perfectly the CFCs are transported with the aqueous phase (Cook and Herczeg, 2000).

2.5.2 Interpretation Factors

2.5.2.1 Recharge Temperature

This refers to the temperature at the water table during recharge, affecting the solubility of the gas. Therefore it is important to know the recharge temperature when analysing sample. A recharge temperature recorded too low gives an apparent age that is too old and vice versa. An error of $\pm 2^0$ C results in an error of ±1 year for water recharged before 1970 and ±1-3 years for water recharged between 1970 and 1990 (Plummer and Busenburg 1999)

2.5.2.2 Unsaturated Zone

One of the assumptions of CFC groundwater dating is that concentrations in the soil gas immediately above the water table are in equilibrium with the atmosphere. However this assumption is not always valid, particularly if the unsaturated zone is thick (Weeks, 1982) and Cook and Solomon (1995) showed that there is a time lag associated with diffusion of these gases through the unsaturated zone. The magnitude of the lag is dependent on the

soil water content and the CFC solubility. The thickness of the zone is also very important, the thicker the zone, the more significant the gas transport process on the apparent age.

2.5.2.3 Loss of CFCs

Microbial degradation of CFCs in anaerobic environments or sorption onto organic matter causes removal of CFCs, giving modelled ages that are too old. However neither process is expected in aerobic conditions and dissolved oxygen concentration in the water can be used to assess the likelihood of these effects. CFC-11 has been found to be more susceptible to such losses than CFC-12 (Happell et al, 2003).

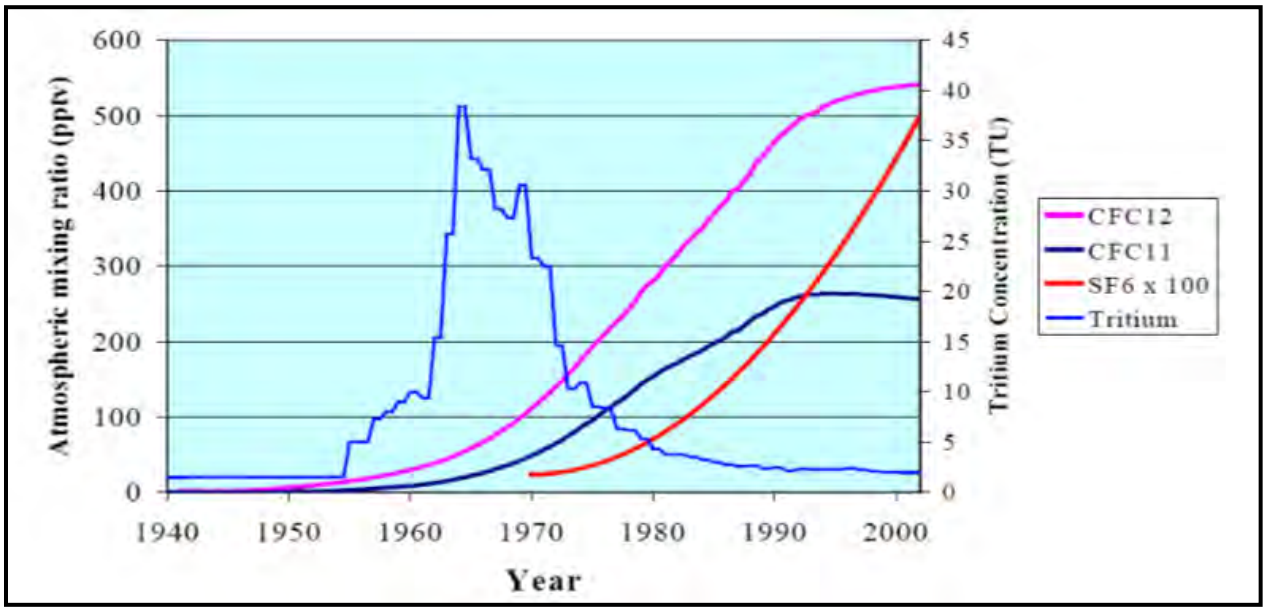

Figure 2.6 CFC concentration in the Southern Hemisphere atmosphere (Source: Stewart, 2002)

2.6 Radiocarbon Dating of Old groundwater

2.6.1 Background

Radiocarbon is the major tool for dating old groundwater. The 5730 year half-life (Libby, 1952) of ^{14}C, and the ubiquity of carbon (as organic and inorganic forms) in groundwater, makes it a potentially ideal tracer of timescales often associated with long residence times in the hydrologic cycle. The geochemistry of carbon in the groundwater system is affected by interactions with the atmosphere, biosphere and geosphere resulting in multiple sources and sinks of carbon that vary in time and space, making interpretations of water age on a basis of C-14 complex and difficult.

The radioactive isotope of carbon (^{12}C), ^{14}C, is generated by cosmic rays interacting with atoms and molecules in the atmosphere. The solar wind and the geomagnetic field of the sun and earth modulate the flux of these rays (Kalin, 2000). When the rays strike the Earth's upper atmosphere they produce thermal (slow) neutrons as they interact with atoms and molecules. These thermal neutrons react to form ^{14}C in the upper atmosphere by the reaction:

$$^{14}N_{(n,p)} \rightarrow {}^{14}C \qquad \textbf{Equation 2.7}$$

The ^{14}C is quickly oxidised to CO_2 and mixes into the lower atmosphere where it is then introduced into living biomass by photosynthesis, and into the hydrosphere by $C0_2$ exchange reactions (Kalin, 2000). Any carbon compound derived from the atmosphere since the late Pleistocene can potentially be dated by radiocarbon. Radio-carbon generally enters the groundwater system through four dominant pathways. First, formation and dissociation of carbonic acid (H_2CO_3) during gas exchange between CO_2 and surface water and groundwater with atmospheric CO_2 . Second, the biological activity of plants results in respired CO_2 in the soil zone that dissolves in water. Third, microbial utilization of organic material in the soil also produces CO_2 that dissolves in water. And finally, through dissolution of mineral phases that contains geologically young carbon (Kalin,2000).

2.6.2 Dating groundwater with Radiocarbon

Rain and surface water dissolve small amounts of atmospheric CO_2, and significantly more is added to water percolating through the soil layer from plant transpiration and decomposition of plant material. Once water reaches the saturated zone of an aquifer it is isolated from the atmosphere and its ^{14}C begins to decay. The decay occurs according to its half-life of 5730 years (Figure 2.7).

Radiocarbon ages are then determined by the direct counting of radioactive decay of the ^{14}C in either the liquid or gas phase. The atoms are counted using Accelerator Mass Spectrometry of a graphite target made from the sample carbon. The Modern activity of ^{14}C is set by convention as 13.56 decays-per-minute per gram of carbon (zero year =1950ad). Therefore, all samples which have an activity lower than this are pre-1950AD, and samples which are higher than this value are younger. This value is also considered to have an activity of 100 percent modern carbon (pmc). Radiocarbon activities expressed as percent "modern" carbon (pmc) represent the activity of carbon prior to the dilution by post-industrial 'dead' fossil fuel carbonate. For example, a carbon sample having "0 pmc" is deemed to be dead or have age beyond the limit detectable by radiocarbon dating.

Most inorganic carbon occurs as HCO_3^- (Cook and Simmons, 2000), when this ion behaves conservatively, groundwater ages can be estimated from measuring ^{14}C concentrations usually by assuming an initial activity of 100pMC, via the equation:

$$t_a = -\lambda^{-1} ln \left(\frac{c}{c_0}\right) \qquad \textbf{Equation 2.8}$$

where c is the measured ^{14}C activity, C_0 is the initial activity (100 pmc), and $\lambda = 1.21 \times 10^{-4}\ yr^{-1}$ is the decay constant for ^{14}C. If the groundwater contains only 50pmc then it will be deemed to be 5730years (Figure 2.7)

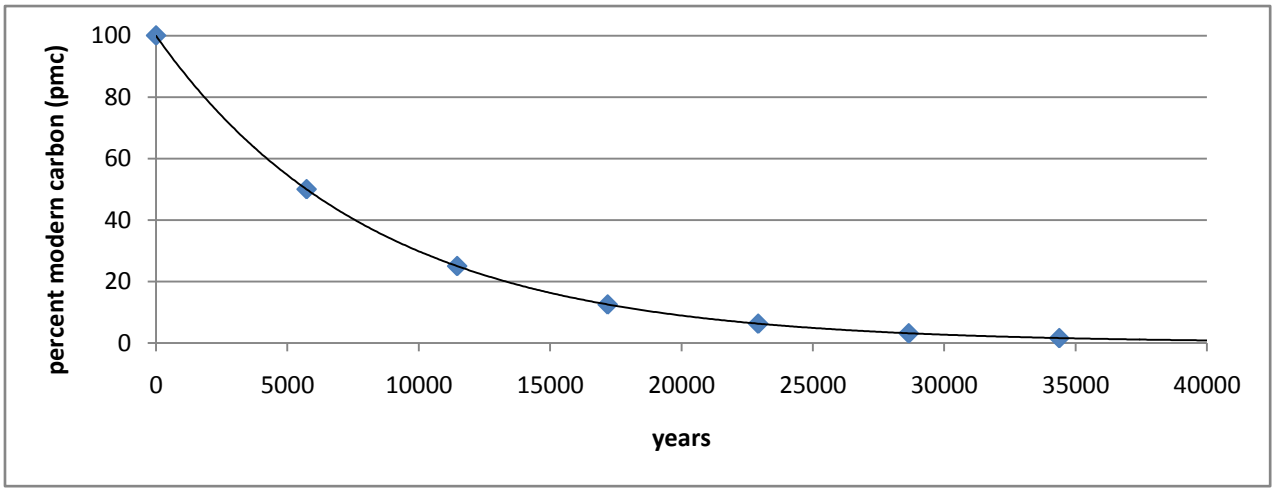

Figure 2.7. Carbon-14 decay curve (half-life 5730y)

2.6.3 Considerations when dating with Radiocarbon

The main problems associated with 14C dating are: (i) the determination of the initial C-14 value, (ii) mixture of waters of different age, (iii) diffusive admixture of CO2 from the atmosphere, (iv) dissolution of carbonates. Despite these problems 14C -age dating is widespread and yields good results in simple situations. The following outlines some methods of correcting for a number of these factors:

2.6.3.1 Radiocarbon fluctuation over geologic time

A major factor in radiocarbon dating of groundwater is being able to accurately determine a correct initial amount of percent modern carbon (pmc) in the atmosphere at the time the groundwater was recharging. However the concentration of ^{14}C in the atmosphere has not stayed constant over time. Considerable effort has therefore been made over the last three decades to accurately measure the variations of ^{14}C as recorded in annual tree rings. Therefore, for the last 24,000 radiocarbon years we can relate the radiocarbon age to actual calendric time periods (Kalin, 2000). After 1950, atmospheric thermonuclear testing doubled the amount of radiocarbon in the atmosphere. When measuring the activity of modern samples , the pmC value is used (Kalin, 2000).

2.6.3.2 Correcting for "Dead" radiocarbon signature

When carbon is sourced from another reservoir, the radiocarbon age can be affected. For example, if water flows through a carbonate aquifer dissolution of the $CaCO_3$ to HCO_3 will occur providing a carbon source to the groundwater. The carbonate source will yield a radiocarbon date which is excessively old (as most if not all of the carbon is 'dead'), therefore the ^{14}C activity in the groundwater sample will become diluted, making the apparent date older than reality. A correction is required to determine an accurate radiocarbon age.

Numerous methods can be used to correct for this error. Firstly, when carbonate does not act conservatively, measurement of the stable isotope ^{13}C and other aquifer chemistry sometimes allows corrections to be made for variations in ^{13}C activities resulting from chemical processes (Kalin, 2000). If the $\delta^{13}C$ of the carbonate material is determined, it can indicate whether it is of marine or terrestrial origin. The $\delta^{13}C$ value varies for different sources of carbon, so it can therefore be determined whether the HCO_3 ions are added from mineral dissolution or atmospheric gases.

Another correction method for determining the effects of "dead carbon" is mass balance modelling. This is where the geochemical evolution of the groundwater is quantified between two points. This can deterimine various dissolution and mixing scenarios which may introduce HCO_3 to a system which will alter the observed ^{14}C date. An example of Mass Balance Modelling Software is NETPATH By L.N. Plummer, E.C. Prestemon, and D.L. Parkhurst (2004).

2.7 Summary

Physical and Chemical processes that occur in the hydrologic cycle determine the hydrochemical composition of groundwater. This unique signature can be used to understand groundwater recharge and discharge dynamics. This study uses the Major Ion compositions, Stable Isotopic and age signature of water samples collected within Karijini Natinal Park to determine whether there is a hydraulic connection with Marandoo Mine.

Chapter 3

Collection and Analysis of Samples

3.1 Introduction

The Hydrochemical study of Karijini National Park involved the collection of groundwater, surfacewater and rock samples from numerous locations in the Karijini National Park. Data was collected both in the field and from laboratory analysis. Sampling was undertaken at Marandoo Mine and the Karijini National Park during September 2008 and May 2009. Samples were collected from 38 sites in 15 locations at a range of different sources with the aim of gaining a hydrochemical overview of the entire study area (Table 3.1, Figure 3.4).

All the water samples were collected to be analysed for Major Ion Concentrations and Stable Isotopes to understand groundwater chemical evolution and recharge-discharge dynamics. While the groundwater samples were also analysed for chloroflurocarbon and radiocarbon concentrations were collected to determine relative ages of the groundwater.

3.2 Collection of Field Data and Samples

3.2.1 Field Testing

Before samples were collected the following field parameters; Temperature, pH, electrical conductivity (EC) and salinity were measured with a TPS Handheld WP-81 pH-Cond-Salinity meter:

Temperature – The temperature of groundwater is a fundamental measurement and is required in all thermodynamic calculations and models (Clark and Fritz 1997). It is also used for correction of EC measurements and for calibrating the pH meter.

Electrical Conductivity (EC) – Electrical conductivity is proportional to the quantity of dissolved ions present in solution and can provide an estimate of the total dissolved solids (TDS).

pH – One of the most important field measurements in the pH. This is an expression of the negative log of H+ activity (ph = -log[H+]. It is fundamental to thermodynamic calculations. In natural waters pH generally ranges from (6.5 – 8).

Dissolved Oxygen (DO) – Dissolved oxygen analysis measures the amount of gaseous oxygen (O2) dissolved in an aqueous solution.

3.2.2 Surface Water samples

Surface water samples were collected from streams and pools located within the gorges of the KNP. Sample locations were generally chosen where the water body was deemed to be a fair representation of the water in the area i.e where possible, samples were not collected from stagnant ponds or locations where significant modification of the hydro-chemistry had changed post groundwater discharge. Samples were collected by rinsing the sample vessel a number of times with the water being sampled, then submerging the sample vessel and allowing the water to fill the bottle and expel all the air. The lid was then tightened while submerged to assure no interaction with the atmosphere. Samples were collected for analysis of Major Ions (500ml PET bottle) and Stable Isotopes (30ml glass McArtney Bottles).

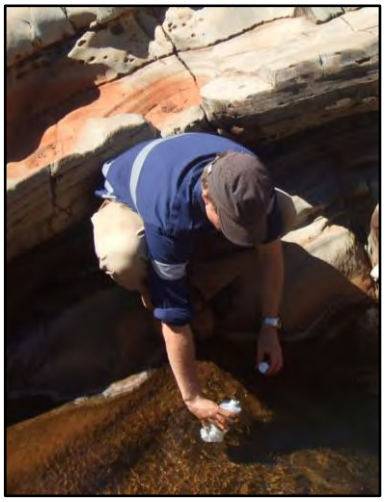

Figure 3.1 Surface water sampling

3.2.3 Groundwater samples

Groundwater samples were collected both from groundwater discharge locations and from groundwater bores. Before samples were collected from the groundwater bores, each bore was purged for an appropriate length of time (dependent on casing volume). The EC, pH and

temperature was monitored continually and the sample was collected when these values had stabilised. This ensured the chemistry of the water was representative of the aquifer and not the bore casing. The groundwater bores had a sample point from which a hose could be attached, and this was used to fill up a bucket in which the sample bottles could be submerged and filled via the method illustrated in Figure 3.2. This method ensured that fresh water from the bore was collected and there was no interaction with the current atmosphere. This is particularly important for CFCs, where any interaction with the atmosphere can dramatically alter the CFC concentration and thus affecting the age.

Samples were collected for analysis of Major Ions (500ml PET bottles), Stable Isotopes (30ml McArtney Bottles), CFCs (150ml glass bottles) and C14 (5L plastic water containers). The groundwater samples that were collected from gorge wall discharge were collected by holding the sample vessel under a continuous drip. No CFC samples were collected in these situations as significant interaction of the water with the atmosphere was occurring.

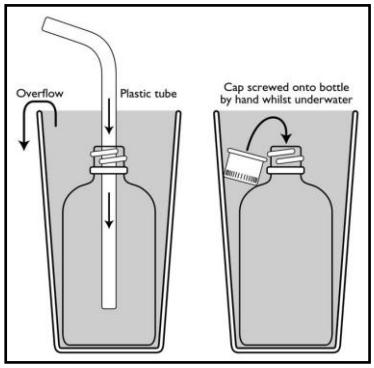

Figure 3.2. Groundwater bore sampling method (provided by SGS)

3.2.4 Solid - Samples

Solid rock samples were collected from a number of locations where water samples had also been collected. The aim was to gain extra information about groundwater evolution by determining their mineralogy using X-ray Diffraction (XRD). Samples included precipitate staining where seepage was occurring, and these samples were collected by scraping the material into a glass vial with a knife blade. A number of rock samples from the Tertiary calcrete were also collected for analysis, as these were believed to be similar to the calcretes found within the surfical aquifers in the area.

Figure 3.3 Example of precipitate staining in Hancock gorge

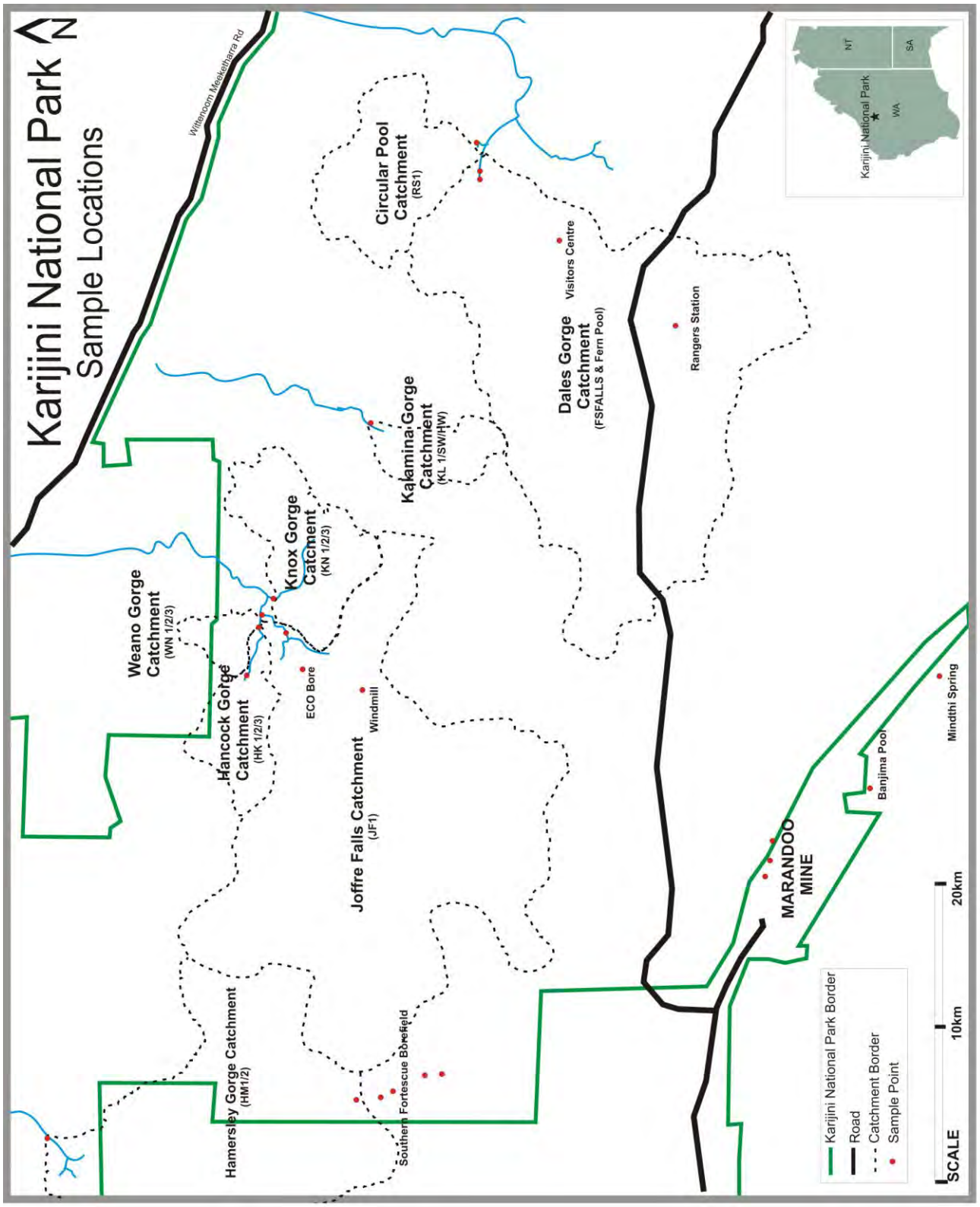

Figure 3.4 Sample Locations within the Study area. The sample location Ids are shown in brackets in each catchment.

Sample Code	Location Name	Number ID	Type of water	δD and δ18O	Major Ions	CFC	C14
SFP10	Southern Fortescue Borefield	001P	GW	O	O	O	
SFP8	Southern Fortescue Borefield	002P	GW	O	O	O	O
SFP7	Southern Fortescue Borefield	003P	GW	O	O	O	
SFP2	Southern Fortescue Borefield	004P	GW	O	O	O	
SFP4	Southern Fortescue Borefield	005P	GW	O	O	O	
SFP5	Southern Fortescue Borefield	006P	GW	O	O	O	
SFP6	Southern Fortescue Borefield	007P	GW	O	O	X	
SFP11	Southern Fortescue Borefield	008P	GW	O	O	O	
SFP12	Southern Fortescue Borefield	009P	GW	O	O	O	O
HM1	Hamersley Gorge	010P	SW	O	O	X	
HM2	Hamersley Gorge	011P	SW	O	O	X	
MR1	Marandoo Production Borefield	012P	GW	O	O	O	O
MR2	Marandoo Production Borefield	013P	GW	O	O	O	O
MR4	Marandoo Production Borefield	014P	GW	O	O	O	O
MN Spring	Mindthi Spring	015P	SW	O	O	X	
BJ Pool	Banjima Pool	016P	SW	O	O	X	
WN1	Weano Gorge	017P	SW	O	O	X	
WN2	Weano Gorge	018P	SW	O	X	X	
WN3	Weano Gorge	019P	SW	X	O	X	
HK1	Hancock Gorge	020P	SW	O	O	X	
HK2	Hancock Gorge	021P	SW	O	O	X	
HK3	Hancock Gorge	022P	SW	O	O	X	
ECO1	Eco Lodge Bore	023P	GW	O	O	X	
Windmill	Windmill Bore	024P	GW	O	O	X	
KN1	Knox Gorge	025P	GW	O	O	X	
KN2	Knox Gorge	026P	SW	O	O	X	
KN3	Knox Gorge	027P	GW	O	O	X	
RS1A GW	Rangers Station Bore	028P	GW	O	O	O	O
VC1	Visitors Centre Bore	029P	GW	O	O	O	
RS1	Circular Pool	030P	GW	O	O	O	
FS Falls	Fortescue Falls (Dales Gorge)	031P	SW	O	O	X	
FS Falls 2	Fortescue Falls (Dales Gorge)	032P	SW	O	O	X	
fern pool 1 GW	Fern Pool (Dales Gorge)	033P	SW	O	O	X	
fern pool 2	Fern Pool (Dales Gorge)	034P	SW	O	O	X	
KL1	Kalamina Falls	035P	GW	O	O	X	
KL2-SW	Kalamina Falls	036P	SW	O	O	X	
KL HW	Kalamina Falls	037P	SW	O	X	X	
JF1	Joffre Falls	038P	SW	O	O	X	

Table 3.1 Sample location details indicating the type of samples that were collected at each location (O = Sample collected X = no Sample collected)

3.2.5 Stream Discharge Measurements

An estimate of the amount of groundwater discharging at the sampled gorges was determined for a number of the catchments. Measurements were determined in locations where all the surface flow was contained within a single channel.

A handheld FP201 Global Water flow probe was used to measure average surface flow velocity, the width and depth of the midpoint of each section was measured, and the average flow velocity used to calculate stream discharge. The flow probe was held in the channel for 30seconds to determine the average flow velocity.

Due to the blocky nature of the BIF, an assumption of a square sided channel was made to determine cross sectional area (WxH) as shown in Figure 3.5. As this process was somewhat arbitrary, the flow measurements presented in this report are indicative only.

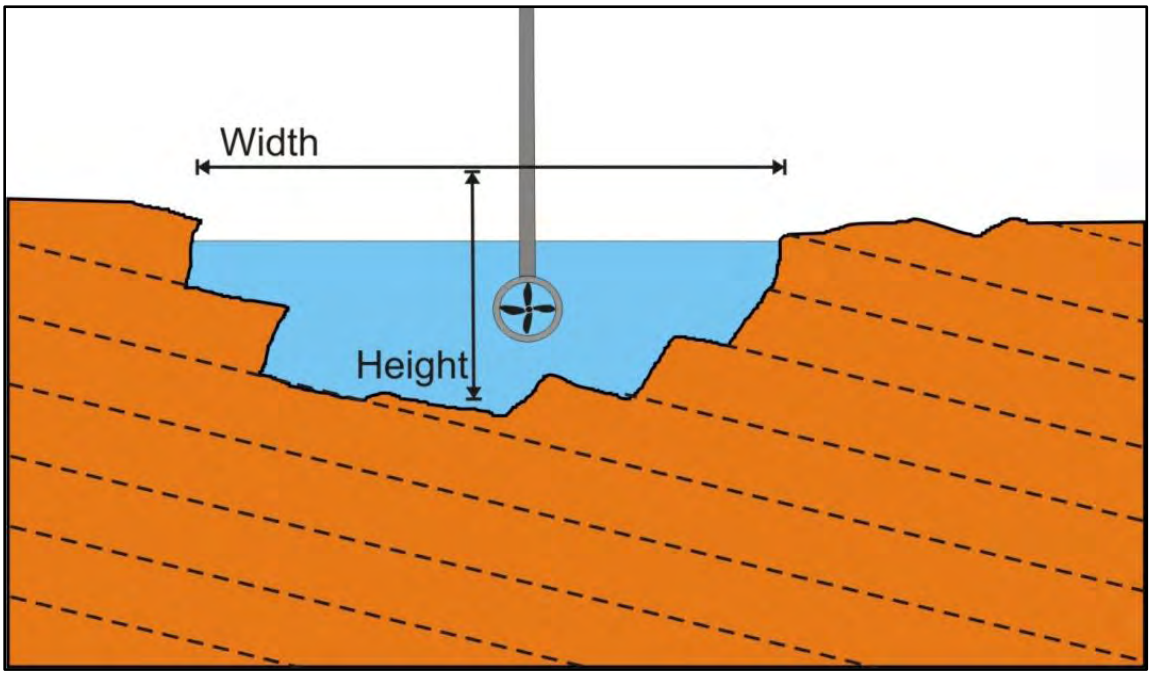

Figure 3.5. Typical set-up for calculating surface water flow volume

3.3 Analytical Methods

After the water samples were collected they were stored in chilly bins (Esky) and freighted directly to the appropriate laboratory for analysis. Stable isotopes (Deuterium and Oxygen-18), CFCs and ^{14}C were analysed by CSIRO Land and Water Adelaide Laboratory, while the analysis of major ions (Ca^{2+}, Mg^{2+}, Na^{+}, $K^{+,}$ Cl^{-}, SO_4^{2-}, HCO_3^{-} , SiO_2) were performed by SGS Environmental Services, WA.

3.3.1 Stable Isotopes (D and ^{18}O)

3.3.1.1 Oxygen-18 Composition (^{18}O)

The standard procedure for analysis of the Oxygen-18 composition of water is that described by Epstein and Mayeda (1953). CSIRO's modification involves equilibration of CO_2 with 1 ml of water in 6.5 ml 'Exetainers' Labco Ltd U.K. in a temperature controlled block held at 50 °C for 8 hours. The preparation and extraction of the CO_2 is automated using a 59 port Water Equilibration System (WES). This is attached to a GEO 20-20 dual inlet stable isotope gas ratio mass-spectrometer (PDZ Europa Ltd. U.K.). Quality control was maintained by placing two tertiary laboratory water standards (deionized water that has been calibrated to the international primary standards V-SMOW and V-SLAP) at the beginning of each run, after every ten samples and at the end of the run. Results were reported as per mille deviation from Vienna Standard Mean Ocean Water (‰ V-SMOW). Analytical uncertainty for naturally occurring waters is $\pm$ 0.15 ‰ (1 s.d).

3.3.1.2 Deuterium Composition (^{2}H)

Dueterium composition of the water was determined with the Water Equilibration Method (WES). WES is used for analysis whenever possible as the method is fully automated and therefore less expensive. The method is similar to ^{18}O analysis via WES, except that for 2H analysis, hydrogen atoms from the water molecules are equilibrated with hydrogen gas rather than oxygen atoms equilibrating with oxygen in CO_2. A platinum catalyst is used to enhance the hydrogen equilibration process allowing complete equilibration within 1 hour. As for ^{18}O analyses, results were reported as per mille deviation from Vienna Standard Mean

Ocean Water (‰ V-SMOW). Analytical uncertainty for naturally occurring waters is ± 1.0 ‰ (1 s.d).

3.3.2 Major Ion Chemistry

The following table details the various methods involved in determining the concentration of various aqueous ions:

Method ID	Species Measured	LOR (mg/L)	Methodology Summary
AN274	**Chloride, Cl-**	**1**	Chloride reacts with mercuric thiocyanate forming a mercuric chloride complex. In the presence of ferric iron, highly coloured ferric thiocyanate is formed which is proportional to the chloride concentration
AN275	**Sulphate, SO_4^-**	**1**	Sulphate is precipitated in an acidic medium with barium chloride. The resulting turbidity is measured photometrically at 405nm and compared with standard calibration solutions to determine the sulphate concentration in the sample.
AN135	**Bicarbonate, HCO_3^-**	**5**	The sample is titrated with standard acid to pH 8.3 (P titre) and pH 4.5 (T titre) and permanent and/or total alkalinity calculated. The results are expressed as equivalents of calcium carbonate or recalculated as bicarbonate, carbonate and hydroxide.
AN020-AN321	**Calcium, Ca^{2+}** **Magnsium,Mg2+** **Potassium, K+** **Sodium, Na+** **Silica, SiO2**	**0.2** **0.1** **0.1** **0.5** **0.05**	After preservation with 10% nitric acid, a wide range of metals and some non-metals in solution can be measured by ICP. Solutions are aspirated into an argon plasma at 8000-10000K and emit characteristic energy or light as a result of electron transitions through unique energy levels. The emitted light is focused onto a diffraction grating where it is separated into components. Photomultipliers or CCDs are used to measure the light intensity at specific wavelengths. This intensity is directly proportional to concentration. Corrections are required to compensate for spectral overlap between elements.
AN245	**Bromide, Br-**	**0.2**	A water sample is injected into an eluent stream that passes through the ion chromatographic system where the anions of interest i.e. Br, Cl, NO2, NO3 and SO4 are separated on their relative affinities for the active sites on the column packing material. Changes to the conductivity and the UV-visible absorbance of the eluent enable identification and quantitation of the anions based on their retention time and peak height or area.

Table 3.2 Summary of major ion analysis methods, compiled from information from SGS (LOR = Limit of Reporting)

3.3.3 Radiocarbon

Carbon-14 (^{14}C) analysis of the DIC in the groundwater was undertaken using Accelerator Mass Spectrometry (AMS). This method was chosen as it only required 5L of sample compared to the cheaper alternative, the Direct Absorption (DA) method, which requires up to 35L of sample. For AMS ^{14}C analysis, firstly the DIC was converted to CO_2. This is undertaken at the CSIRO laboratory. The CO_2 samples were then sent to the AMS machine at Australian National University (ANU), Canberra, Australia.

The Single-Stage AMS at ANU provides an average precision of ~4‰ (around 40 years at 10,000 years) and currently has a limit of detection of ~45, 000 years (CSIRO,2009).

3.3.4 Chlorofluorocarbons

CFC-11 and CFC-12 concentrations in groundwater were measured by firstly stripping the CFC gas from the water sample under a stream of ultra-high purity nitrogen gas. The CFC gas/nitrogen was then passed through a gas chromatograph where the CFC-11 and CFC-12 peaks are identified and measured separately. The set up at CSIRO closely follows that described by Bussenberg and Plummer (1992).

The CFC-11 and CFC-12 concentrations measured were those of the water, which are then converted to an age, by comparing to an assumed atmospheric CFC concentration at time of recharge. This is calculated with the salinity of the water, the recharge temperature of the water and the surface elevation. This value is then matched to measured atmospheric data to give a CFC-11 and CFC-12 age.

Analytical precision for CFC-11 is approximately ± 2% at 500 pg kg-^{1}, ± 5% at 100 pg kg^{-1}, and ± 20% at 20 pg kg^{-1}. Analytical precision for CFC-12 is ± 2% at 500 pg kg^{-1}, ± 10% at 100 pg kg^{-1}, and ± 30% at 20 pg kg^{-1}. Corresponding errors in apparent CFC ages are approximately ± 2 years for ages less than 20 years, increasing to ± 4 years for ages of 30 years. The detection limit for both CFCs is usually approximately 5 pg kg^{-1}, which equates to an age of ~ 1961 although potential errors in sampling means that the lab does not usually do not quote CFC-

11 and CFC-12 ages older than 1965. It is not possible to determine ages prior to that date. Where large peaks interfere with CFC peaks in the chromatograms, detection limits may be higher than this. The sampling blank is estimated to be approximately 10 pg kg^{-1} for CFC-12 and 20 pg kg^{-1} for CFC-11 (CSIRO, 2009)

3.3.5 X-Ray Diffraction Analysis

X-Ray Diffraction analysis is a powerful method by which X-Rays of a known wavelength are passed through a sample to be identified in order to identify the crystal structure. XRD analysis is based on Bragg's equation which relates the angel of incidence (θ) of the x-ray beam, the distance between atomic layers in a crystal (d) and the wavelength of the incident x-ray beam (λ). The Principle assumes that each mineral will have different crystal lattice spacing so altering the angle of incidence of the x-ray will produce a unique diffraction pattern for each mineral. This is produced as at certain orientations the x-ray reflection is enhanced due to constructive interference (resonant frequency).

XRD was under taken in the XRD lab and the University of Canterbury using a Philips PW1820/1710 X-ray Diffractometer system. This method allows the mineralogy of a material to be determined by measuring the characteristic diffraction angles each crystalline structure features.

Chapter 4

Results of Analysis and Field Observations

4.1 Introduction

The following chapter details physical, chemical and observational data determined from both in-field and laboratory analysis. The accuracy and associated errors involved in analysis and reporting will also be considered.

The **chemical** data has been determined from laboratory analysis of the water samples collected from the study area and includes; Major Ion concentrations, Stable Isotopes (Deuterium and Oxygen), Chlorofluorocarbons and Radiocarbon. Mineralogical data of rock and solid precipitate samples has also been determined with X-ray Diffraction.

The **physical** data includes, flow discharge volumes as determined from stream gauging, annual rainfall data extracted from the Bureau of Meteorology and various area calculations determined for different catchment parameters through GIS.

The **observations** made in the field have been interpreted to produce conceptual modes of discharge for groundwater in the area.

This data is further explored and discussed in Chapter 5 where a hydrochemical story of groundwater evolution in the Karijini National Park is developed with in-depth discussion.

4.2 Major Ion Concentrations

As water travels through the ground it interacts with the aquifer materials resulting in the dissolution of the rock minerals to add ions to the water. More than 90% of the dissolved solids in groundwater can be attributed to eight ions: Na^+, Ca^{2+}, K^+,Mg^{2+},SO_4^{2-}, Cl^-,HCO_3^- and CO_3^- (Fetter, 1994). The variation in the concentration of these ions is dependent on the flow path, therefore different flow paths can be distinguished with contrasting ionic concentrations.

4.2.1 Data Quality Assurance

Before any analysis of the data is undertaken it must be first determined whether the quality of the data has been affected at any stage. It is also important to understand the limits of reporting and the associated errors so it can be determined if variation in the data is significant. The limit of reporting (LOR) and analysis errors are detailed for each parameter in the above methods section.

4.2.1.1 Charge-Balance (Reaction Error)

As a basic check of the accuracy of the water sample analysis, a simple charge-balance error calculation was performed. This is based on the fundamental property of an aqueous solution that it is electrically neutral. The total number of equivalents of cations must equal the total number of equivalents of anions. This was determined with the following equation:

$$\textbf{Reaction Error} = ([\textstyle\sum_{CATIONS} - \sum_{ANIONS}] / \sum_{IONS}) * 100. \qquad \textbf{Equation 4.1}$$

The reaction error is therefore expressed as a percentage of the total ion concentration. Freeze and Cherry (1979) recommended that 5% is a reasonable limit for accepting the analysis as valid. The reaction errors for the data collected in KNP in May 2008 range from -5% to 3%. This is deemed to be acceptable. Where the reaction error is large, this may indicate that an analytical error exists or an ion that was not included in analysis exists in the solution at a significant concentration (Table 4.2).

4.2.1.2 Checking field data with Laboratory data

An easy check to determine whether there has been any error in data collection is to compare the total dissolved solids (SAL) value that was determined in the field, with the sum of the measured ions reported from laboratory analysis. These two parameters are obviously proportional to each other and should therefore plot a long a straight line. Figure 4.1, shows the relationship between these two parameters, and highlights the data points that do not correlate to the linear trend. These points either result from an error in field data collection or a laboratory error in analysis. In each case the sample was requested to be re-sampled.

From this process it was determined that the sample for Hamersley Pool had been incorrectly reported by the SGS lab and was amended accordingly. However the values for Kalamina and Windmill were not erroneous, suggesting that either the data in the field was not collected accurately, or that there is a significant concentration of an ion in solution that was not included in the suite of major ion analysed.

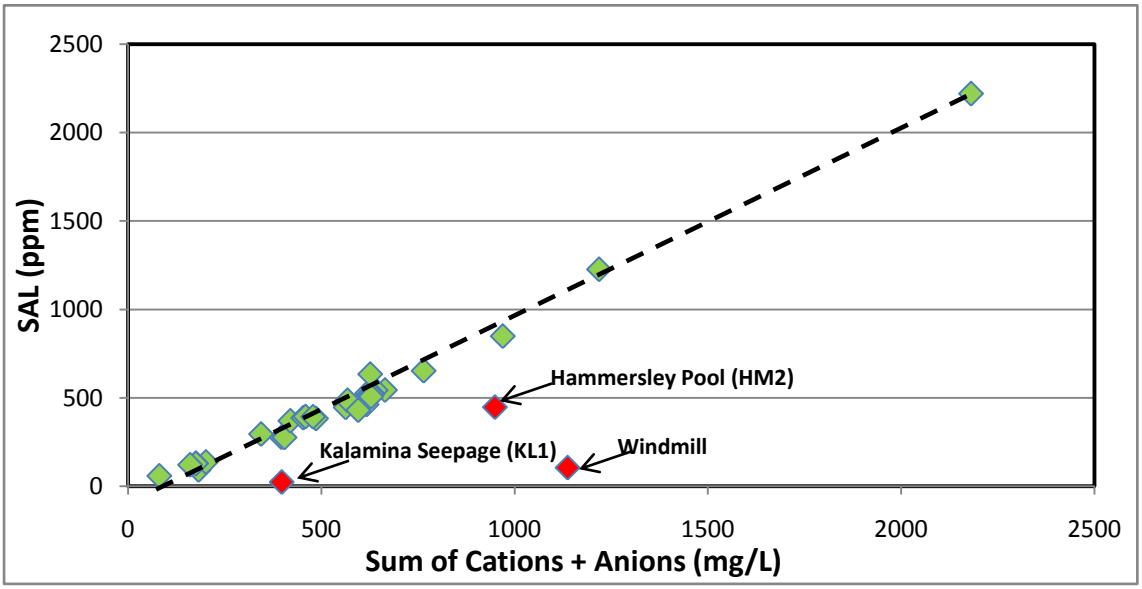

Figure 4.1 Relationship of SAL measured in the field with (handheld meter) against the sum of the ions determined via laboratory analysis.

4.2.2 TDS Distribution

The total dissolved solids (TDS) concentrations in the ground and surface water sampled within study area in September 2008 ranges from 84 mg/L at Banjima Pool (BJ pool) to 2182 mg/L at the Rangers Station Bore (RS1GW) (Figure 4.2). For groundwater samples TDS ranges from 351mg/L to 2182mg/L and for surface water TDS ranges from 84mg/L to 1241mg/L. The average TDS concentration over the entire study area is 543mg/L, indicating the values are evenly spread. The data is shown in Table 4.1

The TDS concentration of the water in the Marra-Mamba (MM) aquifer bores (MR2,MR4 and MR1) exhibited TDS concentrations of 628, 630 and 768 mg/L respectively, which is higher than the TDS concentrations in any discharged groundwater from the Gorges at the KNP, apart from Joffre Falls.

The most prevalent ions in all waters are bicarbonate (HCO_3^-) and chloride (Cl^-), making up 35% and 22.5% of the total dissolved solids respectively, followed by sodium (Na^+) and sulphate (SO_4^{2-}) at 8.4 % and 9.0%, and calcium (Ca^{2+}) and magnesium (Mg^{2+}) at 6.8% and 7.2% of TDS. Minor species are bromide (Br-) and potassium (K+). Silica is also present in solution. The order of anion abundance is HCO_3>Cl> >SO_4, and cation abundance is Na >Mg>Ca>K.

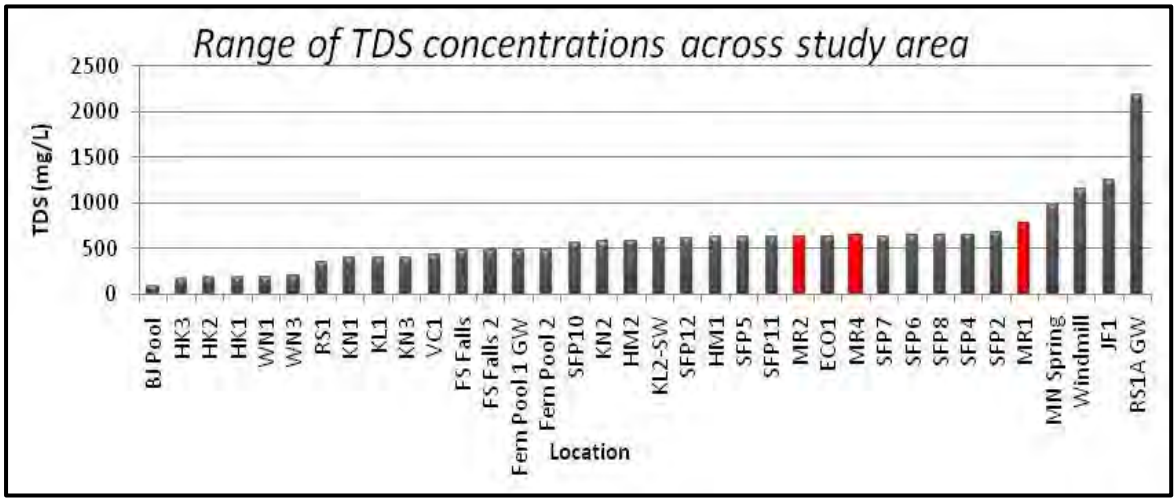

Figure 4.2 The range of TDS concentrations across the Study area

4.2.3 Ternary Diagram Presentation

Ternary diagrams are another method of displaying major ion chemistry (Figure 4.3). The diagrams show the percentage composition of three ions, and by grouping Na^+ and K^+ together all the major ions can be displayed. Each apex of the triangle represents 100% concentration of one of the three constituents. A point is plotted within the x-y space, dependent on the ratio of the three species being displayed. A point is created for each sample therefore displaying the trend and variation of the water in the region.

The cation diagram shows that the water chemistry is fairly evenly balanced between the three apices, although there is a slight trend towards a higher magnesium concentration. The anions are heavily favoured towards HCO_3^- and Cl^-. Neither diagram really shows any obvious grouping apart from where multiple samples were taken from the same location.

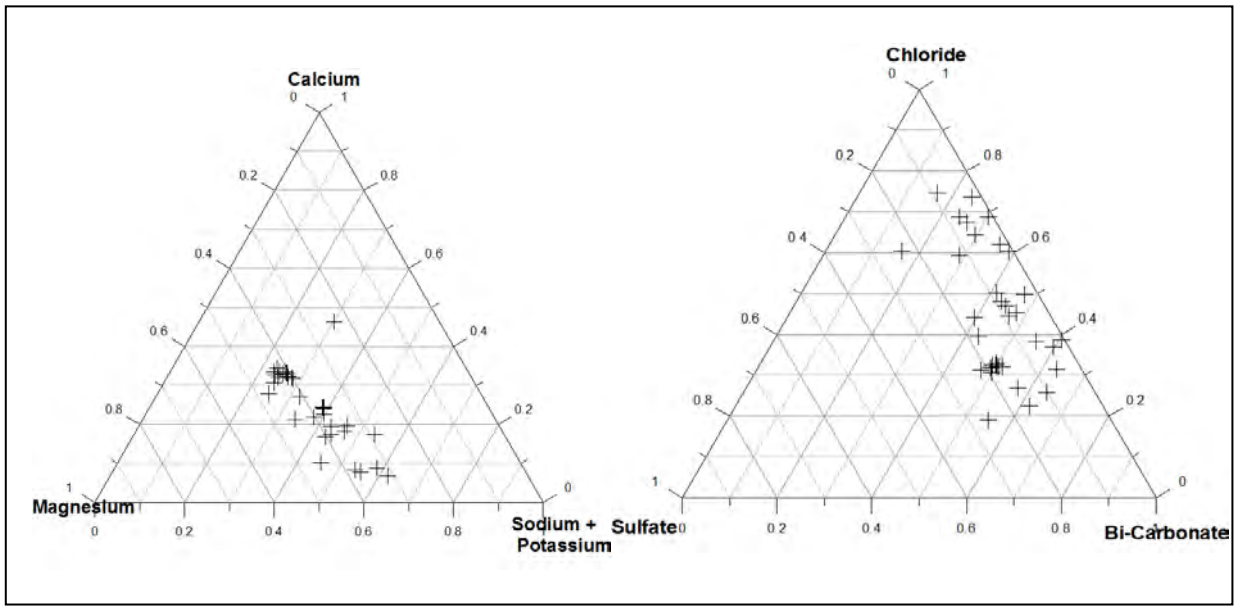

Figure 4.3 Ternary Diagram Representation, illustrating the data spread (Cations:left, Anions:Right)

4.2.4 Schoeller Diagram

The Schoeller Diagram is a method of displaying the chemical composition of multiple samples simultaneously. Figure 4.4 shows the major ion composition of local rainfall, Marandoo's groundwater and a selection of sample locations within the KNP.

BJ Pool exhibits a similar ion pattern as the rainfall with a consistent concentration increase across all ions. The ionic composition of Hancock gorge water (HK) is significantly different to Marandoo, while the Rangers Station Bore (RS1aGW) follows a more similar trend however it is significantly more concentrated in all ions.

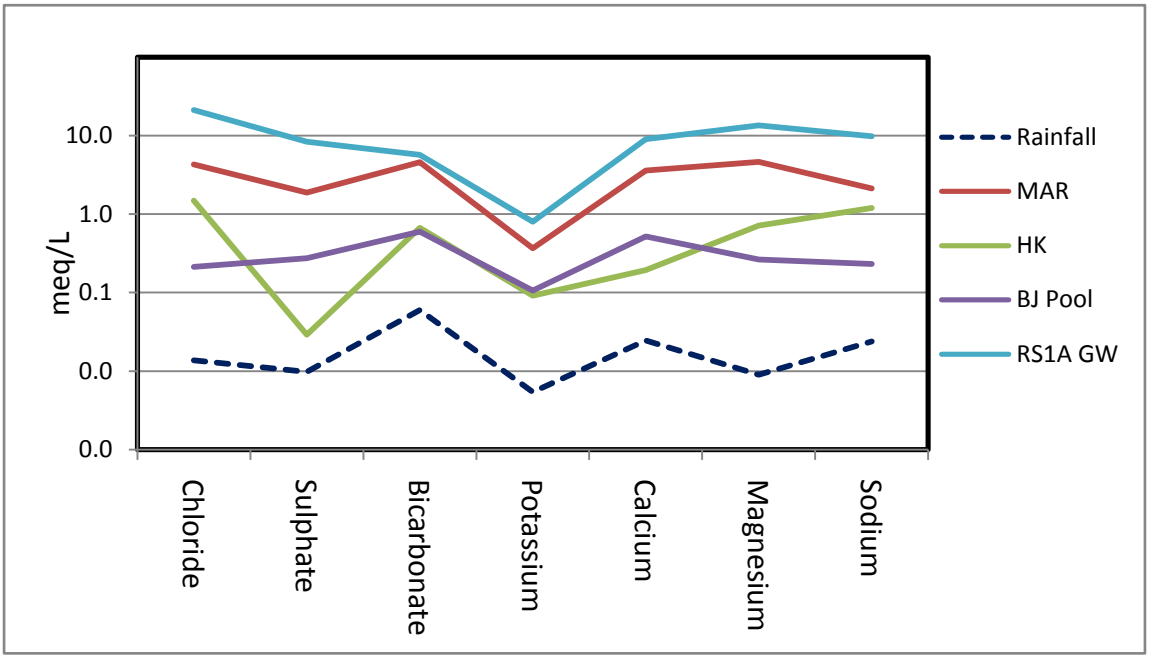

Figure 4.4 Schoeller Diagram to illustrate the variation in major ion composition of local rainfall, Marandoo's MM Aquifer and a selection of KNP sample locations.

4.2.5 Stiff plot representation

Stiff plots for each water sample are presented in Figure 4.5 This provided an excellent tool for visualising the variation in water chemistry across the study region, and created a starting point to further investigate the patterns and trends that exist in the data. At full scale it is clear that there is a large variation in major ion concentrations across the study area. Hancock and Weano Gorges exhibit the freshest water, while Joffre Falls and the

Rangers Station Bore (RS1aGW) exhibit the highest concentration of dissolved solutes. Each catchment was looked at individually to investigate inter-catchment major ion relationships.

Firstly, at Southern Fortescue borefield there is very little variation between the nine bores sampled, however there is a clear similarity between the chemistry of the groundwater sampled at the borefield and Hamersley Gorge. The gorge is located down the hydraulic gradient from the borefield. The borefield has been in operation since early 1972 and has drawn down the water table an average of 50m (AGC,1985). This water is relatively high in all species, especially HCO_3^- which is in excess of 250mg/L.

At Weano and Hancock, the major ion concentrations in the water sampled are all relatively low. They both display similar ion abundance ratios, with Cl^- and Na+K being the dominant ion species, contrasting Hamersley gorge where HCO_3^- dominates. Knox and Kalamina Gorges are also relatively fresh. They both exhibit similar ionic concentrations as emphasised by the similar stiff polygon shape, and again HCO_3^- is the dominant anion.

In the Marandoo area the water collected from the bores is all similar but there is a significant contrast between the mine water and the adjacent Mindthi Spring and Banjima Pool. The water in Banjima Pool is very low in dissolved ions, and this chemical signature suggests that is it primarily a collection of rainwater. Mindthi spring has a very unique chemical signature dominated by Na+K, Cl^- and Mg^{2+}.

At Dales gorge the water chemistry is consistant throughout the length of the gorge, the water is dominated by Cl^-, Na+K and Mg^{2+}, which is similar to the Visitors Centre Bore (VC1). Upgradient from these two locations is RS1aGW which exhibits the highest concentrations of all ions in the study area, and the water is dominated by high Cl^- level.

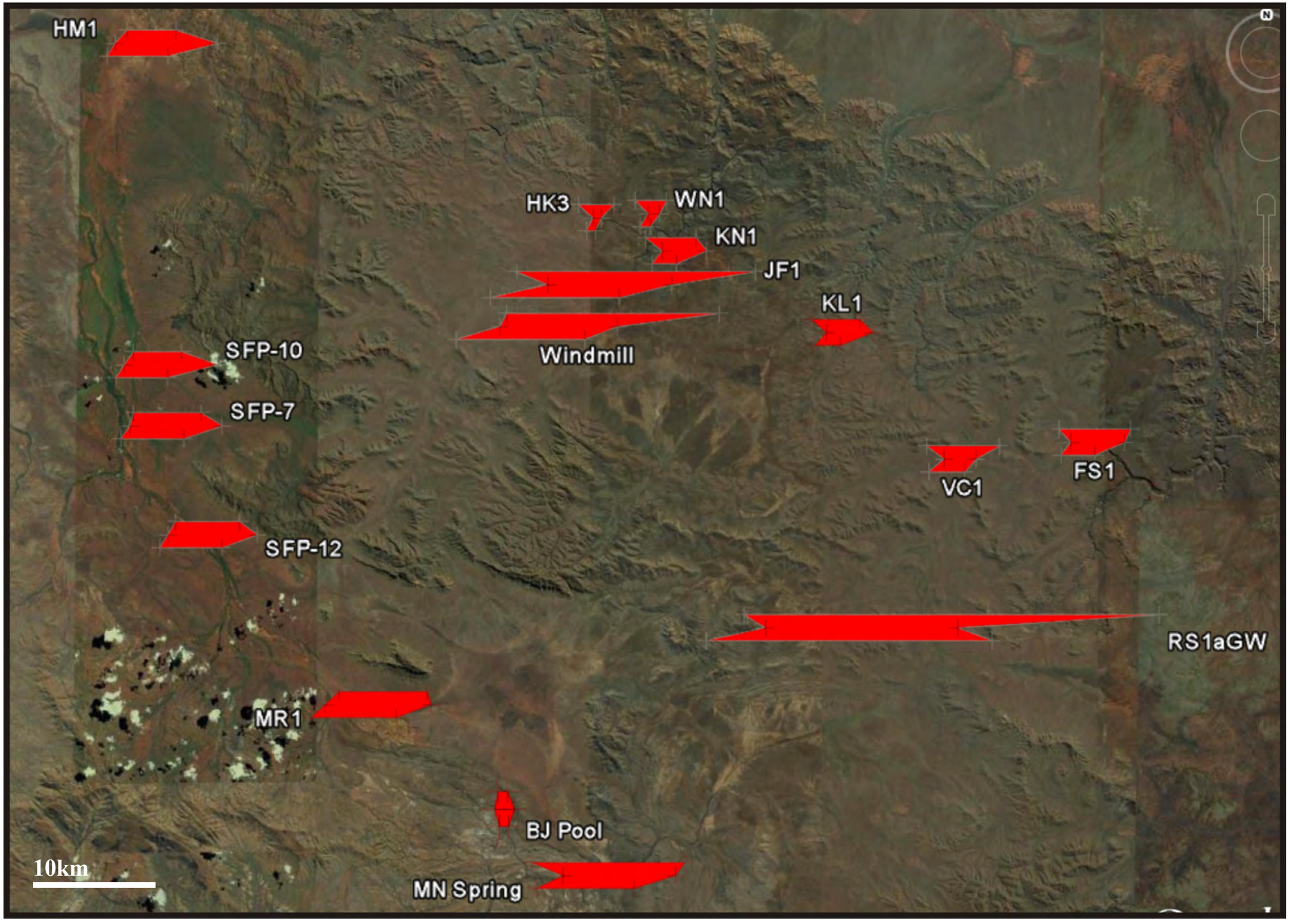

Figure 4.5 Stiff plot of all samples across study area, illustrating the large variation in major ion concentrations between and within catchments. (For each site see appendix II

Location ID	Northing	Easting	Cl	SO4	HCO3	Ca	Mg	K	Na	Br	SiO2	pH	SAL	EC (uS)	Temp (°C)	Type
SFP10	-22.439518	117.990717	66.1	35.0	282.0	51.6	39.1	9.5	37.6	0.4	42.8	7.01	445	742	34.3	GW
SFP8	-22.46552	117.990599	98.7	71.2	274.5	53.9	41.2	11.1	48.9	0.7	40.3	7.27	533	910	31.3	GW
SFP7	-22.473799	117.993963	98.1	67.8	268.0	54.9	42.0	11.3	50.0	0.6	39.3	7.33	520	903	30.9	GW
SFP2	-22.489215	117.989096	104.6	85.5	278.4	57.6	43.9	11.9	50.6	0.6	34.5	7.27	543	947	31.1	GW
SFP4	-22.498897	117.992307	104.6	73.0	271.7	58.8	45.0	12.5	48.9	0.5	32.3	7.29	542	938	31.5	GW
SFP5	-22.505279	117.988382	100.0	71.5	262.7	57.8	44.4	11.9	44.1	0.4	29.0	7.55	524	911	31.9	GW
SFP6	-22.50903	117.99629	98.2	78.9	264.1	59.7	44.2	12.1	45.1	0.4	34.1	7.27	522	906	32.1	GW
SFP11	-22.529183	118.008586	98.2	71.8	261.7	58.1	43.5	11.9	45.7	0.5	34.6	7.38	520	906	31.7	GW
SFP12	-22.534774	118.017218	96.1	65.7	248.9	56.8	42.0	12.1	44.9	0.5	39.2	7.38	515	895	30.3	GW
HM1	-22.258573	117.985979	65.6	60.8	310.7	56.6	41.9	9.6	38.2	0.3	33.6	7.63	461	804	23.6	SW
HM2	-22.257595	117.986906	63.2	53.1	289.1	49.1	43.4	10.0	39.6	0.3	33.9	8.42	446	779	21.4	SW
MR1	-22.629336	118.117401	152.8	90.8	279.6	72.1	56.5	14.4	49.1	0.6	52.1	7.45	652	1121	29.1	GW
MR2	-22.63824	118.143232	102.1	76.0	255.6	55.7	45.4	12.9	41.6	0.3	38.3	7.48	519	904	30.6	GW
MR4	-22.630673	118.12281	78.9	62.5	291.8	56.9	45.7	13.0	39.9	0.5	40.6	7.4	506	878	30.4	GW
MN Spring	-22.724015	118.263008	221.0	111.2	338.6	63.0	63.7	17.0	117.6	1.3	34.3	7.19	848	1440	27	SW
BJ Pool	-22.687258	118.199284	7.5	13.1	36.6	10.5	3.2	4.2	5.4	0.3	2.8	8.37	57.6	110	20.4	SW
WN1	-22.351913	118.28465	45.3	2.0	44.7	3.2	9.3	3.8	24.1	0.2	50.0	6.8	90.9	170	21.2	SW
WN2	-22.356624	118.28716										7.48	153	245	20	SW
WN3	-22.357277	118.286769	50.2	1.4	56.9	4.0	10.9	4.0	27.1	0.3	48.7	7.78	136	250	21.1	SW
HK1	-22.358755	118.285269	52.8	1.4	40.7	3.9	8.7	3.6	27.4	0.3	37.7	7.95	129	239	24.1	SW
HK2	-22.359804	118.286538	52.7	1.4	40.7	3.9	8.6	3.5	27.1	0.4	37.8	7.78	127	234	19.9	SW
HK3	-22.359885	118.286397	52.8	2.4	30.9	2.8	7.7	2.7	27.1	0.4	35.3	6.68	120	222	22.4	SW
ECO1	-22.354592	118.251358	253.3	40.5	93.7	19.4	51.8	17.7	88.9	1.5	61.9	6.38	633	1087	29.6	GW
Windmill	-22.385528	118.260653	428.7	79.4	256.8	97.6	100.4	19.1	88.6	3.5	77.5	7.00	105.2	1954	27.7	GW
KN1	-22.372471	118.300158	63.6	13.6	159.4	16.8	19.6	7.7	44.5	1.1	68.6	8.35	276	495	22.9	GW
KN2	-22.372609	118.300171	143.8	11.5	230.0	26.6	35.7	10.4	71.2	0.7	41.7	8.49	485	845	22	SW
KN3	-22.372327	118.300253	51.6	12.1	177.3	17.7	18.5	7.3	43.6	0.5	72.7	7.14	275	488	27.8	GW
RS1A GW	-22.371691	118.299048	758.9	405.3	351.6	181.7	166.1	31.5	228.3	4.6	54.5	7.13	2220	3640	28.1	GW
VC1	-22.582637	118.459033	120.8	35.6	97.6	17.3	25.1	8.6	45.9	0.3	71.2	6.28	369	649	27.4	GW
RS1	-22.487664	118.476355	87.4	18.3	106.5	18.4	20.5	6.4	32.9	0.7	59.7	6.40	294	520	26.2	GW
FS Falls	-22.475277	118.562007	113.2	18.9	167.3	29.1	27.0	8.8	48.7	0.5	55.8	8.32	386	678	23.4	SW
FS Falls 2	-22.477105	118.56278	111.4	25.4	175.5	29.1	26.6	8.8	48.1	0.5	56.8	7.75	393	690	24.2	SW
fern pool 1 GW	-22.477273	118.556583	109.4	26.1	176.5	29.2	26.8	8.9	48.3	0.4	57.4	6.21	382	671	26.2	GW
fern pool 2	-22.4778	118.550428	110.3	26.1	174.7	30.3	27.9	9.1	49.4	0.4	56.4	7.69	392	688	23.5	SW
KL1	-22.477165	118.548236	60.8	7.2	166.9	18.2	21.4	7.6	41.9	0.3	71.1	8.28	23.4	46	24.9	GW
KL2-SW	-22.41747	118.401955	103.6	2.4	271.7	27.4	27.4	12.9	88.8	0.4	66.6	8.33	429	752	21.8	SW
KL HW	-22.417472	118.401959														SW
JF1	-22.391992	118.268026	426.6	72.2	340.8	80.7	102.9	23.3	134.6	1.4	58.9	8.20	1226	2050	24.9	SW
RAINFALL			0.9	0.5	3.7	0.5	0.1	0.1	0.6							

Table 4.1 Major Ion Analysis Data from all sample locations in mg/L , including field parameters

LOCATION	CATIONS meq/L				ANIONS meq/L				∑ Ions	∑Cation - ∑ Anion	Reaction Error %
	Mg	Ca	Na	K	SO_4	HCO_3	Cl	Br			
SFP10	3.22	2.58	1.64	0.24	0.73	4.62	1.86	0.00	14.90	0.46	3.1
SFP8	3.39	2.69	2.13	0.28	1.48	4.50	2.78	0.01	17.27	-0.28	-1.6
SFP7	3.46	2.75	2.17	0.29	1.41	4.39	2.76	0.01	17.24	0.09	0.5
SFP2	3.61	2.88	2.20	0.30	1.78	4.56	2.95	0.01	18.30	-0.30	-1.7
SFP4	3.70	2.94	2.13	0.32	1.52	4.45	2.95	0.01	18.02	0.16	0.9
SFP5	3.65	2.89	1.92	0.30	1.49	4.31	2.82	0.00	17.38	0.14	0.8
SFP6	3.64	2.98	1.96	0.31	1.64	4.33	2.77	0.01	17.63	0.15	0.8
SFP11	3.58	2.90	1.99	0.30	1.50	4.29	2.77	0.01	17.33	0.22	1.3
SFP12	3.46	2.84	1.95	0.31	1.37	4.08	2.71	0.01	16.73	0.40	2.4
HM1	3.45	2.83	1.66	0.25	1.27	5.09	1.85	0.00	16.40	-0.02	-0.1
HM2	3.57	2.45	1.72	0.26	1.11	4.74	1.78	0.00	15.64	0.37	2.4
MR1	4.65	3.60	2.14	0.37	1.89	4.58	4.30	0.01	21.54	-0.03	-0.1
MR2	3.74	2.79	1.81	0.33	1.58	4.19	2.88	0.00	17.32	0.01	0.1
MR4	3.76	2.84	1.74	0.33	1.30	4.78	2.22	0.01	16.99	0.36	2.1
MN Spring	5.25	3.15	5.11	0.43	2.32	5.55	6.22	0.02	28.05	-0.16	-0.6
BJ Pool	0.26	0.52	0.23	0.11	0.27	0.60	0.21	0.00	2.22	0.04	1.6
WN1	0.76	0.16	1.05	0.10	0.04	0.73	1.28	0.00	4.13	0.02	0.4
WN3	0.90	0.20	1.18	0.10	0.03	0.93	1.41	0.00	4.76	0.00	-0.1
HK1	0.72	0.19	1.19	0.09	0.03	0.67	1.49	0.00	4.38	0.01	0.2
HK2	0.71	0.19	1.18	0.09	0.03	0.67	1.49	0.00	4.36	-0.02	-0.4
HK3	0.63	0.14	1.18	0.07	0.05	0.51	1.49	0.00	4.07	-0.03	-0.7
ECO1	4.27	0.97	3.87	0.45	0.84	1.54	7.13	0.02	19.09	0.02	0.1
Windmill	8.27	4.88	3.85	0.49	1.65	4.21	12.08	0.04	35.47	-0.50	-1.4
KN1	1.62	0.84	1.93	0.20	0.28	2.61	1.79	0.01	9.29	-0.12	-1.2
KN2	2.94	1.33	3.10	0.27	0.24	3.77	4.05	0.01	15.70	-0.44	-2.8
KN3	1.52	0.88	1.90	0.19	0.25	2.91	1.45	0.01	9.11	-0.13	-1.4
RS1A GW	13.67	9.09	9.93	0.81	8.44	5.76	21.38	0.06	69.13	-2.15	-3.1
VC1	2.06	0.87	2.00	0.22	0.74	1.60	3.40	0.00	10.89	-0.60	-5.5
RS1	1.68	0.92	1.43	0.16	0.38	1.75	2.46	0.01	8.80	-0.40	-4.5
FS Falls	2.22	1.45	2.12	0.22	0.39	2.74	3.19	0.01	12.35	-0.31	-2.6
FS Falls 2	2.19	1.46	2.09	0.23	0.53	2.88	3.14	0.01	12.52	-0.59	-4.7
Fern Pool 1 GW	2.21	1.46	2.10	0.23	0.54	2.89	3.08	0.01	12.52	-0.53	-4.2
Fern Pool 2	2.30	1.51	2.15	0.23	0.54	2.86	3.11	0.01	12.71	-0.33	-2.6
KL1	1.76	0.91	1.82	0.20	0.15	2.74	1.71	0.00	9.29	0.09	0.9
KL2-SW	2.25	1.37	3.86	0.33	0.05	4.45	2.92	0.00	15.24	0.39	2.5
JF1	8.47	4.04	5.85	0.60	1.50	5.59	12.02	0.02	38.08	-0.17	-0.4

Table 4.2 Major Ion Conentrations (meq) for samples collected in the KNP in September 2008

4.3 Stable Isotopic Variations across Karijini National Park

By determining the stable isotopic ratio of Deuterium (D) and Oxygen-18 (^{18}O) in water samples collected in the study area, an indication of the groundwater recharge processes occurring within the KNP can be determined. A total of 36 water samples (16 surface, 21 ground) were collected within the KNP and analysed for stable ^{18}O and D isotopic ratios, as presented in Table 4.3. The samples have been divided into groundwater and surface water as there is a distinct contrast in the observed values. The groundwater shows the most depleted signature with a tight $\delta\ ^{18}O$ range from -9.55 to -8.52 ‰ and a δD range from -64.1 to -56.4‰. The surface water has a wider range from -9.04 to -2.37‰ $\delta\ ^{18}O$ and -60.8 to -29.5‰ δD. The amounts of D and ^{18}O present in a sample are expressed as a deviation from the reference Standard Mean Ocean Water (SMOW) using standard delta (δ) notation:

δ = [(Rsample / Rstandard) - 1] x 1,000 **Equation 4.2**

where: δ is reported in units of per mil (‰) for D or ^{18}O, and R is D/H or $^{18}O/^{16}O$.

Surface water sample	δ O18 ‰ (VSMOW)	δ D ‰ (VSMOW)	Ground water sample	δ O18 ‰ (VSMOW)	δ D ‰ (VSMOW)
BJ POOL	-2.37	-29.5	SFP 2	-8.65	-58.3
FERN POOL 2	-8.93	-60.8	SFP 4	-8.75	-59.8
MN SPRING	-8.5	-56.7	SFP 5	-8.87	-60.4
HK 1	-7.67	-53.7	SFP 6	-8.76	-60.7
HK 2	-7.57	-52.9	SFP 7	-8.52	-58.9
HK 3	-7.72	-55.3	SFP 8	-8.63	-57.7
KL HW	-5.81	-43.8	SFP 10	-9.49	-64.1
KL 2	-8.26	-55.7	SFP 11	-8.79	-60.4
KN 2	-5.53	-43.5	SFP 12	-8.78	-60.0
WN 1	-8.64	-58.2	FERN POOL	-9.15	-60.3
WN 2	-8.11	-56.2	ECO RETREAT	-8.67	-57.9
FS FALL 2	-9.04	-59.8	KN 3 GW	-9.39	-61.7
FS FALLS	-8.86	-59.2	KN 1	-9.02	-60.2
HM 2 POOL	-8.54	-59.5	MR 1	-9.17	-62.7
JF 1 11/9	-7.54	-52.5	MR 2	-9.38	-61.5
HM 1 DP	-8.87	-58.7	MR 4	-9.08	-62.9
			WINDMILL	-8.70	-56.4
			RS 1	-8.96	-59.4
			RS 1A GW	-8.53	-61.4
			VC 1	-9.55	-62.1
			KL 1	-8.76	-58.1

Table 4.3 Stable isotopic data for the KNP samples collected in September 2008

It is common practice to present ground and surface water data on a δD - $\delta^{18}O$ diagram, along with the Global and Local Meteoric Water Line of the local precipitation (GWML &LMWL) as a reference. The LMWL for the area is defined by the relationship δD = 7.6 $\delta^{18}O$ + 3.83 (J.D Reeves Pers. Comms) and shows enrichment modification from the Global trend (GMWL) as defined by Craig (1961) section 2.4 .

The data from the water samples collected in the KNP has been split into plots for ground and surface water. The surface water data (Figure 4.6) has a wide spread and correlates to the regression line δD = 4.6 $\delta^{18}O$ - 18.2, this line is further enriched from the LMWL, likely as a result of evaporation. The groundwater data (Figure 4.7), exhibits a much tighter grouping, and plots around the GMWL suggesting minimal modification has occurred to the rainfall recharge. The stable isotope trends are further discussed in Section 5.2.

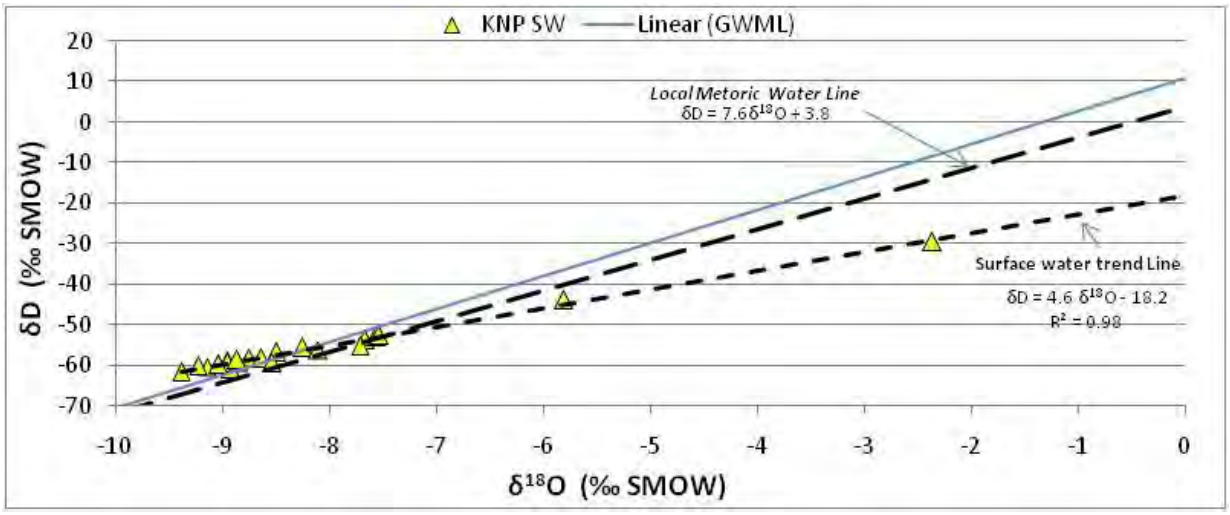

Figure 4.6 Relationship of δD to $\delta^{18}O$ determined from surface water samples collected in the KNP

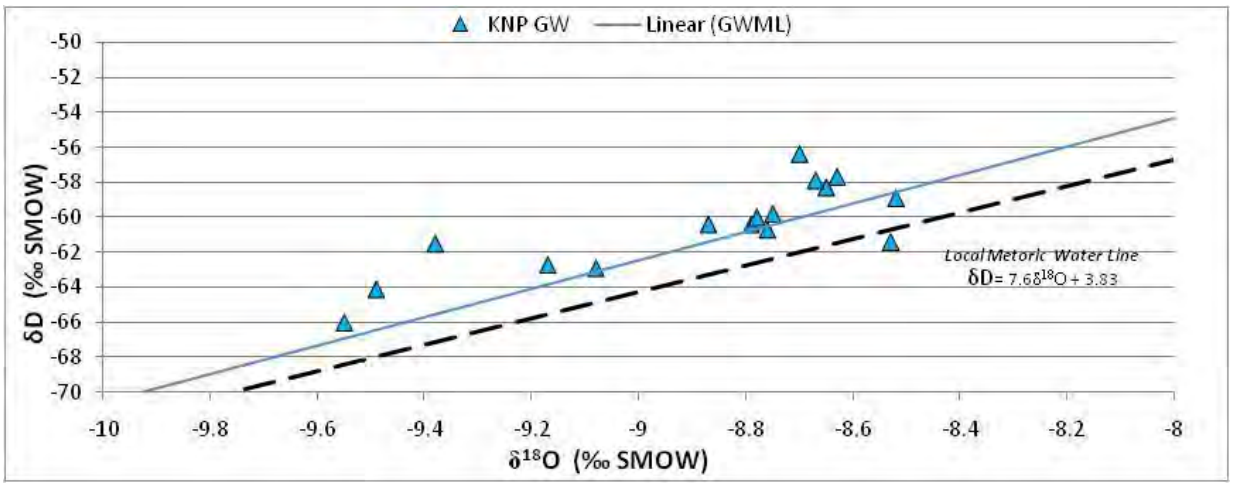

Figure 4.7 Relationship of δD to δO determined from ground samples collected in the KNP

4.4 Age Dating of groundwater

4.4.1 Chlorofluorocarbon data

CFCs can be used as an effective method of dating modern water (i.e. with an age of <50years). The concentration of the CFCs in the atmosphere has changed over time. CFCs are highly soluble and therefore the concentration of CFCs in groundwater reflects the concentration of CFCs in the atmosphere at the time of recharge.

The CFC data is presented in Table 4.4, which shows the concentrations of CFC-11 and CFC-12 measured in the water sample, and equivalent atmospheric concentration required to allow this. From this measurement an apparent age of groundwater is deduced.

	Measured CFC Concentration in Water		Equivalent Atmos. Concentration		Apparent Age	
Sample	**CFC11**	**CFC12**	**CFC11**	**CFC12**	**CFC11**	**CFC12**
units	(pg/kg)	(pg/kg)	(pptv)	(pptv)	(years)	(years)
SFP2	46	38	38	127	1968	1971
SFP4	75	54	62	178	1971	1974
SFP5	91	50	75	165	1972	1973
SFP7	72	50	59	167	1971	1973
SFP8	<25	<20	<25	<50	<1965	<1965
SFP10	54	39	45	130	1969	1971
SFP11	124	21	102	70	1975	1966
SFP12	<25	<20	<25	<50	<1965	<1965
MR1	1464	76	1207	251	NA	1978
MR2	404	146	333	485	NA	1991
MR4	300	34	247	112	1990	1970
VC1	225	71	185	236	1984	1977
GWRS1	198	127	163	421	1981	1988
RS1	197	122	37	108	1968	1969

Table 4.4 CFC data. Where CFC concentrations are given as NA, it is due to either interference on the chromatogram, or to poor reproducibility of replicate samples.

The equivalent atmospheric CFC concentration is based on assumed values of recharge temperature, recharge elevation and excess air. These were assumed to be 26°C, 600m and 0cm^3/kg respectively. Variation of these values can significantly alter the date, therefore the values were kept constant for every sample location so any error is constant for all results.

4.4.1.1 CFC Data quality

The CFC concentration in groundwater is very susceptible to contamination during the sampling process. The quality of the data can be investigated with a plot of CFC-11 vs CFC-12 (Figure 4.8). A linear relationship should exist if both CFC-11 and 12 dates agree with each other. The majority of the data does lie along this line however there are three points that show a much younger age for the CFC-11 date. Erroneous data is generally due to contamination occurring during sampling or analysis.

To further investigate this, the relationship between CFC-11 and CFC-12 plotted in pg/kg can be determined (Figure 4.9). All the data should fall within this triangle, and when this is not the case it indicates that at least one CFC is not behaving conservatively. Figure 4.9, shows that most of the data plots close to the expected line, however there four points that are clearly show that CFC-11 contamination has occurred. Possible reasons for this will be discussed in Chapter 6.

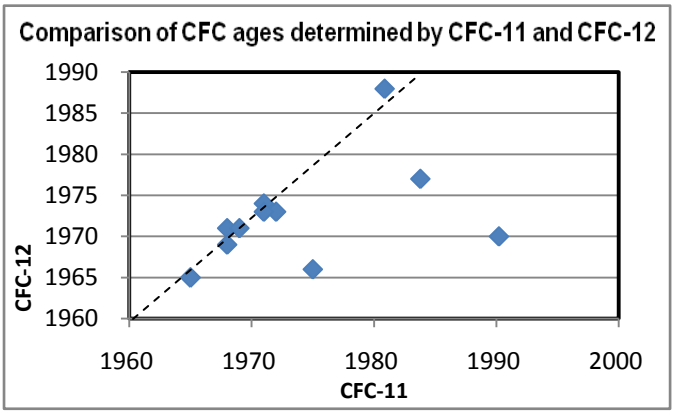

Figure 4.8 Comparison of CFC dates, revealing a number of erroneous data values

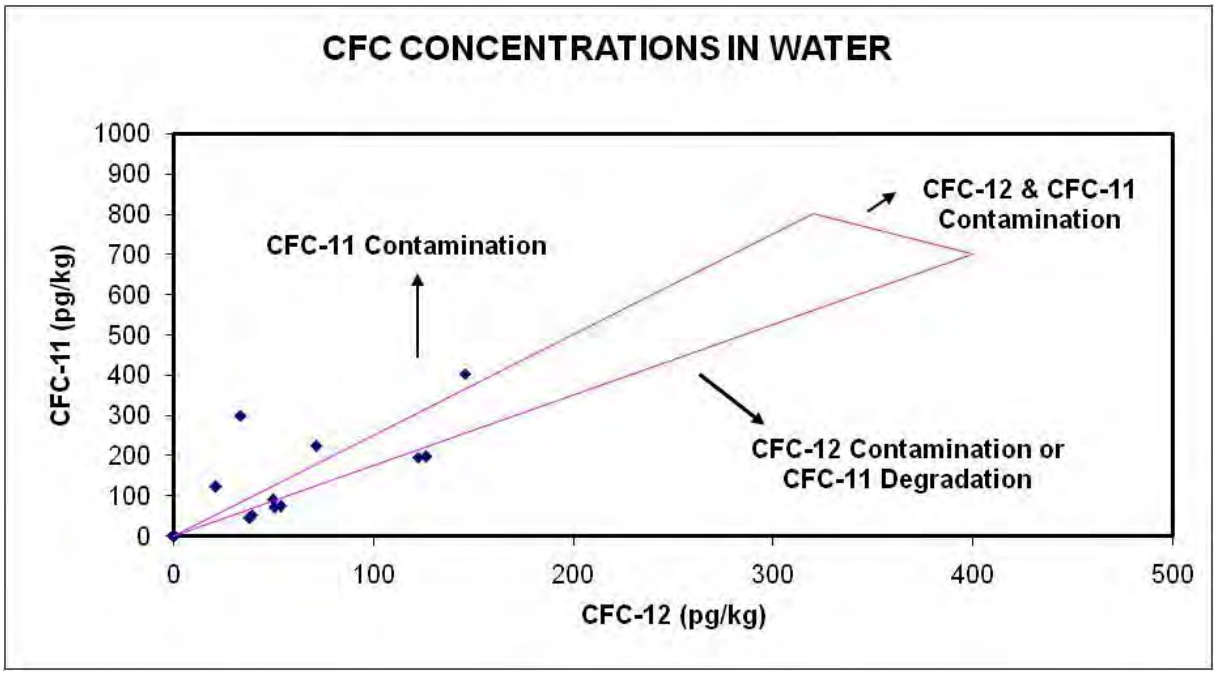

Figure 4.9 CFC Concentrations in water, illustrating the quality of the data

4.4.2 Radiocarbon dating (C-14)

Radiocarbon data for KNP is presented in Table 4.5, Radiocarbon concentration is expressed as percent Modern Carbon, $\delta^{14}C$ and conventional radiocarbon age. Concentrations of ^{14}C in samples from the KNP ranged from 9.18-23.24pMC. The stable isotope $\delta^{13}C$ was also determined for each sample as this gives an indication of the source of the carbon. The interpolation method to determine an apparent groundwater age is shown in Figure 4.10.

Sample	$\delta^{13}C$	±	Percent Modern Carbon (pMC)	±	D ^{14}C	±	^{14}C age (years)	±
sfp12	-8.49	0.05	13.09	0.12	-869.1	1.2	16330	80
mr1	-9.98	0.05	23.24	0.16	-767.6	1.6	11720	60
sfp8	-9.26	0.05	16.14	0.12	-838.6	1.2	14650	60
mr2	-9.92	0.05	9.18	0.12	-908.2	1.2	19180	110

Table 4.5 Radiocarbon data showing apparent ages of groundwater samples The quoted age is in radiocarbon years using the Libby half life of 5568 years and following the conventions of Stuiver and Polach (Radiocarbon, v. 19, p.355, 1977). The age is years before 1950.

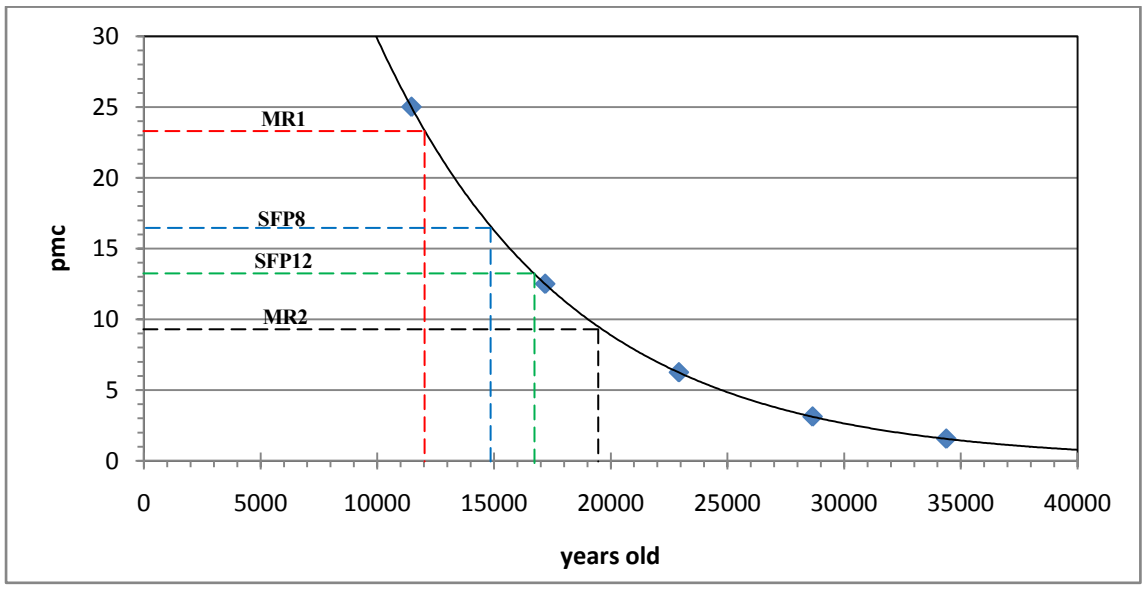

Figure 4.10 Radiocarbon Decay curve, determine by the decay of 100pmc with a half life of 5570years. The curve is interpolated to determine groundwater age for each sample.

4.5 XRD results

The following results detail the mineral composition of various handsamples of rocks and precipitates collected from a selection of the studied groundwater locations. This was undertaken to gain a greater understanding of the hydrochemical evolution occurring. The precipitate type show distinct variation between each sample location.

Sample Location	Sample Type	Mineral Present (%)	Molecular Composition
Circular Pool	Precipitate scraping from seepage	Landsfordite (55) Dolomite (45)	$MgCO_3 \cdot 5H_2O$ $CaMg(CO_3)_2$
Fortescue Falls	Powdery precipitate from gorge wall	Starkeyite (100)	$MgSO_4$
Kalamina Falls	Precipitate scraping from seepage	Dolomite (65) Landsfordite (35)	$CaMg(CO_3)_2$ $MgCO_3 \cdot 5H_2O$
Knox Gorge	Precipitate scraping from seepage	Aragonite (65) Calcite (35)	$CaCO_3$ CaCO3
Minthi Spring	Rock hand sample	Dolomite (85) Calcite (15)	$CaMg(CO_3)_2$ CaCO3
	Nodule in rock sample	Quartz (75) Opal (25)	SiO_2 $SiO_{2.n}H_2o$

Table 4.6 XRD results from analysis of precipitate and aquifer material collected in the KNP. There is a distinct variation in the mineralogy of the various precipitates collected. The Diffraction pattern for each sample is located in appendix V

Common errors in XRD analysis are associated with sample preparation and mis-identification of the diffraction pattern. However in this case the results are assumed to be correct, as for all samples the diffraction patterns showed a good fit to the characteristic pattern (Appendix V)

4.6 Groundwater Discharge

The results detailed in the table below are estimations of surface water flow volumes from various gorges within the study area. The arbitrary nature of the parameters determined during this technique (section 3.2.5) are such that the results should only be used as a guide.

In attempt to quantify the accuracy of the measurements, a conservative estimate would be around ± 20% inaccuracy in the cross-sectional area, as the stream was obviously not perfectly rectangular, with a similar inaccuracy for the Flow rate as this varies depending on the depth the probe is submerged.

This accuracy of the flow volume therefore is not enough for interpretation of gains or losses within the gorge, however they can be useful for inputting into a hydrologic budget for the catchment (section 5.9).

Site	Section Length (m)	Section depth (cm)	Mean velocity (m/sec)	Flow (m^3/sec)	Flow (L/sec)	Flow (m^3/day)
Hamersley 1	0.20	7	0.70	0.0098	9.8	847
Hamersley 2	0.10	9	0.64	0.0058	5.8	498
Fortescue 1	2.30	18	0.13	0.0538	53.8	4650
Fortescue 2	1.60	13	0.19	0.0395	39.5	3415
Kalamina 2	1.20	5	0.21	0.0126	12.6	1089
Joffre 2	0.85	6	0.37	0.0189	18.9	1630
Weano 2	0.19	14	0.15	0.0039	3.9	336
Weano 3	0.40	2	0.64	0.0051	5.1	442
Hancock 2	0.81	4	0.67	0.0217	21.7	1876

Table 4.7 Surface water flow volume (Source Wade Dodson, RTIO)

4.7 Conceptual Models from field observations

The following section details the physical observations made whilst in the field. Various observations were made regarding such factors as: the orientation of the geologic units, the presence of groundwater discharge and the location of vegetation. Conceptual models of groundwater discharge were developed as a result.

4.7.1 Modes of groundwater discharge

All springs and streams that were observed occur within natural drainage lines, and generally occur where the local topography intersects a groundwater table. Three different modes of groundwater discharge were observed within the study area, these included, (1) progressivedischarge from the intersection of the water-table and topography, (2) discharge from the Tertiary Sequence/Brockman Iron Formation (TR/BRF) contact and (3) Structurally controlled discharge.

4.7.1.1 Water-table intersection

This form of discharge is thought to supply the majority of the water to all the Gorges (excluding Circular Pool). It occurs where the main drainage channel within a catchment deepens to the point at which it intersects the regional water table (Figure 4.11). The length over which this occurs is highly variable across the gorges; at Joffre Gorge water was observed to be seeping from the ground up to a couple of kilometres from the head of the Gorge. This water table from which discharge is occurring is situated within the TR aquifer, and the drainage channels are typically lined with vegetation.

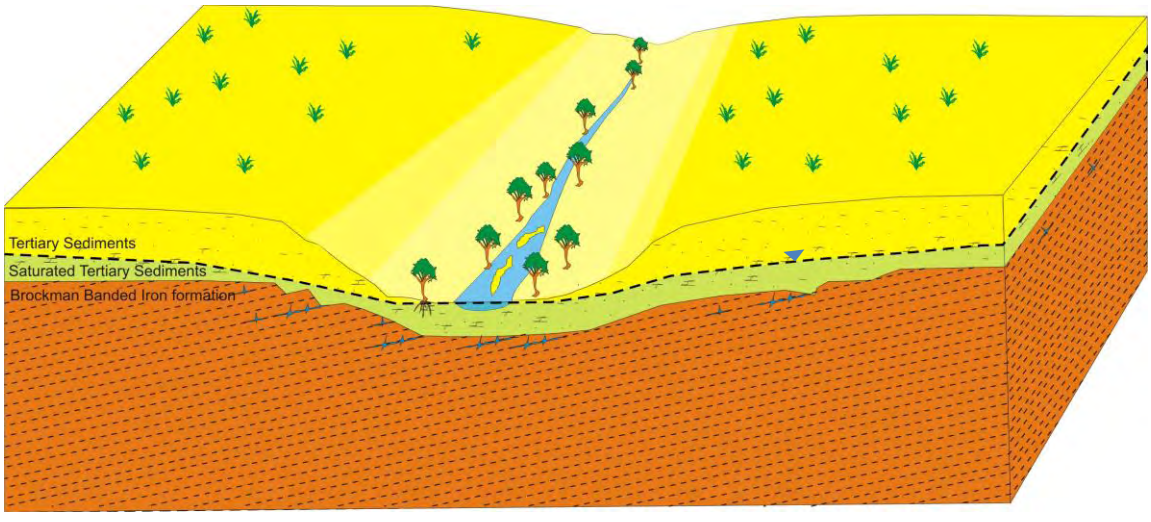

Figure 4.11 Intersection of Water table and Topography groundwater discharge

4.7.1.2 Tertiary-Brockman Boundary discharge

As the drainage channel deepens further, BRF bedrock begins to outcrop defining the head of the gorge. At this point the contact between the Brockman Iron Formation and Tertiary material outcrops and groundwater discharge occurs. There is a significant variation in permeability between these two units and therefore groundwater will naturally exhibit horizontal flow along this feature. Vegetation was observed to line the edges of each gorges indicating the presence of this mode of discharge.

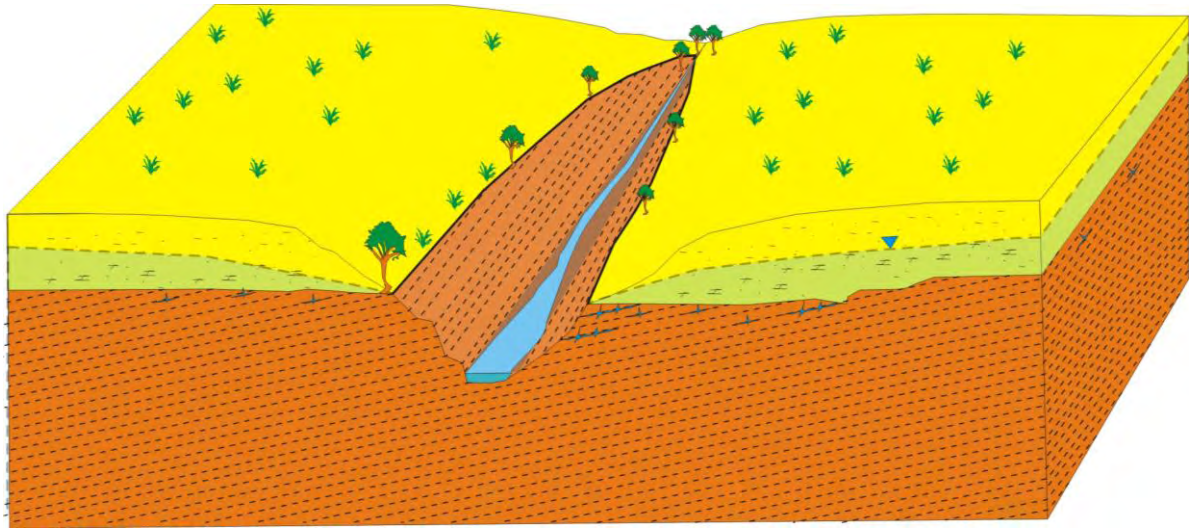

Figure 4.12 Discharge from TR-BIF boundary

4.7.1.3 Structurally Controlled Discharge

On rare occasions groundwater is also discharged from the bedrock fractures on the gorge walls. This was observed at both Knox, Dales and Kalamina Gorge, where a significant amount of water was seen to seep from the rock face. It is thought that this discharge is controlled by the structure of the BIF as it was only ever noted on a single side of the gorge (Figure 4.13). Groundwater percolates downwards through the fractures in the BIF which are a conduit for flow. The banded nature of the BRF bedding orientation creates a direction for the groundwater to flow. In a number of locations a white precipitate was seen below fractures, this suggests that groundwater discharge occurs at these locations (perhaps during wetter periods when the water table is higher). Vegetation was observed on the gorge walls located presumably where this discharge process was occurring (Figure 4.13).

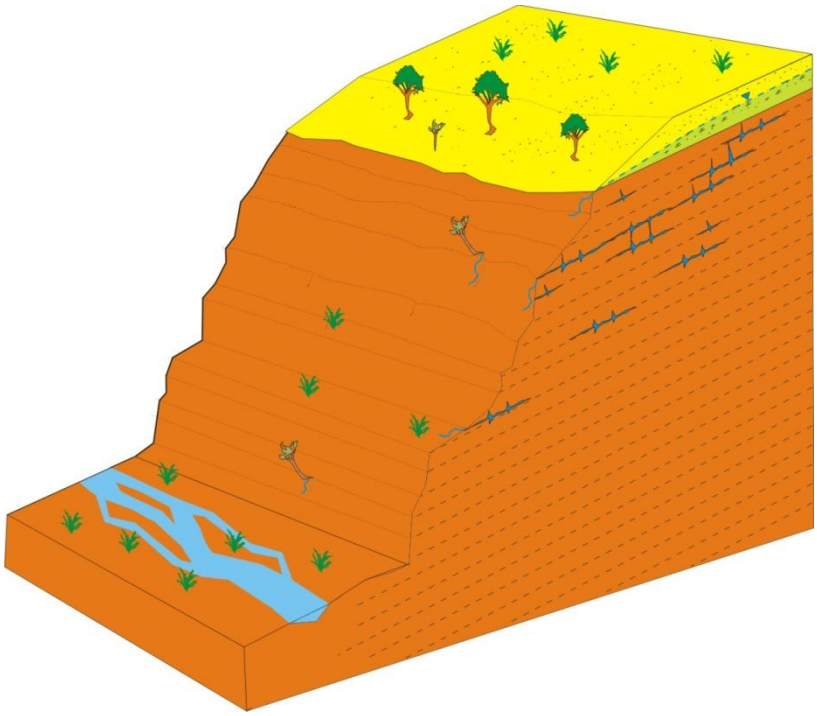

Figure 4.13 Discharge from bedding planes and fractures within a typical gorge. Discharge is structurally controlled by bedding plane orientation. Vegetation is often located on the gorge walls where discharge is occurring

4.7.2 Circular Pool: Case Study

At Circular Pool both structurally controlled and TR-BIF contact groundwater discharge is exhibited. Circular Pool is a good location to illustrate the above concepts, as the stratigraphy and groundwater discharge is clearly observed in the cliff face.

The top unit visible at Circular Pool is composed of cemented Tertiary alluvials, below this is a BIF conglomerate layer cemented with Teritary material, that overlies the BRF bedrock (Figure 4.14). The BRF varies from highly weathered to fractured to fresh bedrock down the succession. Groundwater is clearly visible discharging at both the TR-BRF boundary, and lower down the face from fractures in the BRF. The discharging groundwater is sourced predominantly from lateral flow along major contacts, however there will be a minor component of vertical flow from infiltration. Vegetation was also observed to exist where groundwater discharge was occurring (Figure 4.14).

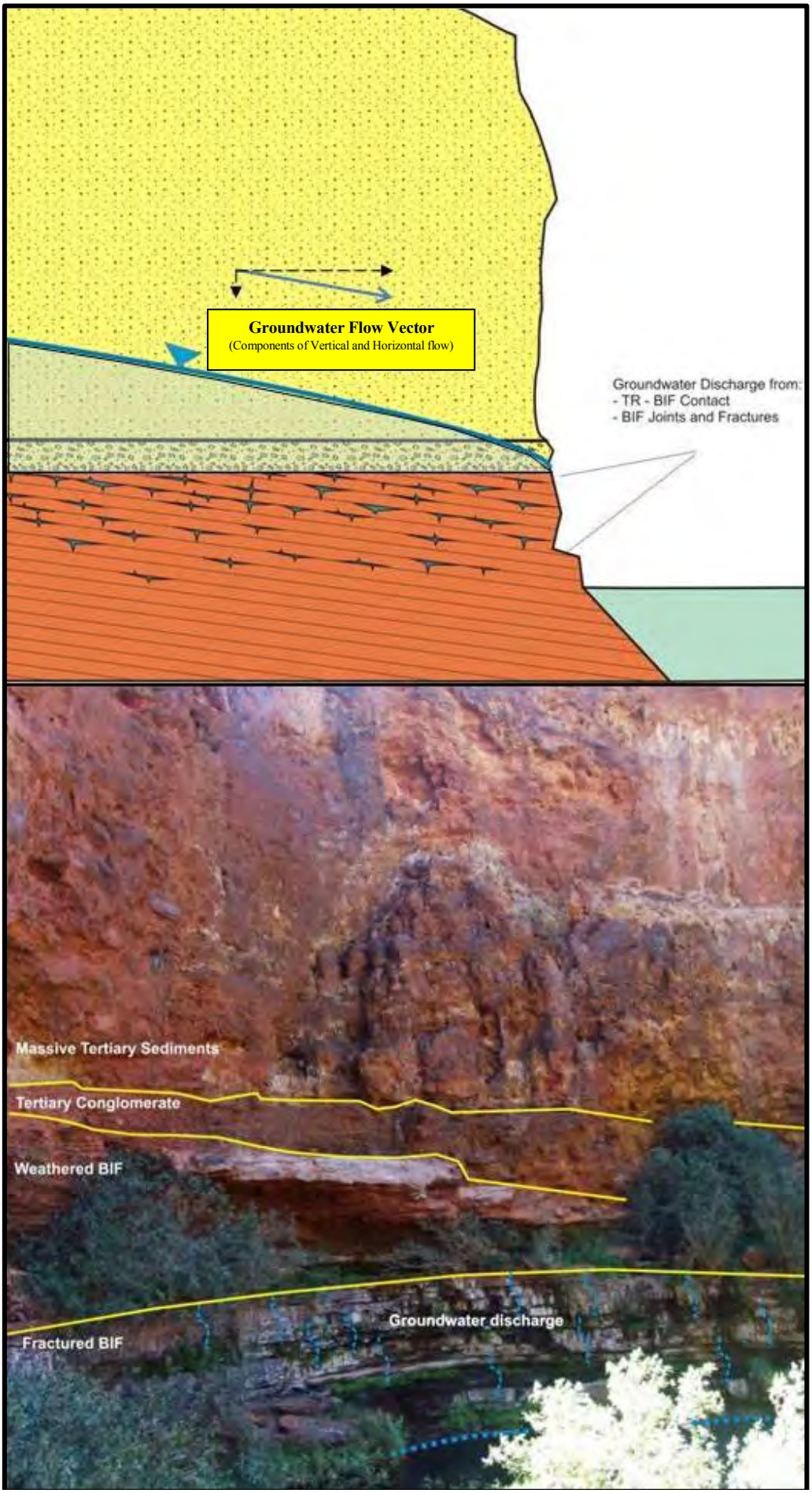

Figure 4.14 Conceptual discharge of groundwater at circular pool. Top: Hydrogeologic Cross-section; Bottom: Cliff face with individual lithologic units labelled (note location of vegetation)

4.8 Defining the Surface Water Catchments

An important aspect of any hydrogeological study is to clearly define various characteristics of the surface water catchment that contribute water to each sample location in the KNP. Remote sensing and GIS interpretation has been effectively used to determine catchment characteristics, including; catchment size, areal extent of various geological formations and the distribution of native vegetation.

The initial step was to define the boundary of each catchment. Remote sensing can be used to understand the surface water flow patterns in the catchment, displayed as a network of drainage lines. This information was displayed and analysed in the form of a hydrology layer within GIS software "ArcGIS". The software allowed the connectivity of the drainage lines to be determined and the extent of all the drainage lines that connect to a single sample location is considered its' catchment (Figure 4.15).

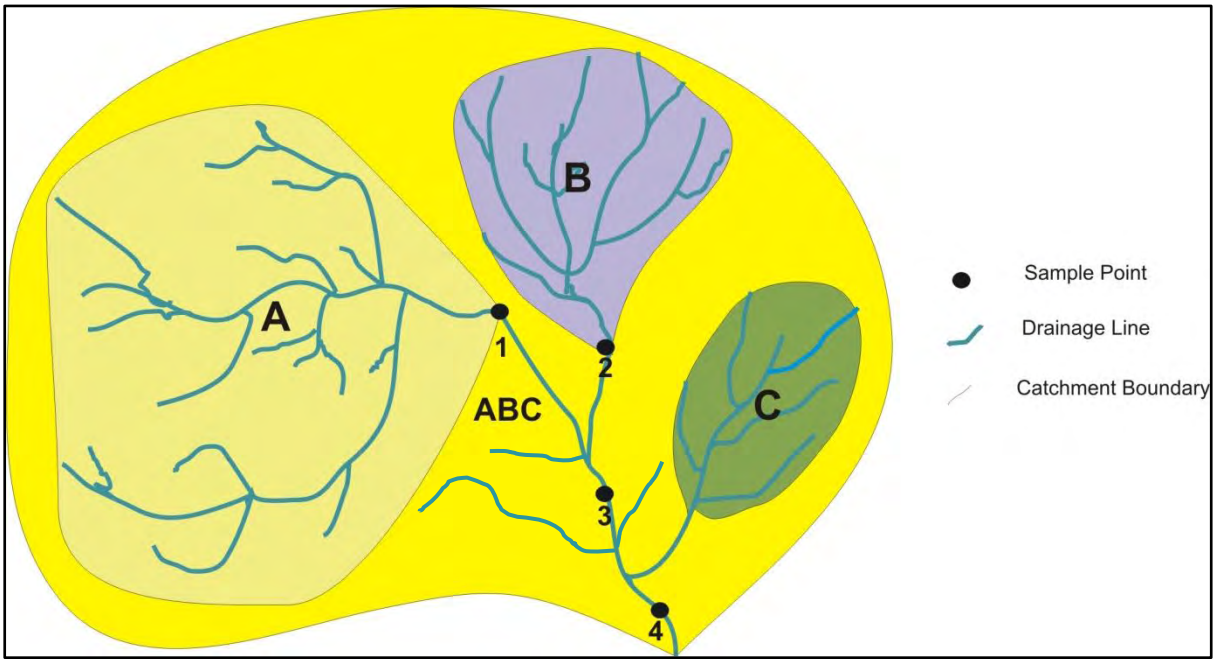

Figure 4.15 Example of a catchment demonstrating how different sample points will reflect different sections of the overall catchment

The figure above illustrates the relationship between a single sample point and its surface water catchment. An example is given for a hypothetical sample collected at four sample locations. The water that is collected at sample point 1 is sourced from Catchment A and

likewise the water that is collected at sample point 2 is sourced from catchment B. Both catchments A and B are considered the surface water catchment for the water collected from sample point 3. Catchment A,B and C all contribute to the sample collected at sample point 4. They can be grouped together to form catchment ABC. The water chemistry at sample point 4 will therefore represent a mixture of each of the three catchments, and the relative input from each contributing catchment should be considered. Once the catchment boundaries have been defined (Figure 1.3) then other physical properties which are of use for hydrochemical studies can be identified. For example, these included the area that different geological units cover, variation in vegetation cover, and the average flow path length.

The proportion of Tertiary material in each catchment was calculated by overlaying the catchment boundaries on a geology map (Thorne, 1996) and undertaking area calculations (Figure 1.10). This was undertaken in GIS program "GPS Utilities". Remote sensing can also be used to infer where water tables are high due to the presence of increased vegetation around flow lines and also from visible surface water.

Catchment	Area (Km^2)	Area of Tertiary	Area of BIF	Other units
Hamersley Gorge	191	35.6	114	41
Weano Gorge	11.0	7.58	3.46	-
Knox Gorge	55.6	24	31.6	-
Kalamina Falls	23.8	15.27	8.53	-
Joffre Falls	340	153.1	194	8
Hancock Gorge	30.8	21.3	9.54	-
Dales Gorge	348	131.8	208	8
Circular Pool	66.5	26.8	39.7	-

Table 4.8 The relative proportions of the total area and outcrop area for each identified catchment.

Chapter 5

Investigating Groundwater Evolution

5.1 Introduction

This chapter investigates the relationships observed within the Stable Isotope and Hydrochemical signatures of the surface and ground waters sampled within the study area. The primary aim is to develop an understanding of the chemical and physical processes that are occurring within the hydrologic cycle, that act to evolve the chemical composition of the natural water.

Understanding how the composition of the water evolves is the key principle behind determining whether two bodies of water are hydraulically connected. This concept is illustrated in the flow diagram below.

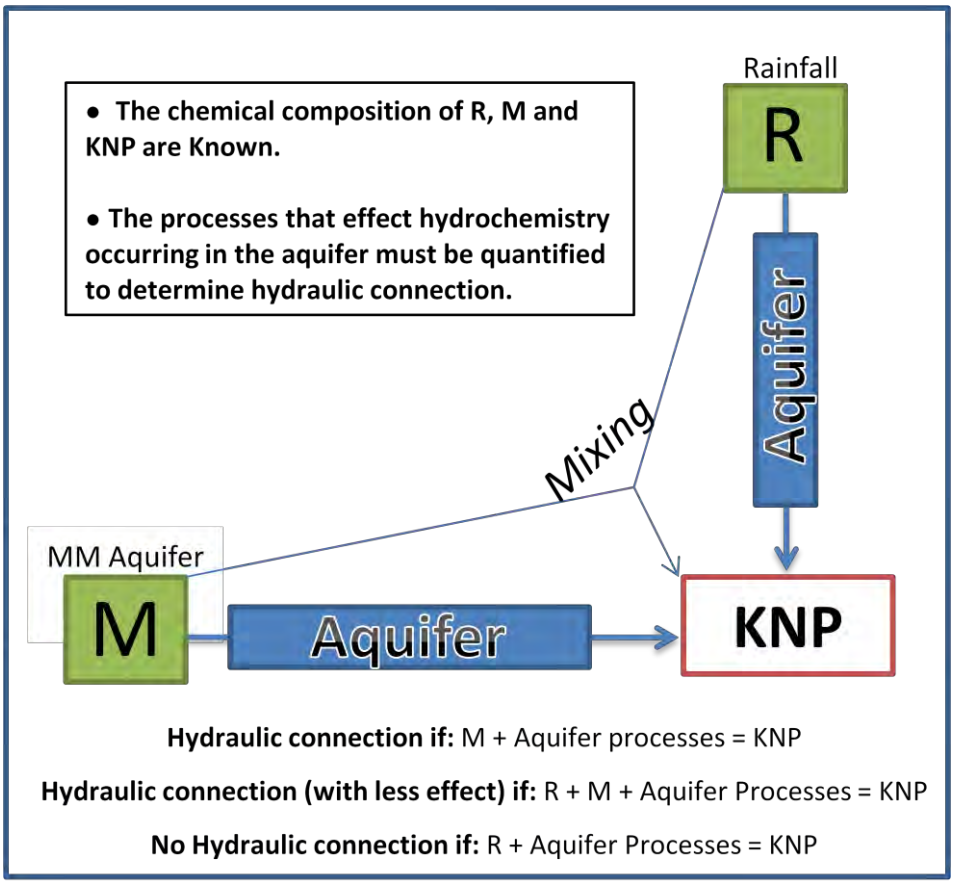

Figure 5.1 Flow diagram to illustrate the concept of understanding physical and chemical aquifer processes to determine hydraulic connection

5.2 Stable Isotope Characteristics of Rainfall and Groundwater Recharge

Stable Isotopic data can give an insight into the rainfall trends and how groundwater recharge is occurring. The isotopic data presented in Figure 4.6 and Figure 4.7 shows a variation in the pattern of stable isotopic ratios between the surface water and the ground water.

The groundwater exhibits a consistently depleted ratio ($\delta^{18}O$: - 9.55 to -8.52 ‰; δD: -64.1 to -56.4‰) this is due to the continental effect, which causes a progressive enrichment of ^{16}O the water vapour as it moves inland, while the surface water shows progressive modification along a linear regression line ($\delta\ ^{18}O$: -9.04 to -2.37‰; δD: -60.8 to -29.5‰). These patterns can be seen in Figure 5.2

Once water is within an aquifer (and isolated from the atmosphere), its isotopic signature is unlikely to change unless groundwater mixing occurs. Figure 4.7 indicated that the groundwater data correlated relatively closely to the LMWL. Considering this, and the fact that the groundwater exhibits such a narrow isotopic range, suggests that very little evaporative modification is occurring prior to recharge. For an arid region (where evapotranspiration greatly outweighs precipitation) this is somewhat surprising.

It is therefore likely that groundwater recharge only occurs when there is heavy and intense precipitation when ET values are low, and this type of rainfall is typical of the cyclonic events which occur in the area. Rainfall during these times must quickly infiltrate into the groundwater system before any significant evaporation can occur. Figure 1.6 illustrated the large amount of surface water that accumulates during these events, which allows rapid infiltration to occur.

It is likely that the lighter rainfall that frequents the area does not contribute to groundwater recharge as it is quickly evaporated before significant infiltration occurs. If it did infiltrate into the aquifer then it would be expected to observe highly enriched isotopic signatures in the groundwater due to evaporative fractionation, this does not occur.

Another factor is that during rainfall the enrichment of δD and $\delta^{18}O$ during intense periods of rainfall under high ambient temperatures is likely to be less, compared to that which occurs during small rainfall events at the same temperatures. This is of the 'Amount Effect' (Clark and Fritz, 1997) which states that "The evaporation of falling raindrops during intense rain is less than during light rainfall". Therefore, precipitation that potentially recharges aquifer systems in such arid areas is isotopically lighter.

Once this groundwater is discharged (as surface water) it is once again exposed to the atmosphere and subsequent isotopic modification. The surface water regression line (Figure 4.6), with a slope of 4.6, suggests that progressive modification likely due to evaporation.

As the groundwater all exhibits a similar isotopic signature, the variation in enrichment of the surface water samples is directly proportional to the amount of evaporation that has occurred subsequently to its exposure to the atmosphere.

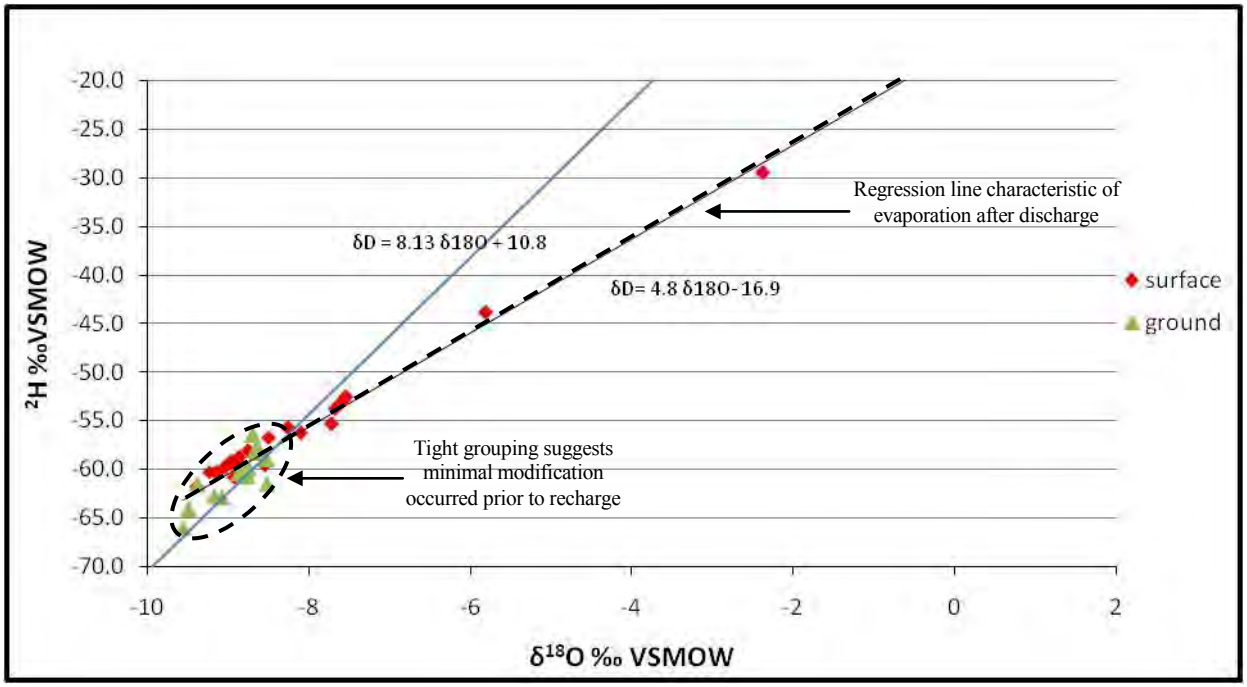

Figure 5.2 The relationship between H and O for Surface and Groundwaters of the Karijini National Park, illustrating the groundwater recharge discharge processes occurring.

5.3 Investigating Catchment Scale Trends

5.3.1 Catchment Area versus TDS concentration Trend

The Isotope data showed that groundwater over the study area is derived from intense rainfall events that have not been significantly affected by evaporation. Although the geologic units are similar across the study area, there is however a large variation in TDS concentration and chemical composition from various aquifers, surface water pools and gorges. This raises the question.

“What is causing the significant variation of TDS concentrations observed across all sample locations?”

It was observed from the field data that the samples collected from small catchments exhibited low TDS concentrations. Aquifer mineralogy and catchment characteristics therefore may have an influence on the variation and composition of the TDS concentrations. To investigate the relationship between catchment size and TDS concentration, the average TDS concentration of the water from each gorge was plotted against the area of its catchment (Figure 5.3). The plot reveals a positive linear trend with a moderate relationship (R^2 = 0.56) and with low TDS concentrations corresponding to small catchment size.

This trend could be explained by a number of factors:

- The greater the area of the catchment, the longer the groundwater travels through the aquifer, allowing more water-rock interactions.

- The larger the catchment, the more surface area, and therefore more evapotranspiration, causing increased ionic concentration.

- The larger catchments have a higher proportion of Tertiary material which is thought to be more reactive in water-rock interactions.

These factors can all be investigated separately to determine which is the most influential on the observed trend.

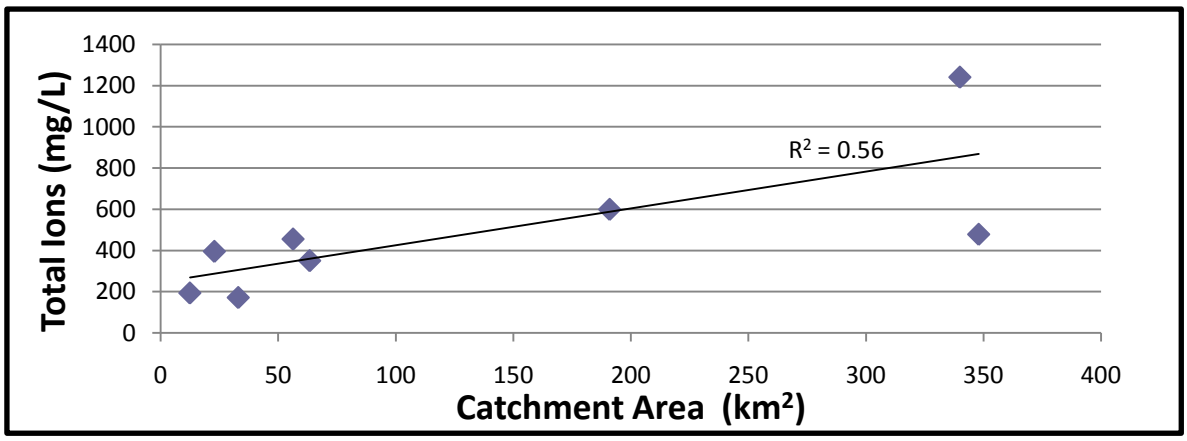

Figure 5.3 The Relationship between the sum total ions versus catchment area.

5.3.2 Length of Flow path from recharge to discharge

To determine whether the length of the flow path has any impact on the TDS concentration of groundwater, Mg:Ca ratios were explored, due to the theory discussed in Section 2.34.

Samples from Southern Fortescue Borefield (Figure 3.4) were used to investigate how the Mg:Ca ratio varies with the length of flow path. These were chosen as they are located progressively down the hydraulic gradient. Increases in Mg:Ca ratio with distance down-gradient were observed (Figure 5.4). It is proposed that the observed increase is due to progressive water rock interaction, including processes such as dissolution of dolomite and calcite precipitation (which may occur in aquifer voids).

Magnesium concentration would tend to increase along the flow path of a ground water undergoing such processes, until a high Mg:Ca ratio is reached (Plummer, 1977; Lohmann, 1988; Wigley, 1973;). This is especially relevant in an arid environment like the Pilbara where carbonate precipitation is commonly observed as white staining where groundwater seepage exists (shown by XRD analysis). HCO_3- concentration was also noted to increase down gradient, possibly as a result of carbonate weathering and/or silicate hydrolysis.

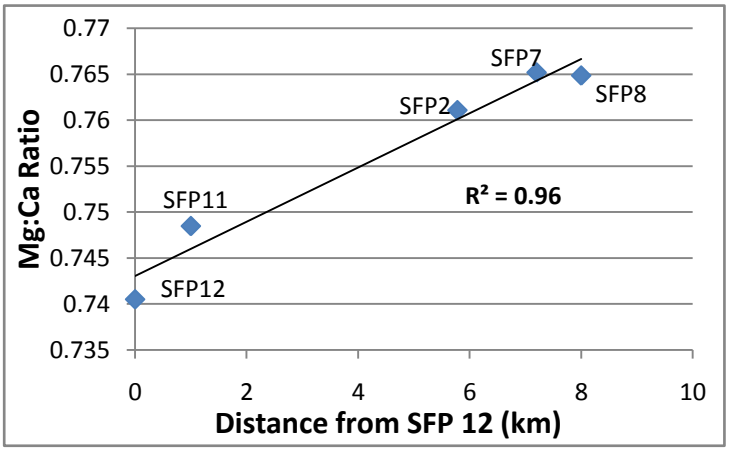

Figure 5.4 Investigating the relationship between Mg:Ca and flow path distance.

5.3.2 Evapotranspiration and Catchment area

To investigate whether the size of the catchment has any effect on the amount of evapotranspiration that occurs, Cl^- was used and was plotted against catchment size. Chloride is a conservative tracer as it is primarily derived from rainfall, is very soluble, does not precipitate out of solution until very high concentration and is not significantly adsorbed on mineral surfaces (Hem, 1985). It is therefore an ideal indicator of evaporation, its concentration in groundwater will reflect the amount of evaporation that has occurred. The plot shows a positive relationship does exist between catchment size and evaporation, however there is a poor relationship (R^2= 0.46) which suggests that a larger catchment area does not necessarily result in increased evapotranspiration.

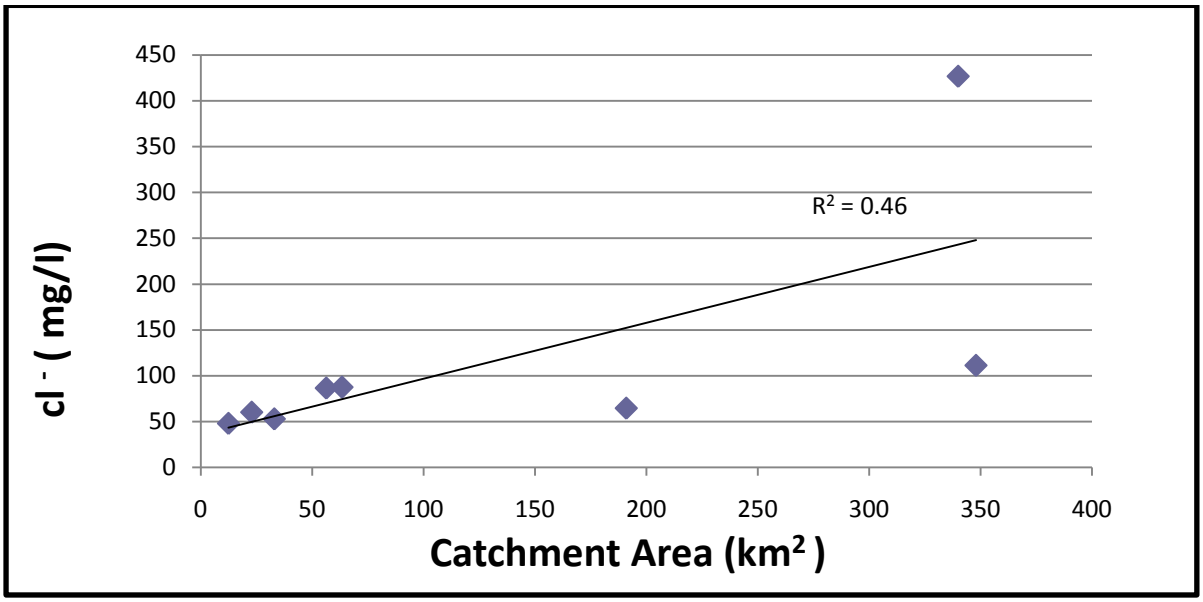

Figure 5.5. The relationship between Cl^- and catchment area for samples collected in KNP to investigate the influence of catchment size on ET

5.3.3 TDS concentration relative to proportion of Tertiary material

The next factor to be investigated is how the unique geology of each catchment determines the groundwater TDS concentration. Each catchment has a varying proportion of Tertiary material to BIF outcrop. The Tertiary material is assumed to be significantly more reactive in the presence of water as it is a deeply weathered sedimentary material. The total area of Tertiary material was plotted against the sum of the major ions.

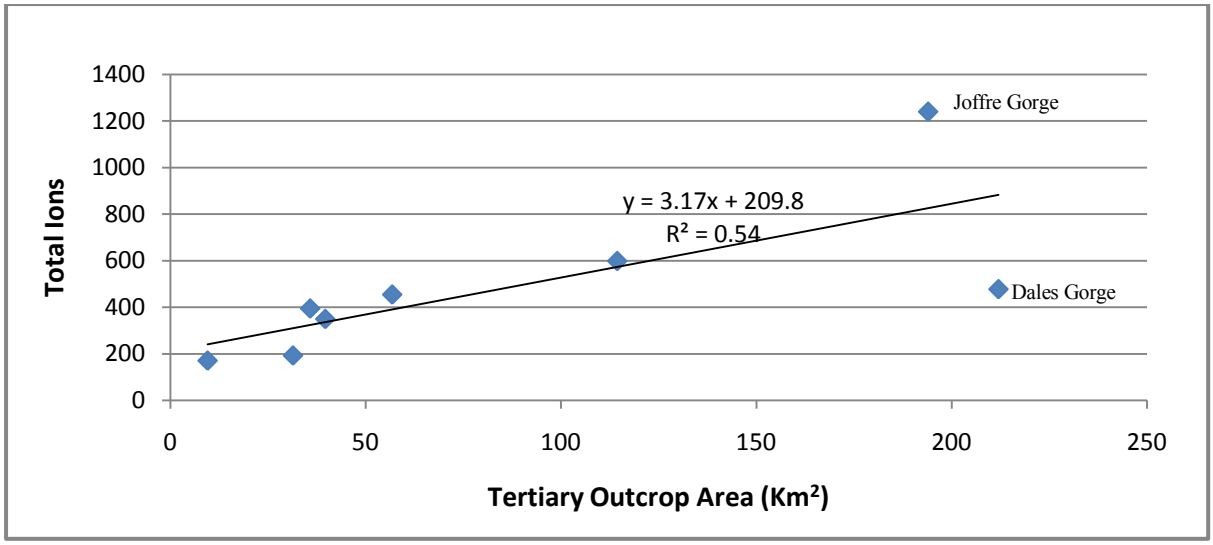

Figure 5.6 The relationship between total dissolved ions measured in solution and the tertiary outcrop area.

There was a positive moderate relationship between the TDS concentration and increasing area of Tertiary outcrop in each catchment. However, there are still two anomalies created by Dales Gorge and Joffre Falls catchments. The anomaly of Dales Catchment is created as it is the largest of the catchments, however it displays an unexpectedly low ionic concentration.

If this anomaly is excluded from the plot then the relationship between Tertiary Outcrop area and TDS increases from 0.54 to 0.95 (Figure 5.7). This reveals that the point representing Joffre Falls Catchment is in fact no longer an anomaly.

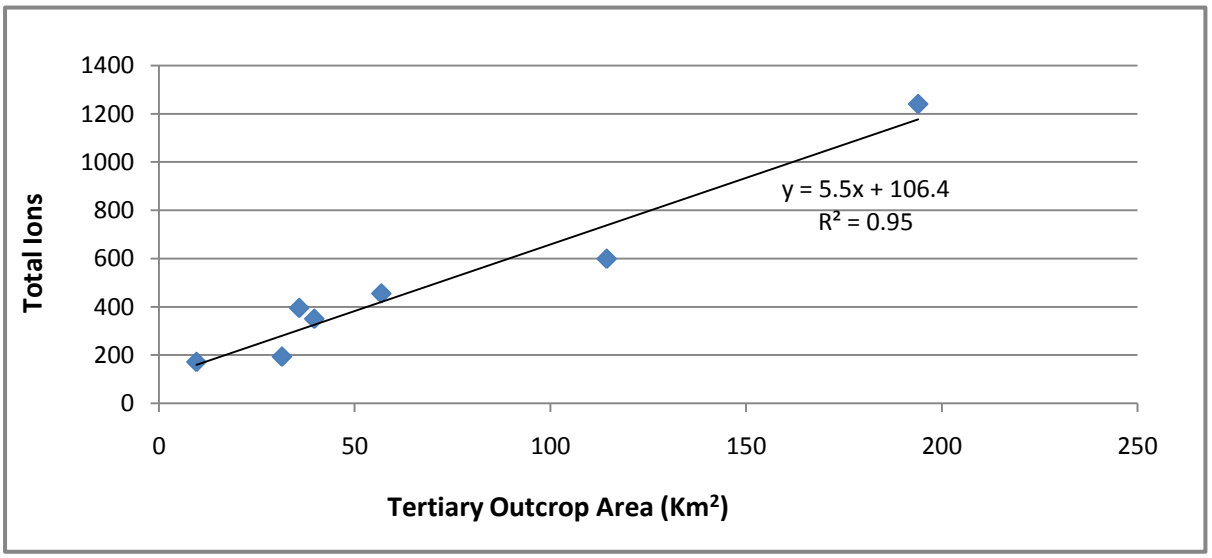

Figure 5.7 The relationship between total dissolved ions measured in solution and the tertiary outcrop area. (Excluding Dales Gorge Catchment)

5.3.4 Investigating the Dales Gorge Catchment Anomaly

The anomaly that Dales Gorge catchment creates on the above plots is somewhat puzzling as all the other catchments appear to follow a common trend. The reason for this anomaly may be explained by looking at the boundary of the catchment in more detail.

The Dales Gorge catchment is dominated by a network of ridges and valleys, and there is a possibility that the large catchment may be split into smaller sub-catchments. Each smaller catchment may contribute a different amount of water to the total volume that is discharged at Dales Gorge, and therefore these different proportions may influence the hydrochemistry of the groundwater discharging at Dales Gorge.

By comparing the water chemistry at the three locations sampled within Dales Gorge catchment it reveals that there is a similarity between the samples collected from within Dales Gorge (Fern Pool, FS Falls, FS2) and from the Visitors centre bore (VC1) as seen in Table 5.1. However the sample collected at the upstream Rangers Station (RS1aGW) exhibits a much higher concentration of dissolved ions.

Location ID	*Cl*	*SO_4*	*HCO_3*	*Ca*	*Mg*	*K*	*Na*	*Br*	*EC (uS)*	*Temp (^oC)*	*Type*
Rangers Station	758.9	405.3	351.6	181.7	166.1	31.5	228.3	4.6	3640	28.1	GW
Visitors Centre	120.8	35.6	97.6	17.3	25.1	8.6	45.9	0.3	649	27.4	GW
Dales Gorge	113.2	18.9	167.3	29.1	27.0	8.8	48.7	0.5	678	23.4	SW

Table 5.1 Comparison of major ion concentrations at Dales Gorge Catchment Locations.

By analysing geological maps and topography it appears that Dales Gorge could be split into two catchments. Figure 5.8 shows the two shaded areas identified as operating separately within the larger catchment. Area 1 and 2 are separated by a BIF ridge which is 835m high (dotted line) and assuming that the surface topography indicates subsurface hydrogeology, the only connection between area 1 and are 2 is a narrow opening in the BIF ridge which is 696m high, shown by the arrow in Figure 5.8. If this is the case then it is likely that the majority of the water which was sampled at Dales Gorge is primarily sourced from catchment area 1, with minimal input from catchment area 2.

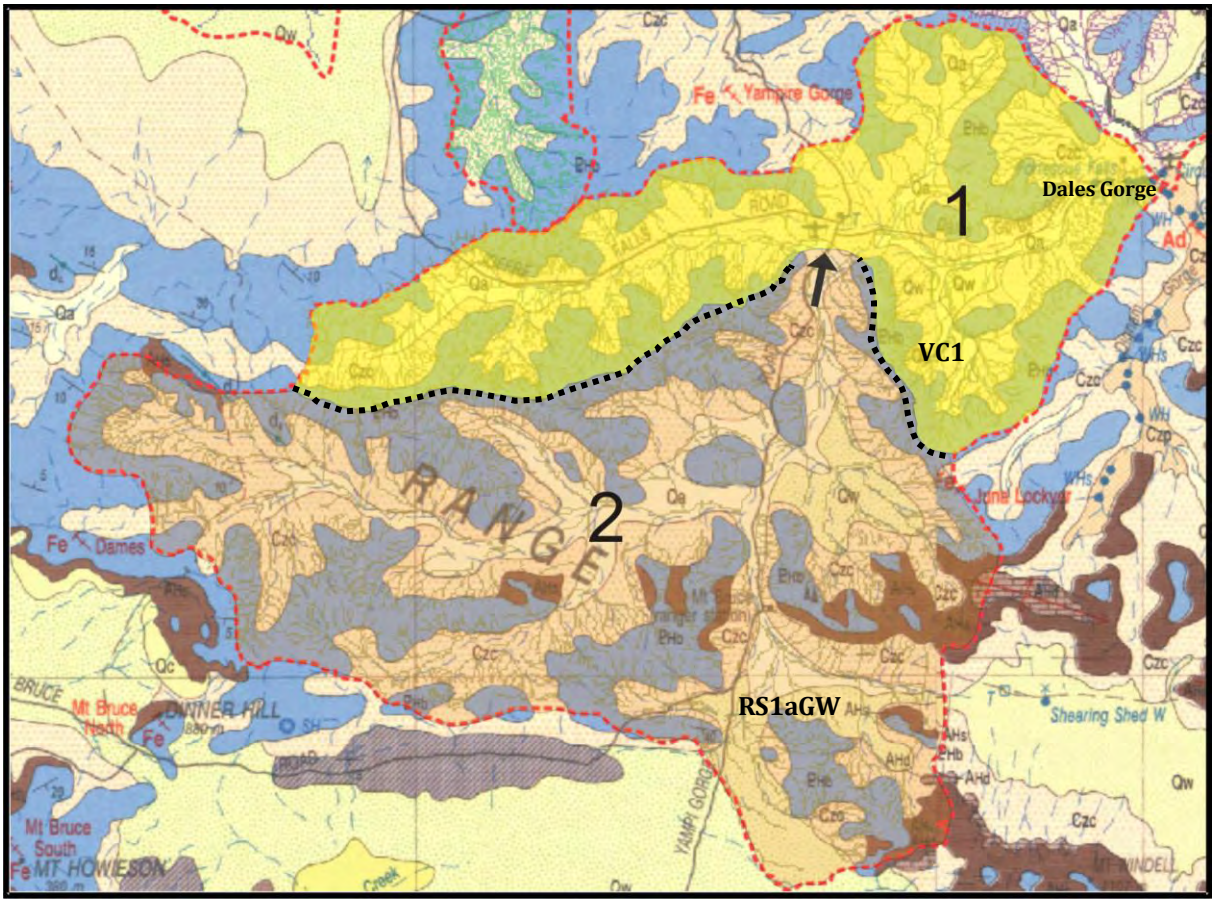

Figure 5.8 Dales Gorge catchment divided into two sub-catchments (for legend see Figure 1.10)

The reconsidered catchment parameters are as follows:

Catchment	Total Area (km^2)	Area of BIF (km^2)	Area of Tertiary(km^2)
DG- Catchment Area 1	119.1	64.1	55
DG-Catchment Area 2	157.2	60	97

Table 5.2 Total area, BIF outcrop area and Tertiary outcrop area determined for Dales sub catchments

If the values for catchment area 1 is used to re-plot the graphs in section 5.3 then a much better relationship exists for both total Catchment Area vs Total Ions and also Area of Tertiary vs Total Ions (Figure 5.9). The relationship of the Catchment area vs total ions plot improves from R^2 = 0.56 to 0.91, while the Tertiary outcrop area vs total ions plot relationship improves from R^2 = 0.54 to 0.94.

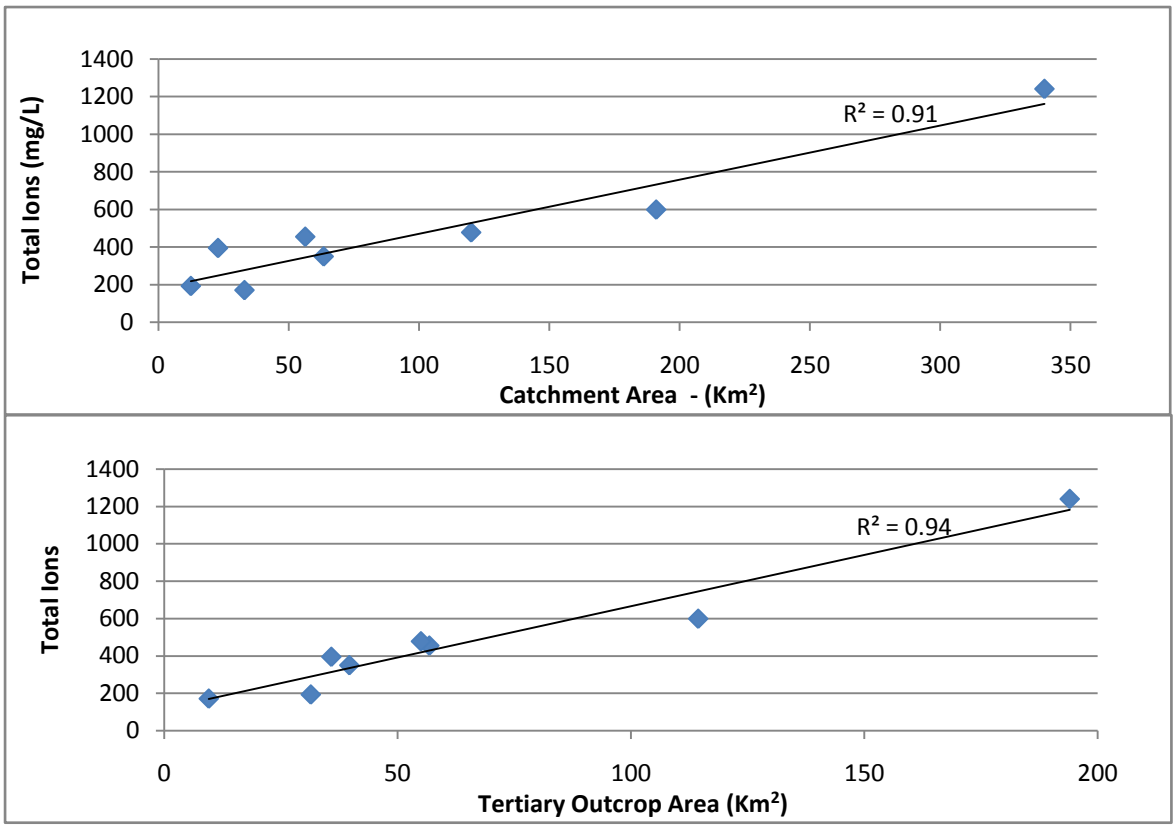

Figure 5.9 Revised plots of catchment area and tertiary outcrop area vs Total Ions for Dales Gorge sub-catchment 1 (excluding Dales Gorge Sub-catchment 2)

5.3.4.1 The High Salinity of Dales Gorge Sub-Catchment 2

By excluding any groundwater input from sub-catchment 2 to the overall discharge at Dales Gorge, the relationsip was dramatically improved. This may suggest that if there is any input flows from Sub-catchment 2 to sub-catchment 1 through the opening in the BIF ridge (shown by the arrow Figure 5.8) then it is very minimal with insignificant effect on the overall hydrochemistry.

This could then be the reason for why the sample collected from sub-catchment 2 was highly concentrated in dissolved solutes. As if minimal discharge is occuring then the sub-catchment is effective a closed basin with a lack of groundwater movement. This will allow and increased amount of time for mineral dissolution to occur and perhaps transpiration from deep rooted vegetation.

5.4 Groundwater Evolution from Evapotranspiration

5.4.1 Introduction

The previous section established that there is significant variation in the water chemistry of the water bodies of the KNP. Various trends were identified between catchment parameters and TDS concentrations. The following section expands from this, and aims to determine the influence of evapotranspiration on groundwater recharge and solute concentrations in groundwater.

5.4.2 Determining the processes involved in hydrochemical evolution

A useful tool to decipher the chemical and physical processes that affect the concentration of dissolved ions in groundwater is through the depiction of chemical species on binary diagrams. Each major ion has been plotted against Cl^- which is commonly used as a reference, as in most groundwater systems it is considered a conservative ion (Drever, 1988). Cl^- is primarily derived from rainfall, it is very soluble , does not significantly enter into oxidation or reduction reactions, forms no important solute complexes with other ions unless the Cl^- concentration is extremely high, does not form salts of low solubility, is not significantly adsorbed on mineral surfaces, and plays few vital biochemical roles (Hem,1985). Therefore the concentration of Chloride in groundwater is dependent on the level of Evapotranspiration that has occurred. The 'cyclic wetting and drying' process (discussed in section 2.2.2) is not thought to be important because the recharge waters do not evaporate to dryness within the soil zone, as shown by the depleted isotopic signature suggesting little evaporative effect before recharge.

The sea-water dilution line (SWL) is also added to the diagram to investigate the influence of evapo-concentration. The SWL defines the chemical progression of rainfall, which should contain solutes at the same ratio as sea-water, due to evapo-concentration. If an ion is purely sourced from rainfall and no precipitation occurs then the progressive evaporation of water will cause the concentration to follow the SWL. Therefore if any processes other than evaporation affect the concentration of a solute in solution, then this will show up as a depletion or excess relative to the seawater line. The plots shown in Figure 5.10 illustrate the trends for all the data collected in the KNP.

The relationship between K^+ and Cl^- is linear and the data all correlates to the SWL. This suggests that K+ is introduced to the system via the dissolved solutes that exist in rainfall. The same is the case for Na+ however at the higher concentrations there is a deficit seen in Na+. This may indicate that Na^+ removed from solution as concentrations increase, perhaps due to ion exchange on clays.

The plots of Cl^- versus Ca^{2+}, Mg^{2+}, and HCO_3^- all show an excess concentration relative to the seawater. Their concentrations can therefore be either attributed to mixing with water bodies that have excess Ca^{2+}, Mg^{2+} and HCO_3^-, or to progressive mineral dissolution. Dissolution of a carbonate is a common process that could be responsible for addition of theses ions to solution.

A number of the samples are depleted in SO_4 relative to the sea-water dilution line. These correspond to the relatively fresh water samples from pools of Weano and Hancock gorges. These samples were collected from stagnant water with significant biological activity as is evidenced from high pH. This may indicate the presence of microbial reduction of sulphate.

Drever (1988), also attributes the reduction of sulphate to the precipitation of anhydrite. This occurs in the presence of high Ca^{2+} concentration and elevated temperatures, both of which are present at the point of groundwater discharge.

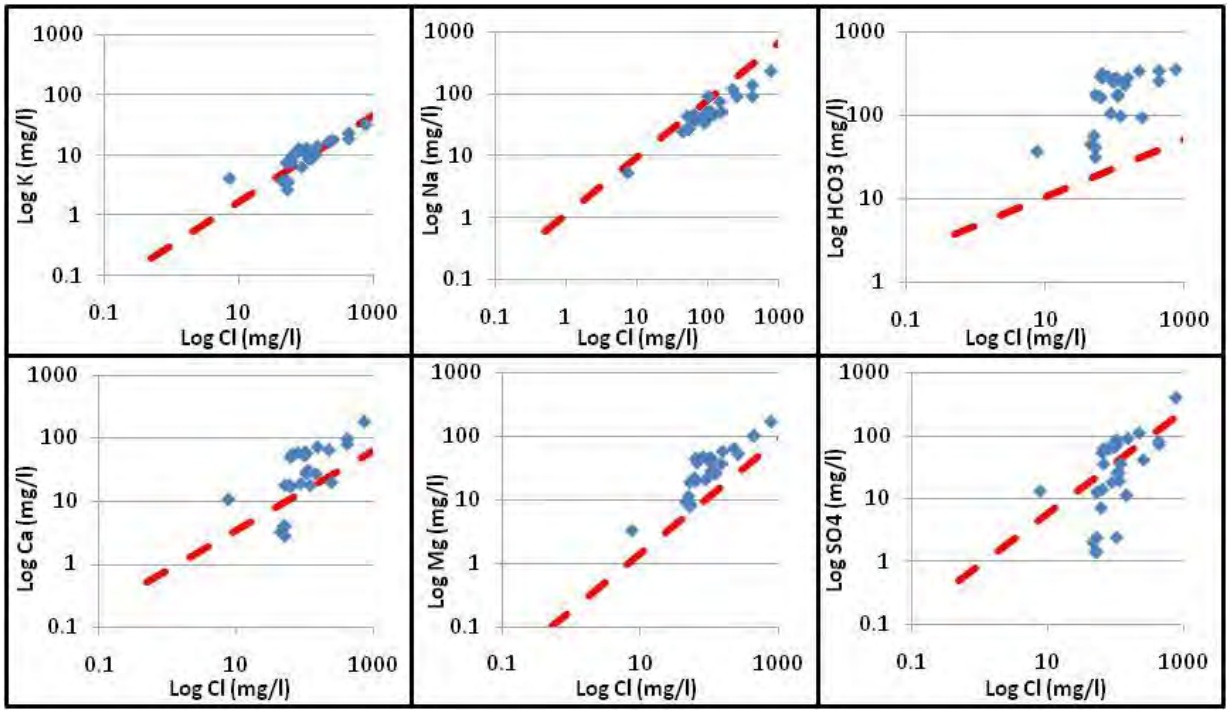

Figure 5.10 Inter-elemental relationships to illustrate the sources of ions (SWL = — — —)

5.4.3 Characterising Evapotranspiration and groundwater recharge

The inter-elemental relationships shown in Figure 5.10 indicate that evapotranspiration is a key process in the evolution of the groundwater within the study area. However the groundwater isotope signature suggested that minimal evaporation was occurring before recharge. Therefore, characterising how and where evapotranspiration is occurring will provide valuable insight into how groundwater recharge processes are occurring in the area.

A common method is to investigate the relationship between Stable Isotope δD and Cl^- (Abdalla, 2007; Zagana et al, 2007). This can give an insight into evaporative processes in the unsaturated zone. As stated earlier, the Cl^- ion can be assumed to be conservative, and therefore the only process that will increase Cl^- concentration in water is through loss of solution through evapotranspiration. The amount of evapotranspiration that is occurring can be estimated by comparing the Cl^- concentration of the sampled waters with that of the cyclonic rainfall. Evaporation will also cause the enrichment of δD in the remaining solution.

The relationship between δD and Cl^- for all the water samples collected in the KNP is illustrated in Figure 5.11. It has been separated into ground and surface water, with the groundwater isolated from the atmosphere and therefore only subjected to enrichment processes during recharge. While surface water is in continual contact with the atmosphere and subsequent modification, it is therefore expected to see variation in the two groups.

5.4.3.1 Groundwater Trends

If evaporation was occurring prior to recharge then an increase in Cl^- concentration would be expected, along with enrichment of the stable isotopes. However the graph shows that the Cl^- concentration is increasing independently to δD (Figure 5.8). This non-fractionating water loss can only be explained by transpiration occurring in the recharge zone. Transpiration can act to concentrate salts in the soil while the residual water remains isotopically unchanged.

Transpiration is a non-fractionating process (Zimmermann et al., 1967; Dincer et al., 1974; Allison et al., 1982) where soil water is taken up by roots and released by the leaves therefore no partitioning can occur (Clark and Fritz, 1997). This process has been extensively shown through many studies. Zimmermann et al. (1967) showed that plants growing in

solution brought about no isotopic fractionation in the liquid remaining after transpiration had removed half the liquid. This same process has been assumed to occur with plants growing in wet soils.

Generally the differences in Cl^- concentration reflect the degree of transpiration that has occurred during infiltration. However it was also observed that in some catchments deep rooted plants were located along the drainage lines. This suggests that the water table was relatively high and that there is the potential for continual transpiration and subsequent concentration of solutes to occur along the drainage lines.

5.4.3.2 Surface water Trends

After discharge the surface water becomes exposed to the atmosphere and subsequently evaporation, this allows both isotopic enrichment and an increase in chloride concentration to occur. However the initial Cl^- concentration of the water at time of discharge will differ depending on the amount of transpiration that has occurred during recharge. This means that there is not a strong relationship seen between δD and Cl^- in the surface water samples. There is an anomalous data point which represent Banjima pool that exhibits the most enriched isotope value yet the lowest Cl^- concentration.

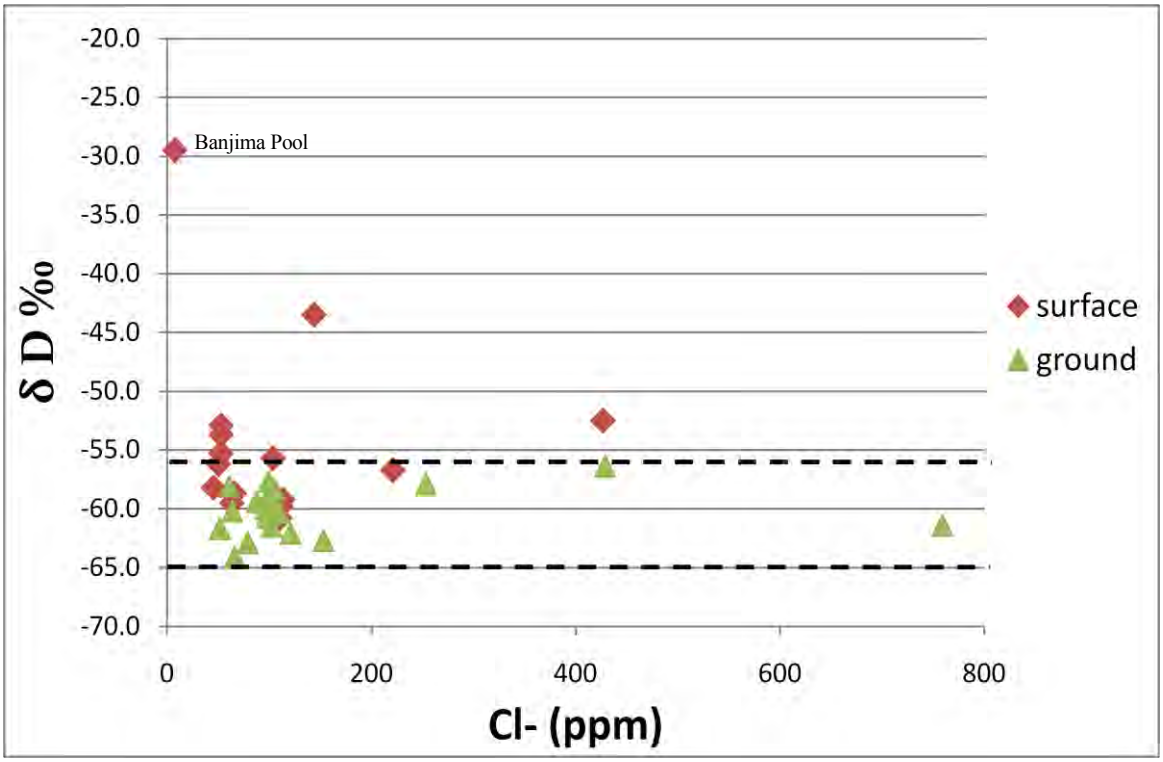

Figure 5.11 Relationship between δD and $\delta^{18}O$ The δD of the ground water lies in a narrow range of ±5‰, while the modified surface water obviously exhibits a broader range of δD‰ values (±15‰).

5.4.4 Summary of Recharge Process

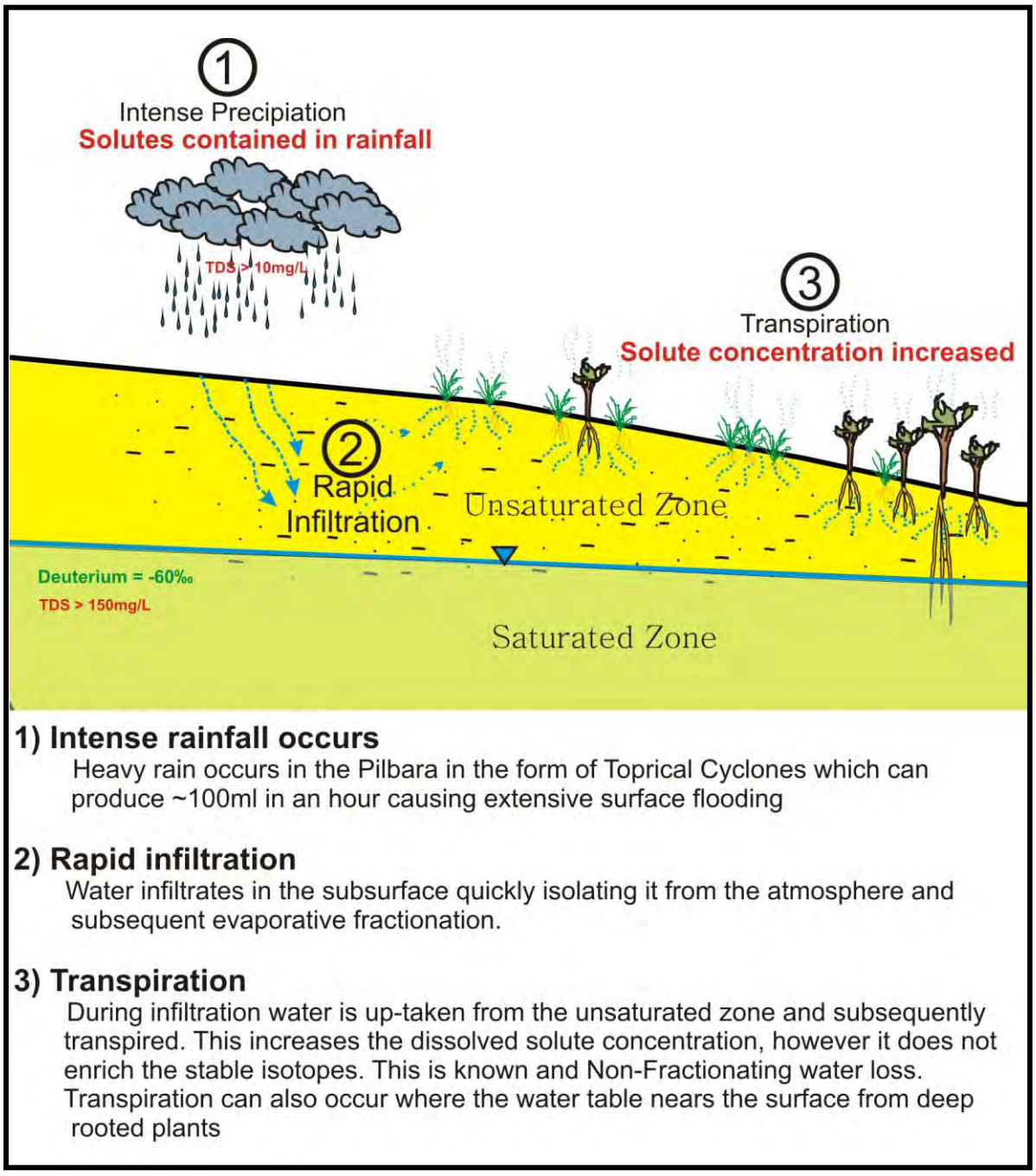

Figure 5.12 Summary of groundwater recharge process

5.4.5 Banjima Pool (Special case)

Banjima Pool is thought to be a collection of rainwater and for this reason it has been investigated separately. The interesting aspect about Banjima Pool is that it has a very low concentration of chloride, yet the most enriched isotope in the area. A comparison in the ion concentrations between Marandoo and Banjima Pool shows that the Marandoo concentrations are 10 fold higher than Banjima Pool.

5.4.5.1 Enrichment of Banjima Pool Case Study

To justify the highly enriched isotopic ration and low Cl^- concentration at Banjima Pool the following processes have been explored as possible explanations.

Evaporation

Evaporation has the effect of enriching stable isotopes through kinetic fractionation and it will also increase the ionic concentrations of the water. To demonstrate evaporation as the cause of the enriched isotope we must determine whether the amount of evaporation required to enrich the isotope will allow the Chloride concentration to remain the lowest in the study area. The Cl- concentration of Banjima Pool is 7.5mg/L. First we must assume that the dissolved chloride in the Banjima Pool is derived entirely from rainfall or surface water runoff. Rainfall and surface-water data from nearby Newman has shown Cl- concentrations of 4.3mg/L and 6.7mg/L respectively.

To determine the amount of evaporation that has occurred in the pool a simple mass balance can be undertaken with the Chloride concentrations. Using the equation :

$$Q = \frac{Clg - Clr}{Clg} x\ 100 \qquad \textbf{Equation 5.1}$$

where Q = the percent of water loss, Clg = the concentrations of chloride in Banjima Pool and Clr = the concentration of Cl in the rainwater or surface water.

The estimated water loss by evaporation was calculated using the data from Newman as an lower and upper limit. This resulted in an evaporation range of 10.6 to 42.6%.

$$\boldsymbol{Qrainfall} = (\mathbf{7.5} - \mathbf{4.3} / \mathbf{7.5})\mathbf{100} = \mathbf{42.6}\% \ (\boldsymbol{upper\ limit})$$
$$\boldsymbol{Qsurface} = (\mathbf{7.5} - \mathbf{6.7} / \mathbf{7.5})\mathbf{100} = \mathbf{10.6}\% \ (\boldsymbol{lower\ limit})$$

Evaporation of water prior to recharge not only increases the major ion concentration but also leads to enrichment in δD and $\delta^{18}O$ isotopes in the remaining water. Simpson and Herczeg (1991) found a δD enrichment of about 0.75‰ per 1 % evaporation loss in surface waters of the semi-arid regions of the Murray Basin by using a model by Gonfiantini (1986). Therefore using the evaporation range calculated above we can determine the amount of enrichment in δD to be between, 7.95 and 32‰. If we use the H value for rainfall of - 50‰ (Reeves et al) then we can expect the D value to be within the range of 18‰ - 42.05‰. The measured δD value in BJ (-29.5‰) is within this range, suggesting the plausibility of evaporation as a process responsible for stable isotope enrichment in BJ pool.

Vapour-Water Exchange

Another explanation is enrichment caused by isotopic exchange between the pool water and vapour above the pool. This process would alter the isotope signature without evaporation therefore it would not concentrate the ions in solution.

This exchange process will only occur if the water in the pool and the air above it are effectively a closed system with minimal evaporation. A closed system is where the material removed from one reservoir accumulates in a second reservoir in such a manner that isotopic equilibrium is maintained throughout the process (Gat, 1981). The opposite end-member is an open system where material is removed continuously under condition of a constant fractionation factor, ie. evaporation.

The pool does have a morphology that would be required to create a closed system environment. The pool is surrounded by high side walls which create a continuous shadow (Figure 5.13). Vapour from evaporation that does occur may be contained by the steep sides increasing the humidity. The high humidity is required for continuous enrichment of the isotopes in the air above the pool and in the pool.

When humidity is involved water-vapour exchange can occur. A number of steps are involved in this process due to the various layers. The boundary layer is a microns-thick atmosphere over the liquid water interface with virtually 100% water saturation. This layer is in isotopic equilibrium with the water body.

Figure 5.13 Banjima Pool (photo by: W. Dodson)

Between the boundary layer and the atmosphere is a transition zone through which water vapour is transported in both directions by molecular diffusion. This layer is where non-equilibrium enrichment occurs.

Figure 5.14 from Gat and Gonfiantini (1981) illustrates how enrichment progresses in an open versus a closed system. Lines A and B represent the δ18O value of the remaining water and the resulting vapour respectively in a open system (0% humidity). And lines D and E represent the same but for a closed system (100% humidity)

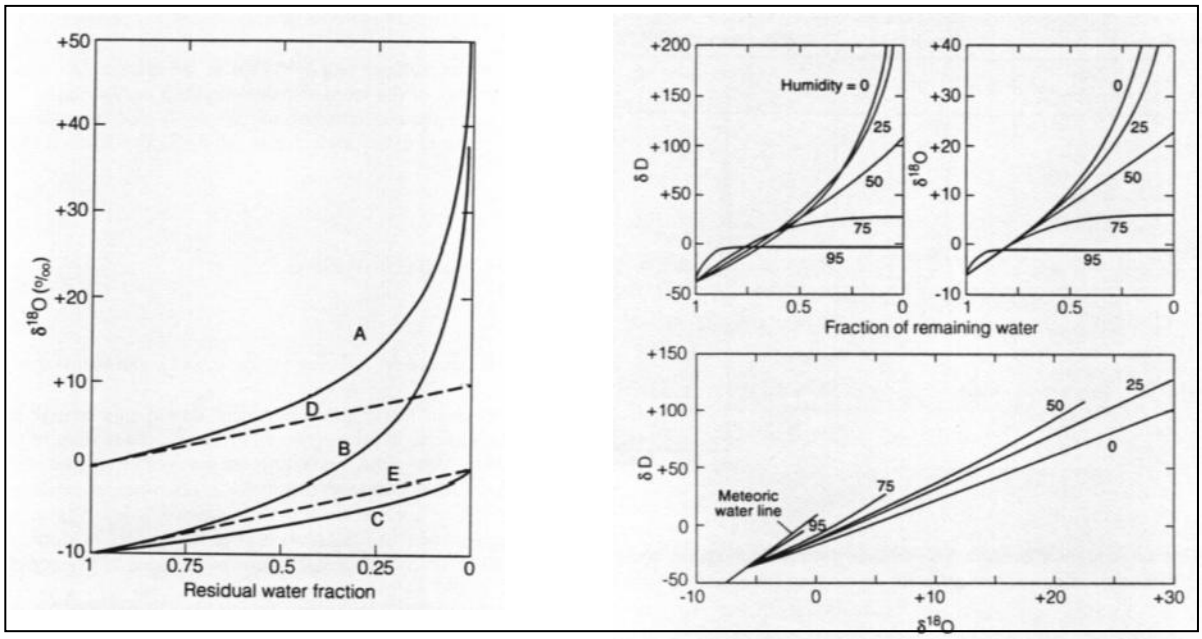

Figure 5.14. a) Isotope enrichment in an open versus closed system b) Effect of humidity on the isotopic enrichment

Figure 5.14, illustrates the effect of humidity on the $\delta^{18}O$ and δD values of the residual water fraction. When there are high humidities the fractionation is less due to the back exchange between water and the vapour, this results in a evaporation line of higher slope (Kendal and McDonnell, 1999).

To estimate evaporation rates at Banjima Pool the Penman-Montieth Model of Evapotranspiration was used. (Monteith, 1965). The aim was to determine how the humidity would affect evaporation. The model was conducted using data from the 27th of February (a randomly picked summer day). A ET value for Marandoo was first calculated using the known input parameters: Latitude (22.4deg), Altitude(709m), Temp(Max: 41.4^{o}, Min: 26.5^{o}), Solar Radiation. (Max:102 Wm-2 Min: 22Wm-2) Humidity(Max: 53.4 Min:11.8) Wind speed (2.7m/s) This produced ET values of: 9.7mm @ 22 Wm-2 and 21.1 @ 101 Wm-2

When applying the model to Banjima Pool the Humidity and Wind speed were used as variable parameters as these were considered unique to the location. A solar radiation of 22wm2 was used as this was the minimum recorded in the area that day. The range of outputs can be seen in Table 1.

Table 5.2 shows that evaporation will be occurring at Banjima Pool regardless of the conditions. However it is highly dependent on both humidity and wind. When humidity is 100% a change in wind speed will not affect the ET value. However as humidity drops the ET value increases and the effect of the wind becomes obvious.

Humidity %	Wind (m/s)	ET (mm)
100	0.1	6.9
100	5	6.9
100	10	6.9
80	0.1	6.43
80	5	9.02
80	10	11.65
50	0.1	5.54
50	5	12
50	10	18.6
0	0.1	2.2
0	5	14.9
0	10	28.1

Table 5.3 ET calculations for variable Humidity and Wind

Banjima Pool is very well sheltered so we can assume that wind speed will be negligible (0.1 m/s) and a conservative approach is considered regarding humidity at the site. We assume that the humidity is 20% higher than the regional annual average of 60%. This produces an ET value of **6.43mm/day**. This value suggests that evaporation is occurring at a high enough rate to prevent equilibrium conditions occurring. Therefore isotopic fractionation at Banjima pool will occur in a non-equilibrium manner, allowing enrichment to occur as a result of evaporation.

5.5 Mass Balance Calculations

5.5.1 Quantifying recharge rates with Chloride method

The relationship between isotopes and Cl^- have shown that transpiration is an active process in the study area. As the water infiltrates through the subsurface unsaturated zone it is susceptible to transpiration processes until it enters the saturated zone where it becomes groundwater recharge. To estimate how much of the annual rainfall actually becomes groundwater recharge in each catchment the Chloride method can be used.

This method makes the assumption that Cl^- acts conservatively. The concentration of Cl- in the ground water can be used as an indicator of the level of transpiration that has occurred prior to recharge. Most plants do not take up Cl^- ; therefore, it is concentrated in the soil in proportion to the amount of transpiration that is occurring.

The following equation adapted from Allison et al, 1985 can be used to estimate the amount of rainfall that becomes groundwater recharge.

$$\boldsymbol{R} = \frac{(\boldsymbol{PCp})}{\boldsymbol{Cg}} \qquad \textbf{Equation 5.2}$$

Where: R = recharge, Cp = concentration of Cl^- in precipitation, P = annual precipitation, Cg = concentration of Cl^- in groundwater.

The annual rainfall at Marandoo is 400mm/ year. The concentration of Cl- in the rainfall is 0.5 mg/L (measured at Yandi) and groundwater concentrations of Cl- average 150 mg/l., Therefore from the 400mm/year the estimated groundwater recharge is 1.33mm (only 0.33% of mean annual rainfall). For Hamersley, Dales, Knox and Joffre Gorges recharge is 0.52%, 0.42%, 0.76%, 0.21% respectively. The relatively small catchments are characterised by lower evapotranspiration and higher recharge rates resulting in relatively fresher waters observed where the groundwater discharges as surface water.

5.5.2 Estimating the influence of the aquifer

This same principle can be used to further understand the sources of solutes to the aquifers via a simple mass balance equation. By quantifying the level of evapotranspiration occurring prior to recharge, the major ion concentration of the infiltrating water can be estimated and therefore the concentration of solutes added by mineral dissolution can be calculated.

If we assume no mixing, then the (elevated) concentration of Cl^- in a groundwater sample will be due to the amount of evapotranspiration that has occurred during infiltration.

If the Cl^- concentration of the rainfall and the groundwater is known, a value for the amount of evapotranspiration (ET) that is occurring prior to recharge can be determined.

$$ET = \frac{[Cl\,(groundwater) - Cl(rainfall)]}{Cl\,(groundwater)} x\ 100 \qquad \textbf{Equation 5.3}$$

$$Concentration\ post\ ET = Conc.\ Factor\ x\ Initial\ conc.\ of\ rainfall \qquad \textbf{Equation 5.4}$$

The ET value calculated from equation 5.3 can be used to determine a concentration factor. This is determined via the following method:

If ET = 97% then from 1000ml only 30ml will remain and has a chance to infiltrate into the saturated zone the ratio of initial water to remaining water is the “concentration factor”. As solutes are not removed during evaporation they are continually concentrated in the remaining solution, therefore the “concentration factor” multiplied by the initial solute concentration will give an estimate of the solute concentration after ET processes have occur. Eg. If the Ca concentration in rainfall is initially 2.3mg/L after ET processes have removed 97% of the water the Ca^{2+} concentration should be 76.6mg/L. This is calculated by equation 5.4.

By comparing this value (Concentration post ET) with the actual concentration of the water extracted from the aquifer we can determine the amount of dissolved solutes that have been added or lost due to interaction with the aquifer. This will be the difference in estimated concentration and actual concentration of the relevant ion.

Table 5.4 shows the estimated influence of the aquifer on the groundwater samples collected within the KNP. The value is the difference between the measured and estimated values and the % change. It illustrates there is variation between each aquifer and the behaviour of the ions present.

When the estimated concentration is higher than the measured, this suggests that the ion involved is being precipitated or reduced. Likewise when the estimated concentration is lower it suggests that ion involved is being added to the system via dissolution of aquifer minerals.

Table 5.4 reveals that the Mg^{2+} concentration increases in all samples after recharge as a result of dissolution of rock minerals. K^{+} concentrations stay relatively constant emphasising its meteoric origin, while Na^{+} shows a slight decrease in concentration from the estimated value. SO_4^{-} is estimated to be consumed in some aquifers while added in others.

Ca^{2+} is seen to be added in some aquifer systems while reduced in others.

Location	ΔCa	%	ΔMg	%	ΔSO_4	%	ΔK	%	ΔNa	%
SFP10	0.37	29	1.31	81	-0.02	-5	0.06	23	-0.28	-17
SFP8	-0.02	-2	1.24	73	0.17	23	0.00	1	-0.74	-35
SFP7	0.01	1	1.28	74	0.14	20	0.01	4	-0.67	-31
SFP2	-0.01	-1	1.33	74	0.29	32	0.01	2	-0.83	-38
SFP4	0.02	1	1.37	74	0.15	20	0.02	7	-0.90	-42
SFP5	0.06	4	1.37	75	0.17	22	0.02	7	0.77	40
SFP6	0.13	9	1.37	75	0.25	31	0.03	10	-0.88	-45
SFP11	0.09	6	1.34	75	0.18	24	0.03	8	-0.86	-43
SFP12	0.08	6	1.29	75	0.13	19	0.04	12	-0.83	-43
MR1	-0.32	-18	1.63	70	0.06	6	-0.07	-18	-2.29	-107
MR2	-0.02	-2	1.40	75	0.20	25	0.04	12	-1.15	-64
MR4	0.33	23	1.52	81	0.19	30	0.11	33	-0.55	-32
Windmill	-3.51	-144	2.17	53	-1.65	-200	-0.73	-149	-8.57	-223
KN1	-0.46	-110	0.52	64	-0.23	-161	0.02	8	0.09	5
KN3	-0.28	-62	0.52	69	-0.17	-136	0.04	22	0.40	21
RS1A GW	-6.00	-132	3.37	49	-0.17	-4	-1.35	-168	-12.07	-122
VC1	-1.25	-288	0.48	46	-0.33	-89	-0.12	-56	-1.51	-75
RS1	-0.75	-163	0.44	53	-0.31	-165	-0.08	-51	-1.10	-77
	(-) Consumed by aquifer (+) Added by aquifer (mmol/L)									

Table 5.4 Influence of the aquifer on the concentration of dissolved ions. Changes illustrate the difference between the estimated concentration and the observed concentration, with the % change

5.6 Addition of solutes from various chemical processes

5.6.1 Carbonate dissolution

It has been established that the dissolution of aquifer minerals is an active process in the evolution of the groundwater in the area increasing solute concentration. The inter-elemental relationship plots in Section 5.4 suggested that the major ions that are added via this process were Ca^{2+}, Mg^{2+} and HCO_3^-. Carbonaceous Calcretes are known to exist in the area which may provide the carbonate source (Johnson and Wright, 2001). The presence of these carbonate deposits may be due to cyclic wetting and drying (Drever, 1988).

This is where the high levels of transpiration that occurs increases the concentration of the water to the point where precipitation of minerals starts to occur. The relative solubility's of the minerals in the water govern the order of precipitation, with carbonates forming first and Chlorides last. This will generally occur at the bottom of the unsaturated zone forming a 'relic groundwater table'. The remaining water will become increasing concentrated in Cl^- as it does not precipitate until concentrations of around 200 g/L (Clark and Fritz, 1997) Subsequent rainfall events will then infiltrate through this zone re-dissolving the carbonate minerals and adding solutes to the water that recharges the aquifers.

Generally dissolution of a carbonate will result in the addition of Ca^{2+}, Mg^{2+} and HCO_3^- to the solution according to the following basic reactions:

$$\textbf{Calcite Dissolution}: \ CaCO_3 + H_2O + CO_2 = Ca^{2+} + 2HCO_3^-$$

$$\textbf{Dolomite Dissolution}: \ CaMg(CO_3)_2 + H_2O = Ca^{2+} + Mg^{2+} + 2HCO_3^-$$

The ratio of one ion to another can give an indication of the type of mineral that is primarily involved in dissolution. If the dissolution of calcite is a dominant process controlling the chemistry of natural groundwater, then Ca^{2+} and HCO_3^- will correlate to a 1:1 regression line when plotted in milliequivalents$^-$ (Drever, 1988; Rosen and Jones 1998). This is because the dissolution products of calcite are HCO_3^- and Ca^{2+} at a molar ratio of 2:1. On an equivalent basis, one mole of Ca^{2+} is given an equal weight two moles of HCO_3.

Figure 5.15a investigates the relationship between Ca^{2+} and HCO_3^-, the plot shows there is an excess of HCO_3^- charge relative to Ca^{2+}. This suggests that HCO_3^- is not only supplied to the system via pure calcite dissolution and must therefore be another cation associated in dissultion reactions. Dolomite has the chemical formula $CaMg(CO_3)_2$. Dissolution of this carbonate mineral will increase the Ca^{2+} and HCO_3^- concentration in solution, and will also provide Mg^{2+}. The chemical composition of Dolomite is such that Ca and Mg exist in 1:1 ratio with HCO_3^- (Wigley, 1973).

Figure 5.15b reveals that when the ionic charge of Mg^{2+} and Ca^{2+} in water samples are summed and plotted against HCO_3^-, then the majority of the data correlates to the 1:1 line, this suggests that dolomite dissolution is an active process in the KNP aquifers.

As a basic requirement in aqueous chemistry is that all cations and anions must balance. Therefore the data that still does not correlate to the Dolomite dissolution line must suggests that Ca or Mg (or both) are balanced with another anion. This was investigated by the addition of SO_4 to the y-axis (Figure 5.15c) which reveals a greater proportion of data correlating to the line, this may suggest the dissolution of a hydrate of $CaS0_4$ or $MgSO_4$:

$$\mathbf{CaSO_4.2H_2O = Ca^{2+} + SO_4^{2-} + 2H_2O}$$

Or it could come from oxidation of pyrite (FeS_2 - which is known to exist in the proterozioc rocks), and reaction with calcite:

$$\mathbf{FeS_2 + 3.75O_2 + 3.5H2O = Fe(OH)_3 + 4H^+ + 2SO_4^-}$$

$$\mathbf{4H^+ + 2CaCO_3 = 2Ca^{2+} + 2H_2CO_3.}$$

There is however no way to distinguish between these alternatives without investigation of the rocks involved (Dreaver, 1988). To follow on from the investigation of Mg:Ca ratio (section 5.3.1) the relationship between Ca and Mg was investigated in Figure 5.15d. At low concentrations (<5meq/L) Ca^{2+} and Mg^{2+} concentration stay around the 1:1 ratio, however as concentration increases the Mg^{2+} accelerates more than Ca^{2+}. This may be due to the precipitation of calcite over dolomtie. When the ion activity product of calcite reaches saturation, Ca^{2+} precipitates as calcite resulting in an increase in the Mg/Ca ratio. This was seen earlier, where the flow path length had an impact on the Mg/Ca ratio.

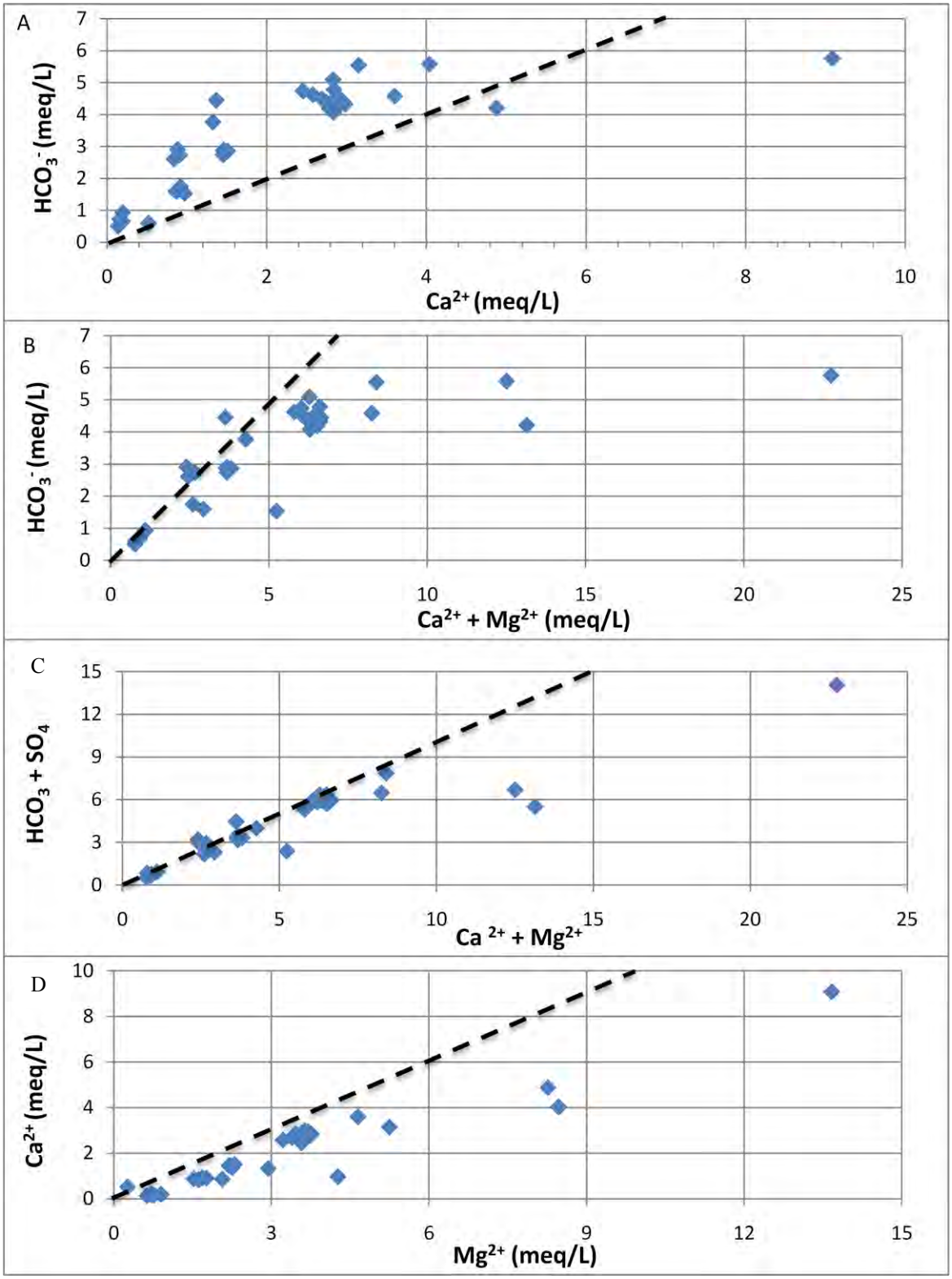

Figure 5.15 The relationships between Ca, Mg and HCO_3, in order to determine whether ionic ratios can indicate the type of carbonate present

5.6.2 Ion- Exchange to remove sodium from solution

It has been shown earlier in this section (section 5.4 and 5.5) that there was a slight depletion in Na. This relationship can be further investigated by plotting the ratio of Na/Cl versus Cl to separate the processes involved, creating a clearer picture.

Figure 5.16, shows that if Evapotranspiration is the dominant processes increasing the Na concentration then the data should plot along a horizontal trend (red arrow) and likewise if the reduction of Na (relative to Cl) is occuring then the data will plot along a vertical line (green arrow). A very common processes responsibly for the reduction of Na from solution is through ion-exchange where Na is commonly absorbed by clays (Hem, 1985).

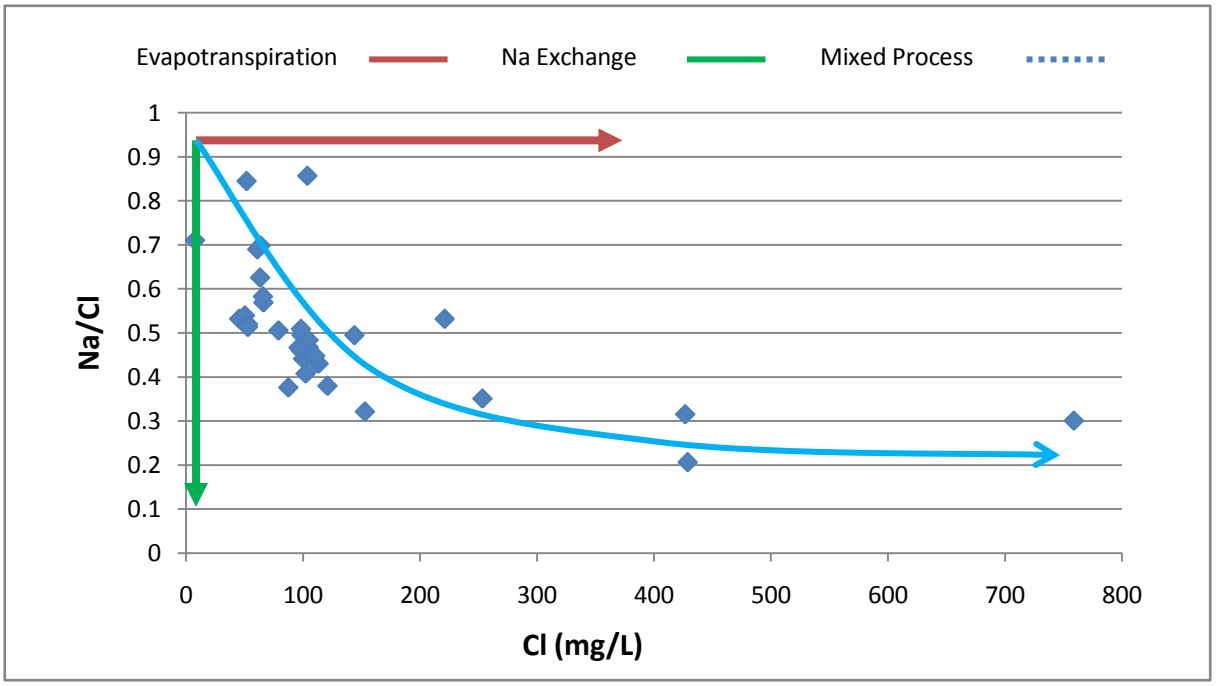

Figure 5.16 Relationship of Na/Cl versus Cl, illustrating that the concentration of Na in the natural water is determined by a combination of both Evapotranspiration and ion exchange processes.

The data initially plots along a curved line suggesting that the concentration of Na in the groundwater is dependent on both evapotranspiration and ion-exchange processes. However as Cl- concentration increases the trend flattens suggesting evapotranspiration is the more dominant process. Hanshaw, 1964 showed that when compacted, clays may preferentially adsorb sodium, but when dispersed in water they may preferentially adsorb sodium. This may therefore also explain why Ca appears to be reduced in some locations where Na is not reduced (Table 5.4).

5.8 Discussion of XRD results

The results from the XRD analysis of various rock and precipitate specimens from within the KNP revealed some interesting results which answer some questions but also create others.

The analysis of the relative major ion concentrations has suggested that Carbonate dissolution is an active process determining the evolution of groundwater. Figure 5.15b shows that although the data correlates to the Dolomite dissolution line but there is slight enrichment in Ca + Mg. This may be the result of calcite or aragonite dissolution also occurring, this is supported by the aquifer rock sample collected at Mindthi spring was 85% Dolomite and 15% Calcite. Once the bi-carbonate saturated groundwater discharges the partial pressure drops and degassing of CO_2 occurs. This reduces the CO_2 content of the water and subsequently precipitation of a carbonate occurs.

A range of different precipitate types were determined through XRD analysis. The precipitate samples collected from Circular Pool and Kalamina Gorges were both magnesium rich carbonates, whereas the sample collected at Knox Gorge, which exhibits similar catchment size and ionic ratios, was pure Calcite/Aragonite. The precipitate collected at Fortescue Falls (Dales Gorge) was pure $MgSO_4$. This leads to two questions, what is the source of Sulphur? And why does Mg-Carbonate precipitate in one area and pure calcite in another?

Firstly, the source of sulphur may be from localised zones of pryitization? Pyrite is known to exist in the Proterozoic rocks in the area (W.Dodson Pers Comms, 2008) so there may indeed be concentration of pyrite in the TR alluvials. Another Sulphate source may be Gypsum ($CaSO_4$) or Epsom salts ($MgSO_4$), the relationships shown in Figure 5.15c, may support this, as it appears that SO_4 ions are in solution and balance Ca^{2+} and Mg^{2+}.

As for the difference in Carbonate precipitations, the controls on precipitation should be addressed. As discussed in section 2.2.3, the precipitation of Carbonate is controlled by changes in pH, temp and partial pressure. It can be assumed that the partial pressure will be consistent at each site, as in each case, groundwater is discharging directly into an open atmosphere. Therefore the differences in precipitation must be due to temperature and chemical variations.

The variation in crystallography between Calcite and Dolomite may provide an answer. Dolomite is a double carbonate, where the cations (Ca^{2+} and Mg^{2+}) are in a regularly alternating pattern with the anion CO_3 -. The regular alternation is important as this is a special highly ordered crystal structure which perhaps takes a long time to grow (Krauskopf and Bird, 1995). The theory matches the fact that Dolomite was seen observed to form in Circular Pool and Kalamina Falls, both of which are located in shady areas where precipitation occurs out of the influence of direct sunlight. Whereas the sample collected at Knox Gorge, which remains in direct sunlight for the majority of the day, was pure calcite. This suggests the shady areas allow crystal growth to occur slower, resulting in different mineralogy.

In the case of the $MgSO_4$ collected at Fortescue Falls, Mg^{2+} salts generally form where cation concentration is relatively high and increased temperatures cause extreme evaporation (Dreaver, 1988; Krauskopf and Bird, 1995). Fortescue Falls may indeed provide these conditions as the morphology and orientation of the gorge allows maximum sunlight resulting in high temperatures (Figure 5.17).

Figure 5.17. Location of Precipitation: Above Shady Circular Pool, Below Sunny Fortescue Falls

5.9 Basic Hydrologic Water Budget

It has been shown that the hydrochemistry observed at each gorge can be justified by groundwater evolution occurring within each respective catchment. Water is collected in the catchment (Figure 5.18a) from rainfall and travels through the local aquifers before being discharged at a gorge (Figure 5.18b). To prove this, a simple hydrological budget calculation can be undertaken.

The hydrologic continuity equation is based on a simple mass balance and states that any input to a system must equal the output plus any change in storage, as follows:

Inflow = Outflow + Δ Storage

Where each of the quantities are expressed are volume per unit time. "Inflow" consists of precipitation in the catchment, surface water runoff and groundwater inflow and any other water flows imported into the system. "Outflow + Δ Storage" consists of evaporation, transpiration, groundwater discharge, exported water flow (pumping) and changes in total reservoir properties (Fetter, 1994) For a system where no groundwater abstraction is occurring, and conditions have stayed constant for an extended period of time, we can assume the system is in dynamic equilibrium. Therefore the Δ Storage will equal zero and Inflow should equal outflow.

It has been shown that each catchment acts individually with no outside inputs, therefore we can assume that all input is due to rainfall within the catchment, and likewise the only output will be base-flow discharge at the gorge. The difference between these two values must therefore be due to losses from Evapotranspiration:

$$\mathbf{Inflow - ET = Outflow}$$

Rearranging this equation allows the calculation of ET for each catchment:

$$\mathbf{ET} = \frac{\mathbf{Inflow}}{\mathbf{Outflow}}$$

Inflow was calculated by multiplying the catchment area by the average annual rainfall (.365m) while Outflow was calculated from surface water flow measurements in the gorges. Table 5.5, below details the respective data with the estimated ET value for each catchment.

A value for ET was also previously quantified with the Chloride Mass Balance Method (section 5.5.1). The values determined via this method are also displayed for comparison. Considering the various errors involved the comparison in ET values are surprisingly similar. This supports the theory that Cl^- is primarily acting conservatively.

This is therefore more evidence to support that the groundwater that discharges from each gorge is in fact sourced entirely from rainfall in its own surface water catchment with no external inputs such as inter-flow from Marandoo's MM aquifer.

Location	Catchment Area Km^2	INPUT Rainfall M^3/yr ($x10^3$)	OUTPUT Discharge M^3/yr ($x10^3$)	IN-OUT Difference M^3/yr ($x10^3$)	ET% (budget)	ET% (Cl method)
Ham	191	80,220	309	79,911	99.6	93.4
Wea	12	5,216	161	5,055	96.9	91.4
Kal	23	9,597	397	9,199	95.9	95.8
Jof	340	142,800	595	142,205	99.6	98.5
Han	33	13,860	685	13,175	95.1	91.8
Dal	120	50,400	1,697	48,702	96.6	96.2

Table 5.5 Hydrologic Budget for each catchment where surface water flow measurements were determined.

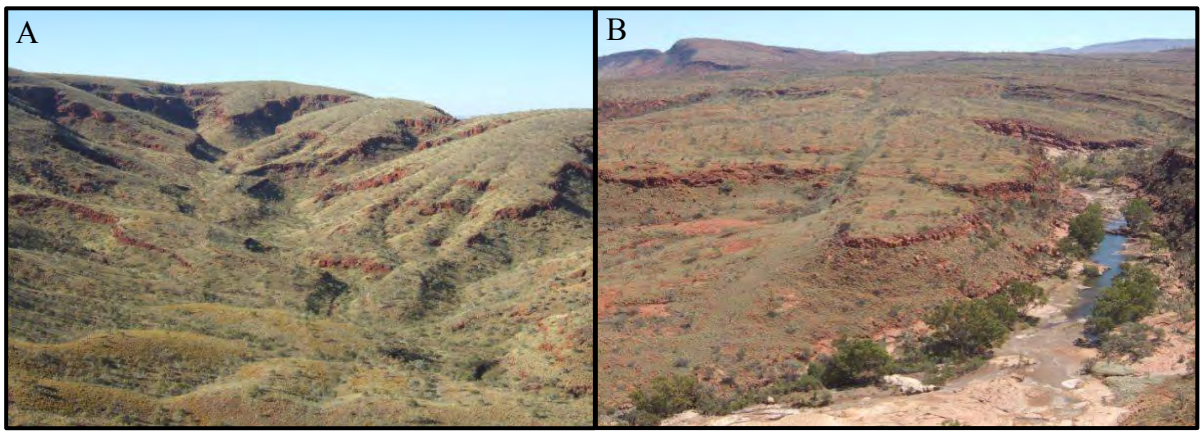

Figure 5.18 a) Typical topography at the head of a KNP catchment b) Typical head of KNP gorge (photos: Pippa Gardner)

5.10 Summary of groundwater chemical evolution

The chemical evolution of the groundwater in the Karijini National Park, as discussed in the previous sections, is summarised in the following diagram (Figure 5.19):

Stage One (Precipitation): Intense rainfall provided by cyclonic events occurs in the Pilbara. The rainfall has a characteristic depleted isotopic signature and contains low concentrations of dissolved solutes sourced from atmospheric dust and oceanic air-entrained particles.

Stage two (Infiltration): The rainfall rapidly infiltrates into the ground before the δD and $\delta^{18}O$ can be significantly modified. During infiltration a significant proportion of the water is absorbed by the vegetation and subsequently transpired. This concentrates the solutes in the remaining solution without enriching the δ D and $\delta^{18}O$.

Stage Three (Mineral Dissolution): The groundwater is hosted in TR aquifers which have a high carbonate concentration. The carbonates are subsequently dissolved increasing the concentration of Ca^{2+}, Mg^{2+} and HCO_3^-.

Stage Four (Transpiration): As the groundwater nears the discharge point at the gorges the water table nears the surface in reach of deep rooted plants. This acts to further concentrate the dissolved solutes in the remaining water.

Stage Five (Discharge): Groundwater discharge occurs at the head of the Gorge. The groundwater is now in contact with atmospheric processes allowing subsequent hydrochemical modification to occur. Precipitates commonly form where the groundwater first is introduced to the atmosphere.

Variations in the rates and residence times of step 2,3 and 4 determines the unique chemical signature observed at each of the gorges within Karijini National Park.

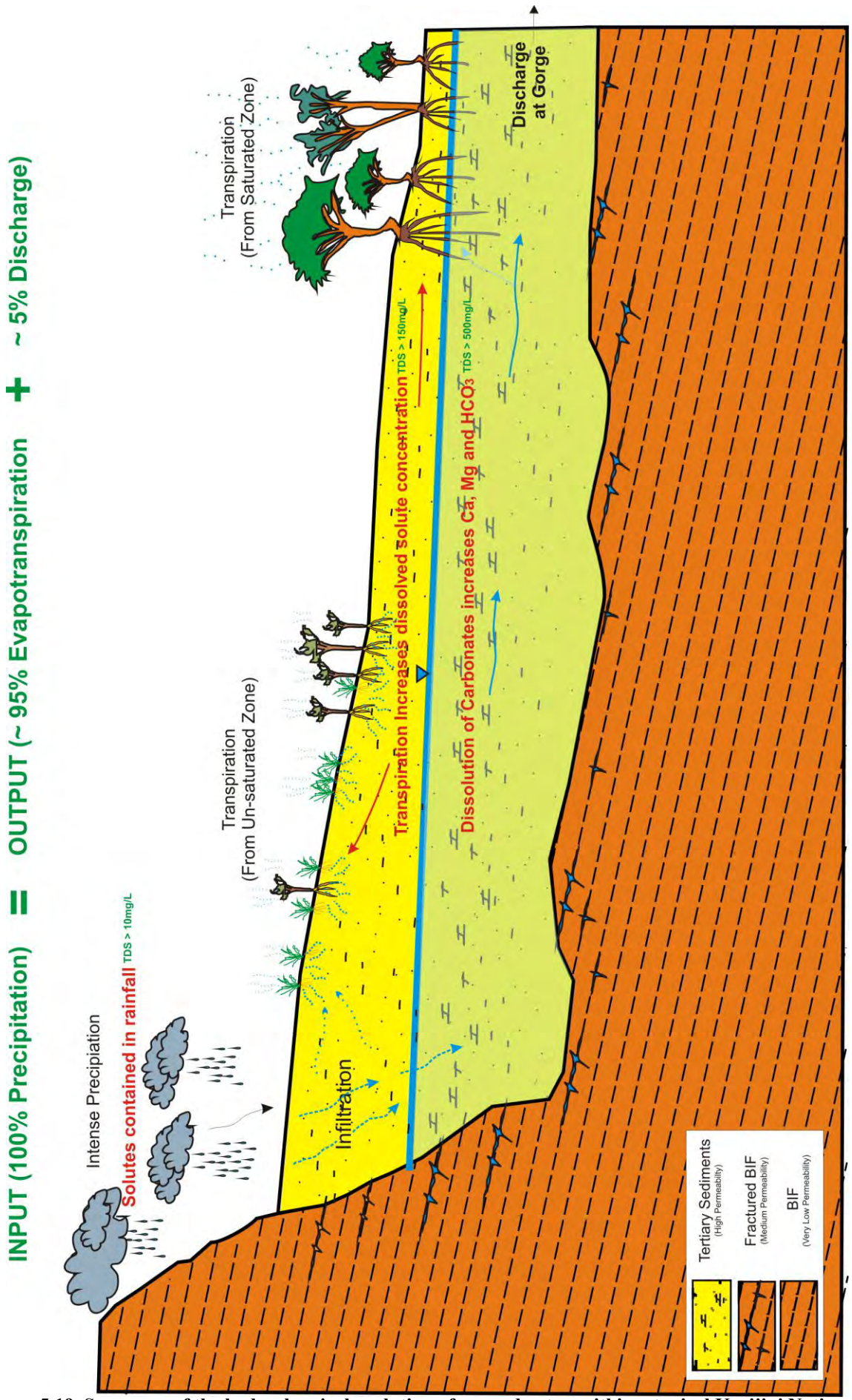

Figure 5.19. Summary of the hydrochemical evolution of groundwater within a typical Karijini National Park Catchment

Chapter 6

Dating and Temporal Variation

The previous chapter investigated the chemical and physical processes responsible for producing the chemical signature of the ground and surface water within the study area. This created a strong understanding of how water is evolving; however without any bearing of temporal scale it is difficult to gain the full picture.

This chapters investigates the temporal variation in the hydrochemical data and attempts to determine relative ages for the water found within the study area. The introduction of a third dimension can add new meaning to the current data.

6.1 Investigating Temporal Variation

Repetition of field measurements and laboratory analyses is an essential part of hydrochemical studies (Mazor, 1991). The source of recharge may vary over the year (eg. summer rains, winter rains) and this may be identified by variation in isotopic composition of the water. Likewise, chemical variations and temperature fluctuations may suggest mixing processes are occurring. Understanding these, can give an indication of the vulnerability of the resource to any change in the hydrologic budget.

To investigate temporal variation in the hydrochemistry a second round of water sampling was conducted in May 09 across the study area, with an emphasis on indentifying any differences in surface and ground water composition pre and post wet season.

This was addressed by re-sampling a selection of the previous locations for major ion concentrations and stable isotopes (δD and δ^{18}O). Repetition of field measurements is an important component of any hydrogeological study. Ideally the more sample repetitions the better, a common rule of thumb is that the water should be studied four times, to cover one hydrological cycle (Mazor, 1991), however for the Pilbara, which only has a wet and dry season, it was decided to only undertake two sampling programmes, one either side of the

wet season (November-April). Around 400ml of water has fallen in the area over the previous few months (BOM, 2009).

Twenty two samples were collected from a select few locations, shown in Table 6.1. The samples were collected at the exact same location as previous, guided by handheld GPS.

6.1.1 Major Ion Concentrations

6.1.1.1 Temperature and TDS Variations

The results of the re-sampling are detailed in table 6.1 and 6.2. The first of which shows the measured concentrations and the second shows the change (mg/L) for each ion between the sampling periods and % change in TDS. The major ions are also compared in Figure 6.1 and 6.2 below in the form of inter-elemental relationships (compared to Figure 5.10). This visually shows the similarity in sampling periods.

When the data from the two sampling programs is compared the data shows that there is no consistent increase or decrease in ionic concentrations between the two periods. The average change in TDS for the surface water is only ±7% and ±2% for groundwater. The temperature for the surface and groundwater water is 3.5 and 2.2 °C lower respectively.

The TDS variation of ±2% for groundwater can be considered insiginifcant when considering the errors associated with sampling and the slight increase in temperature can be justified by the 15-20°C difference in average air temperature. It can therefore be concluded that there is no significant difference in the water between the two sampling periods.

6.1.1.2 Significance of Variation

This suggests that similar groundwater recharge processes occur annually resulting in similar groundwater chemistries. It also suggests that groundwater inter-aquifer mixing is not a significant process, or if it does occur, it proceeds in a very constant manner.

The fact that the variation in the surface water hydrochemistry is also minimal, emphasises the theory that the gorges are sourced entirely from baseflow groundwater discharge. This would infer that the contribution from surface water runoff is minimal throughout the majority of the year. The constant hydrochemistry is also another indicator to show that the hydraulic budget of the system is in dynamic equilibrium.

	Cl	SO_4	HCO_3	Ca	Mg	K	Na	Br	SiO2	SAL	EC	TEMP	DO %	pH
SFP10	73	48	260	52	39	9.1	34	0.3	42	557.4	693	30.39	26.3	7.45
SFP2	100	75	270	59	44	11	47	0.6	34	640.6	828	29.52	39.4	7.59
SFP12	98	72	250	58	42	11	40	0.5	38	609.5	790	28.88	17.4	7.66
HM1	70	57	300	58	45	9.9	36	0.3	33	609.2	715	20.27	74.7	8.75
HM2	71	54	300	56	45	10	37	0.3	33	606.3	712	18.88	65.6	8.49
MR1	79	51	310	60	47	12	32	0.4	48	639.4	765	27.62	44.7	7.44
MR2	100	78	260	56	45	12	37	0.5	36	624.5	775	28.18	31.9	7.74
MR4	79	63	280	56	45	12	35	0.4	40	610.4	733	27.6	34.8	7.56
WN1	48	<1	65	4.2	11	4.3	25	0.3	49	206.8	247	18.11	57.1	
WN3	49	<1	70	4.3	12	4.2	26	0.3	51	216.8	246	20	65.7	8.3
HK1	69	<1	50	5.1	11	4.4	29	0.4	40	208.9	271	17.1	65.8	8.3
Windmill	450	76	240	100	100	19	85	3.2	72	1145.2	1648	20.58	56.4	8.06
KN1	56	12	150	17	20	7.4	39	0.3	64	365.7				
KN2	120	7	190	24	32	9.2	49	0.7	39	470.9	625	17.09	44.5	8.58
VC1	100	19	95	16	23	8.1	38	0.6	69	368.7	481	20.4	44.6	7.49
RS1	93	23	110	20	23	7.4	32	0.5	57	365.9	446	24.06	46.3	7.55
FS Falls 2	120	24	170	32	29	9	47	0.6	54	485.6	611	20.12	67.3	7.96
Fern Pool 2	110	24	180	32	29	9.1	47	0.6	56	487.7	606	20.99	40.7	8.1
KL1	65	7	170	19	22	7.5	38	0.4	72	400.9	719	16.27	61.2	9.54
KL2-SW	110	<1	300	30	30	14	92	0.7	66	642.7				
JF1	460	38	320	85	100	21	140	3.1	55	1222.1	1782	20.5	72.4	8.34
Mn Spring	310	150	330	72	72	19	140	1.7	16					

Table 6.1 Data collected for secondary sampling program from field and labratory analysis

Location	ΔCl	ΔSO_4	ΔHCO_3	ΔCa	ΔMg	ΔK	ΔNa	ΔBr	ΔSiO_2	TDS 1st	TDS 2nd	% Δ
SFP10*	-6.9	-13.0	22.0	-0.4	0.1	0.4	3.6	0.1	0.8	564	557	1.2
SFP2*	4.6	10.5	8.4	-1.4	-0.1	0.9	3.6	0.0	0.5	668	641	4.0
SFP12*	-1.9	-6.3	-1.1	-1.2	0.0	1.1	4.9	0.0	1.2	606	610	-0.5
HM1	-4.4	3.8	10.7	-1.4	-3.1	-0.3	2.2	0.0	0.6	617	609	1.3
HM2	-7.8	-0.9	-10.9	-6.9	-1.6	0.0	2.6	0.0	0.9	582	606	-4.2
MR2*	2.1	-2.0	-4.4	-0.3	0.4	0.9	4.6	-0.2	2.3	628	625	0.6
MR4*	-0.1	-0.5	11.8	0.9	0.7	1.0	4.9	0.1	0.6	630	610	3.1
WN1	-2.7	1.0	-20.3	-1.0	-1.7	-0.5	-0.9	-0.1	1.0	183	207	-13.2
WN3	1.2	0.4	-13.1	-0.3	-1.1	-0.2	1.1	0.0	-2.3	204	217	-6.5
HK1	-16.2	0.4	-9.3	-1.2	-2.3	-0.8	-1.6	-0.1	-2.3	176	209	-18.5
Windmil*	-21.3	3.4	16.8	-2.4	0.4	0.1	3.6	0.3	5.5	1152	1145	0.6
KN1*	7.6	1.6	9.4	-0.2	-0.4	0.3	5.5	0.8	4.6	395	366	7.4
KN2	23.8	4.5	40.0	2.6	3.7	1.2	22.2	0.0	2.7	572	471	17.6
RS1*	-5.6	-4.7	-3.5	-1.6	-2.5	-1.0	0.9	0.2	2.7	351	366	-4.3
FS Falls 2	-8.6	1.4	5.5	-2.9	-2.4	-0.2	1.1	-0.1	2.8	482	486	-0.7
Fern Pool 2	0.3	2.1	-5.3	-1.7	-1.1	0.0	2.4	-0.2	0.4	485	488	-0.6
KL1*	-4.2	0.2	-3.1	-0.8	-0.6	0.1	3.9	-0.1	-0.9	396	401	-1.4
KL2-SW	-6.4	1.4	-28.3	-2.6	-2.6	-1.1	-3.2	-0.3	0.6	601	643	-6.9
JF1	-33.4	34.2	20.8	-4.3	2.9	2.3	-5.4	-1.7	3.9	1241	1222	1.6
Mn Spring	89.02	38.81	-8.55	8.96	8.25	1.99	22.43	0.43	-18.28	967	1110	15

Table 6.2 Change in ionic concentrations pre and post-wet season (* denotes groundwater)

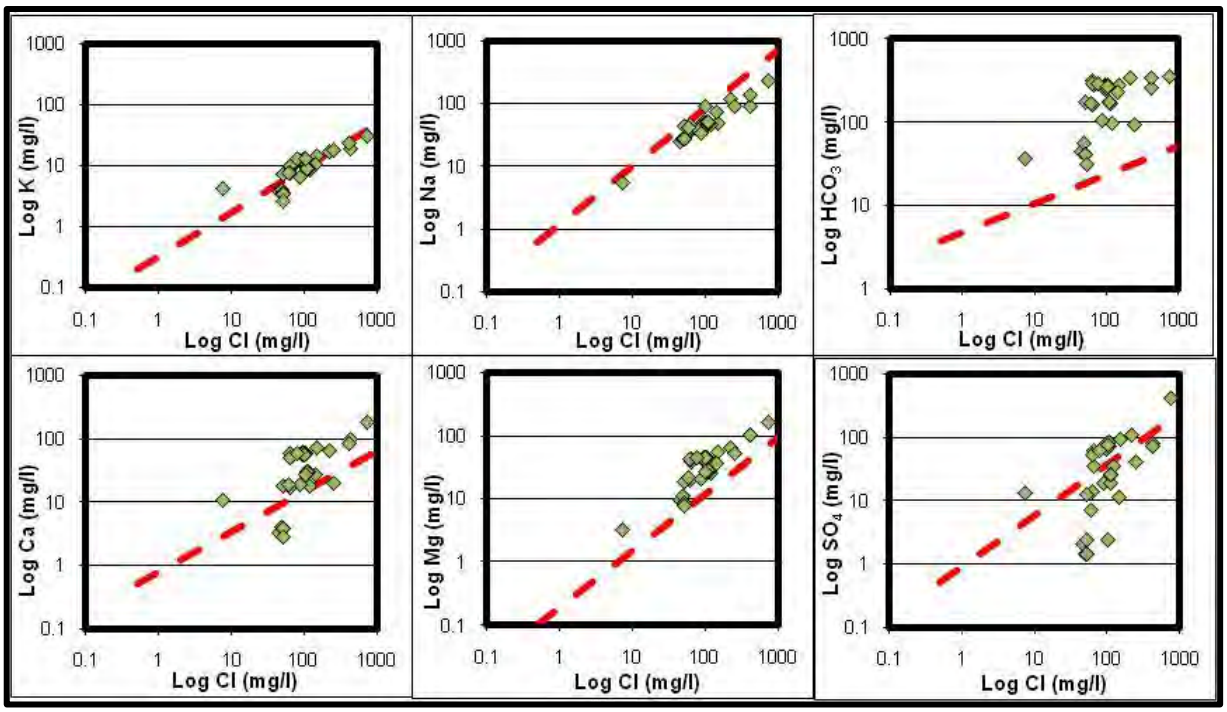

Figure 6.1 Inter-elemental relationships from water samples collected in September 2008

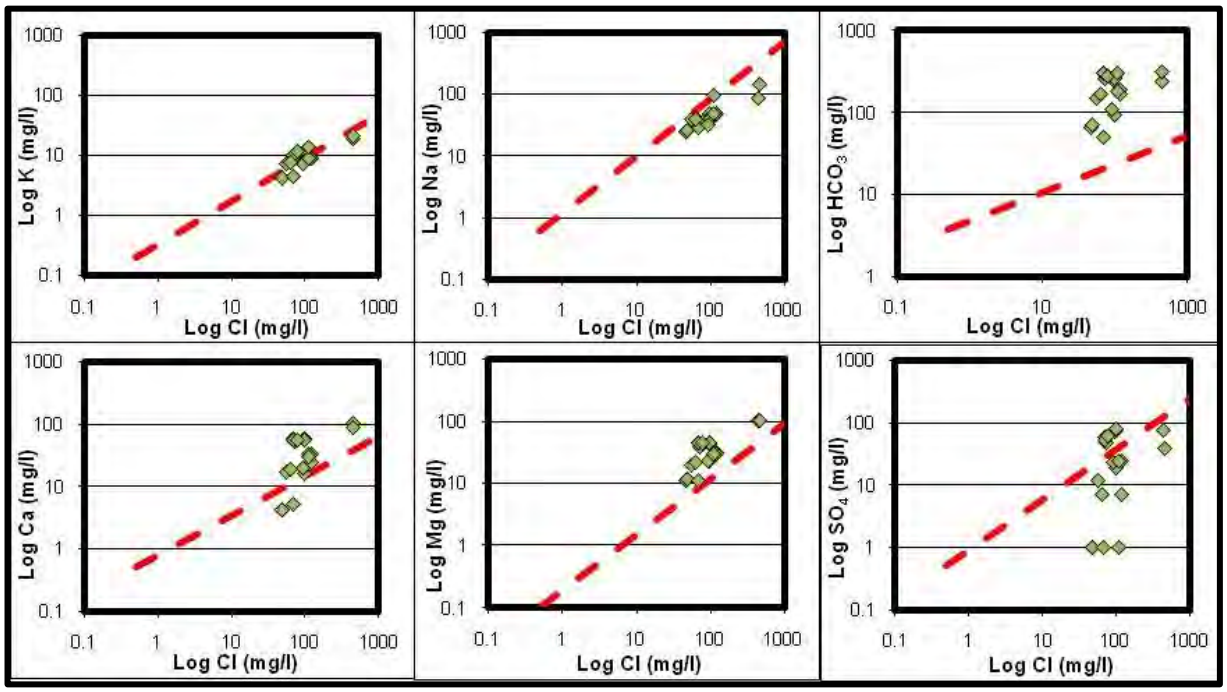

Figure 6.2 Inter-elemental relationships from water samples collected in May 2009

6.1.2 Comparison of Stable Isotopes (δD and $\delta^{18}O$ Data)

The stable isotopic composition of the ground and surface water samples for samples collected in May 2009 is shown in table 6.3 below. It shows that there is very little change between the May 2009 and Sep 2008 sampling programmes. As would be expected, the surface water exhibits a larger variation than the groundwater, which is not exposed to modification.

Type	$\delta^{18}O$ ‰ SMOW	Δ	δD ‰ SMOW	Δ
Surface water	-7.8	*-0.56*	-55.93	*-1.04*
Groundwater	-8.72	*-0.36*	-61.07	*-0.62*

Table 6.3 Average Isotopic composition of ground and surface water samples collected within the KNP during May 09, with average change from Sep 08 sampling

When the data is plotted on a "δD‰ vs $\delta^{18}O$‰" plot it can be seen the data follows a similar linear regression line, characteristic of evaporation after discharge. The variation between two data sets is within the limits of accuracy and therefore deemed insignificant. However the fact that the data all shows a slight horizontal shift of the data to the right (ie. A constant change) suggests that the difference may be due to a variation in the analytical proceedure. This could perhaps be due to a slight calibration difference in the machine or a different composition of the SMOW laboratory standard.

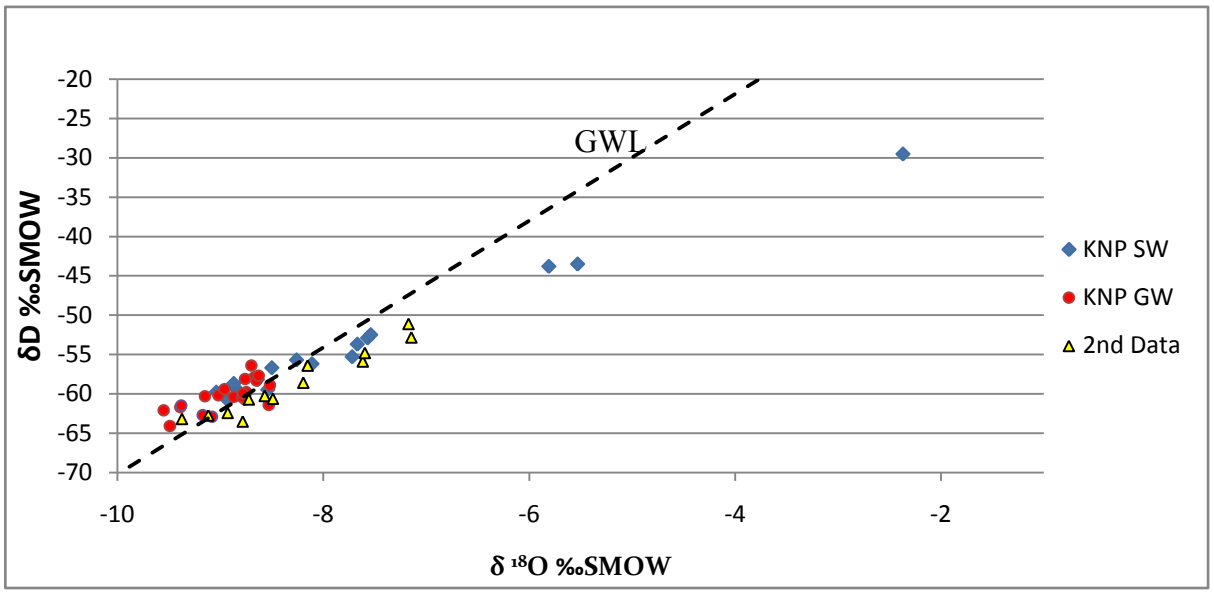

Figure 6.3 Comparison of the relationship between δD‰ SMOW versus $\delta^{18}O$‰ SMOW

6.2 Discussion of Groundwater Dating Results

6.2.1 Introduction

Now it has been established that there is no significant variation in the composition of the water with time, the next step is to identify the relative ages of the different bodies of groundwater. The dating of groundwater gives an indication of important hydrogeological factors such as residence time and inter-aquifer mixing processes.

Using Age dating as a tool in hydrogeological studies is not a definitive tool. Analysis of the data can be complex and can require manipulation through geochemical modelling to acquire a reasonable date (beyond the scope of this thesis). However without this data manipulation it still has uses for providing relative ages and underground residence times to help to understand such factors as inter-aquifer mixing and resource sustainability.

Note: The dates were determined from samples collected at production bores at Marandoo and Southern Fortesuce Borefields. These bores extract water from a number of aquifers. Therefore the sample collected will be a mixture of different waters and therefore different ages.

6.2.2 Discussion of Dating Results

The un-modelled and un-corrected dates for both methods are as follows:

CFC method = 20-45 years old

C-14 method = 11,000-19,000 years old

There is obviously a large discrepancy between the two methods, however from this data we can make two initial conclusions. Firstly, the fact that CFC's exist in the water suggests there is a component of modern recharge water (post-1950) into the aquifer. Secondly the C-14 activity appears to exhibit decay suggesting that there is an input of ancient water. Both dating methods however, are based on a number of assumptions which can dramatically affect the date. The accuracy of these assumptions should be addressed to determine whether the dates are reasonable.

6.2.3 C-14 Assumptions Addressed

Firstly, the dates produced from C-14 dating are calculated simply by measuring the pmc (percent modern carbon) level observed in groundwater and determining the length of time it would take to decay the level of INITIAL pmc to the OBSERVED pmc. These dates are based on an initial concentration of 100pmc and assume the reduction from the INITIAL pmc to OBSERVED pmc is purely due to radioactive decay. In a complex aquifer system, this is a too simplistic view of reality.

6.2.3.1 'Dilution from Dead carbon ' pmc correction

The previous discussion of major ion relationships has shown that carbonate dissolution is an active process associated with water infiltrating through the 2.6 - 65 million year old TR sequence, this may cause a dilution in the groundwater age. As stated in section 3.3.3, when groundwater flows through aquifers containing carbonates the c-14 activity can be diluted due to mineral dissolution.

The carbonates in the TR sequence will contain no ^{14}C due to the length of time past since their formation compared to the ^{14}C Half Life of 5730years. The ^{14}C has all subsequently decayed resulting in "dead carbon". Recharged water containing CO_2 reacts with the carbonates to form dissolved bicarbonate. The dissolved CO_2 in the water (assumed to be **100pmc**) reacts with the rock (**0pmc**) to produce a 50pmc bicarbonate (Mazor, 1991):

$$\underset{}{H_2O} + \underset{100\text{pmc}}{CO_2} + \underset{0\text{pmc}}{CaCO_2} \rightarrow Ca^{2+} + \underset{50\text{pmc}}{2HCO_3}$$

50pmc is therefore assumed to be the initial C-14 activity of the freshly recharged groundwater. Therefore the difference between this value (50pmc) and the observed value will be due to radioactive decay. In contrast the pmc of groundwater in a silicate aquifer, where there is no interaction with carbonates, will show reduction only as a result of radioactive decay.

If 50pmc is infact the initial value then the resulting date will obviously be younger as less apparent decay has occurred. (Eg. If 50pmc is the initial value and the observed is 13pmc then the corrected pmc value will be 26pmc resulting in a age of 11,100yrs because) The corrected dates can be seen in (Table 5.4)

Location	Percent Modern Carbon (pmc)	Corrected pmc	^{14}C age	^{14}C age
SFP12	13.09	26.18	16330	11070
MR1	23.24	46.47	11720	6417
SFP8	16.14	32.27	14650	9365
MR2	9.18	18.37	19180	13950

Table 5.4. Corrected dates by assuming initial concentration of 50pmc

6.2.3.2 Application of $\delta^{13}C$ to correct ^{14}C values for changes caused by interactions with carbonate rocks.

The $\delta^{13}C$ value may be applied to evaluate the extent by which ^{14}C in groundwater is altered by exchange with rocks (Pearson and Hanshaw, 1970). ^{13}C is an excellent tracer of carbonate evolution in groundwaters, because there are large variations in the various carbon reservoirs (Clark and Fritz, 1997). The method takes into consideration the sources of carbon in the system that may be involved in carbon mass transfers, diluting the pmc value, the method requires the knowledge of three values:

- The $\delta^{13}C$ of the studied groundwater
- The $\delta^{13}C$ of the local soil material, representing the initial composition of groundwater, prior to interaction with rocks.
- The $\delta^{13}C$ of the local aquifer rocks

In this study the last two parameters were not determined due to the difficulty of collecting relevant samples. The values can however been assumed to be -25‰ for the $\delta^{13}C$ of soil material and 0‰ for the $\delta^{13}C$ in the rock (Mazor, 1991).

The equation below is used to determine a correction factor which is multiplied by the measured pmc value to correct for ^{14}C losses during reaction with aquifer carbonates. This value can then be applied to the decay curve (Figure 4.10) and a corrected age obtained.

$$[-\delta^{13}C_{(carb)} - (-\delta^{13}C_{(soil)})] / [-\delta^{13}C_{(carb)} - \delta^{13}C_{(water)}] = \text{Correction factor}$$

The correction calculation and corrected dates are shown in table 5.5 below.

Location	$\delta^{13}C$	Correction factor	Corrected pMC	^{14}C age	Corrected ^{14}C age
SFP12	-8.49	2.945	38.55	16330	7879
MR1	-9.98	2.505	58.21	11720	4473
SFP8	-9.26	2.700	43.56	14650	6868
MR2	-9.92	2.520	23.14	19180	12100

Table 5.5 Corrected C-14 ages with $\delta^{13}C$

6.2.4 CFC Assumptions Addressed

As shown in section 4.4.1 there was an element method of error associated with the dates determined from the CFC dating method. Both CFC molecules do not seem to be acting conservatively leading to a erroneous date.

An erroneous date may be due to a number of reasons, firstly:

The solubility of CFCs means that the CFC signature of the groundwater is highly susceptible to contamination if it comes in contact with the atmosphere before analysis. This may slightly occur during the pumping of the bore as air is sucked back into the hose connection on the bore sampling point. Secondly, if the assumed values for recharge temp, recharge altitude and salinity are incorrect further error could be introduced.

6.2.5 Conclusions from Dating

Both C-14 correction methods calculated a component of the groundwater to be in excess of 5000years old, while the CFCs present suggest that there is a component on modern (post 1950s) recharge. The fact that old groundwater and young groundwater both exist in each sample suggests that two end members may be contributing to the water which is extracted from the production bores.

The existence of CFCs in all sites suggests that this represents the component of modern rainfall recharge from rapid vertical infiltration. However the older groundwater (indicated by the decayed radiocarbon) may represent the component of horizontal flow (Figure 6.4).

The proportion of each component (modern:ancient) to the total discharge is however unknown and can obviously be an infinite number of scenarios (eg. 90% recent, 10% ancient). However it is likely that the modern rainfall recharge is the dominant component,

due to knowledge of the recharge processes developed through the hydrochemistry and the fact that ancient groundwater would be a finite resource which constant groundwater discharge at the gorges would exhaust.

From a de-watering perspective it should be noted that, the smaller the portion of the ancient water, the less vulnerable a location will be to un-sustainable dewatering.

Assuming that the CFC age is the time it takes for the rainfall to infiltrate to the depth of the bores (appendix IV) it is possible to calculate an approximate rate of infiltration of 3m/year which seems to be a reasonable value.

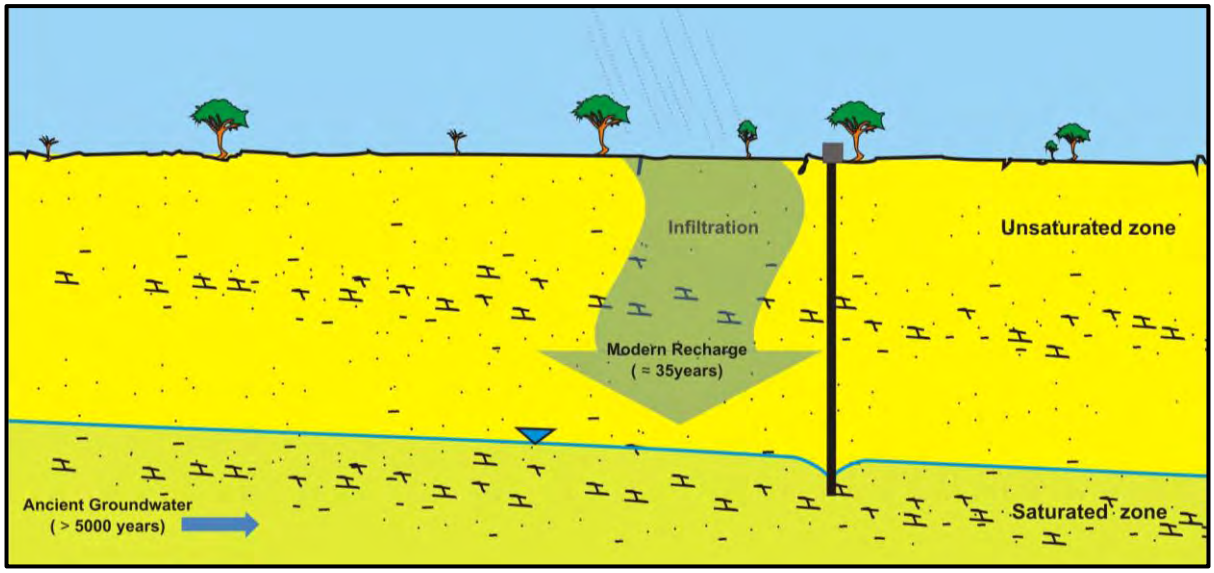

Figure 6.4 Possible scenario for the relationship of the groundwater components identified by dating methods. This scenario is based on the raw data at face value.

There is level of uncertainty in the dating data which leads to a reluctancy in making any statements regarding groundwater ages. If there is indeed a component of ancient water, it is difficult to believe that it would not be mixing with water that is discharging at the gorges, and therefore exhausting the resource.

It is therefore more likely that dilution occurs from carbon transfers. However it is impossible to make this statement without a lot more in-depth analysis undertaken on the dating data to provide more sophisticated model of the various geo-chemical processes that affect the pmc value.

Chapter 7

Analysis of each sample location

7.1 Introduction

The previous chapters were aimed at clearly defining the hydrochemical processes that are occurring within the aquifers of the Karijini National Park over time. This chapter takes this knowledge and uses it to determine whether there is any plausible concern for hydraulic connection between the Mara-Mamba aquifer at Marandoo Mine and the Gorges and Springs of Karijini National Park, that may lead to adverse effects from dewatering.

This analysis has been achieved by investigating each location individually to determine, with the acquired knowledge of groundwater chemical evolution, whether it is possible for the groundwater at Marandoo to "evolve" to the water seen at the Gorges of Karijini National Park. Groundwater will evolve from recharge to discharge through physical and chemical processes that occur in the hydrologic cycle, such as mineral dissolution and ET.

7.2 Banjima Pool

As detailed in the Banjima Pool case study (section 5.4.5), the Pool has been shown to be simply a collection of rainfall. The reason for this is summarised below:

Banjima Pool exhibits a very low Cl^- concentration of 7.5mg/L compared to the Mara-Mamba Aquifer (Cl^- = 110mg/L) and it also has an enriched isotopic ratio (δO^{18} -2.37‰ δD -29.5‰). If Banjima Pool was sourced by groundwater, a much higher Cl^- concentration would be expected. It can be assumed that the most depleted groundwater value in the KNP (-65‰) is the closest reflection of rainfall. Therefore if Banjima Pool is a collection of rainfall an enrichment of 36‰ must have occurred to produce the observed δD -29.5‰. Simpson and Herczeg (1991) found a δD enrichment of about 0.75‰ per 1 % evaporation loss in

surface waters of the semi-arid regions of the Murray Basin by using a model after Gonfiantini (1986).

This suggests that the Banjima pool sample was evaporated by approximately 48%. This level of evaporation is supported by the change in the Cl^- concentration of rainfall. This corroborates the scenario that evaporation of rainfall is the process causing the enriched isotopes despite the relatively low Cl^- concentrations.

7.3 Knox and Kalamina Gorges

Knox and Kalamina Gorges both have relatively small catchments. The TDS concentration sampled at the discharge locations were 391mg/L and 395mg/L respectively. These values are significantly lower than that of the water sampled at MM aquifer (650mg/L). If the MM aquifer was hydraulically connected to these gorges, then one of two processes must be occurring; either dilution as a result of groundwater mixing, or dissolved solute attenuation within the aquifer.

Groundwater mixing could be occurring either by input from rainfall, or by dilution from a ancient groundwater source. The latter is implausible because as the surface water samples were collected from discharge points, an ancient water body would be a finite resource that would quickly run-out if it was mixing with discharging water.

If dilution was caused by rainfall then this would require a large amount of water low in TDS to infiltrate into the aquifer. The ≈ 90% evapotranspiration that has been shown to occur makes this process also implausible.

If attenuation (sorption, precipitation, bioremediation) of the dissolved solutes was occurring within the aquifers, the Cl^- concentration would be expected to remain constant as it is uninvolved in such processes. This is not the case, because in all groundwater discharge locations the Cl^- concentration is significantly lower than that of the MM aquifer. Also, there has been no evidence to suggest that any other dissolved solutes are being significantly attenuated within the aquifers of the KNP.

Figure 7.1 Kalamina Falls at the head of the gorge. Photo emphasises the variation in water chemistry between the surface water (KLSW) and groundwater (KL1), and the similarity in $\delta^{18}O$

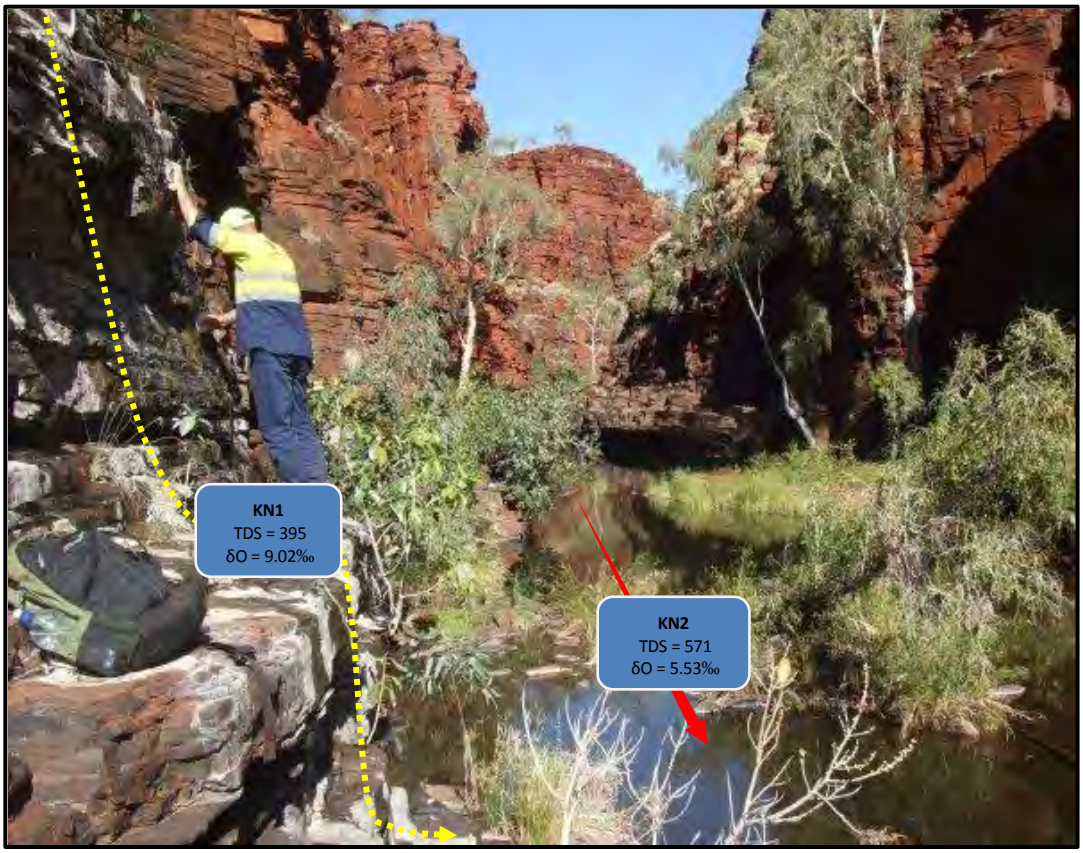

Figure 7.2 Knox Gorge. Photo emphasises the variation in water chemistry between the surface water (KN2) and the groundwater (KN1).

The chemical evolution that is occurring within the gorges of the KNP is illustrated in Figure 7.1 and Figure 7.2. In Kalamina Gorge two samples were collected from contrasting sources. The first sample was collected from a water fall at the head of the gorge, and the second from groundwater discharge from the gorge wall. The isotope values were similar in both samples, however the TDS concentration was 601mg/L and 395mg/L respectively. This suggests that transpiration processes, which increase soluted concentraition without enriching stable isotopes, were dominant in the drainage line leading up to the gorge.

In contrast, at Knox Gorge a similar difference in TDS was observed, however there was also a significant modification in stable isotopic signature. This suggests that evaporative processes were dominant in the drainage line leading up to the gorge. The contrast in the drainage lines between Kalamina and Knox Gorge is shown in Figure 7.3. It is clearly visible that the Kalamina drainage line (left) has a large proportion of trees allowing transpiration to occur, while Knox Gorge water flows for a significant portion of time as surface water exposed to evaporative processes.

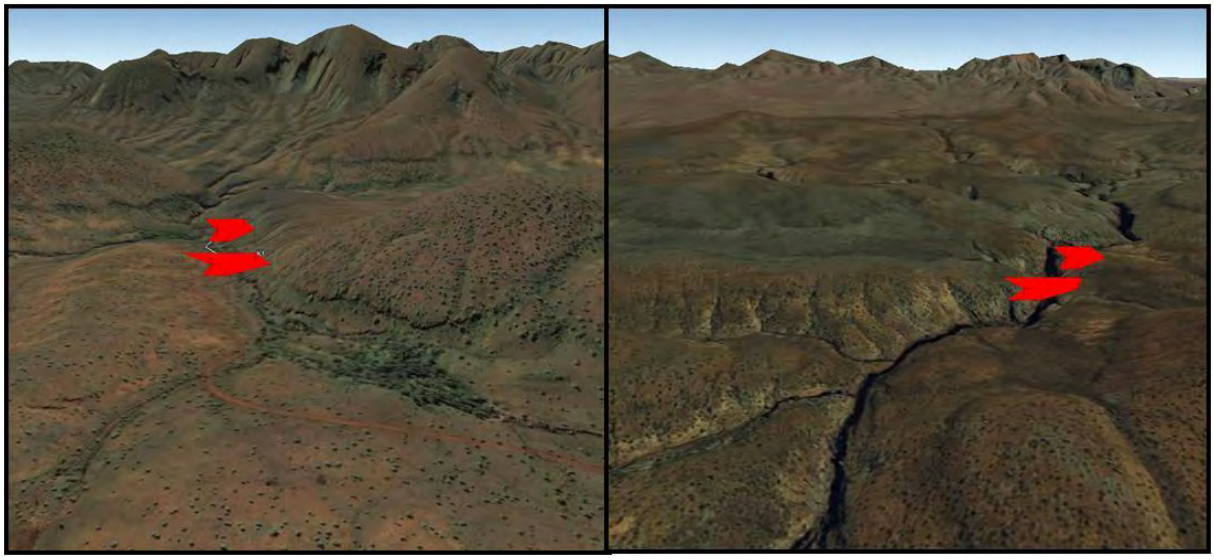

Figure 7.3 Drainage lines leading up to Kalamina (left) and Knox Gorge (right). Note the large amount of vegetation located on Kalamina Drainage line compared to the deep open valley of Knox gorge. (source:googleEarth)

7.4 Hancock and Weano Gorges

Hancock and Weano Gorge have the smallest catchments within the KNP, and they also exhibit the lowest TDS concentrations recorded in any of the gorges, at 182mg/l and 176mg/L respectively. Their Cl^- concentrations are similar to Kalamina and Knox gorge, suggesting a similar amount of evapotranspiration has occurred, however the other major ion concentrations are significantly lower. The discharged groundwater at Hancock and Weano have very low concentrations of Ca^{2+}, Mg^{2+} and especially HCO_3^-, and in fact the measured concentrations are very similar to Banjima Pool. This suggests that the residence time within the aquifer is relatively short compared to other catchments, allowing minimal mineral dissolution to occur.

The catchments of the two gorges also start in the north and extend south-east, and it is therefore logical to assume that the hydraulic gradient follows this same trend. Taking this into consideration and the hydrochemical evidence, dewatering of the MM aquifer at Marandoo will most certainly have no effect on Weano and Hancock Gorge.

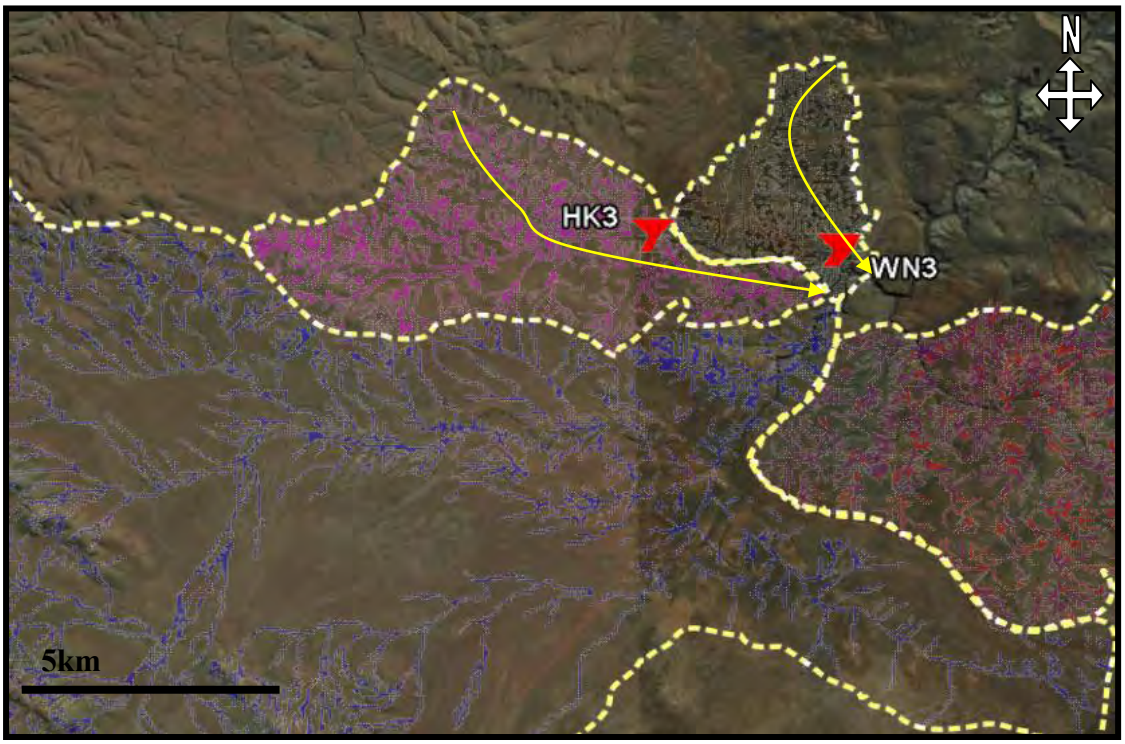

Figure 7.4 Hancock and Weano catchments emphasising their orientation. Marandoo is 33km SE. Arrows show hydraulic gradient

7.5 Joffre Gorge

The surface water sample collected at Joffre Gorge is the only groundwater discharge location in the KNP that has a TDS concentration (1240mg/L) higher than that of the MM aquifer, and its TDS concentration is approximate double. A plausible explanation for the increased TDS concentration could be due to chemical evolution as the water travels from Marandoo, but a detailed examination of the data from surrounding sources does not support this interpretation. A groundwater sample was collected from a small windmill powered bore, and it was assumed that the windmill would only have the power to extract a total of 20m head, thus the sample was entirely sourced from the surficial TR aquifer.

The major ion composition of the groundwater sampled from the windmill bore showed a very similar signature to Joffre Gorge. This suggests that the water sampled at Joffre Gorge is primarily sourced from base flow from the local TR aquifer. The higher than expected TDS concentration is due to the relatively shallow water table within the Tertiary aquifer. This is evidenced by a long drainage line that is dominated by groundwater-dependent native vegetation particularly paper bark (Figure 7.6). This allows for transpiration to occur over a considerable distance down gradient, concentrating the remaining solutes. The water table may even be close enough to the surface to allow direct evaporation to occur, and this can be inferred by the δD isotope enrichment of 4‰ between Windmill Bore and Joffre Gorge which are only 4km apart (Figure 7.5).

The increased TDS concentration observed at Joffre Gorge is also a result of dissolution of minerals within the Tertiary detritus (indurated chemical calcrete). This dissolution is seen by higher Mg:Ca and Na:Ca ratios than Marandoo, which is located in a fractured BIF aquifer. These ratios are increased due to the higher carbonate content of the tertiary aquifer compared to the fractured BIF aquifer.

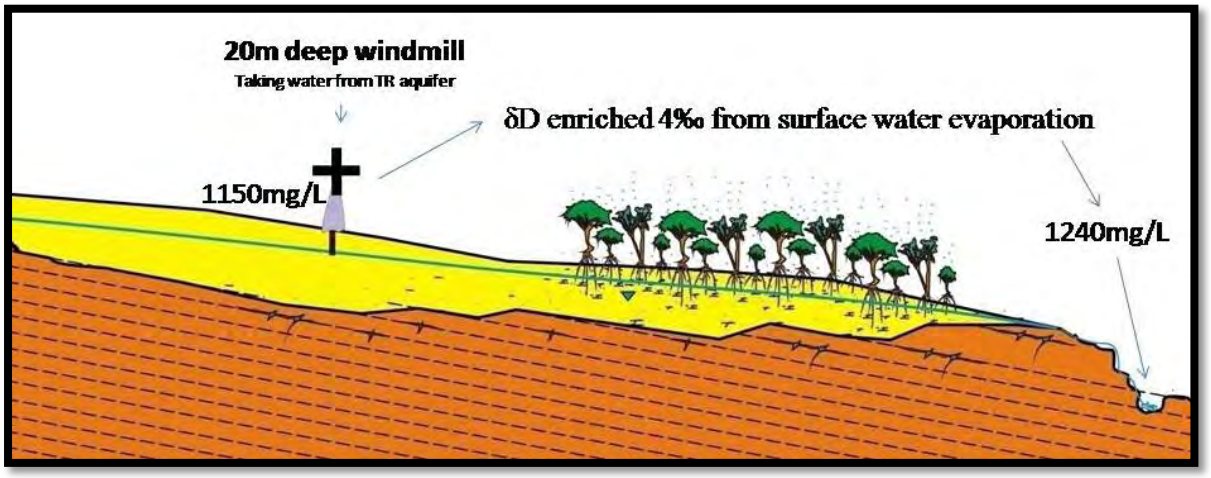

Figure 7.5 Conceptual cross section of Joffre Gorge catchment emphasising the groundwater evolution between the windmill bore and the sample collected at Joffre Falls.

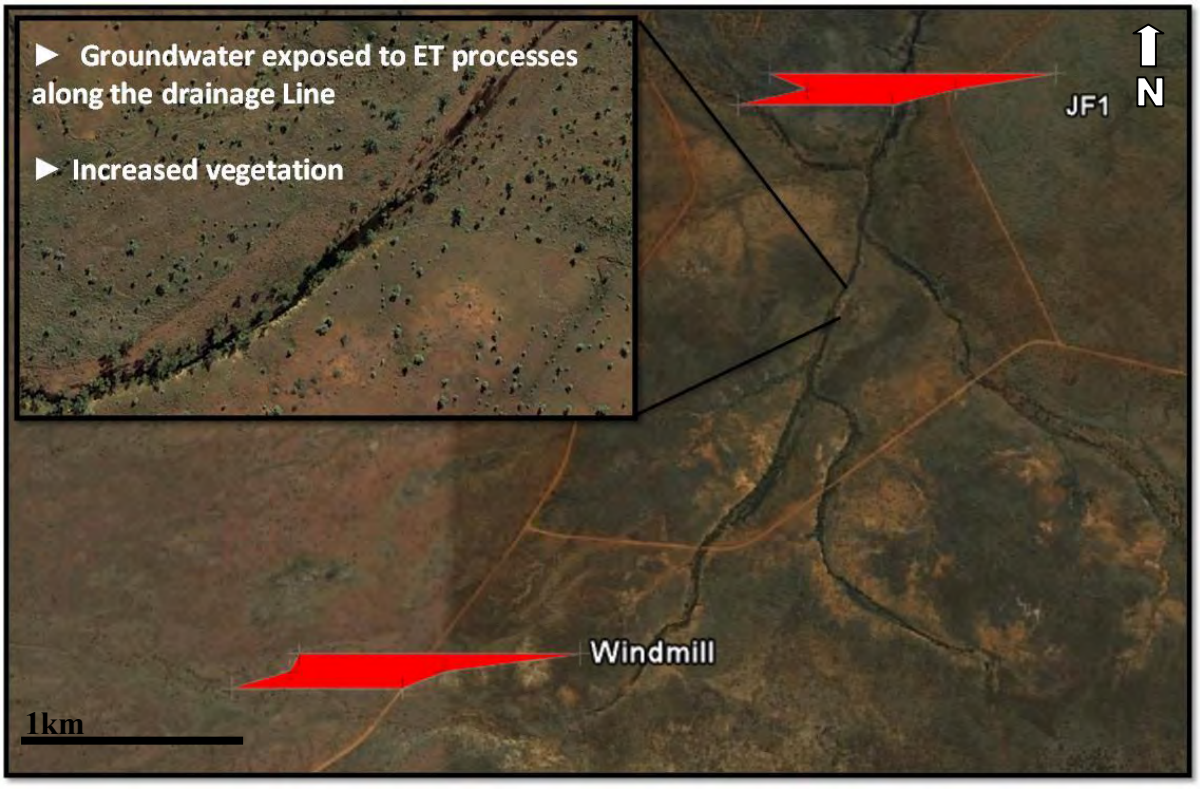

Figure 7.6 Map showing the main drainage lines leading up to Joffre Gorge

7.6 Dales Gorge

As stated in section 5.3.4, Dales Gorge seems to be fed from a large catchment that can be split into two sub-catchments, each of which supplies a different proportion of water to the Gorge. Dales Gorge exhibits a TDS concentration of ≈ 480mg/L, which is lower than the MM aquifer water at 650mg/L, but higher than the groundwater sampled from the TR aquifer upstream at the Visitors Centre (VC1) where it is 420mg/L.

When examining the major ion data it is clear that the water from the visitors centre can evolve to what was sampled at Dales Gorge. Both the δD and Cl^- values are very similar between the two locations, as would be expected if the water was flowing from one location to another (isolated within an aquifer) without evapotranspiration processes occurring.

The 60mg difference in TDS between the two locations is partly due to the increases in the concentration of Ca^{2+}, Mg^{2+} and HCO_3^- as a result of carbonate dissolution within the TR aquifer as it flows from the VC1 bore to the gore. This trend was seen during both sample programs suggesting it is a constant process with limited mixing from other sources between the Visitors Centre and Dales Gorge. This is strong evidence to suggest that groundwater at Dales Gorge is also sourced from the local TR aquifer and therefore connection to Marandoo is most unlikely.

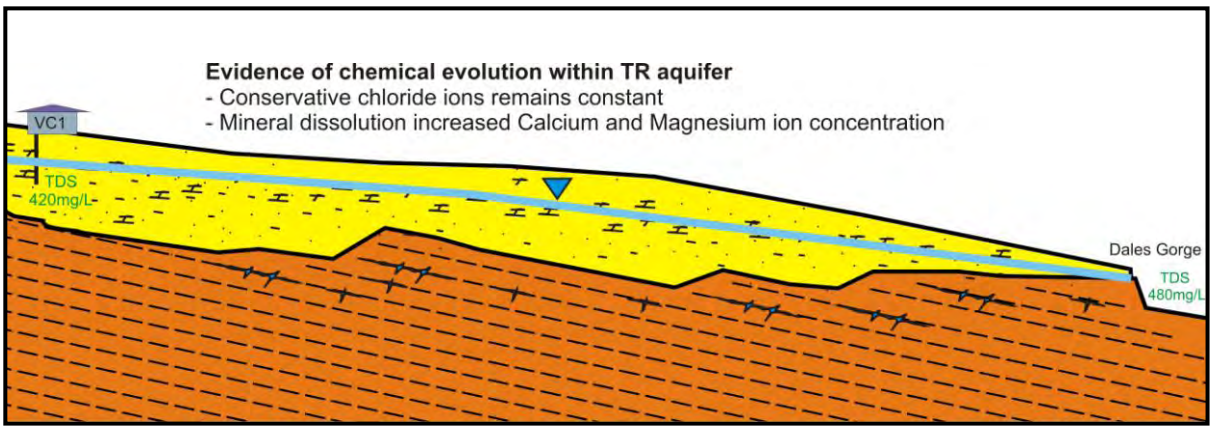

Figure 7.7 Cross-section of Dales Gorge, emphasising the evolution of groundwater from VC1 to where it discharges at the gorge.

7.7 Mindthi Spring

Apart from increased Cl^- and Na^+ concentrations, the water chemistry of Mindthi Spring is relatively similar to Marandoo. The conceptual model for groundwater discharge is shown in Figure 7.8. It is likely that groundwater is sourced from outcropping of the water table within the surficial calcrete aquifer. This is emphasised by the high concentration of HCO_3. Mg^{2+} and Ca^{2+} . The XRD analysis of calcrete outcrop nearby showed that it was 85% Dolomite, this corroborates the fact that equal concentrations of Mg^{2+} and Ca^{2+} were measured in the Mindthi Spring water sample (63mg/L), as the dissolution of dolomite produces Mg^{2+} and Ca^{2+} at 1:1 ratio (Section 5.6.1).

If Mindthi Spring is sourced from this aquifer then it is unlikely that dewatering will have an effect, as dewatering will target the deeper aquifer. However due to the proximity of the mine to Mindthi spring there is a level of concern, as even if the two are not currently connected a large drop in water table may indeed reverse hydraulic gradients in the area causing subsequent adverse effects.

Therefore ongoing monitoring should be continued throughout the dewatering process and the mode of occurrence should be further investigated to be confident that it will not be affected

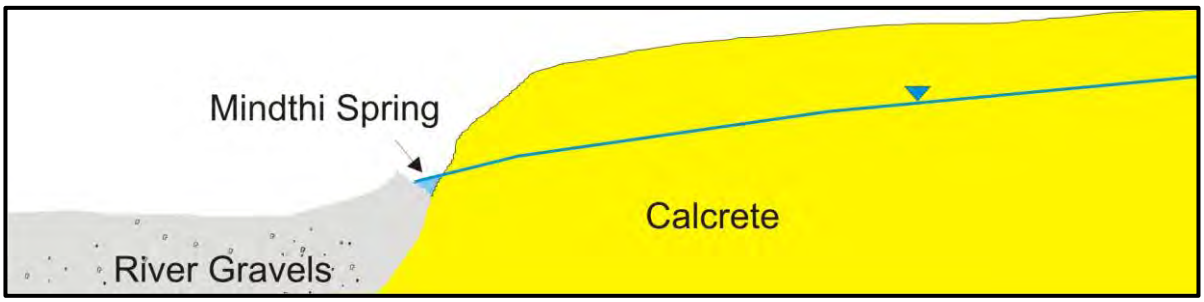

Figure 7.8 Conceptual Model of groundwater discharge at Mindthi Spring

7.8 Circular Pool

Circular Pool is unique in the fact that it is sourced entirely from base flow, and the pool itself is surrounded by 50m high vertical walls. All the surface water contained within the pool has its origins from groundwater discharge from the TR/BIF boundary and from bedding defined joints and fractures in the BIF.

The water contains much lower concentrations of Cl^-, HCO_3^-, Ca^{2+} and Mg^{2+} than that of the MM aquifer suggesting a lot less groundwater evolution has occurred. It is similar to Weano and Hancock gorge in the fact that its catchment begins on the north side of the Park.

7.9 Hamersley Gorge

The water discharged at Hamersley gorge has very similar water chemistry to the MM aquifer. It is however around 40km away. Hamersley Gorge also has the same water chemistry as Southern Fortescue Borefield (which is upstream), suggesting the two are hydraulically connected. However water has been extracted from Southern Fortescue Borefield for the last 30 years dropping the water table 10s of metres. Hamersley Gorge is less than 20km away and has not experienced any detrimental effects from groundwater extraction exhibiting perennial discharge (Figure 7.8).

This can be seen as an active example for the gorges of Karijini which are 30-40km away from where de-watering will be undertaken at Marandoo and are not even within the same catchment.

There is also a similar CFC age for both Marandoo and the Southern Fortescue Borefield suggesting that both systems have a large proportion of modern recharge. Therefore if groundwater from Marandoo was contributing to discharge at Hamersley it would be a minor amount and therefore the effects of dewatering insignificant. Figure 7.8 shows how once the water has infiltrated through the TR sequence it is stored in the Wittenoom Dolomite karstic aquifer (WT). This could explain why no significant increase in TDS is observed between HM1 and SFP, as karst terrain is known for very fresh water due to

minimal mineral dissolution. Therefore the TDS concentration observed at Hamersley Gorge is considered to be due to the mineral dissolution that occurs as the water infiltrates through the 100m thickness of TR material to reach the WT aquifer (appendix Figure A4.2).

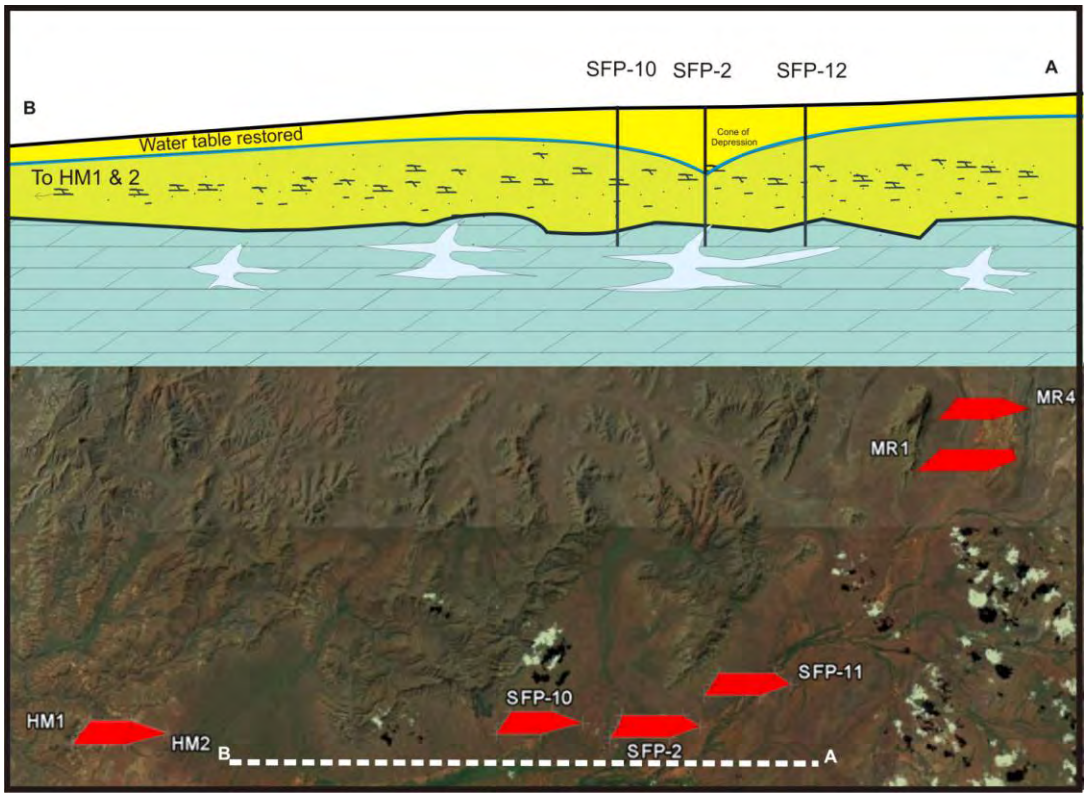

Figure 7.8 ***Top)*** **20km long section illustrating how the water table reduced by the cone of depression from Southern Fortescue Borefield is restored before Hamersley Gorge** ***Bottom)*** **The stiff plot illustrating the similarity in water chemistry between SFP and Hamersley**

7.10 Summary

By investigating each gorge separately, it has been illustrated how the hydrochemistry of the water is evolving purely within the local aquifers for each gorge. The hydrochemical evolution appears to occur primarily during processes in the Tertiary aquifer such as mineral dissolution and evapotranspiration. Therefore, it can be concluded that the groundwater from Marandoo's MM aquifer is not related to the waters of Karijini National Park, and dewatering will not have any impact on these locations. The possible exception in Mindthi spring, where its proximity to Marandoo causes concerns. This may justify an increase in monitoring and further local studies.

Chapter 8

Conclusions and Suggested Future Work

8.1 Project Summary

This study was undertaken to determine whether there was a hydraulic connection between Karijini National Park's iconic water features, and the Iron Ore at Marandoo, Pilbara, WA. The mine is proposing to significantly lower the surrounding water table to extend the life of the mine, this may have a negative impact on the surrounding water features.

Conceptual hydrogeology was aided by a hydrochemical study of the Karijini National Park, which aimed to prove that the composition of the water of each gorge can be justified by chemical evolution within the local aquifers within its own catchment.

The Hydrochemical study consisted of collecting surface and groundwater samples during September 2008 and May 2009 from thirty eight sites in 15 locations across the study area. Locations included two major borefields and numerous surface water features throughout the study area. The samples were analysed for Major Ion concentration, Stable Isotopes (δD and $\delta^{18}O$), Chloroflurocarbons and Radiocarbon.

These components of water composition can give an indication of the key processes in groundwater evolution such as recharge, residence time, chemical and physical process that affect the hydrochemistry, and discharge.

8.2 Principal Conclusions

8.2.1 Groundwater Evolution

▪ A combination of physical hydrogeology, geochemistry and stable isotope data suggests that the chemical evolution of groundwater in the Karijini National Park is dominated by processes that occur during vertical infiltration and secondly lateral movement through the surficial Tertiary sequence. As the water infiltrates through this sequence the concentration of Ca^{2+}, Mg^{2+} and HCO_3^- are significantly increased due to the dissolution of carbonates. Ion ratios suggest that dolomite is the most prevalent mineral being dissolved. The concentration of Cl^- ions is primarily dependent on the level of evapotranspiration that has occurred, as in this study Cl^- is considered a conservative ion that is only concentrated by evaporative processes.

▪ The isotope data shows that recharge occurs from intense rainfall events when recharge water quickly infiltrates before any significant evaporative modification of the groundwater isotopic signature can occur. Once in the unsaturated zone, transpiration processes act to concentrate major ions in the remaining water without enriching the stables isotope. This process varies between catchments depending on the water table depth as deep rooted plants may reach the saturated zone in places and subsequently concentration dissolved solutes by transpiration.

8.2.2 Groundwater age and temporal variation

▪ The dating data suggests that the majority of aquifer recharge occurs from direct vertical infiltration of modern local rainfall. This is indicated by the existence of CFCs, which only exist in post 1950s rainfall. There may also be a small component of ancient groundwater as evidenced by the radioactive decay of ^{14}C in the groundwater. There is some concern, however, about the quality of the dating data. This leads to a reluctancy to make any bold statements around groundwater age.

▪ There is no significant temporal variation in the chemical composition of the gorge waters suggesting that there is no significant input from surface water, as this would be a variable source. Therefore the gorges are entirely base-flow sourced which must have a constant hydrochemical composition. This suggests that the system is in dynamic equilibrium with minimal inter-aquifer mixing occurring.

8.2.3 Catchment scale hydrochemistry

▪ The major catchment variables are catchment area, the ratio of BIF to Tertiary material, the thickness of the Tertiary material, and the length of the flow path. These characteristics determine the relative ionic concentration of the discharged groundwater which will therefore be unique to the individual catchment. The amount of tertiary material is particularly important as it is a major source of mineral dissolution reactions.

▪ The contrast in the chemical characteristics of the natural waters between the key surface water features of the Karijini National Park and Marandoo Mine suggests that they are each supported by different catchments, with the exception of Mindthi Spring. The hydrochemistry of each ground and surface water location in the Karijini National Park has been shown to result from groundwater evolution within the local aquifers with no input from the MM aquifer groundwater.

8.3 Recommended Future work

As with any scientific study, more data can make the picture clearer. The following work is suggested with the aim of defining certain unknowns with more clarity.

8.1.1 Monitoring and Sampling

As is the nature of any large scale dewatering project, impacts should be continually monitored over time, as suggested for Mindthi Spring. The aim of this monitoring would be to identify any changes in flow rate that are not associated with typical seasonal fluctuations. The groundwater level, ph and Salinity of Mindthi Spring are currently monitored quarterly, when de-watering commences this should be increased to monthly, as

this is considered a realistic resolution for indentifying any changes. The water chemistry should also be analysed regularly to identify any temporal variations that may indicate a change in the groundwater flow dynamics. The major ions suggested for analysis are Ca^{2+}, Mg^{2+}, HCO_3^- and Cl^-. Which have been shown to be the major ions in groundwater evolution and may indicate a source change.

It is also recommended that rainfall samples are collected and analysed for both stable Isotope and rainfall chemistry. This should be undertaken for numerous precipitation events to allow more accurate calibration of ET models and gain better understanding on the recharge processes occurring in the area.

There is also room for an extensive hydrochemical survey of the Mount Bruce flats to be conducted. This would required more in depth analysis of the shallow and deep aquifers and whether these show any relationship to Mindthi Spring.

8.1.2 Modelling.

The hydrochemistry of the water has revealed a number of geochemical processes that are thought to be occurring. These processes can be further explored with geochemical modelling software such as PHREEQC from the USGS. PHREEQC is a computer program that is designed to perform a wide variety of low-temperature aqueous geochemical calculations.

PHREEQC is based on an ion-association aqueous model and has capabilities for (1) speciation and saturation-index calculations; (2) batch-reaction and one-dimensional transport calculations involving reversible reactions, which include aqueous, mineral, solid-solution, surface-complexation, and ion-exchange equilibria, and irreversible reactions, which include specified mole transfers of reactants, kinetically controlled reactions, mixing of solutions, and temperature changes; and (3) inverse modelling, which finds sets of mineral transfers that account for differences in composition between waters, within specified compositional uncertainty limits (USGS, 2009).

Therefore if the concentration of the end-member at a gorge is known, and there is an indication of the active geochemical processes, reverse modelling can be used to determine whether the rainfall can evolve to what is observed at the gorge

8.1.3 Dating

Although the data obtained from groundwater dating has provided some important information, it has also been shown that the dating of groundwater is a very complex process with many assumptions required in the process. To improve the quality of the radiocarbon dating, it would be appropriate to determine the initial ^{14}C for freshly recharged groundwater after water rock interaction has occurred. This will give an apparent age which can be applied to the age calculation of older water of aquifers with similar rocks. To undertake this it would be necessary to collect water from a shallow bore where it is known that recharge has occurred recently from vertical infiltration.

Another widely accepted modern method involves modelling the geochemical and isotopic evolution of groundwater between initial and final points along a flow path using the NETPATH geochemical code (Plummer et al., 1991). This is a mass-balance model that takes into consideration the carbon mass transfers along a flow path that may cause subsequent ^{14}C dilution. This model can be further refined by using $\delta^{13}C$ values which indicate the type of carbon involved in transfer (as in section 6.2.3). In this study the values for the local aquifer materials and soil were assumed. Obviously if samples of local soil and rock are analysed for their correct $\delta^{13}C$ values, the model will be far more accurate.

References

AAR , (2007) Annual Aquifer Review of Marandoo Borefield, Rio Tinto Internal Document

Abdalla, O. (2007). "Groundwater recharge/discharge in semi-arid regions interpreted from isotope and chloride concentrations in north White Nile Rift, Sudan." Hydrogeology Journal: pp. 1-14.

AGC Pty Ltd, 1985, Tom Price Water Supply Review of Long Term Capacity

Allison, G. B. (1982). "The relationship between 18O and Deuterium in water sand columns undergoing evaporation." Journal of Hydrology 55: 163-169.

Aquaterra (2001). Marandoo Wellfield Assessment: For Rio Tinto Iron Ore, Aquaterra Consulting Pty Ltd.

Balleau, W. P. (1972). "Outline of Groundwater in the Fortescue Valley: Western Australia Geologic Survey." Hydrogeology Report No. 977.

Baskaran, S., Ransley, T., Brodie, R. S. and Baker, P.(2009)'Investigating groundwater-river interactions using environmental tracers',Australian Journal of Earth Sciences,56:1,13 — 19

Beckett, K. (2008). "Phase II surface water management." unpublished report prepared for Rio Tinto Iron Ore Expansion Projects.

Busenberg, E. and Plummer, L. N. (1992) Use of chlorofluorocarbons (CCl3F and CCl2F2) as hydrologic tracers and age dating tools: the alluvium and terrace system of central Oklahoma. Water Resources Research, 28(9):2257-2283.

Cardenal, J., J. Benavente, et al. (1994). "Chemical evolution of groundwater in Triassic gypsum-bearing carbonate aquifers (Las Alpujarras, southern Spain). ." Journal of Hydrology 161(3-30).

Clark, I. and P. Fritz (1997). Environmental Isotopes in Hydrogeology, CRC Press.

Cook, P. and A. Herczeg (2000). Environmental Tracers in subsurface hydrology, Springer.

Cook, P.G. and Solomon, D.K., 1995. The transport of atmospheric trace gases to the water table: implications for groundwater dating with chlorofluorocarbons and krypton 85. Water Resour. Res., 31: 263-270.

Craig, H. (1961). "Isotopic variations in meteoric waters." Science 133: 1702-1703.

CSIRO, 2009 Chlorofluorocarbon (CFC) Analysis of Groundwater. Information Sheet CSIRO Land and Water

CSIRO, 2008 Carbon-14 (14C) Analysis of DIC in Groundwater Using Accelerator Mass Spectrometry (AMS)

Cunnold, D.M.. Fraser, P.J., Weiss, R.F., Prinn, R.G., Simmonds, P.G., Miller, B.R.. Alyea, F.N. and Crawford,A.J., 1994. Global trends and annual releases of CClsF and CClsFr estimated from ALE&AGE and other measurements from July 1978 to June 1991. J. Geophys. Res., 99: 1107-l 126.

DEC, (1999) Karijini National Park Management Plan, Department of Conservation and Land Management Report No 40.

Dincer, T., AI-Mugrin, A. and Zimmermann, U., (1974). Study of the infiltration and recharge through the sand dunes in arid zones with special reference to the stable isotopes and thermonuclear tritium. J. Hydrol., 23: 79--109.

Dindane, K. a., Bouchaou, L.a , Hsissou, Y.a , Krimissa, M.a b (2003). "Hydrochemical and isotopic characteristics of groundwater in the Souss Upstream Basin, southwestern Morocco." Journal of African Earth Sciences 36(4): 315-327.

Drever (1988). The Geochemistry of Natural Waters, Prentice Hall, Englewood Cliffs, New Years 07632

Dodson, W. (2008). Marandoo Phase II spring and gorge water assessment unpublished report prepared for Rio Tinto Iron Ore Expansion Projects, Resource Development, Technical Projects

Edmunds, W.M. and Smedley, P.L. (2000) Residence time indicators in groundwaters: The East Midlands Triassic sandstone aquifer. *Applied Geochemistry*, 15: 737-752

Edmunds, W. M., J. M. Cook, et al. (1987). "Baseline geochemical conditions in the chalk aquifer, Berkshire, UK: a basis for groundwater quality management." Appl. Geochem 2: 251-274.

Epstein S. and Mayeda, T.K., 1953. Variations of the 18O/16O ratio in natural waters. Geochim. et Cosmochim. Acta, 4: 213.

Eriksson, E., 1985. Principles and applications of hydrochemistry. Chapman and Hall Ltd, New York.

Eugster, H. and B. Jones (1979). "Behavior of major solutes during closed-basin brine evolution." American Journal of Science 279(June 1979): 609-631.

Fetter, C. W. (1994). Applied Hydrogeology, Prentice Hall. Upper Saddle River, New Jersey 07458

Feth, J.H. (1965) Calcium, Sodium, Sulfate, and Chloride in stream water of the western conterminous United States to 1957: U.S Geological Survey Hydrologic Investigations Atlas HA-189

Freeze, R.A. and J.A. Cherry.(1979). Groundwater. Prentice-Hall, Inc., Englewood Cliffs, NJ, 604 pp

Gat, J. R. (1981) Isotopic fractionation In: J.R. Gat and R. Gonfiantini (eds) Stable isotope Hydrology, Deuterium and Oxygen-18 in the water cycle. IAEA, Tech. Rept. Series No 210

Gonfiantini, R. (1986). Environmental isotopes in lake studies. In: P. Fritz and J.Ch. Fontes, Editors, *Handbook of Environmental Isotope geochemistry, 2: The Terrestrial Environment*, B. Elsevier, Amsterdam (1986), pp. 113–163.

Groves, D.I, Barley, M.E; Shepard,J.M. (1994) Geology and mineralisation of Western Australia, ASEG Special Publications 1994 (1) 1-28. CSIRO Publishing. www.publish.csiro.au

Hanshaw, B.B, (1964), Cation-Exchange constants for clay from electrochemical measurements: National Conference on Clays and Clay Minerals, 12th, Atlanta 1962, Proceeding, p. 397-421

Happell, J.D; Price, R.M; Top,Z; Swart, P K (2003) *Evidence for the removal of CFC-11, CFC-12, and CFC-113 at the groundwater–surface water interface in the Everglades* Journal of Hydrology, Volume 279, Issues 1-4

Hem, J. (1985). "Study and Interpretation of the Chemical Characteristics of Natural Water." U.S GEOLOGICAL SURVEY WATER-SUPPLY PAPER 2254.

Johnson, S. L. and A. H. Wright (2001). "Central Pilbara Groundwater Study." Water and Rivers Commission,Perth.

Jones, B. F., Eugster, H.P., Rettig, S.L, (1977). "Hydrochemistry of Lake Magadi Basin, Kenya." Geochim. Cosmochim. Acta 41: 53-73.

Kalin,R.M (2000). Radiocarbon dating of groundwater systems. In: Cook, P. and A. Herczeg (2000). Environmental Tracers in subsurface hydrology, Springer.

Kehew, A. E. (2001). Applied Chemical Hydrogeology. New Jersey, Prentice Hall.

Kendall, C and McDonnell, J (1998) Isotope Tracers in Catchment Hydrology, Elsevier Science B.V., Amsterdam.

Kendrick, T. (2006). Triennial Aquifer review, Pilbara Iron Company (Services) Pty Ltd.

Khider,K. (2004) Geochemical dispersion of elements in Byrock-Hermidale Groundwaters, Grobar Region NSW. Regolith 2004,

Kloppmann, W., L. Dever, et al. (1998). "Residence time of Chalk groundwaters in the Paris Basin and the North German Basin: a geochemical approach." Applied Geochemistry 13(5): 593-606.

Krauskopf, K and Bird, D(1995) Introduction to Geochemistry, Third Edition, WCB-McGraw-Hill

Kresic, N (2007) Hydrogeology and Groundwater Modelling, CRC Press, Tailor & Francis Group

Libby WF (1952). *Radiocarbon dating* . Chicago: University of Chicago Press

Liquid Earth, (2005) Marandoo Hydrogeological Investigation Report, Report produced for: Pilbara Ion Pty Limited

Lo´pez-Chicano, B. M., et al. (2001). "Factors which determine the hydrogeochemical behaviour of karstic springs. A case study from the Betic Cordilleras, Spain." Appl. Geochem 16: 1179-1192.

Lohmann, K. C. (1988). Geochemical patterns of meteoric diagenetic systems and their application to studies of paleokarst. Paleokarst, Springer-Verlag,New York. pp. 58-80.

Mackenzie, F (2005) Sediments, Diagensis, and Sedimentary Rocks, Elsevier Science

Mazor, E. (1991). Applied chemical and isotopic groundwater hydrology, St Edmundsbury Press.

McIntonsh, J. C. and L. M. Walter (2006). "Paleowaters in Silurian- Devonian carbonate aquifers: geochemical evolution of groundwater in the Great Lakes region since the Late Pleistocene. ." Geochim. Cosmochim. Acta 70: 2454-2479.

Monteith JL (1965) Evaporation and the environment. In The state and movement of water in living organisms*,* Fogg GE (ed). Cambridge University Press: London.

Musgrove, M. and J. L. Banner (2004). "Controls on the spatial and temporal variability of vadose dripwater geochemistry: Edwards aquifer." Geochim. Cosmochim. Acta 68: 1007-1020.

NRC, (1987). The Mono Basin Ecosystem: Effects of changing lake level, by the National Research Centre. National Academy Press, Washington.

Pearson, Jr. F.J., Hanshaw,B.B (1970) Sources of dissolved carbonate species in groundwater and their effects on carbon-14 dating. In: *Isotope Hydrology 1974, IAEA,* Vienna, 1,45-56

Plummer. (1977). " Defining reactions and mass transfer in part of the Floridan Aquifer. ." Water Resour. Res 13: 801-812.

Plummer, L.N., Prestemon, E.C., and Parkhurst, D.L., 1991, An interactive code (NETPATH) for modeling NET geochemical reactions along a flow PATH: U.S. Geological Survey Water-Resources Investigations Report 91-4078, 227 p.

Polevoy, S (2003) Water Science and Engineering (2nd Ed.), Taylor & Francis, 1996

Rosen, M. R. J., S (1998). "Controls on the groundwater composition of the Wanaka and Wakatipu basins, Central Otago, New Zealand." Hydrogeology Journal 6: 264-281.

RTIO (2006). "Triennial Aquifer Review." Internal Document.

Simonson, B M, Hassler, S W and Schuble, A, 1993. Litho logy and proposed revisions in stratigraphic nomenclature of the Wittenoom Formation (Dolomite) and overlying formation, Hamersley Group, Western Australia, Western Australia

Simpson, H. J. and A. L. Herczeg (1991). "Salinity and evaporation in the River Murray Basin, Australia." Journal of Hydrology 124(1-2): 1-27.

Simpkins, W. W. (1995). "Isotopic composition of precipitation in central Iowa." Journal of Hydrology 172(1-4): 185-207.

Stewart, M., Trompetter,Van der Raaij, R. (2002). Age and Source of Canterbury plains groundwater, Institute of Geological and Nuclear Sciences .

Stumm,W (1992) Chemistry of the solid-water interface: Processes at the Mineral-Water and Particle-Water Interface in Natural Systems. A Wiley Interscience publication

Thorne, A.M and Tyler, I.M (1996) Mt Bruce, WA, Sheet SF51-11 (2nd edition): Western Australia Geological Survey 1:250,000 series.

Thorne, A.M. , Tyler, I.M. 1997 Mount Bruce, Western Australia. 1:250 000 geological series explanatory notes. Sheet SF 50-11. Second edition. Geological Survey of Western Australia 28

Urey H.C. (1947) Thermodynamic properties of isotopic substances. J. Chem. Soc.: 562-581

Weeks, E.P., Earp, D and Thompson, G (1982) Use of atmospheric fluorocarbons F-11 and F-12 to determine the diffusion parameters of the unsaturated zone in the southern high plains of Texas. Water Resour. Res, 15, 1365-1378

Wigley (1973). "The incongruent solution of dolomite." Geochim.Cosmochim. Acta 37: 1397-1402.

Woodward-Clyde, A. (1995). Contribution of CID groundwaters to the Fortescue Valley Groundwater System: For Hamersley Iron Pty. Ltd, for Fluor Daniel Pty. Ltd

Youngs, J. (2006). Marra Mamba BWT Project - Dewatering and Reinjection Program. Prepared by MWH for Pilbara Iron.

Zagana E, Obeidat M, Kuells Ch, Udluft P (2007) Chloride, hydrochemical and isotope methods of groundwater recharge estimation in eastern Mediterranean areas: a case study in Jordan. Hydrol Process 21:2112–2123

Zimmermann, U., Ehhalt, D. and Miinnich, K.-O., (1967). Soil-water movement and evapotranspiration: changes in the isotopic composition of the water. Proc. Syrup. Isotopes in Hydrology, Vienna, 1966, Int. At. Energy Agency, Vienna, pp. 567—584

Websites

ANRA (Saturday, 22-Nov-2008). "Pilbara Climate." Retrieved 20/10/08, from <http://www.anra.gov.au/topics/rangelands/overview/wa/ibra-pil.html>.

BOM, 2009 . “Bureau of Meteorology” Retrieved 30/09/09 from www.bom.gov.au

USGS, Retrieved 30/09/09 from:
http://wwwbrr.cr.usgs.gov/projects/GWC_coupled/phreeqc/html/final-1.html

Laboratorys where Analysis was undertaken.

SGS Australia Pty Ltd
10 Reid Road Newburn, WA

CSIRO Land and water
Contact Fred Leaney, Principal Research Scientist
Phone +61 8 8303 8728

APPENDIX I : Description of the Gorges of Karijini National Park

A1.1 Hamersley Gorge

A1.1.1 Location

Hamersley Gorge is located at the North-Western edge of Karijini National Park at grid reference GDA94 50,601,610mE, 7,538,370mN. It is approximately 45km North-Northwest of Marandoo and is a tributary to the Southern Fortescue Catchment.

Figure A1.1 Hamersley Gorge

A1.1.2 Description

The Gorge cuts through Tertiary gravely clays and the top of the Bee Gorge Member shales, the base of the surface flow lies on the Main Tuff Interval (Simonson, et, al).. It contains numerous perennial pools and small waterfalls that are groundwater fed.

A1.1.3 Catchment

Hamersley Gorge has a large catchment approximately 191km^2. Water is accumulated on a large alluvial plane, and there is also significant runoff from Mt McLeod and Mt Fredrick. For the majority of the year there is no surface water flow. The only water exists where the groundwater table intersects the surface within the gorge. Groundwater discharge occurs at ~580m RL.

A1.1.4 Location of Samples

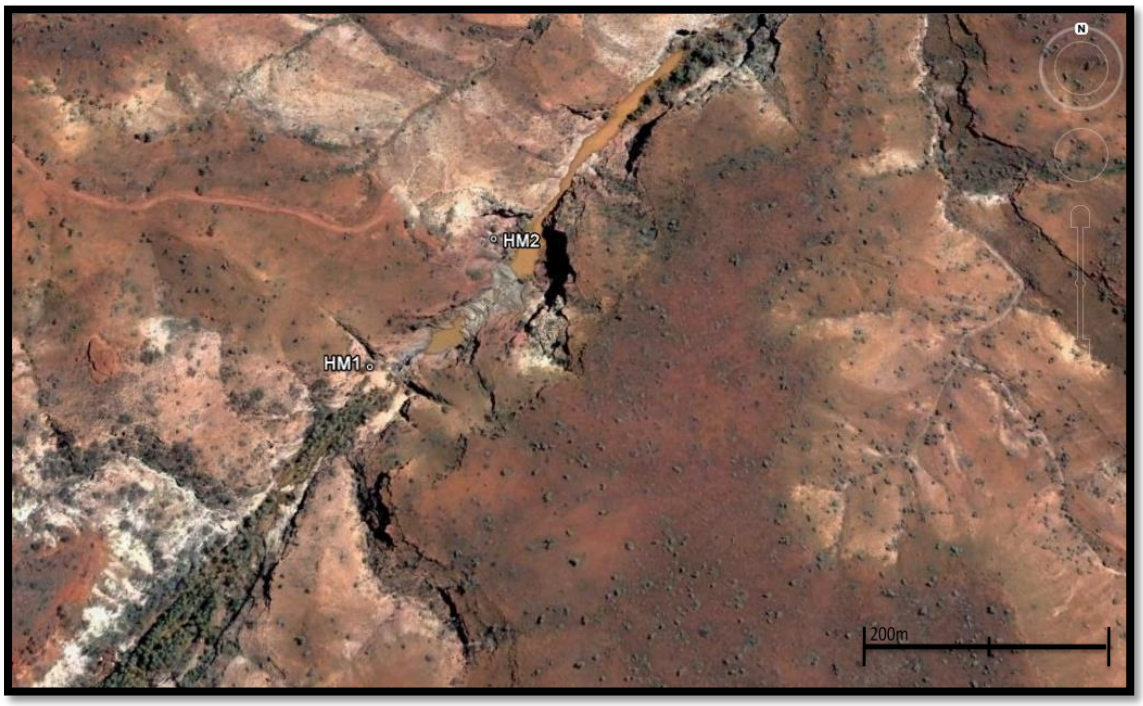

Figure A1.2 Location of samples at Hamersley Gorge

A1.1.5 Analysis undertaken

Samples were collected and analysed for major ions and stable isotopes ($\delta^{18}O$ & δD) from two locations within Hamersley Gorge (Figure A1.2):

HM1 - Close to the groundwater discharge point where water collects in a valley full of trees.

HM2 – A large pool at the end of a succession of small pools and small waterfalls.

A1.2 Hancock Gorge

A1.2.1 Location

Hancock Gorge is located at the northern edge of central Karijini National Park approximately 34km north of Marandoo mine site on small a tributary to the Fortescue River catchment. (50,631,440mE, 7,526,410mN)

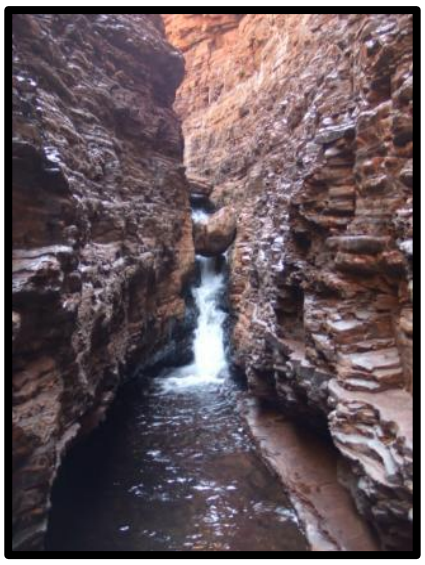

Figure A1.3 Spider walk (Hancock Gorge)

A1.2.2 Description

The Gorge is incised through a thickness of Tertiary cover into the BRF. It contains numerous perennial pools and that are groundwater fed. The Gorge tapers off to stream that contains surface water for a significant distance upstream. It is a popular tourist attraction for the more advanced climber, with access via ladders and abseiling required in places.

A1.2.3 Catchment

The Hancock Gorge is relatively small (30km^2) and extends west. The catchment is lined with saturated Tertiary colluvium overlying relatively low permeable Joffre Member basement. Groundwater discharges at ~700m RL

A1.2.4 Location of Samples

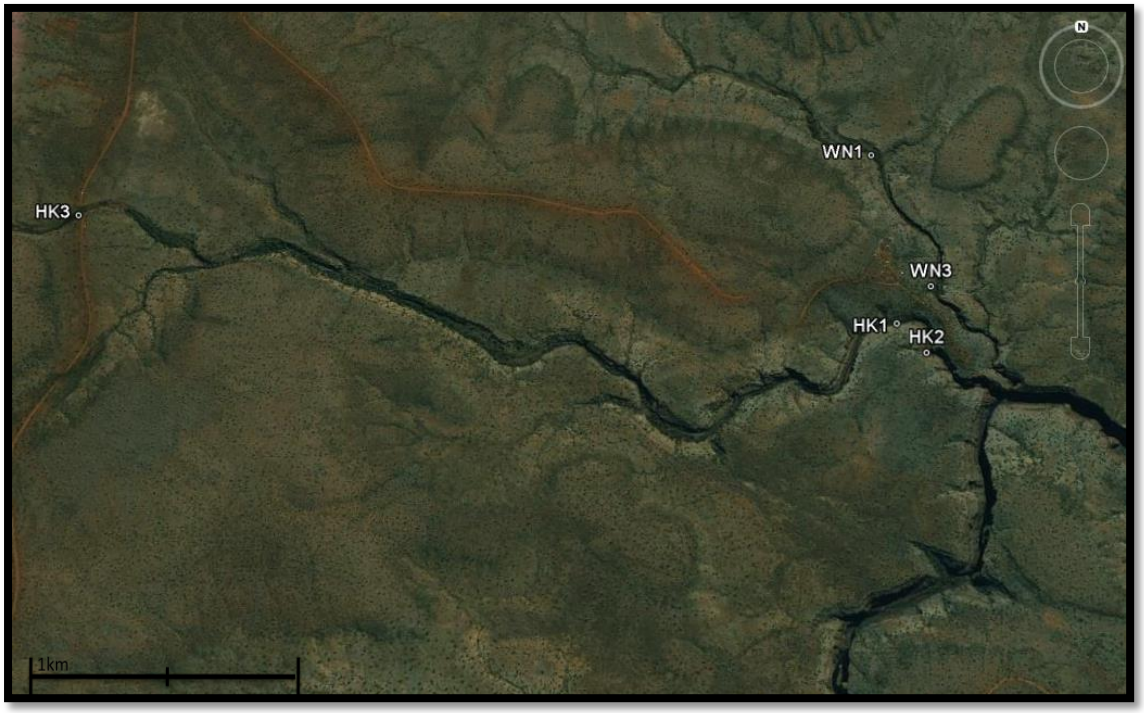

Figure A1.4 Locations of Samples at Hancock gorge. (HK3 upstream of HK1 and 2)

A1.2.5 Analysis undertaken

Samples were collected and analysed for water chemistry and stable isotopes ($\delta^{18}O$ & δD) from two locations within Hancock Gorge and one from Hancock stream 4km upstream of the gorges:

HK1&2 – These samples were collected from small pools within the gorge. HK1 was collected upstream of the famous spider walk section of the gorge and HK2 downstream.

HK3 – This sample was collected from the point where Hancock stream crosses the gorge access road. It was taken where water was collecting on the upstream side of the road.

A1.3 Weano Gorge

A1.3.1 Location

Weano Gorge is located within a few hundred meters of Hancock Gorge and is tributary to the Fortescue River. It is approximately 35km north of Marandoo mine site (50,631,440mE, 7,526,410mN)

Figure A1.5 Pool at head of Weano Gorge

A1.3.2 Description

The Gorge cuts through Joffre Member of the Brockman Iron Formation, Hamersley Group. Minor Tertiary colluvium cover occurs at top of catchment outside of gorge. The gorge features many large pools which attract tourists particularly for swimming.

A1.3.3 Catchment

Weano Gorge has a very small catchment approximately 12 km^2 to the north and west of the gorge. Groundwater discharges at ~660mRL

A1.3.4 Location of Samples

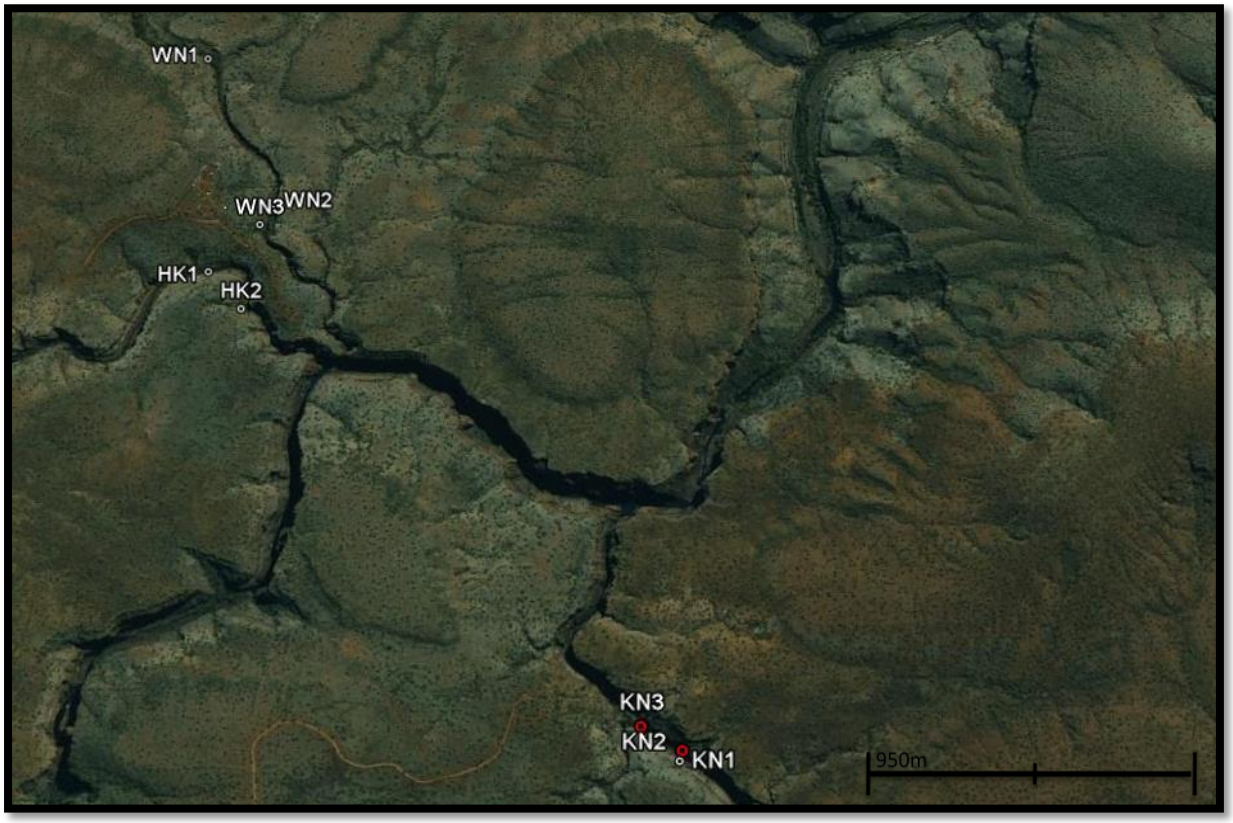

Figure A1.6 Locations of Samples at Weano Gorge

A1.3.5 Analysis undertaken

Samples were collected and analysed from two locations within Weano Gorge (Figure A1.6):

WN1 - Close to the groundwater discharge point where water collects in a small stagnant pool full of orange algae. A sample for both water chemistry and stable isotopes ($\delta^{18}O$ & δD were collected

WN3 – A large pool at the end of a succession of small pools and small waterfalls. A sample was only collected for water chemistry analysis.

A1.5 Knox Gorge

A1.5.1 Location

Knox Gorge is located within a few kilometers of Hancock Gorge and Weano Gorge and is also a tributary to the Fortescue River. It is approximately 33km north of Marandoo mine site

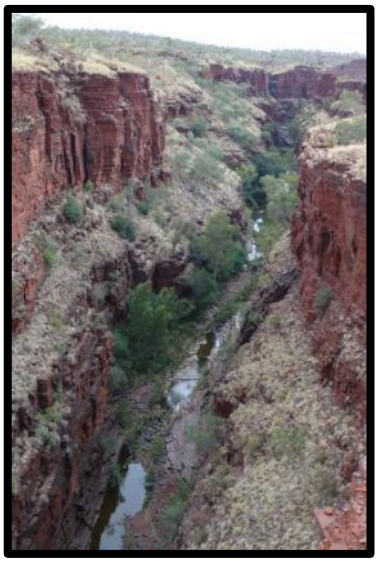

Figure A1.7 Knox Gorge

A1.5.2 Description

The Gorge cuts through Joffre Member of the Brockman Iron Formation, Hamersley Group. Little to no tertiary sediment overlies the BIF. The BIF provides many conduits of flow and groundwater can be observed to be seeping out of the Gorge walls in numerous locations. There is a significant amount of flow within the Gorge

A1.5.3 Catchment

Knox Gorge has a medium sized catchment approximately 56 km^2 to the north and East of the gorge. There is a small amount of tertiary sediment in the catchment however it is primarily comprised of BIF terrain. Groundwater discharge occurs ~640mRL.

A1.5.4 Location of Samples

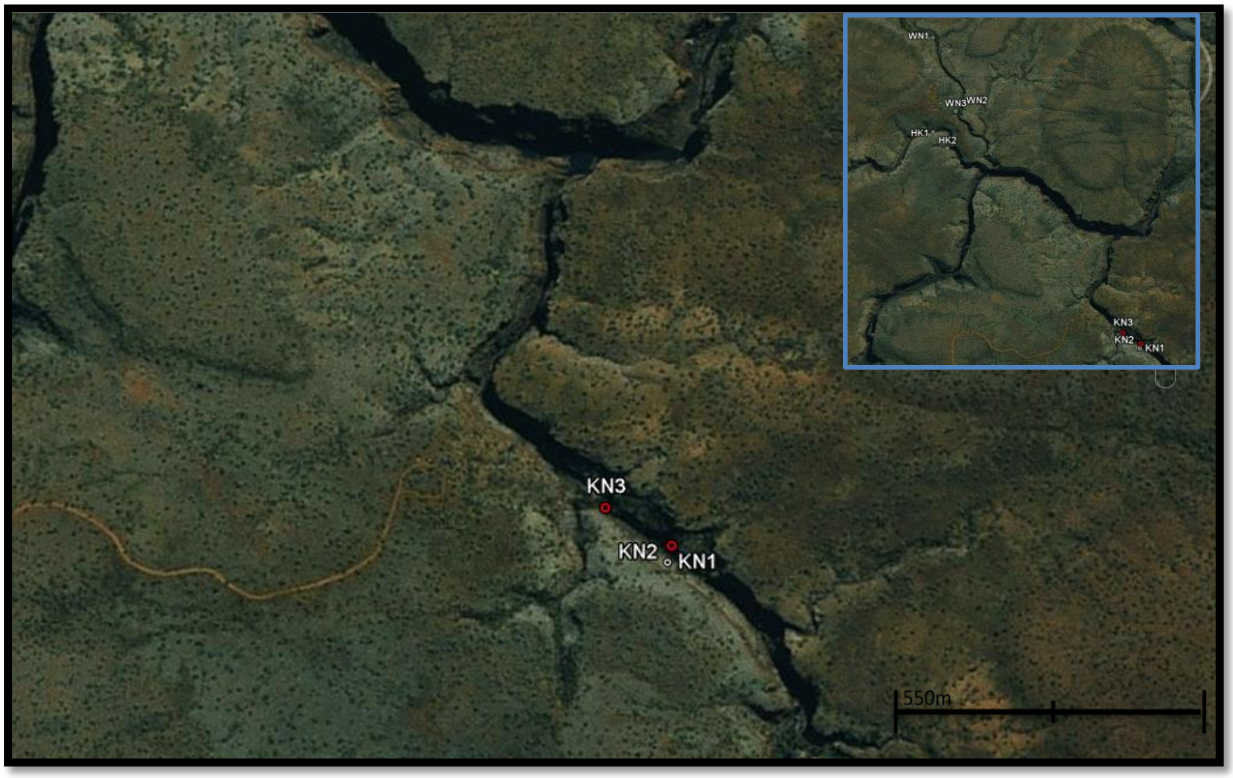

Figure A1.8 Locations of Samples at Weano Gorge

A1.5.5 Analysis undertaken

Samples were collected and analysed for water chemistry and stable isotopes ($\delta^{18}O$ & δD) from three locations within Knox Gorge (Figure 4):**KN1** – A sample was collected from groundwater that was seeping from the Gorge wall. The water was emerging from the bedding planes and dripping down the face. **KN2** – This sample was collected from the flowing stream at the foot of the wall where the KN1 sample was collected. **KN3** – Groundwater seeping out of the footwall of the gorge was collected from a constant trickle of water.

A1.6 Joffre Falls

A1.6.1 Location

Joffre Falls is located within Karijini National Park approximately 30km north northeast of Marandoo mine site on small a tributary to the Fortescue River catchment. 50,630,561mE, 7,523,332mN

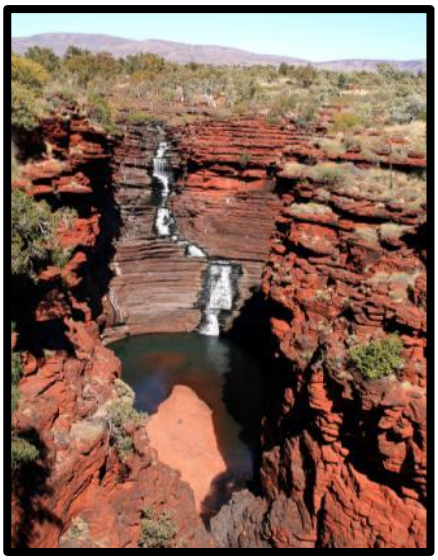

Figure A1.9 Joffre Falls

A1.6.2 Description

The Falls cascade over the Joffre Member of the Brockman Iron Formation, Hamersley Group. The Falls are at the head of a deep gorge that contains a number of pools. The head of the falls is at ~680m RL.

A1.6.3 Catchment

Knox Gorge has a large catchment approximately 400 km^2 to the South and West of the gorge. The catchment contains numerous drainage lines with near surface water indicated by a concentration of Paper Bark Trees. The Falls appear to be purely surface water fed as there is no obviously groundwater seepage from the Joffre member.

A1.6.4 Location of Samples

Figure A1.10 Locations of Samples at around Joffre Falls.

A1.6.5 Analysis undertaken

One sample was collected and analysed for water chemistry and stable isotopes ($\delta^{18}O$ & δD) from Joffre Falls**(JF1)** . The sample was collected from where the surface water emerged from a mass of rubbly BIF. Nearby groundwater was also sampled from a shallow **Windmill** bore and the water supply for Eco Lodge **(ECO1)**.

A1.7 Kalamina Gorge

A1.7.1 Location

Kalamina Gorge is located within Karijini National Park approximately 37km northeast of Marandoo mine site on small a tributary to the Fortescue River catchment. 50,644,288mE, 7,520,320mN

Figure A1.11 Kalamina Gorge

A1.7.2 Description

The Kalamina Falls cascade over the Joffre Member of the Brockman Iron Formation, Hamersley Group. Upstream of the falls comprises an upper catchment of Brockman Iron Formation with a valley fill of Tertiary Colluvium and scree shedding from the basement areas (Dodson, 2008). Note there are several other tributaries to Kalamina Gorge with larger catchment areas downstream of the falls.

A1.7.3 Catchment

Kalamina Falls has a small catchment approximately 24km^2 to the South the gorge. The drainage line leading up to the falls is swampy and lined with trees. There are also other tributaries that feed the lower section of the Gorge below the falls. Groundwater discharges at ~ 675mRL.

A1.7.4 Location of Samples

Figure A1.12 Locations of Samples at around Kalamina Falls

A1.7.5 Analysis undertaken

Samples were collected and analysed for water chemistry and stable isotopes ($\delta^{18}O$ & δD) from two locations at Kalamina Falls:**KL1** – A sample was collected from groundwater that was flowing out of the bedding structure of the BIF. There was Calcite staining of the BIF.

KL2- A sample was collected from water running over the falls. **KLHW** – Sample was also collected and analysed for $\delta^{18}O$ & δD only. This sample was collected from a swampy area lined with trees and small shurbs

A1.8 Dales Gorge and Circular Pool

A1.8.1 Location

Dales Gorge is the eastern most gorge sampled within Karijini National Park. It is located ~48km northeast of Marandoo at Grid Ref:50,660,692mE, 7,513,758mN

A1.8.2 Description

Dales Gorge cuts through the tertiary detritus into the Dales Gorge member of Brockman Formation. The gorge is relatively steep sided and contains numerous water features including Fern Pool, Fortescue Falls and Circular Pool.

Fortescue Falls cascade over a staircase of BIF bedrock. The total flow discharge is relatively small at 3.5ML/day.

Cicular Pool is unique in the fact that it is is fed entirely by groundwater discharge. It is a collapse feature that defines the starting point for a side arm of the main part of Dales Gorge.

A1.8.3 Catchment

Fern Pool and Fortescue Falls: A large catchment extends south from the head of Dales Gorge, the catchment has as complex structure and is defined by a network of channels and valleys defined by BIF ridges. Groundwater discharges at ~655m RL.

Circular Pool: A small catchment extends North from around Circular Pool. Rainfall Groundwater discharge occurs at depth of ~40m from flow conduits on the walls of the pool. Groundwater discharges at ~635m RL.

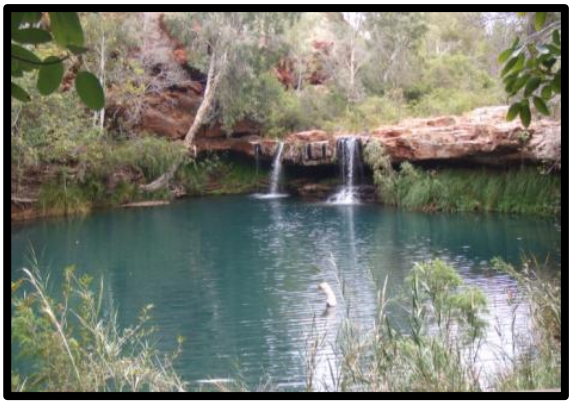

Figure A1.12 Fern Pool

Figure A1.13 Circular Pool

Figure A1.14 Fortescue Falls

A1.8.4 Location of Samples

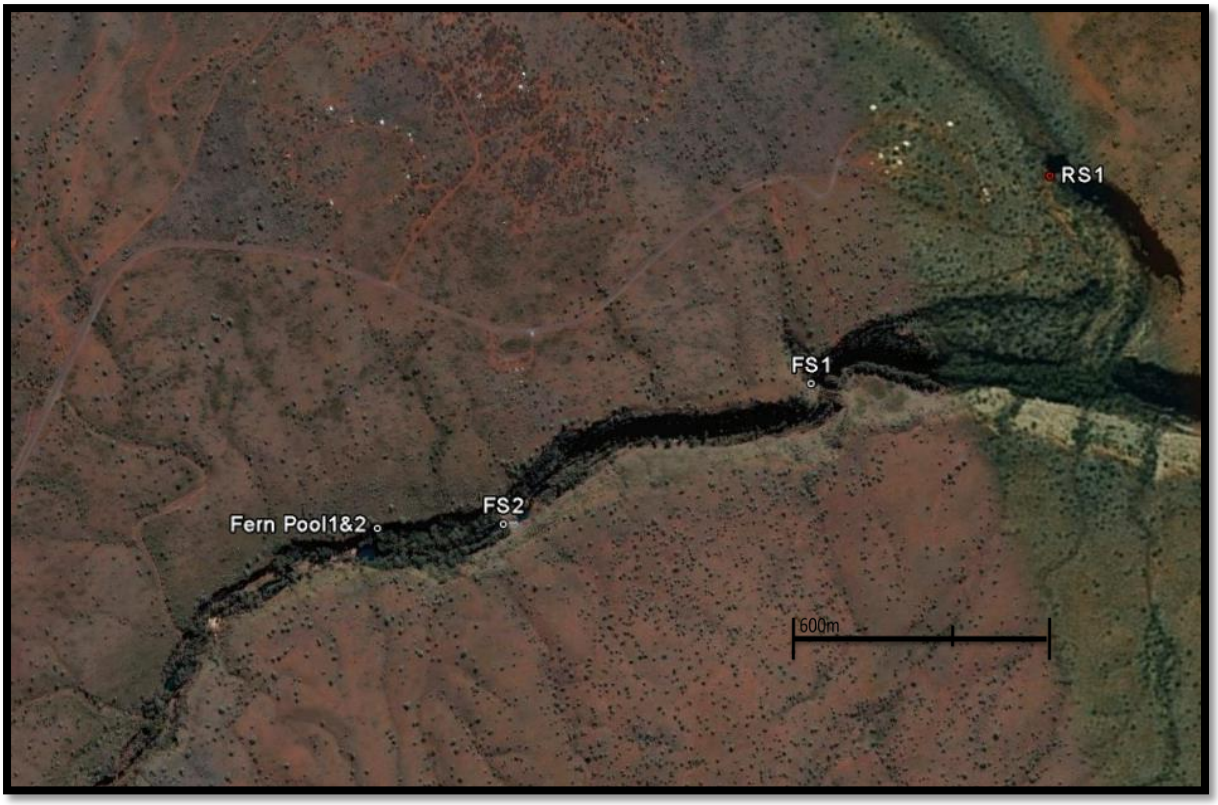

Figure A1.15 Locations of Samples from Dales Gorge

A1.8.5 Analysis undertaken

Samples were collected and analysed for water chemistry and stable isotopes ($\delta^{18}O$ & δD) from five locations in the Dales Gorge area:

Fern Pool – Two samples were collected here. Fern Pool 2 was a sample of water from the pool and

Fern Pool 1 was collected from groundwater seepage from a nearby embankment. The water was seeping out the the face and trickling through leaves.

FS1 – A small step in the stream where water was flowing at a moderate rate and not stagnant.

FS2 – A sample was collected from the head of Fortescue Falls.

RS1 – Samples were collected from the large amount of groundwater that was seeping out of the Cliffs around circular pool.

A1.9 Mindthi Spring

A1.9.1 Location

Mindthi Spring is located 18km southeast of Marandoo Mine in a tributary to the Turee Creek drainage system. Grid Ref – 50,629,719mE, 7,486,482mN.

A1.9.2 Description

Mindthi spring occurs on the side of the creek banks and is thought to be supported by groundwater discharge from a near surface calcrete aquifer. It is likely that groundwater discharge is due to intersection of topography with the shallow water table located in the calcrete aquifer.

A1.9.3 Catchment

The catchment for Mindthi Spring is not clearly defined, but may extend out into Mount Bruce Flats. Groundwater discharge occur at ~678m RL.

Figure A1.16 Collecting Sample from Mindthi Spring Photo Source : W.Dodson RTIO

A1.9.5 Analysis undertaken

Samples were collected and analysed for water chemistry and stable isotopes ($\delta^{18}O$ & δD). Solid samples were also collected from the aquifer material nearby to be analysed via x-ray diffraction to determine its mineral composition.

A1.10 Banjima Pool

A1.10.1 Location

Banjima Pool is a non-permanent rock pool approximately 10km south east of the mine and outside of the Marandoo mine lease .The pool elevation is approximately 705m RL which is ~25m above the local groundwater table. It is located at Grid Ref : 50,623,207mE, 7,490,600mN

A1.10.2 Description

The pool is located at the base of a small waterfall where scouring has occurred and is surrounded by rock faces on three sides. The morphology of the pool is such that it is very sheltered limiting its exposure to direct sunlight. The pool is at an altitude of 710m RL

A1.10.3Hydrogeology and Catchment

The Catchment for Banjima Pool appears to be very local and and related to immediate surface water run-off.There does not appear to be any groundwater inputs as groundwater levels are estimated at least 25 – 30m below ground level (pers Comms W.Dodson, 2008)

Figure A1.17 Banjima Pool (Photo Source: W.Dodson)

A1.10.5 Analysis undertaken

Samples were collected and analysed for water chemistry and stable isotopes ($\delta^{18}O$ & δD).

APPENDIX II: Additional Stiff plot Maps of Sample Locations

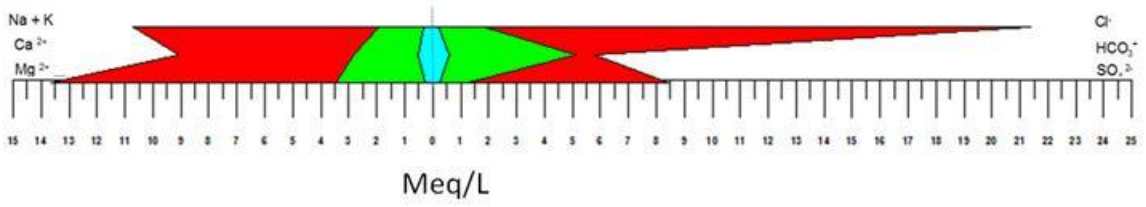

Figure A2.1 Relative scale used for stiff plots in following diagrams (from biggest to smallest: RS1aGW, HM1, BJ Pool)

Figure A2.2. Stiff Plots at Marandoo Production Bores

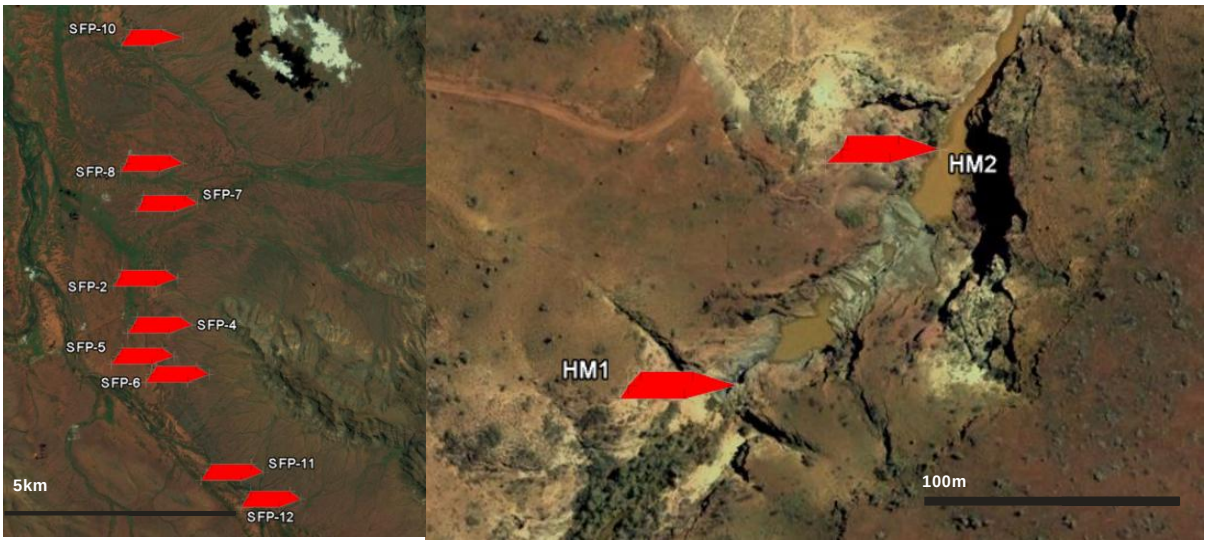

Figure A2.3 Sitff plots for Southern Fortescue Borefeild (left) and Hamersly Gorge (right)

Figure A2.4 Stiff Plots for Hancock and Weano Gorge

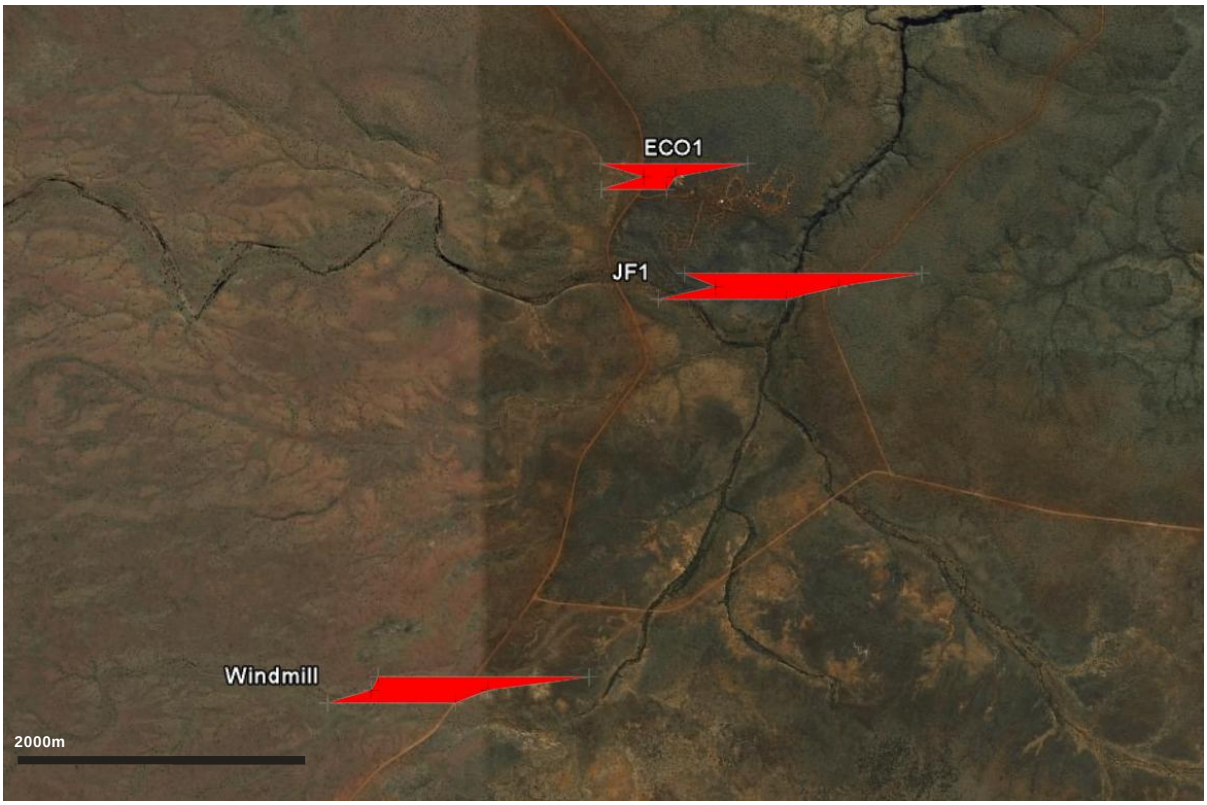

Figure A2.5 Stiff plots for the Joffre Falls Catchment. Showing the two bores; Windmill and Eco Lodge and the samples collected from surface water at the falls

Figure A2.6 Stiff plots of Dales Gorge (Fern Pool, Fortescue Falls and Circular Pool

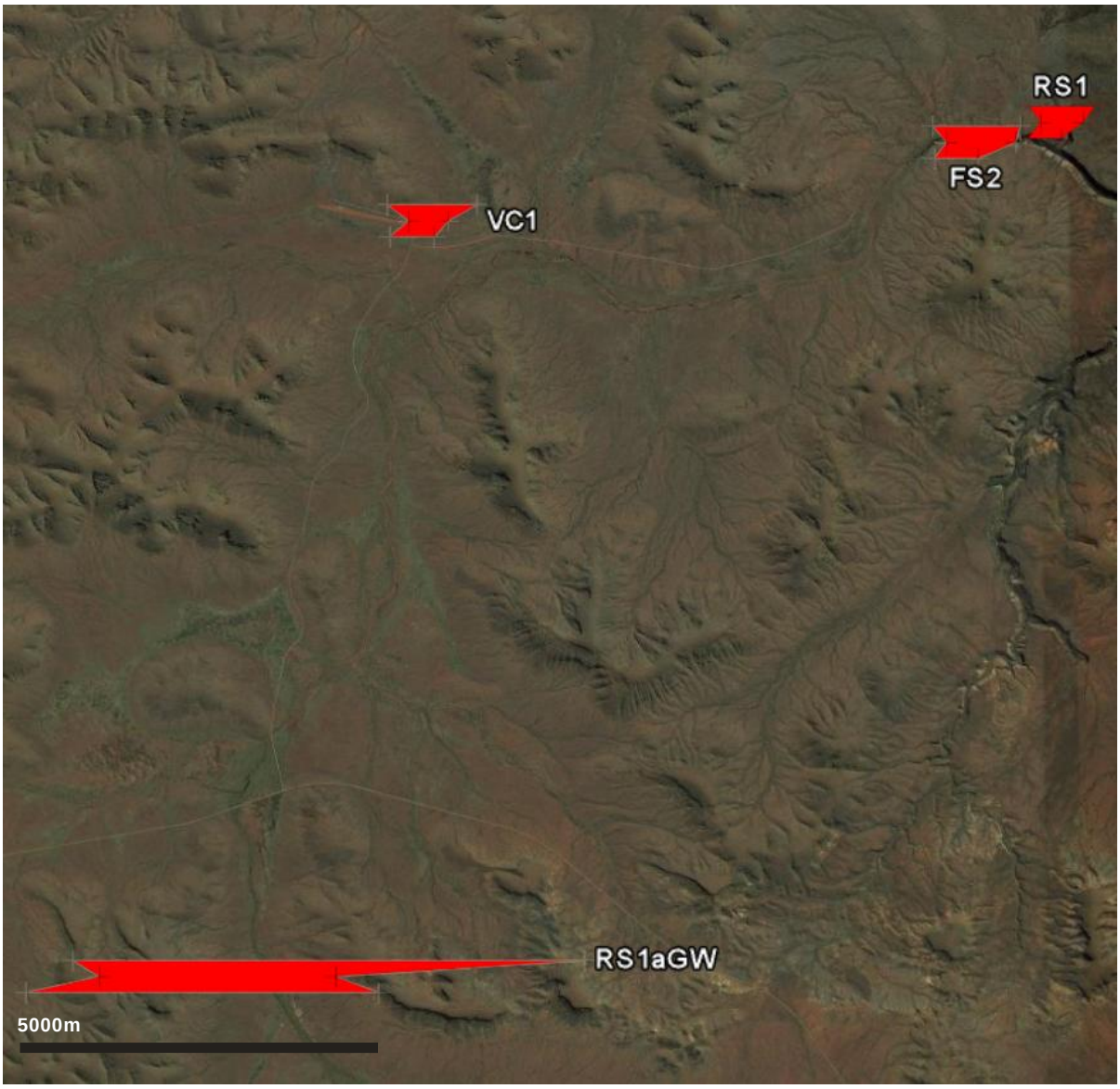

Figure A2.7 Stiff Plots for Dales Gorge Catchment (sub catchment one includes VC1; Subcatchment 2 includes RS1aGW

APPENDIX III – The use of Major Ions and Stable Isotope (δ D and δ18O) to distinguish groundwater flow in Karijini National Park, Pilbara, WA

Publication produced during thesis (prepared for AusIMM Water in Mining Conference, 2009)

The Use of Major Ion Analysis and Stable Isotopes δO^{18} and δH^{2} to Distinguish Groundwater Flow in Karijini National Park, Western Australia

P Hedley[1], S Dogramaci[2] and W Dodson[3]

ABSTRACT

Isotopes and hydrochemistry were used to define groundwater flow systems and better understand the hydrogeological setting of the Karijini National Park, which is in the Central Pilbara region adjacent to the Marandoo iron ore mine. Based on the stable isotope composition of the water samples, the data can be divided into two main groups. Groundwater is characterised by depleted δD and $\delta^{18}O$, suggesting no significant evaporation effect. Surface water on the other hand is more enriched in δD and $\delta^{18}O$ due to evaporation. The relatively high concentration of Cl^- compared to rainfall and depleted δD and $\delta^{18}O$ values of groundwater indicate that recharge of the aquifers is occurring during intense rainfall events when rapid infiltration occurs. Evapotranspiration then acts to concentrate ionic species prior to recharge. Relationships between the major ion concentration and catchment area, surficial Tertiary cover and distance between recharge and discharge were identified. The results show that these catchment variables combine to determine unique water chemistry for each sub catchment in Karijini National Park.

The TDS concentration of the groundwater in the Marra Mamba Iron Formation that hosts the Marandoo ore body is higher than most of the water bodies surrounding the mining area suggesting significant modification or different recharge mechanisms to that of the Karijini groundwater.

INTRODUCTION

When there is a restriction on obtaining subsurface hydrogeologic information via methods that involve ground disturbance, hydrochemistry can be used as a non-evasive low cost investigation method to supplement conventional hydrogeological investigations (Demlie, 2007; Barbieri, 2005). The chemistry of the water is determined by the physical and chemical processes it has been subjected and it can be used to better understand aquifer hydraulics, inter-aquifer mixing and groundwater aquifer matrix interaction. In this study Major ion concentrations and stable isotopes (δD and $\delta^{18}O$) have been used as a tool to determine the relationship between Marra Mamba (MM) aquifer at the Marandoo Mine and Tertiary sediment (TR) aquifers and Brockman Iron Formation (BIF) of Karijini National Park (KNP).

Rio Tinto's Marandoo Mine is located within the KNP, in Central Pilbara Region, Western Australia. Rio Tinto Iron Ore (RTIO) has undertaken a prefeasibility study into expanding the mine below watertable and has proposed a significant dewatering scheme to access the ore below the water table.

The proposed mine plan dictates the required dewatering in the vicinity of the pits for effective and safe extraction of the iron ore (Dodson, 2008). A lowering of the regional water table has the potential to have adverse effects on surrounding areas. To assess the potential impact of dewatering on the water features of the KNP, the hydrogeology must be understood to determine groundwater interaction and flow dynamics. As ground disruption within the National Park off mining tenure is not permitted, a drilling program to define the hydrogeology in the park is not an option. Therefore, a hydro-geochemical study of groundwater has been conducted in an attempt to better understand the hydrogeology of the region.

The mine produces Marra Mamba lump and fine ore which is a vital part of their Pilbara Blend Product. Extending Marandoo's life will be important in continuing to produce a constant product. Therefore, it is imperative that enough evidence is collected to allow mine operations to continue.

Description of study area

The Pilbara region of Western Australia is located 1100 km N-NE of Perth. It is a region that is rich in mineral resources which have been extracted over the last century. The Pilbara region covers an area of 507 896 km^2. Karijini National Park is a located in the Centre of the Pilbara within the Hamersley Ranges (Figure 1). It covers an area of 6274 km^2 making it the second largest national park in Australia. The Park's main features are the picturesque natural gorges, which have incised down deep through the Brockman Iron Formation. The gorges developed due to the significant erosion of the BIF along the main catchment drainage lines and a significant thickness of colluvium and alluvium has been deposited as valley-fill material.

Climate and hydrology

The Pilbara Region has a semi-arid climate dominated by two distinct seasons (wet summers and dry winters). These are influenced by two air masses over the region, the Indian Tropical Maritime air moving in from the west or northwest, and the tropical continental air from the inland (ANRA, 2007). In the summer months (November to February) the average maximum temperature is often over 40°C, while during the winter months it falls to about 25°C.

Average rainfall over the area ranges from about 200 mm to 350 mm, although rainfall may vary widely from the average from year to year. Most of this rain falls between December and March, but can continue through until June. Distinct dry periods are observable predominantly between August and November. The average yearly evapotranspiration (about 2500 mm) exceeds average yearly rainfall (ANRA, 2007). Average rainfall near Marandoo is approximately 365 mm and is characterised by frequent, low-intensity events related to localised thunderstorms and tropical upper air disturbances, however there are also rare high-intensity events associated with tropical cyclones (Beckett, 2008). Tropical cyclones occur in the area, usually between January and April, with a frequency of about seven every decade. They produce a massive amount of rainfall, contributing 40 per cent to 60 per cent rainfall to the region (ANRA, 2007). These high-intensity events often cause over 100 - 200 mm of rain within 24 hours (Beckett, 2008). These intense high volume rainfall events produce significant surface flow that may recharge the aquifers in the region.

The local hydrology is affected by a prominent east-west ridge of the Hamersley Range which divides Marandoo Mine and the

1. Masters Student, Geological Sciences, University of Canterbury, Private Bag 4800, Christchurch 8140, New Zealand. Email: paulhedley@gmail.com
2. Specialist Hydrogeologist, Riotinto Iron Ore, Level 9, 182 St Georges Terrace, Perth WA 6000. Email: shawan.dogramaci@riotinto.com
3. Principal Hydrogeologist, Riotinto Iron Ore, Level 9, 182 St Georges Terrace, Perth WA 6000. Email: wade.dodson@riotinto.com

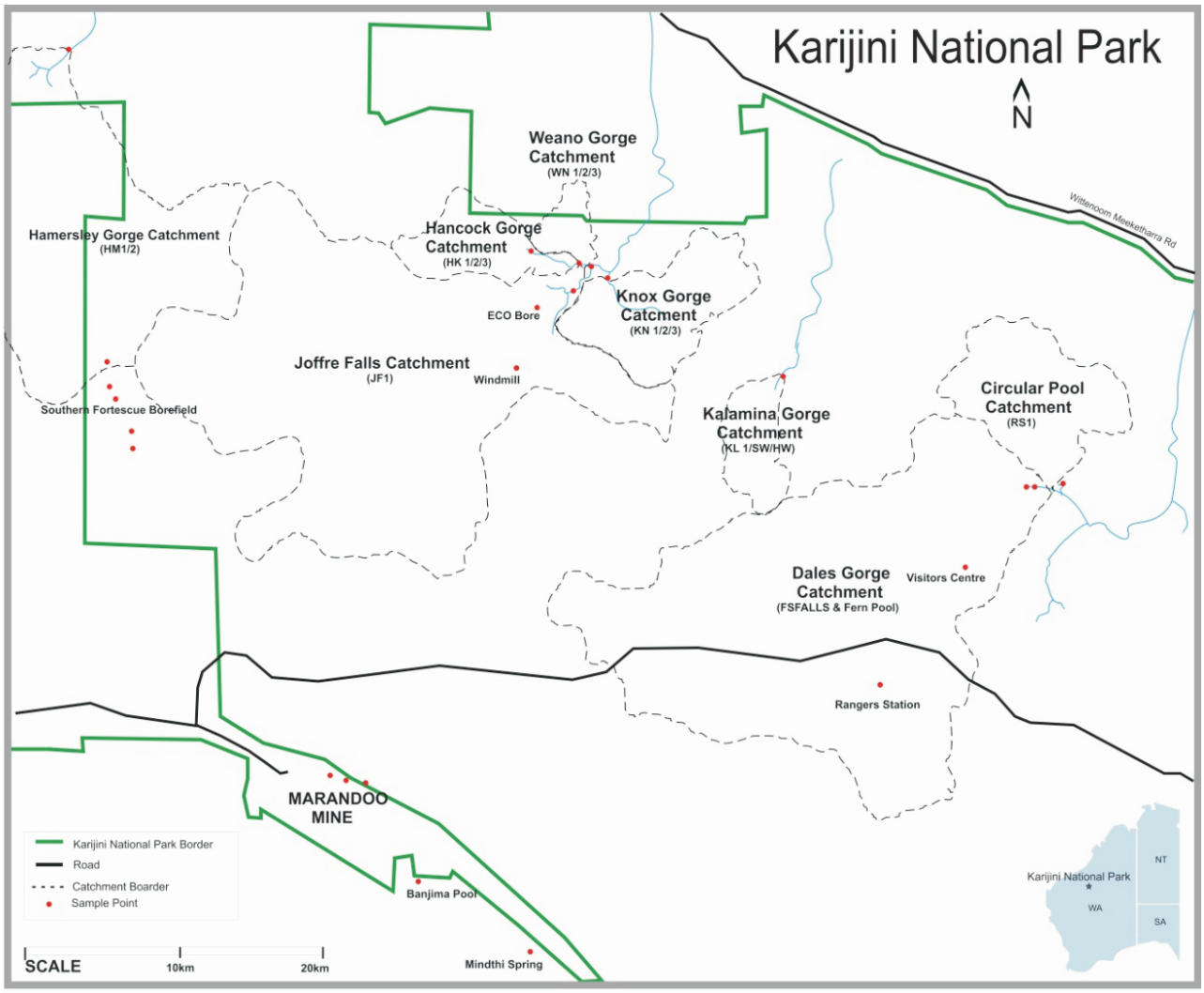

FIG 1 - Map of the study area with catchment names and sample locations.

KNP (Figure 2). Rainfall that falls on the north side of the ridge will be collected by a number of catchments ranging in size from 12 km^2 - 350 km^2. Each catchment has an incised gorge as its main or only discharge point. The structure of each catchment is defined by the resistant BIF ridges in the area; zones of weakness have been eroded away resulting in considerable bedrock relief. Variations in area of BIF outcrop, amount of Tertiary valley fill and flow path length combine to create a range of different catchment characteristics. For the majority of the year, surface water flow rates in the KNP are relatively low, as the water is derived completely from base flow and exists in the form of small pools and low-flow streams. Rainfall that occurs on the south side of the ridge will fall on the Mount Bruce flats which are an internally draining system. Surface water outflows from these flats only occur during extreme rainfall events.

Regional and local geology and hydrogeology

Regional characteristics

The geology of the region is comprised of a succession of Achaean to Lower Proterozoic sedimentary rocks from the Hamersley Group. The group consists of various metasedimentary rocks including banded iron formations, inter-bedded with minor felsic volcanic rock and intruded dolerite dykes (Johnson and Wright, 2001). Marandoo Mine is located in the mineralised section of the Mara-Mamba Iron Formation (MM), which is overlain by the Wittenoom Formation (WT) and the relatively impermeable Mount McRae Shale (Figure 2). These are overlain by the Brockman Iron Formation (BIF). The eroded drainage lines are filled with Tertiary sediments (TR) and groundwater may exist in both Tertiary sediments and in fractures in the bedrock (Dodson, 2008).

The TR aquifers consist of alluvium and colluvium which are shallow and tend to be unconfined. The alluvium is often clayey with inter-bedded sand and gravel lenses, whereas the colluvium comprises cobble-sized detritus within a clay matrix. The thickness of Tertiary material is highly variable. Groundwater is contained in the primary porosity of the clastic sediments. There may be a hydraulic connection with the underlying BIF in the KNP and MM at Marandoo Mine site, particularly where the basement is weathered and fractured (Woodward-Clyde, 1995).

The MM groundwater occurs where secondary porosity has developed in fractured, mineralised, weathered zones and along bedding plane partings or joints. Where the rock is not fractured there is little to no-porosity and therefore no groundwater exits, this is particularly true for the BIF in the KNP catchments. The relatively low hydraulic property of the unmineralised BIF is evident by the absence of seepage from most of the gorge walls at the KNP. In contrast to unmineralised BIF formation, Wittenoom Formation is characterised by significant porosity and karstic features can develop due to the dissolution of dolomite via percolating groundwater (Balleau, 1972), particularly where over lain by Tertiary cover.

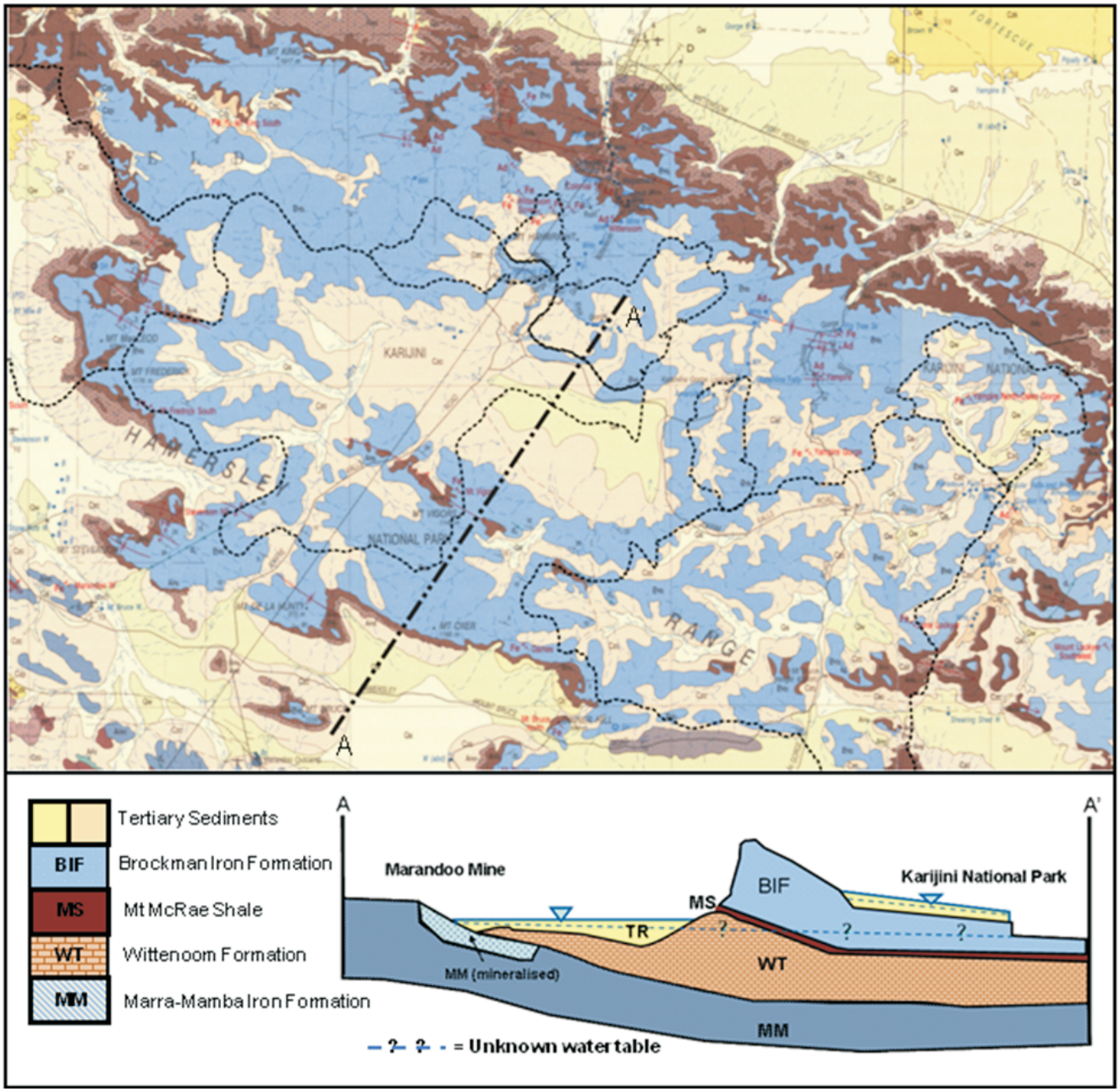

FIG 2 - 1:250 000 geologic map of Karijini National Park, with cross-section of the regional hydrogeology, Hamersley Group (map extracted from Thorne and Tyler, 1996).

Local characteristics

The groundwater of the KNP occurs primarily in the TR aquifers and in fractured sections of the BIF. The Tertiary sediments comprise loosely consolidated alluvium, colluvium and indurated chemical (calcrete/goethitic) sediments that act predominantly as sedimentary aquifers (Dodson, 2008). The BIF has zones where it is fractured and jointed and also where bedding planes have parted. These zones may support groundwater flow which is assumed to be sourced from downward percolation from the unconfined Tertiary aquifers.

The gorges of the KNP are incised up to 60 m into the BIF bedrock with near vertical walls, and have a thin layer of Tertiary material on the top, as shown by Figure 3. Groundwater is primarily discharged into the gorges from the BIF-TR boundary. Generally there is no groundwater discharging from the walls throughout the entire length of the gorge. There are a few cases where groundwater can be seen to seep out of the fractured BIF, in other cases this seepage is indicated by white precipitate staining on the walls of the gorge.

Tertiary and Marra Mamba iron formation groundwater

There are two main borefields associated with this study, Marandoo Mine and Southern Fortescue Borefields. At Marandoo both Tertiary and MM aquifers exist. The permeability of the Mara-Mamba is gained during mineralisation when silicates are stripped from the banded Iron formation and vugs develop. Transmissivities derived from the MM aquifer range between 50 m^2/d and 1800 m^2/d (Youngs, 2006).

The Southern Fortescue borefield is located in the catchment of the Southern Fortescue River. The borefield is located in a thick Tertiary sequence of alluvial, colluvial and other deposits formed from secondary diagenetic process (calcretes, ferricretes,

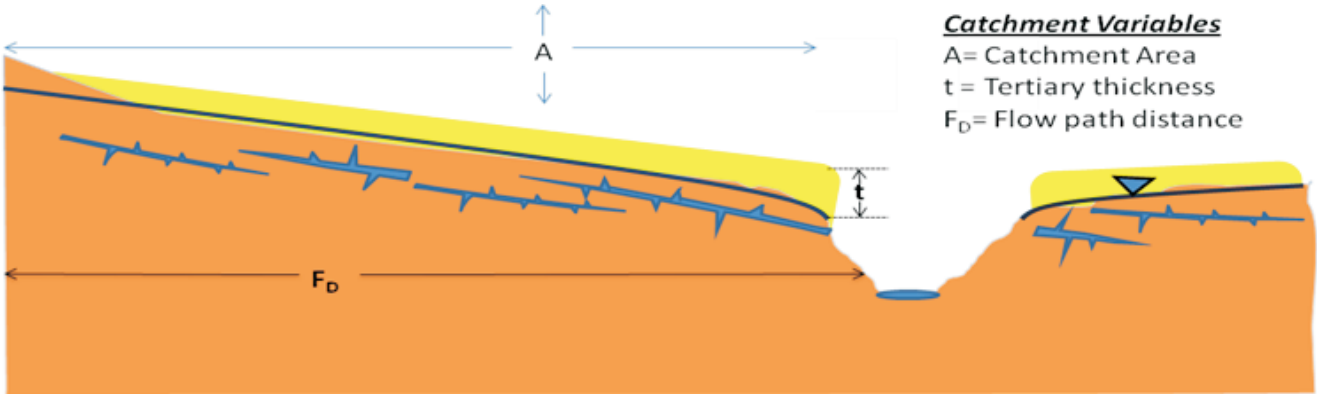

FIG 3 - Conceptual cross-section of a typical gorge within Karijini National Park.

etc) that has developed in a palaeovalley. The valley has eroded down to the underlying Wittenoom Formation. These Tertiary aquifers host a large amount of water with hydraulic properties commensurate to that of the MM aquifer (Kendrick, 2006).

METHOD

Sampling method

Groundwater sampling was undertaken at Marandoo Mine and the KNP during September 2008. Samples were collected from 38 sites in 15 locations; these were collected from a range of different sources with the aim of gaining a hydrochemical overview of the entire study area.

Samples collected from Marandoo Mine were taken from production bores located in the Marra Mamba Iron Formation at a depth of 70 - 100 m. Within the KNP, samples were collected from groundwater bores from Southern Fortescue Borefield and bores in the National Park, the bores were all to purged so the water chemistry was representative of the aquifer and not the bore. Surface water samples were collected from two locations nearby Marandoo (Mindthi Spring and Banjima Pool) and also eight gorges spreading across the entire National Park (Figure 1).

The analysis of major ions (Ca^{2+}, Mg^{2+}, Na^{+}, K^{+}, Cl^{-}, SO_4^{2-}, HCO_3^{-}) was performed by SGS Environmental Services. Stable isotopes (Deuterium and Oxygen-18) were analysed by CSIRO Adelaide Laboratory.

Samples were collected in 500 ml PET bottles (major ions) and 30 ml glass McArtney Bottles (Stable Isotopes). The results are detailed in Table 1. The location map (Figure 1) shows the extent of the KNP and the catchment boundaries for the gorges involved in this study. Field parameters; Temperature, pH, electrical conductivity (EC) and salinity were measured with a TPS Handheld WP-81 pH-Cond-Salinity metre.

The use of hydrochemistry and isotopes

The geo-chemical composition of water is modified as it evolves from rainfall to groundwater. A unique chemical signature is developed as water interacts with its surroundings, which can be used as a diagnositic tool to understand the history of the water (Fetter, 2001). As rainfall infiltrates the unsaturated zone, evapotranspiration processes will increase the concentration of the dissolve solutes in the water (Abdalla, 2007; Allison, 1982). Once in the aquifer the relative concentrations of individual major ions are then modified by the water-rock interactions depending on the mineralogy of the aquifer matrix. The mass balance calculation can be carried out along the flow path to determine the likely connection and to quantify the amount of dissolved or precipitated minerals. Furthermore, by understanding chemical evolution of groundwater we will be able to determine connectivity by establishing whether the TDS signature of the MM groundwater can evolve to the observed TDS signature in the surrounding water features.

Similar to the major ion concentrations the evaporation and condensation of rainfall and water that recharges the aquifers cause a variation in the isotopic composition of hydrogen (^{1}H and ^{2}H) and oxygen (^{16}O and ^{18}O). Therefore stables isotopes are used to determine the main processes of recharge and discharge in the area (Chambers, Bartley and Herczeg, 1996). The measured δD and $\delta^{18}O$ of groundwater of the local water can be compared to a global relationship defined by the line $\delta D = 8 .\delta ^{18}O + 10$ (Craig, 1961), which is known as Global Meteoric Water Line (GMWL). In addition each region is characterised by the Local Water Meteoric line (LMWL) that is affected by local climatic conditions. The Local Meteoric Water Line LMWL calculated for the Pilbara region (Dogramaci and Dodson, 2009) is $\delta 2H = 6.31\ \delta 8O + 9.3$ and shows a characteristically depleted value for recharge with no apparent evaporation effect. Any variation from the LMWL illustrates a modification of the isotopes due to processes such as mixing, evaporation or isotopic exchange. Evaporation progressively enriches the remaining water in heavy isotopes resulting in the shift away from the LMWL to produce a lower regression slope

Catchment variables

Key factors in determining the chemical composition of groundwater are the processes occurring within the catchment. Remote sensing and GIS can be used effectively to gain information on the areal extent of various geological formations and the distribution of native vegetation. Remote sensing can be used to understand the surface water flow patterns in the catchment, displayed as a network of drainage lines. The extent of these drainage lines that connect to a single gorge is considered its' catchment. With the catchment defined other parameters including average flow path length and the area of Tertiary sediment can be calculated. There is obviously a variation in these parameters between catchments. The variables can be subsequently used to investigate relationships between the chemical composition of the water discharging from the gorge and its catchment.

The proportion of Tertiary material in each catchment was calculated by overlaying the catchment boundaries on a geology map (Thorne and Tyler, 1996) and undertaking area calculations. This was undertaken in GIS program MapINFO. Remote sensing can also be used to infer where water tables are high due to the presence of increased vegetation around flow lines and also visible surface water.

TABLE 1

Full data set from all sample locations, all concentrations shown in parts per million (ppm).

Location ID	Catchment	Northing	Easting	Date	δO18	δD	Cl	SO_4	HCO_3	Ca	Mg	K	Na	Br	SiO_2	pH	SAL	EC	Temp
Units					‰SMOW	‰SMOW	ppm	ppm	ppm	ppm	ppm	ppm	ppm	ppm	ppm		ppm	uS	°C
SFP10†	HAM	-22.439518	117.990717	8/09/2008	-9.49	-64.1	66.1	35.0	282.0	51.6	39.1	9.5	37.6	0.4	42.8	7.01	445	742	34.3
SFP8†	HAM	-22.46552	117.990599	8/09/2008	-8.63	-57.7	98.7	71.2	274.5	53.9	41.2	11.1	48.9	0.7	40.3	7.27	533	910	31.3
SFP7†	HAM	-22.473799	117.993963	8/09/2008	-8.52	-58.9	98.1	67.8	268.0	54.9	42.0	11.3	50.0	0.6	39.3	7.33	520	903	30.9
SFP2†	HAM	-22.489215	117.989096	8/09/2008	-8.65	-58.3	104.6	85.5	278.4	57.6	43.9	11.9	50.6	0.6	34.5	7.27	543	947	31.1
SFP4†	HAM	-22.498897	117.992307	8/09/2008	-8.75	-59.8	104.6	73.0	271.7	58.8	45.0	12.5	48.9	0.5	32.3	7.29	542	938	31.5
SFP5†	HAM	-22.505279	117.988382	8/09/2008	-8.87	-60.4	100.0	71.5	262.7	57.8	44.4	11.9	44.1	0.4	29.0	7.55	524	911	31.9
SFP6†	HAM	-22.50903	117.99629	8/09/2008	-8.76	-60.7	98.2	78.9	264.1	59.7	44.2	12.1	45.1	0.4	34.1	7.27	522	906	32.1
SFP11†	HAM	-22.529183	118.008586	8/09/2008	-8.79	-60.4	98.2	71.8	261.7	58.1	43.5	11.9	45.7	0.5	34.6	7.38	520	906	31.7
SFP12†	HAM	-22.534774	118.017218	8/09/2008	-8.78	-60	96.1	65.7	248.9	56.8	42.0	12.1	44.9	0.5	39.2	7.38	515	895	30.3
HM1	HAM	-22.258573	117.985979	9/09/2008	-8.87	-58.7	65.6	60.8	310.7	56.6	41.9	9.6	38.2	0.3	33.6	7.63	461	804	23.6
HM2	HAM	-22.257595	117.986906	9/09/2008	-8.54	-59.5	63.2	53.1	289.1	49.1	43.4	10.0	39.6	0.3	33.9	8.42	446	779	21.4
MR1	MBF	-22.629336	118.117401	9/09/2008	-9.17	-62.7	152.8	90.8	279.6	72.1	56.5	14.4	49.1	0.6	52.1	7.45	652	1121	29.1
MR2	MBF	-22.63824	118.143232	9/09/2008	-9.38	-61.5	102.1	76.0	255.6	55.7	45.4	12.9	41.6	0.3	38.3	7.48	519	904	30.6
MR4	MBF	-22.630673	118.12281	9/09/2008	-9.08	-62.9	78.9	62.5	291.8	56.9	45.7	13.0	39.9	0.5	40.6	7.4	506	878	30.4
MN Spring	UKN	-22.724015	118.263008	9/09/2008	-8.5	-56.7	221.0	111.2	338.6	63.0	63.7	17.0	117.6	1.3	34.3	7.19	848	1440	27
BJ Pool	UKN	-22.687258	118.199284	9/09/2008	-2.37	-29.5	7.5	13.1	36.6	10.5	3.2	4.2	5.4	0.3	2.8	8.37	57.6	110	20.4
WN1	WNO	-22.351913	118.28465	10/09/2008	-8.64	-58.2	45.3	2.0	44.7	3.2	9.3	3.8	24.1	0.2	50.0	6.8	90.9	170	21.2
WN2	WNO	-22.356624	118.28716	10/09/2008	-8.11	-56.2										7.48	153	245	20
WN3	WNO	-22.357277	118.286769	10/09/2008			50.2	1.4	56.9	4.0	10.9	4.0	27.1	0.3	48.7	7.78	136	250	21.1
HK1	HCK	-22.358755	118.285269	10/09/2008	-7.67	-53.7	52.8	1.4	40.7	3.9	8.7	3.6	27.4	0.3	37.7	7.95	129	239	24.1
HK2	HCK	-22.359804	118.286538	10/09/2008	-7.57	-52.9	52.7	1.4	40.7	3.9	8.6	3.5	27.1	0.4	37.8	7.78	127	234	19.9
HK3	HCK	-22.359885	118.286397	10/09/2008	-7.72	-55.3	52.8	2.4	30.9	2.8	7.7	2.7	27.1	0.4	35.3	6.68	120	222	22.4
ECO1†	JOF	-22.354592	118.251358	10/09/2008	-8.67	-57.9	253.3	40.5	93.7	19.4	51.8	17.7	88.9	1.5	61.9	6.38	633	1087	29.6
Windmill†	JOF	-22.385528	118.260653	10/09/2008	-8.7	-56.4	428.7	79.4	256.8	97.6	100.4	19.1	88.6	3.5	77.5	7	105.2	1954	27.7
KN1†	KNX	-22.372471	118.300158	10/09/2008	-9.02	-60.2	63.6	13.6	159.4	16.8	19.6	7.7	44.5	1.1	68.6	8.35	276	495	22.9
KN2	KNX	-22.372609	118.300171	10/09/2008	-5.53	-43.5	143.8	11.5	230.0	26.6	35.7	10.4	71.2	0.7	41.7	8.49	485	845	22
KN3†	KNX	-22.372327	118.300253	10/09/2008	-9.39	-61.7	51.6	12.1	177.3	17.7	18.5	7.3	43.6	0.5	72.7	7.14	275	488	27.8
RS1A GW†	DAL	-22.371691	118.299048	11/09/2008	-8.53	-61.4	758.9	405.3	351.6	181.7	166.1	31.5	228.3	4.6	54.5	7.13	2220	3640	28.1
VC1†	DAL	-22.582637	118.459033	11/09/2008	-9.55	-62.1	120.8	35.6	97.6	17.3	25.1	8.6	45.9	0.3	71.2	6.28	369	649	27.4
RS1†	CIR	-22.487664	118.476355	11/09/2008	-8.96	-59.4	87.4	18.3	106.5	18.4	20.5	6.4	32.9	0.7	59.7	6.4	294	520	26.2
FS Falls	DAL	-22.475277	118.562007	11/09/2008	-8.86	-59.2	113.2	18.9	167.3	29.1	27.0	8.8	48.7	0.5	55.8	8.32	386	678	23.4
FS Falls 2	DAL	-22.477105	118.56278	11/09/2008	-9.04	-59.8	111.4	25.4	175.5	29.1	26.6	8.8	48.1	0.5	56.8	7.75	393	690	24.2

† Denotes groundwater.

TABLE 1 cont ...

Location ID	Catchment	Northing	Easting	Date	δO18	δD	Cl	SO_4	HCO_3	Ca	Mg	K	Na	Br	SiO_2	pH	SAL	EC	Temp
Units					‰SMOW	‰SMOW	ppm	ppm	ppm	ppm	ppm	ppm	ppm	ppm	ppm		ppm	uS	°C
fern pool 1 GW†	DAL	-22.477273	118.556583	11/09/2008	-9.15	-60.3	109.4	26.1	176.5	29.2	26.8	8.9	48.3	0.4	57.4	6.21	382	671	26.2
fern pool 2	DAL	-22.4778	118.550428	11/09/2008	-8.93	-60.8	110.3	26.1	174.7	30.3	27.9	9.1	49.4	0.4	56.4	7.69	392	688	23.5
KL1†	KAL	-22.477165	118.548236	11/09/2008	-8.76	-58.1	60.8	7.2	166.9	18.2	21.4	7.6	41.9	0.3	71.1	8.28	23.4	46	24.9
KL2-SW	KAL	-22.41747	118.401955	11/09/2008	-8.26	-55.7	103.6	2.4	271.7	27.4	27.4	12.9	88.8	0.4	66.6	8.33	429	752	21.8
KL HW	KAL	-22.417472	118.401959	11/09/2008	-5.81	-43.8													
JF1	JOF	-22.391992	118.268026	11/09/2008	-7.54	-52.5	426.6	72.2	340.8	80.7	102.9	23.3	134.6	1.4	58.9	8.2	1226	2050	24.9

Notes: WNO = 68 per cent BIF; 32 per cent TR KAL = 64 per cent BIF; 36 per cent TR HCK = 65 per cent BIF; 35 per cent TR KNX = 43 per cent BIF; 57 per cent TR CIR = 42 per cent BIF; 58 per cent TR HAM = 20 per cent BIF; 63 per cent TR JOF = 44 per cent BIF; 66 per cent TR DAL = 38 per cent BIF; 62 per cent TR UKN = unknown MBF = Mount Bruce Flats

BIF/TR percentage determined from Thorne and Tyler (1996).

† Denotes groundwater.

RESULTS

Total dissolved solids distribution

The total dissolved solids (TDS) concentrations in the ground and surface water samples within study area range from 84 mg/L Banjima Pool (BJ pool) to 2182 mg/L Rangers Station Bore (RS1GW). The TDS for groundwater and surface water range from 351 mg/L to 2182 mg/L and 84 mg/L to 1241 mg/L respectively. The TDS from the MM aquifer bores (MR2, MR4 and MR1) exhibited TDS concentrations of 628 630 and 768 mg/L respectively, which is higher than the TDS concentrations in any discharged groundwater from the gorges at the KNP, apart from Joffre Gorge (Table 1).

The most prevalent ions are bicarbonate (HCO_3^-) and chloride (Cl^-) making up 35 per cent and 22.5 per cent of the total dissolved solids respectively, followed by sodium (Na^+) and sulfate (SO_4^{2-}) at 8.4 per cent and 9.0 per cent and calcium (Ca^{2+}) and magnesium (Mg^{2+}) at 6.8 per cent and 7.2 per cent of TDS. Minor species are bromide (Br^-) and potassium (K^+). Silica is also present in solution. The order of anion abundance is HCO_3 >Cl > >SO_4 and cation abundance is Na >Mg >Ca >K.

Stable isotope distribution

There is a wide range of isotopic abundances in water sampled from the study area (Figure 4). When ratios are plotted the data falls to the left of the GMWL with a slope of 4.8, this suggests significant modification has occurred.

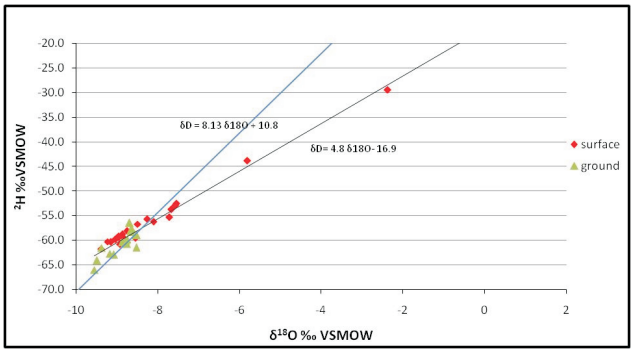

FIG 4 - The relationship between δ^2H and $\delta^{18}O$ for both ground and surface water samples collected within Karijini National Park, relative to Craig's (1961) GMWL.

The groundwater shows the most depleted signature with a $\delta^{18}O$ range from -9.55 to -8.52 ‰ and a δD range from -64.1 to -56.4‰. The surface water ranges from -9.04 to -2.37‰ $\delta^{18}O$ and -60.8 to -29.5‰ δD. The surface water ranges from a ratio similar to the groundwater to strongly enriched in ions. The surface water samples show a strong linear relationship suggesting evaporative fractionation.

Once water is within an aquifer and isolated from the atmosphere, its isotopic signature is unlikely to change unless groundwater mixing occurs. The narrow isotopic range of the groundwater (Figure 4) suggests that very little evaporation is occurring prior to recharge. Therefore it is likely that groundwater recharge occurs from heavy and intense precipitation. Such rainfall patterns are typical of cyclonic events which occur in the area. The more frequent light and short-term precipitation is less likely to contribute to groundwater recharge in the semi-arid Pilbara as evaporation exceeds infiltration rate. The enrichment of δD and $\delta^{18}O$ during intense periods of rainfall under higher ambient temperatures is less, compared to that which occurs during small rainfall events at the same temperatures.

This may be due to a number of factors. Firstly the sheer volume of water rapidly infiltrating the recharge zone, and

secondly the 'amount effect' (Clark and Fritz, 1997). The amount effect is where evaporation of the falling raindrops during intense rain is less than during light rainfall (Simpkins, 1995). Therefore, precipitation that potentially recharges aquifer systems in such arid areas is isotopically lighter.

The regression line with a slope of 4.8 for surface water samples represents progressive surface water evaporation. As the groundwater is all relatively similar in isotopic composition the different levels of enrichment seen in the surface water is determined by the amount of evaporation that has occurred since it was discharged. This is a function of humidity, temperature and time since exposure.

DISCUSSION OF RESULTS

Regional trends (catchment scale)

Isotope data shows that groundwater over the study area is derived from intense rainfall events that have not been affected by evaporation. There is however a large variation in TDS concentration and chemical composition from various aquifers, surface water pools and gorges (Table 1). Once infiltration occurs subsequent chemical evolution of water occurs due to mineral dissolution and/or precipitation or mixing. Aquifer mineralogy and catchment characteristics therefore may have an influence on the variation and composition of the TDS concentrations. Some key catchment variables that may influence groundwater chemistry are catchment size, which determines the distance between recharge and discharge zones and the thickness and area of Tertiary sediments (Figure 3).

The relationship between total dissolved solids and catchment area

The average TDS concentration for the surface water was plotted against the area for each catchment (Figure 5a). The graph shows that the Low TDS values correspond to smaller catchments.

The plot reveals a positive trend with a moderate relationship ($R^2 = 0.56$). The trend could be explained by a number of factors:

- the greater the area of the catchment, the longer the groundwater travels through the aquifer, allowing more water-rock reactions;
- the larger the catchment, the more surface area, and therefore more evapotranspiration, causing increased ionic concentration; and
- the larger catchments have a higher proportion of Tertiary material which is more reactive in water-rock interactions.

Length of flow path from recharge to discharge

To determine whether the length of the flow path has any impact on the TDS concentration of groundwater Mg:Ca ratios were explored. Various studies have shown that this is a reliable indicator of the residence time of the water in the aquifer (Cardenal, Benavente and Cruz-Sanjulián, 1994; Kloppmann, Dever and Edmunds, 1998; Edmunds and Smedley, 2000; Lo´pez-Chicano *et al*, 2001; Musgrove and Banner, 2004; McIntonsh and Walter, 2006).

Samples from Southern Fortescue Borefield were used to investigate how the Mg:Ca ratio varies with the length of flow path. These were chosen as they are located progressively down the hydraulic gradient. Increases in Mg:Ca ratio with distance down-gradient were observed. It is proposed that the observed increase is due to progressive water rock interaction, processes such as dissolution of dolomite and calcite precipitation. Magnesium concentration would tend to increase along the flow path of a ground water undergoing such processes, until a rather high Mg:Ca ratio is reached (Wigley, 1973; Plummer, 1977; Lohmann, 1988). This is especially relevant in an arid environment like the Pilbara where carbonate precipitation is common observed as white staining where groundwater seepage exists. It was also observed that HCO_3^- concentration increases down gradient, possibly as a result of carbonate weathering and/or silicate hydrolysis.

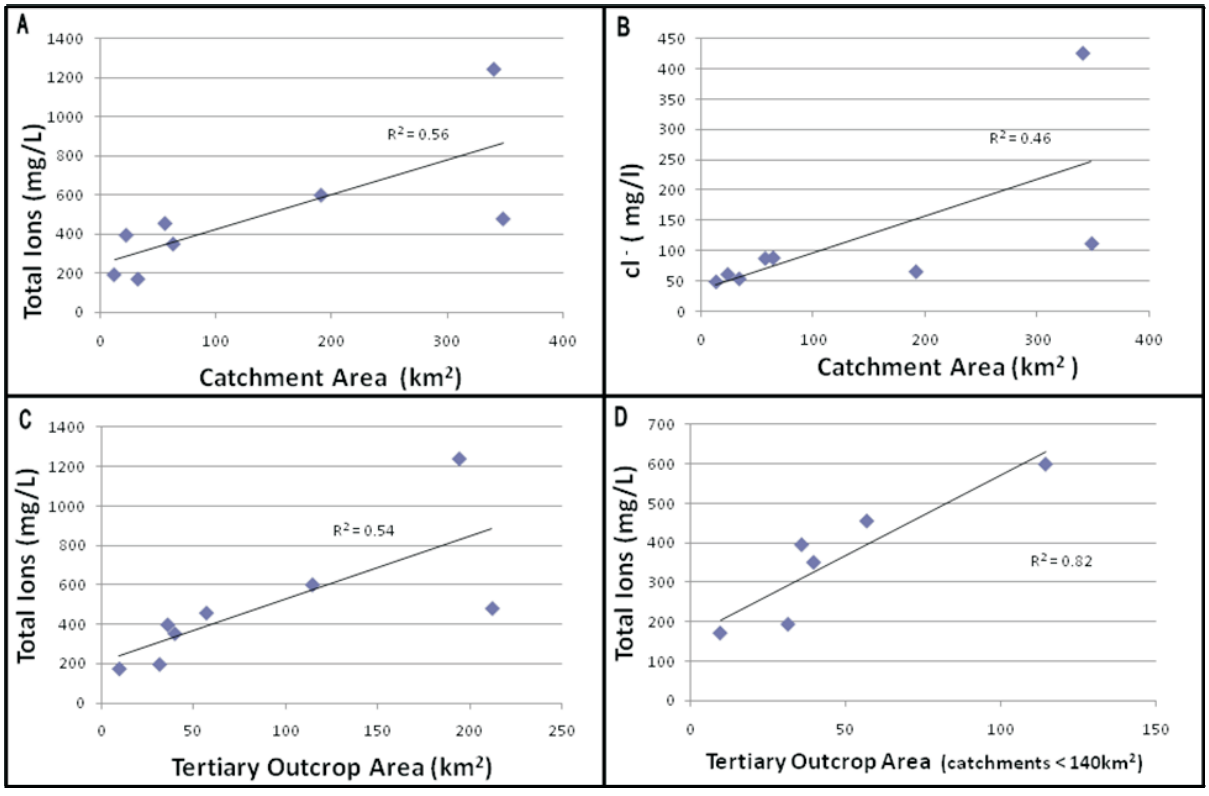

FIG 5 - The relationship between TDS and Cl^- concentration versus catchment and tertiary area. To investigate catchment scale trends.

The relationship between evapotranspiration and catchment area

To investigate whether the size of the catchment has any effect on the amount of evapotranspiration that occurs, Cl^- was used and was plotted against catchment size (Figure 5b). Chloride is a conservative tracer as it is primarily derived from rainfall, is very soluble, does not precipitate out of solution until very high concentration and is not significantly adsorbed on mineral surfaces (Hem, 1985). It is therefore an ideal indicator of evaporation, its concentration in groundwater will reflect the amount of evaporation that has occurred. The plot shows a positive relationship does exist between catchment size and evaporation, however there is a poor relationship (R^2 = 0.46) which suggests that a larger catchment area does not necessarily result in increased evapotranspiration.

Total dissolved solids concentration relative to proportion of tertiary material

The next factor to be investigated is how the unique geology of each catchment determines the groundwater TDS concentration. Each catchment has a varying proportion of Tertiary material to BIF outcrop. The Tertiary material is thought to be significantly more reactive in the presence of water. The total area of Tertiary material was plotted against the sum of the major ions to (Figure 5c). There was a positive moderate relationship between the TDS concentration and increasing area of Tertiary outcrop in each catchment. However, there are still some anomalies. The relationship appears to be much stronger in the small catchments. When only the small catchments are plotted (Figure 5d) a much better relationship (R^2 = 0.82) is produced.

The best relationship exists when the anomaly is removed (R^2 = 0.95). The anomaly was Dales Gorge catchment, which is the largest of the catchments; however it displays an unexpectedly low ionic concentration. This anomaly may be explained by the thickness of the Tertiary material and depth to the water table. The variation of TDS over tenfold therefore is most likely attributed to the catchment characteristics that define the amount of recharge, and the relative groundwater residence times.

Interelemental relationships to determine the source of solutes in groundwater

A useful tool to decipher the chemical and physical processes that affect groundwater TDS is depiction of chemical species on binary diagrams (Figure 6). The seawater dilution line (SWL) that relates evaporation and/or evapotranspiration of rainfall is added to the diagram to investigate the influence of evapo-concentration. The SWL defines the progression of rainfall (which should contain solutes at the same ratio as seawater) due to evapo-concentration. If no water-rock interaction or precipitation is occurring, then progressive evapo-concentration should cause points to lie along the SWL.

In the Na^+ versus Cl^- and K^+ versus Cl^- plots, the samples fall along the line. This suggests that Na^+ and K^- are introduced to the system via rainfall. There is a slight deficit of Na^+ showing that it is being taken out of solution possibly due to mineral precipitation.

The plots of Cl^- versus Ca^{2+}, Mg^{2+}, and HCO_3^- all show an excess concentration relative to the seawater. Their concentrations can therefore be either attributed to mixing with water bodies that have excess Ca^{2+}, Mg^{2+} and HCO_3^- or mineral dissolution.

A number of the samples are depleted in SO_4 relative to the sea-water dilution line. These correspond to the relatively fresh water samples from pools of Weano and Hancock Gorges. These samples were collected from stagnant water with significant biological activity as is evidenced from high pH. This may indicate the presence of microbial reduction of sulfate.

Characterising evapotranspiration

The isotopic composition and binary diagrams indicate evapotranspiration is a key process in the evolution of the groundwater within the study area. The rate of evapotranspiration can be estimated by comparing the Cl^- concentration of the sampled waters with that of rainfall. Evaporation will cause the enrichment of δD and the increase in Cl^- concentration in the remaining solution.

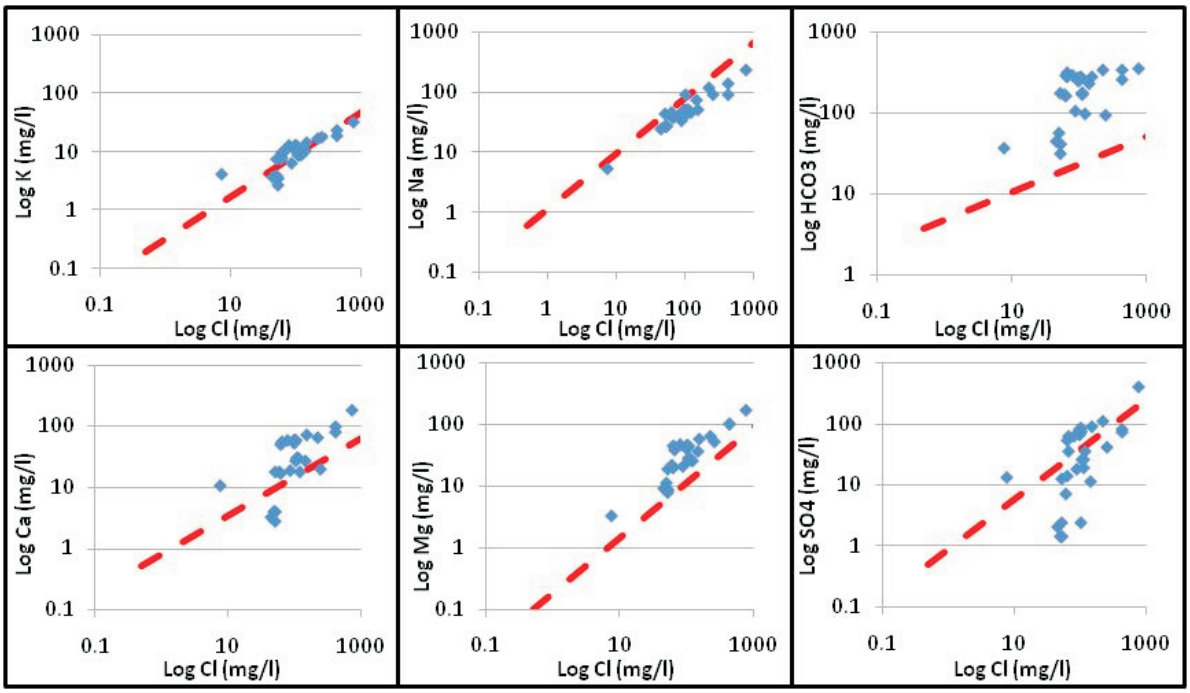

FIG 6 - Interelemental relationships with conservative Cl^- ion against other major ions, for all water samples from study area. Correlations emphasise the meteoric origin of K^+ and Na^+ and the introduction of HCO_3^-, Mg^{2+} and Ca^{2+} from other processes.

Figure 7 has been separated into ground and surface water, groundwater is isolated from the atmosphere and therefore has only been subjected to enrichment processes during recharge. The δD of the ground water falls in a narrow range (±10‰), however the Cl^- ranges tenfold from 66 - 759 mg/L (between black dotted lines). The surface water exhibits a broader range of δD‰ values. There is an anomalous data point that represents Banjima Pool which is characterised by the highest isotope values and the lowest Cl^- concentration.

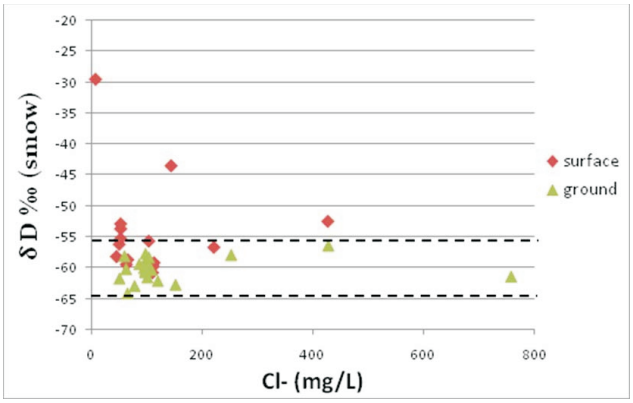

FIG 7 - δD‰ (smow) values versus chloride concentration for both surface and groundwater samples to investigate recharge processes.

If evaporation was occurring prior to recharge then you would expect to see an increase in Cl^- concentration along with enrichment of the stable isotopes. However the graph shows that the Cl^- concentration is increasing independently to δD. This nonfractionating water loss can only be explained by transpiration occurring in the recharge zone. Transpiration can act to concentrate salts in the soil while the residual water remains isotopically unchanged. This is because transpiration is a nonfractionating process (Zimmermann, Ehhalt and Miinnich, 1967; Dincer, AI-Mugrin and Zimmermann, 1974; Allison, 1982). Soil water is taken up by roots and released by the leaves therefore no partitioning can occur (Clark and Fritz, 1997). Generally the differences in Cl^- concentration reflect the degree of transpiration that has occurred during infiltration.

However it was also observed that in some catchments deep rooted plants were located along the drainage lines. This suggests that the water table was relatively high and there was the potential for continual transpiration and subsequent concentration of solutes to occur along the drainage lines.

Estimating recharge

To determine how much of the annual rainfall actually becomes groundwater recharge in each catchment the Chloride method can be used. The concentration of Cl^- in the ground water can be used as an indicator of the level of evapotranspiration that has occurred prior to recharge. Most plants do not take up Cl^-; therefore, it is concentrated in the soil in proportion to the amount of evapotranspiration that is occurring.

Equation 1, adapted from Allison (1985) can be used to estimate the amount of rainfall that becomes groundwater recharge.

$$R = (PCp) / Cg \quad (1)$$

where:

R = recharge

Cp = concentration of Cl^- in precipitation

P = annual precipitation

Cg = concentration of Cl^- in groundwater

The annual rainfall at Marandoo is 365 mm/year. The concentration of Cl^- in the rainfall is 0.5 mg/L (measured at Yandi) and groundwater concentrations of Cl^- average 100 mg/L. Therefore from the 365 mm/year the estimated groundwater recharge is 1.21 mm (only 0.45 per cent of mean annual rainfall). For Hamersley, Dales, Knox and Joffre Gorges, recharge is 0.52 per cent, 0.42 per cent, 0.76 per cent, 0.21 per cent respectively. The relatively small catchments are characterised by lower evapotranspiration and higher recharge rates resulting in relatively fresher waters observed where the groundwater discharges as surface water.

Mass balance calculations

This same principle can be used to further understand the sources of solutes to the aquifers via a simple mass balance equation. By quantifying the level of evapotranspiration occurring prior to recharge the major ion concentration of the infiltrating water can be estimated. If we assume no mixing, then the (elevated) concentration of Cl^- in a groundwater sample will be due to the amount of evapotranspiration that has occurred during infiltration.

If the Cl^- concentration of the rainfall and the groundwater is known, a value for the amount of evapotranspiration (ET) that is occurring prior to recharge can be determined.

$$ET = [Cl\ (groundwater) - Cl(rainfall)]/Cl\ (groundwater) \times 100 \quad (2)$$

$$\text{Ion concentration after ET} = \text{concentration factor} \times \text{initial concentration of rainfall} \quad (3)$$

The ET value calculated from Equation 2 can be used to determine a concentration factor, which is proportional to the amount of water lost during ET. The concentration of the solutes prior to recharge (when their concentration is only effected by ET) can then be estimated. The concentrations are determined by Equation 3.

By comparing this value (concentration post ET) with the concentration of the water extracted from the aquifer we can determine the amount of dissolved solutes that have been added or lost due to interaction with the aquifer. Table 2 shows the estimated influence of the aquifer on the groundwater samples collected within the KNP. The values are the difference between the measured and estimated values, with the per cent change shown. The table illustrates that there is variation between each aquifer and the behaviour of the ions present in solution.

When the estimated concentration is higher than the measured, this suggests Ca^{2+} is being precipitated. Mg^{2+} concentration increases in all samples after recharge as a result of dissolution of rock minerals. K^+ concentrations stay relatively constant emphasising its meteoric origin, while Na^+ shows a slight decrease in concentration from the estimated value. SO_4^- is estimated to be consumed in some aquifers while added in others.

Addition of solutes from carbonate dissolution

Carbonate dissolution will result in the addition of Ca^{2+}, Mg^{2+} and HCO_3^- to the solution according to the following reactions:

$$\text{Calcite dissolution: } CaCO_3 + H_2O + CO_2 = Ca^{2+} + 2HCO_3^- \quad (4)$$

$$\text{Dolomite dissolution: } CaMg(CO_3)_2 + H_2O = Ca^{2+} + Mg^{2+} + 2HCO_3^- \quad (5)$$

TABLE 2

The influence of the aquifer on groundwater composition. Values indicate the difference between measured and estimated groundwater concentrations with the per cent change from measured value.

Location	Ca	%	Mg	%	SO4	%	K	%	Na	%
SFP10	0.37	29	1.31	81	-0.02	-5	0.06	23	-0.28	-17
SFP8	-0.02	-2	1.24	73	0.17	23	0.00	1	-0.74	-35
SFP7	0.01	1	1.28	74	0.14	20	0.01	4	-0.67	-31
SFP2	-0.01	-1	1.33	74	0.29	32	0.01	2	-0.83	-38
SFP4	0.02	1	1.37	74	0.15	20	0.02	7	-0.90	-42
SFP5	0.06	4	1.37	75	0.17	22	0.02	7	0.77	40
SFP6	0.13	9	1.37	75	0.25	31	0.03	10	-0.88	-45
SFP11	0.09	6	1.34	75	0.18	24	0.03	8	-0.86	-43
SFP12	0.08	6	1.29	75	0.13	19	0.04	12	-0.83	-43
MR1	-0.32	-18	1.63	70	0.06	6	-0.07	-18	-2.29	-107
MR2	-0.02	-2	1.40	75	0.20	25	0.04	12	-1.15	-64
MR4	0.33	23	1.52	81	0.19	30	0.11	33	-0.55	-32
Windmill	-3.51	-144	2.17	53	-1.65	-200	-0.73	-149	-8.57	-223
KN1	-0.46	-110	0.52	64	-0.23	-161	0.02	8	0.09	5
KN3	-0.28	-62	0.52	69	-0.17	-136	0.04	22	0.40	21
RS1A GW	-6.00	-132	3.37	49	-0.17	-4	-1.35	-168	-12.07	-122
VC1	-1.25	-288	0.48	46	-0.33	-89	-0.12	-56	-1.51	-75
RS1	-0.75	-163	0.44	53	-0.31	-165	-0.08	-51	-1.10	-77

(-) Consumed by aquifer.

(+) Added by aquifer (mmol/L).

Rosen and Jones (1998) showed that if dissolution of calcite controls the chemistry of natural groundwater, then Ca^{2+} and HCO_3^- will correlate to a 1:1 regression line when plotted in milliequivalents. This is because the dissolution products of calcite are HCO_3^- and Ca^{2+} at a molar ratio of 2:1 (Equation 4). On an equivalent basis, one mole of Ca^{2+} is given an equal weight to two moles of HCO_3^-.

If calcite dissolution a dominant process the HCO_3^- against Ca^{2+} concentration (Figure 8a) would be expected to plot around the 1:1 line (Drever, 1988). The relationship between calcium and bicarbonates, however, shows an excess of HCO_3^- charge relative to Ca^{2+}. The high concentration of HCO_3^- could be the result of dolomite (Equation 5) dissolution. Dolomite has the chemical formula $CaMg(CO_3)_2$. When the ionic charge of Mg^{2+} and Ca^{2+} in water samples are summed, then most of the data falls on the 1:1 line (Figure 8b), suggesting a dolomitic source.

At low concentrations (<5 meq/L) Ca^{2+} and Mg^{2+} stay around the 1:1 ratio (Figure 8d), however as concentration increases the Mg^{2+} accelerates more than Ca^{2+}. This may be due to the precipitation of calcite. Dissolution of dolomite results in the production of Ca^{2+}, Mg^{2+} and HCO_3^-. When the ion activity product of calcite reaches saturation, Ca^{2+} precipitates as calcite resulting in an increase in the Mg/Ca ratio. This was seen earlier, where the flow path length had an impact on the Mg/Ca ratio.

Summary and specific data on each location

Based on the chemical composition and mass balance calculations the predicted order of processes for the rainfall evolution to groundwater are intense rainfall rapidly infiltrates into the unsaturated zone without significant evaporative effect. Once in this zone simultaneous evapotranspiration and carbonate dissolution of the TR aquifer increase major ion concentrations. During discharge, groundwater is further concentrated by evaporation and SO_4^- reduction may occur in stagnant pools. Most of these processes occur during infiltration of rainfall to the aquifer, it is therefore concluded that the chemical composition of the discharged groundwater water at each gorge is evolved during recharge; the vertical flow through the Tertiary sediments therefore dominates lateral flow. This water is supplied by rainfall that falls in the particular catchment of each gorge, which suggests mixing with water from the MM aquifer (approximately 40 km south) is an unlikely process.

Banjima pool

Banjima pool exhibits a very low Cl^- concentration of 7.5 mg/L compared to the Mara-Mamba Aquifer (Cl^- = 110 mg/L). It also has an enriched isotopic ratio (δO^{18} -2.37‰ δD -29.5‰). If Banjima pool was sourced by groundwater we would expect a much higher Cl^- concentration. It can be assumed that the most depleted groundwater value in the KNP (-65‰) is the closest reflection of rainfall. Therefore if Banjima pool is a collection of rainfall an enrichment of 36 per cent must have occurred to produce the observed δD - 29. 5‰. Simpson and Herczeg (1991) found a δD enrichment of about 0.75‰ per one per cent evaporation loss in surface waters of the semi-arid regions of the Murray Basin by using a model (after Gonfiantini, 1986). This suggests that the Banjima pool sample was evaporated by approximately 48 per cent. This level of evaporation is supported by the change in the Cl^- concentration of rainfall, which corroborates the scenario that evaporation of rainfall is the process causing the enriched isotopes despite the low Cl^- concentrations.

Knox and Kalamina Gorges

Knox and Kalamina Gorge both have relatively small catchments. The TDS concentration at each discharge location is significantly lower than that of the water sampled at MM aquifer. If the MM aquifer was hydraulically connected to these gorges then one of

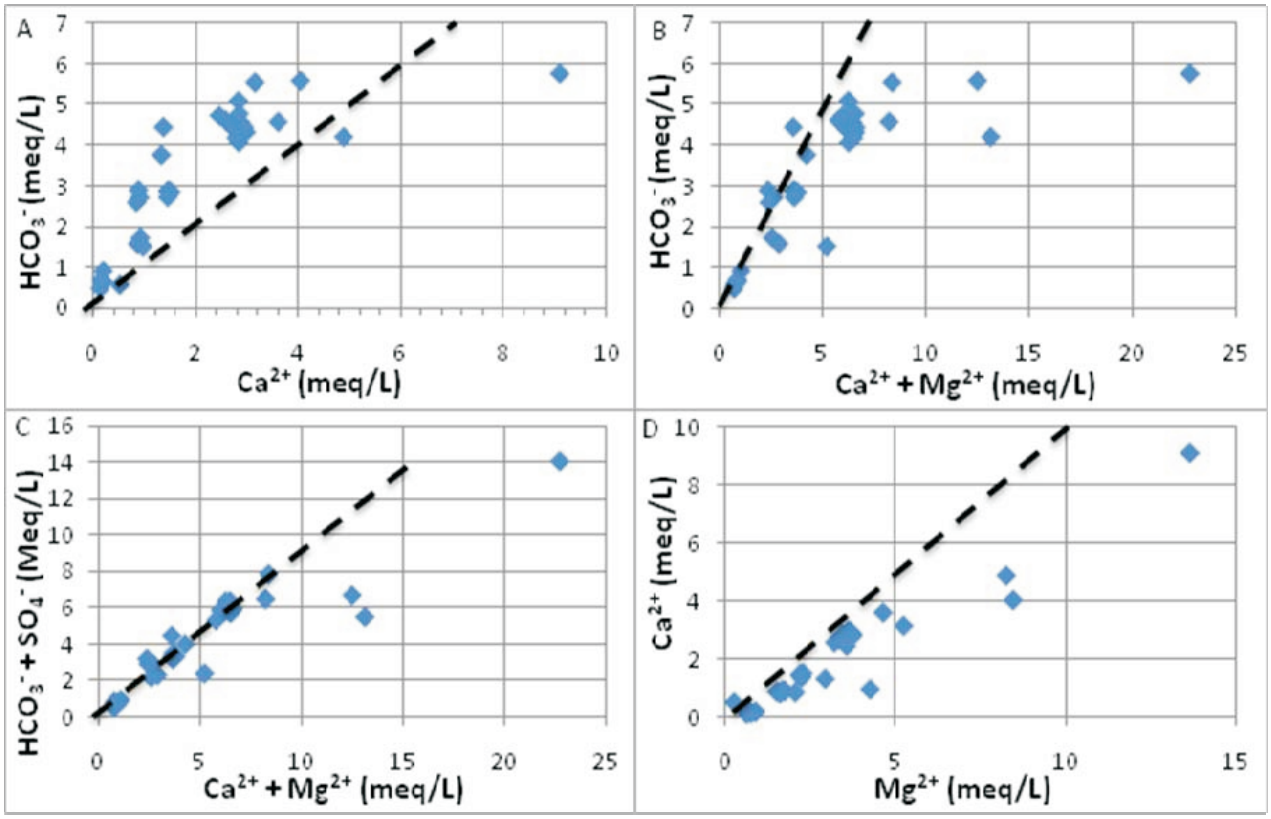

FIG 8 - Investigating carbonate dissolution: (A) concentration of Ca relative to HCO_3; (B) concentration of Ca + Mg relative to HCO_3; (C) concentration of Ca + Mg relative to HCO_3 + SO_4; (D) concentration of Ca relative to Mg.

two processes must be occurring; either dilution is occurring as a result of groundwater mixing, or dissolved solutes are being attenuated within the aquifer.

Groundwater mixing could be occurring either by input from rainfall, or by dilution from a relic groundwater source. The latter is implausible because if the surface water samples were collected from discharge points, a relic water body would be a finite resource that would quickly run-out if it was mixing with discharging water. If dilution was caused by rainfall then this would require a large amount of water low in TDS to infiltrate into the aquifer. The evapotranspiration that has been shown to occur makes this process also implausible.

If attenuation (sorption, precipitation, bioremediation) of the dissolved solutes was occurring within the aquifers we would expect the Cl^- concentration to reamin constant as it is uninvolved in such processes. This is not the case, in all groundwater discharge locations the Cl- concentration is significantly lower than that of the MM aquifer. Also, there has been no evidence to suggest that any other dissolved solutes are being significantly attenuated within the aquifers of the KNP.

Hancock and Weano Gorges

Hancock and Weano Gorge have the smallest catchments within the KNP, they also exhibit the lowest TDS concentrations of any groundwater discharge. Their Cl^- concentrations are similar to Kalamina and Knox Gorge, suggesting a similar amount of evapotranspiration has occured, however the other major ion concentrations are significantly lower. The discharged groundwater at Hancock and Weano have very low concentrations of Ca^{2+}, Mg^{2+} and especially HCO_3^-. In fact, the measured concentrations are very similar to Banjima pool. This suggests that the residence time is relatively short compared to other catchments and there is little effect from evapotranspiration or mineral dissolution.

Joffre Gorge

The surface water sample collected at Joffre Gorge is the only groundwater discharge location in the KNP that has a TDS concentration higher than that of the Marandoo groundwater. Its TDS concentration is in fact two fold higher. The major ion composition of groundwater sampled from a bore in the TR aquifer upstream of Joffre Gorge shows an identical major ion signature to that of the water sampled at the gorge. This suggests that Joffre Gorge groundwater discharge is dominated by groundwater flow from TR aquifer. The higher than expected TDS concentration is due to the relatively shallow water table within the Tertiary aquifer, evidenced by a long drainage line that is dominated by groundwater dependent native vegetation particularly paper bark resulting in higher transpiration rates. The water table may even be close enough to the surface to allow direct evaporation to occur, this is seen by a δD isotope enrichment of 4‰ between Windmill Bore and Joffre Gorge which are only 4 km apart.

Dales Gorge

Dales Gorge exhibits a TDS concentration slightly lower than the MM aquifer water but higher than the groundwater sampled from the TR aquifer upstream. However, the Cl^- concentration of TR groundwater and the groundwater discharged at Dales Gorge are identical. The increased level of Ca^{2+} and HCO_3^- in the discharge water compared to TR groundwater is more likely due to carbonate dissolution in the TR aquifer. This suggests that groundwater at Dales Gorge is sourced from the local TR aquifer.

Hamersley Gorge and Mindthi Spring

There are two locations where the chemical signature of groundwater is similar to that of Marandoo hydrochemistry

making hydraulic connection plausible. These locations are Hamersley Gorge and Mindthi Spring. The water discharged at Hamersley Gorge also has the same water chemistry as Southern Fortescue Borefield (which is upstream), suggesting the two are hydraulically connected.

Apart from increased Cl^- and Na^+ concentrations, the water chemistry of Mindthi Spring is relatively similar to Marandoo. Considering its proximity to the mine it is plausible that the two may be hydraulically connected. Even if the two are not currently connected a large drop in water table may indeed reverse hydraulic gradients in the area causing subsequent adverse effects. Therefore ongoing monitoring should be continued throughout the dewatering process and the mode of occurrence should be further investigated to be confident that it will not be affected

CONCLUSION

Based on the comparative analysis of the water chemistry discussed above the following conclusions are drawn:

- A combination of physical hydrogeology, geochemistry and stable isotope data suggests that the chemical evolution of groundwater is dominated by processes that occur during vertical infiltration and secondly lateral movement through the surficial TR sequence.
- The isotope data shows that recharge occurs from intense rainfall events when recharge water quickly infiltrates before any significant evaporation can occur. Once in the unsaturated zone transpiration processes act to concentrate major ions in the remaining water without enriching the stables isotopes. This process varies between catchments depending on the water table depth.
- The characteristics of the catchment determine the relative ionic concentration of the discharged groundwater. The major catchment variables are catchment area, the ratio of BIF to Tertiary material, the thickness of the Tertiary material and the length of the flow path.
- The contrast in the chemical characteristics of the natural waters between the key surface water features of the Karijini National Park and Marandoo Mine suggests that they are *each* supported by *different* catchments, with the exception of Mindthi Spring. The results have therefore shown no evidence to justify any restriction on the future operations at Marandoo Mine.

REFERENCES

Abdalla, O, 2007. Groundwater recharge/discharge in semi-arid regions interpreted from isotope and chloride concentrations in north White Nile Rift, Sudan, *Hydrogeology Journal*, pp 1-14.

Allison, G B, 1982. The relationship between ^{18}O and deuterium in water sand columns undergoing evaporation, *Journal of Hydrology*, 55:163-169.

Allison, G B, Stone, W J and Hughes, M W, 1985. Recharge in karst and dune elements of a semi-arid landscape as indicated by natural isotopes and chloride, *Journal of Hydrology*, 76:1-25.

Australian Natural Resources Atlas (ANRA), 2007. Pilbara climate [online]. Available from: <http://www.anra.gov.au/topics/rangelands/overview/wa/ibra-pil.html> [Accessed 20 October 2008].

Balleau, W P, 1972. Outline of groundwater in the Fortescue Valley: Western Australia geologic survey, hydrogeology report no 977.

Barbieri, M, 2005. Stable isotope (^2H, ^{18}O and $^{87}Sr/^{86}Sr$) and hydrochemistry monitoring for groundwater hydrodynamics analysis in a karst aquifer (Gran Sasso, Central Italy), *Applied Geochemistry*, 20:2063-2081.

Beckett, K, 2008. Phase II surface water management, unpublished report prepared for Rio Tinto Iron Ore Expansion Projects.

Cardenal, J, Benavente, J and Cruz-Sanjulián, J J, 1994. Chemical evolution of groundwater in Triassic gypsum-bearing carbonate aquifers (Las Alpujarras, southern Spain), *Journal of Hydrology,* 161:3-30.

Chambers, L A, Bartley and Herczeg, A L, 1996. Hydrogeochemical evidence for surface water recharge to a shallow regional aquifer in northern Victoria, Australia, *Journal of Hydrology*, 181(1-4):63-83.

Clark, I D and Fritz, P, 1997. *Environmental Isotopes in Hydrogeology*, First Edition, 352 p (CRC Press: Queensland).

Craig, H, 1961. Isotopic variations in meteoric waters, *Science*, 133:1702-1703.

Dincer, T, AI-Mugrin, A and Zimmermann, U, 1974. Study of the infiltration and recharge through the sand dunes in arid zones with special reference to the stable isotopes and thermonuclear tritium, *Journal of Hydrology*, 23:79-109.

Dodson, W, 2008. Marandoo phase II spring and gorge water assessment, unpublished report prepared for Rio Tinto Iron Ore expansion projects, resource development, technical projects.

Dogramaci, S and Dodson, W, 2009. The use of stable isotopes of oxygen, hydrogen and carbon to understand groundwater dynamics in the Hamersley Basin, western Pilbara region, northwest Australia, in *Proceedings Water in Mining 2009*, pp 89-98 (The Australasian Institute of Mining and Metallurgy: Melbourne).

Drever, J I, 1988. *The Geochemistry of Natural Waters: Surface and Groundwater Environments* (Prentice Hall: New Jersey).

Edmunds, W M and Smedley, P L, 2000. Residence time indicators in groundwaters: The East Midlands Triassic sandstone aquifer, *Applied Geochemistry*, 15:737-752.

Fetter, C W, 2001. *Applied Hydrogeology, Upper Saddle River, NJ,* fourth edition (Prentice Hall: New Jersey).

Gonfiantini, R, 1986. Environmental isotopes in lake studies, in *Handbook of Environmental Isotope Geochemistry 2: The Terrestrial Environment* (eds: P Fritz and J Ch Fontes), pp 113-163 (Elsevier: Amsterdam).

Hem, J, 1985. Study and interpretation of the chemical characteristics of natural water, *US Geological Survey Water-Supply Paper 2254.*

Johnson, S L and Wright, A H, 2001. *Central Pilbara Groundwater Study,* Water and Rivers Commission, Perth.

Kendrick, T, 2006. *Triennial Aquifer review*, Pilbara Iron Company (Services) Pty Ltd.

Kloppmann, W, Dever, L and Edmunds, W M, 1998. Residence time of chalk groundwaters in the Paris Basin and the North German Basin: a geochemical approach, *Applied Geochemistry*, 13:593-606.

Lohmann, K C, 1988. Geochemical patterns of meteoric diagenetic systems and their application to studies of paleokarst, in *Paleokarst*, pp 58-80 (Springer-Verlag: New York).

López-Chicano, M, Bouamama, M, Vallejos, A and Pulido-Bosch, A, 2001. Factors which determine the hydrogeochemical behaviour of karstic springs: A case study from the Betic Cordilleras, Spain, *Applied Geochemistry,* 16:1179-1192.

McIntonsh, J C and Walter, L M, 2006. Paleowaters in Silurian-Devonian carbonate aquifers: Geochemical evolution of groundwater in the Great Lakes region since the Late Pleistocene, *Geochim Cosmochim Acta,* 70:2454-2479.

Musgrove, M and Banner, J L, 2004. Controls on the spatial and temporal variability of vadose dripwater geochemistry: Edwards aquifer, central Texas, *Geochim Cosmochim Acta,* 68:1007-1020.

Plummer, L N, 1977. Defining reactions and mass transfer in part of the Floridan Aquifer, *Water Resources Research,* 13:801-812.

Rosen, M and Jones, S, 1998. Controls on the groundwater composition of the Wanaka and Wakatipu basins, Central Otago, New Zealand, *Journal of Hydrology*, 6:264-281.

Simpkins, W W, 1995. Isotopic composition of precipitation in central Iowa, *Journal of Hydrology,* 172(1-4):185-207.

Simpson, H J and Herczeg, A L, 1991. Salinity and evaporation in the River Murray Basin, Australia, *Journal of Hydrology*, 124(1-2):1-27.

Thorne, A M and Tyler, I M, 1996. *Mt Bruce, WA, Sheet SF51-11,* second edition, Western Australia geological survey 1:250 000 series.

Wigley, T M L, 1973. The incongruent solution of dolomite, *Geochim Cosmochim Acta*, 37:1397-1402.

Woodward-Clyde, A, 1995. *Contribution of CID groundwaters to the Fortescue Valley Groundwater System*, for Hamersley Iron Pty Ltd, for Fluor Daniel Pty Ltd.

Youngs, J, 2006. Marra Mamba BWT project – Dewatering and reinjection program (MWH).

Zimmermann, U, Ehhalt, D and Miinnich, K-O, 1967. Soil-water movement and evapotranspiration: Changes in the isotopic composition of the water, *Proceedings Syrup Isotopes in Hydrology*, pp 567-584 (International Atomic Energy Agency: Vienna).

APPENDIX IV: Bore Completion Data

Bore No	Easting	Northing	RL (TOC) (mAHD)	Casing Material	Cased Depth (mbgl)	Casing Diam (mm)	Screened Interval (mbgl)	Screened Formation	Status
Dewatering Bores									
PB1	614575	7496935		ABS	77	202 ID	53-65 (sl) 65-77 (sc)	Ore body - Marra Mamba Iron Formation	Active
PB2	615250	7496590		ABS	104.3	202 ID	68.3 – 104.3 (sl)	Ore body - mineralised Marra Mamba, West Angelas Shale and Wittenoom Dolomite	Active
PB3	617050	7496050		PVC	70.5	197 ID	34.5 – 70.5 (sl)		Active
PB4	617340	7495930		ABS	68.7	202 ID	48.7 – 50.7 (sl) 50.7 – 62.7 (sc) 62.7 – 68.7 (sl)	Ore body - Marra Mamba Iron Formation	Active
PB5	617700	7495650		ABS	77.1	202 ID	35 – 59 (sl) 59 – 71 (sc) 71 – 77 (sl)	Ore body - Marra Mamba Iron Formation	Active

Figure A4.1 Bore completion data for Marandoo Production Bores

Bore No	Easting	Northing	RL (TOC) (mAHD)	Casing Material	Total Depth (mbgl)	Casing Diam (mm)	Screened Interval (mbgl)	Screened Formation	
SFP2	601623	7512495	663.39	150mm ND Steel	125	244,200,150	100.6-125 (slotted)	0-67 m: 67-104 m: 104-? m:	Alluvium Calcrete / goethite Wittenoom Dolomite
SFP4	601919	7511456	666.90	150mm ND Steel	196.3	244, 178	68.4-71.4 (sl) 87.6-102.7 (sl) 110.7-151.4 (sl) 166.3-186.3 (sl)	0-34 m: 34-107 m: 107-? m:	Alluvium 34-107m: Calcrete / goethite Wittenoom Dolomite
SFP5*	601517	7510788	667.10	FRP Casing	129.1	408, 254	77.4-83.4 (sl) 83.4-86.4 (sc) 86.4-104.2 (sl) 104.2-107.2 (sc) 107.2-125 (sl)	0-65 m: 65-120 m: 120-? m:	Alluvium Calcrete / goethite Wittenoom Dolomite
SFP6	602345	7510330	-	150mm ND Steel					
SFP7	602075	7514242	667.38	150mm ND Steel	114.3	244, 178	57.9-79.9 (sl) 84.7-114.3 (sl)	0-53 m: 53-? m:	Alluvium Calcrete / goethite
SFP8	601797	7515185	663.65	150mm ND Steel					
SFP9	601827	7516458	661.90	FRP Casing	86.8	408, 254	59.3-68.2 (sl) 68.2-74.6 (sc) 74.6-80.6 (sl)	0-39 m: 39-82 m: 82-? m:	Alluvium Calcrete / goethite Wittenoom Formation
SFP10	601878	7518014	658.79	FRP Casing					
SFP11	603552	7508102	679.09	FRP Casing			64.9-82.8 (sl) 82.8-86.1 (sc) 86.1-104 (sl) 104-107.4 (sc) 107.4-131.2 (sl)	0-70 m: 70-120 m: 127-? m:	Alluvium Calcrete / goethite Wittenoom Dolomite
SFP12	604469	7507462		FRP Casing			83.1-101 (sl) 101-104.3 (sc) 104.3-137.1 (sl) 137.1-140.4(sc)	0-100 m: 100-137 m: 137-? m:	Alluvium Calcrete / goethite Wittenoom Dolomite

Figure A4.2 Bore Completion data for Southern Fortescue Borefield

APPENDIX V: XRD Diffraction Patter

(Please see hard copy for original XRD Plots)

APPENDIX VI: Karijini Photography

A 6.1 View into Knox Gorge (Photo: P.Hedley)

A6.2View across Karijini National Park (Photo: P.Hedley)

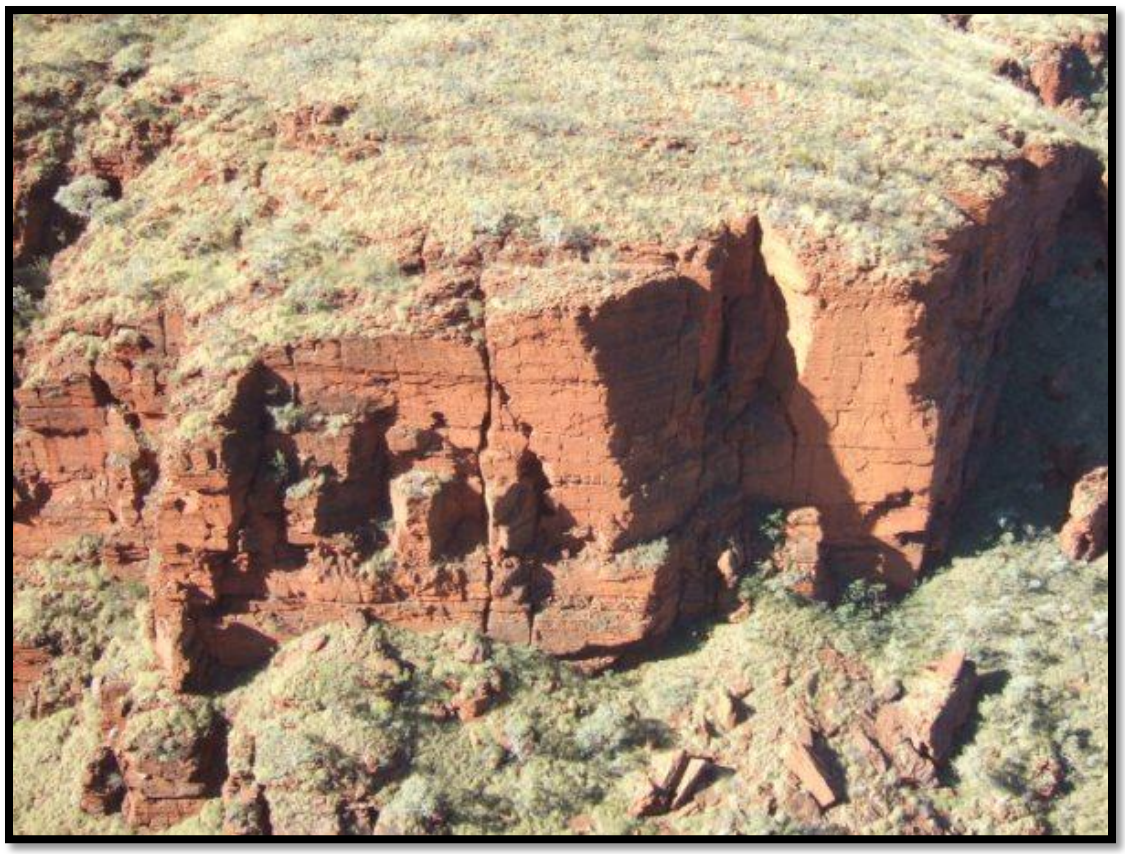

A6.3 Aerial View of a gorge in the Karijiji National Park (Photo: Pippa Gardner)

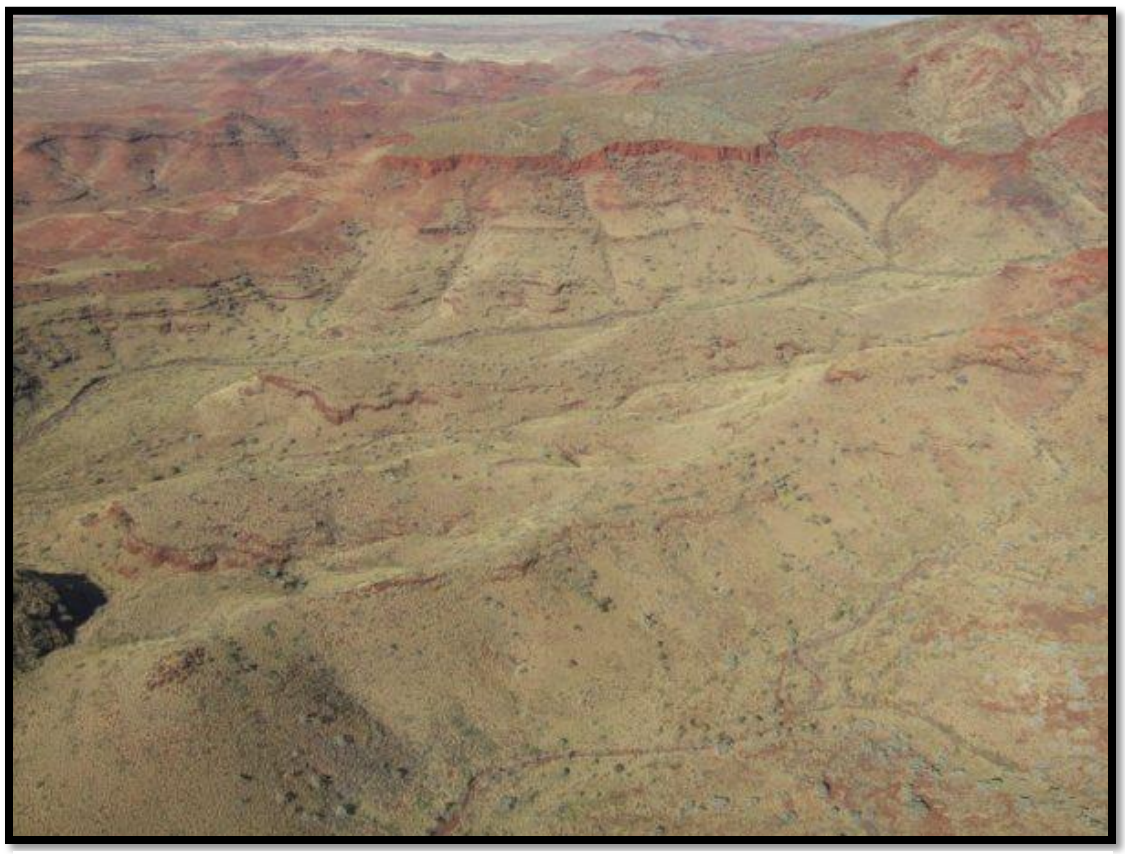

A6.4 Aerial view over Karijin National Park (Photo: Pippa Gardner)

A6.5 Hancock Gorge (upstream of spider walk) (Photo:P.Hedley)

A6.6 Sub-Horizontal Bedding of BIF in the Karijini National Park (photo: Pippa Gardner)

A6.7 Large pool in Weano Gorge (Photo:P.Hedley)

A6.8 View into Hancock Gorge (Photo:P.Hedley)

A6.9 Fern Pool (Photo:P.Hedley)

A6.10 Water sampling in Fern Pool (Photo: Jay Matta)

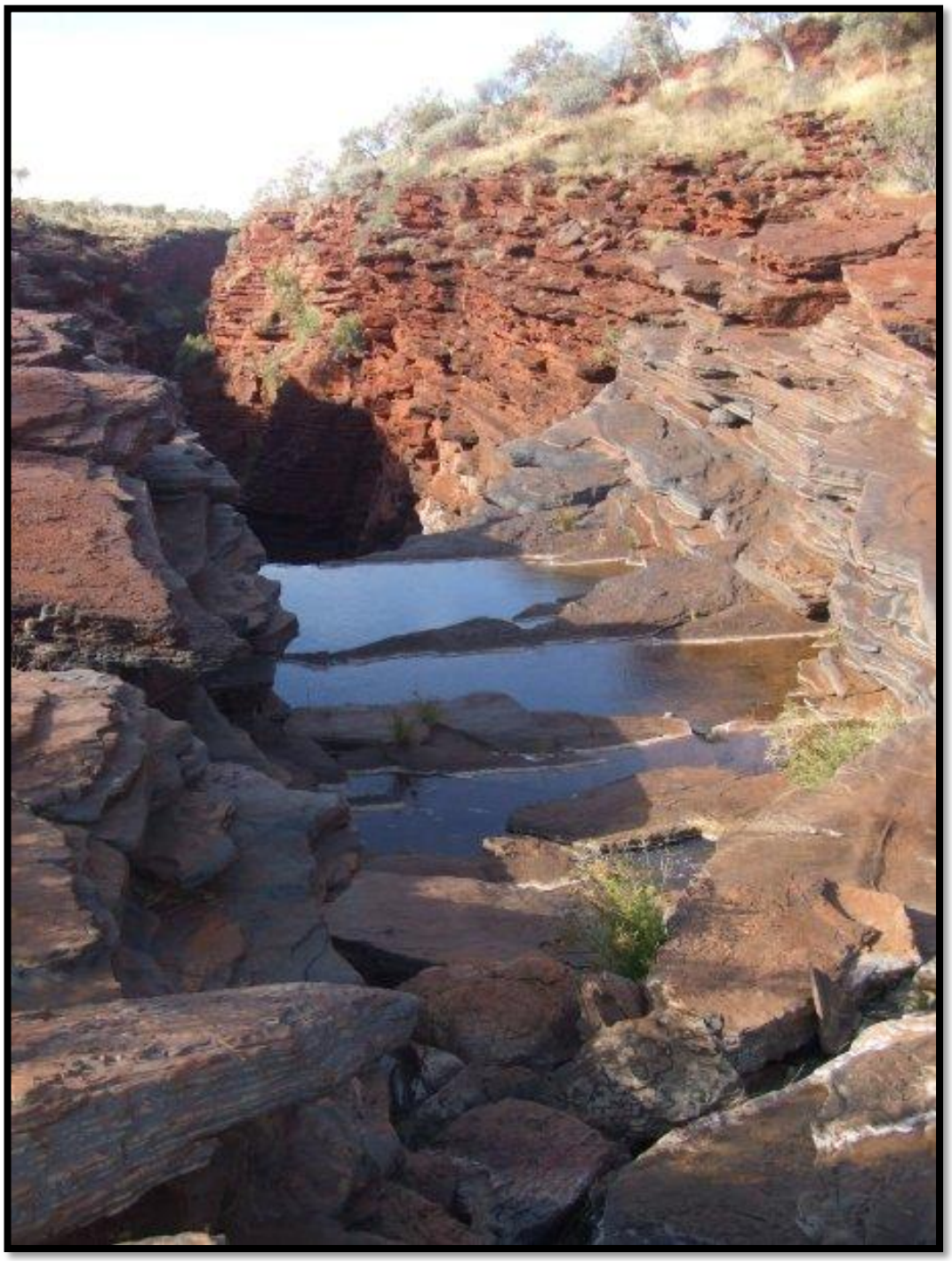

A6.11 The Head of Joffre Falls (Photo:P.Hedley)